NASA TECHNICAL NOTE

NASA TN D-7345

NASA TN D-7345

COMPUTER PROGRAM FOR DEFINITION OF TRANSONIC AXIAL-FLOW COMPRESSOR BLADE ROWS

by James E. Crouse

Lewis Research Center

Cleveland, Ohio 44135

NATIONAL AERONAUTICS AND SPACE ADMINISTRATION • WASHINGTON, D. C. • FEBRUARY 1974

1. Report No.	2. Government Accession No.	3. Recipient's Catalog No.
NASA TN D-7345		

4. Title and Subtitle

COMPUTER PROGRAM FOR DEFINITION OF TRANSONIC AXIAL-FLOW COMPRESSOR BLADE ROWS

5. Report Date

February 1974

6. Performing Organization Code

7. Author(s)

James E. Crouse

8. Performing Organization Report No.

E-7094

9. Performing Organization Name and Address

Lewis Research Center
National Aeronautics and Space Administration
Cleveland, Ohio 44135

10. Work Unit No.

501-24

11. Contract or Grant No.

12. Sponsoring Agency Name and Address

National Aeronautics and Space Administration
Washington, D.C. 20546

13. Type of Report and Period Covered

Technical Note

14. Sponsoring Agency Code

15. Supplementary Notes

16. Abstract

A method is presented for designing axial-flow compressor blading from blade elements defined on cones which pass through the blade-edge streamline locations. Each blade-element centerline is composed of two segments which are tangent to each other. The centerline and surfaces of each segment have constant change of angle with path distance. The stacking line for the blade elements can be leaned in both the axial and tangential directions. The output of the computer program gives coordinates for fabrication and properties for aeroelastic analysis for planar blade sections. These coordinates and properties are obtained by interpolation across conical blade elements. The program is structured to be coupled with an aerodynamic design program.

17. Key Words (Suggested by Author(s))		18. Distribution Statement
Compressor design	Turbomachinery	Unclassified - unlimited
Blade design	Blade stacking	
Aerodynamic design		

19. Security Classif. (of this report)	20. Security Classif. (of this page)	21. No. of Pages	22. Price*
Unclassified	Unclassified	224	Domestic, $5.50 Foreign, $8.00

* For sale by the National Technical Information Service, Springfield, Virginia 22151

PRECEDING PAGE BLANK NOT FILMED

CONTENTS

COMPUTER PROGRAM FOR DEFINITION OF TRANSONIC AXIAL-FLOW COMPRESSOR BLADE ROWS

by James E. Crouse

Lewis Research Center

SUMMARY

A method is presented for designing axial-flow compressor blading from blade elements defined on cones which pass through the blade-edge streamline locations. A blade-element centerline is composed of two segments which are tangent to each other. The centerline and surfaces of each segment have constant change of mean-camber-line angle with path distance. The blade elements are stacked along a line which can be leaned in both the axial and tangential directions. The output of the computer program gives coordinates for fabrication and properties for aeroelastic analysis for planar blade sections. These coordinates and properties are defined by interpolation across conical blade elements to the planes perpendicular to a radial line through the hub stacking point. The output blade-section properties are area, center-of-area location, stacking-point location, maximum and minimum moments of inertia along with their orientation, torsion constant, and twist stiffness.

The computer program uses velocity diagrams that have been established from some aerodynamic design process. The velocity diagrams are applicable to some fixed locations near the blade edges. Blade-element angles are obtained from the velocity diagrams (1) by correcting the velocity diagrams from the fixed locations to the edges of the blade as stacking adjustments are made, (2) by determining and applying incidence and deviation angles at the edges of the blade with one of several common methods chosen with optional controls, and (3) by correcting the inlet and outlet blade-edge angles on a streamline of revolution to the blade-element layout cone with the use of appropriate direction derivatives. The iterative stacking adjustments are made by translating the blade elements along the cone so that the center of area of the associated blade section is alined on the stacking axis.

INTRODUCTION

In an axial-flow compressor design method, the general objective is to define hardware which will give suitable and predictable flow conditions. For subsonic and transonic flows, the solidity of blade elements is generally low enough so that blade elements at most locations in a blade row can more reasonably be treated as a cascade of airfoils rather than channel flow. Also, since the axial dimension in axial-flow compressor stages is usually short with respect to blade height, there is reasonable freedom in the selection of blade-element shapes which, when stacked, will define a structurally sound blade. Where possible, those blade-element shapes which have demonstrated good performance with enough experimental data to yield useful parametric correlations are usually selected. One shape commonly used in present-day aircraft compressors is some variation of the circular-arc type of blade element.

Most compressor design systems utilize experimental data correlated from similar blade shapes in either two-dimensional or three-dimensional flow. In order to have a meaningful relation between the correlated data and the design application, the blade-element definition properties should be as nearly alike as possible. It is recognized, for example, that all the blade-element properties of a two-dimensional layout cannot be preserved when it is applied to compressor streamlines of revolution. So some decisions must be made as to which properties fundamentally control the data correlations. The most desirable properties to preserve are blade-element thickness distribution and blade-edge angles along streamlines of the compressor.

The camber distribution used to achieve the prescribed turning is a property which has significant effect on the blade-surface pressure distribution. The camber distribution can be simulated in various ways. For example, an element can be laid out directly on the surface of revolution, or it can be laid out on a plane or cylinder and then projected to the streamline. In reference 1 it was shown that these methods produce varying rates of change of blade angle with blade-element centerline-path distance at significant streamline slopes. From strictly a geometric point of view, the rate of change of blade angle with blade-element centerline-path distance is most directly related to the local chordwise rate of aerodynamic loading. So there appears to be some merit in preserving the rate of change of blade angle with blade-element centerline-path distance in the flow direction. This concept was developed and programmed in reference 1 for the simulation of a circular-arc blade element which has a constant rate of change of blade angle with blade-element centerline-path distance. The computer program of reference 1 mathematically describes and then stacks blade elements to define a blade after the blade-edge angles are established.

The coupling of an aerodynamic program with such a blade design program avoids iterative computer entries by the designer; but for the design of multistage compressors, program coupling places particular premium on speed, reliability, and accuracy. It was apparent that, to use the concepts of reference 1 in a coupled program, improved mathematical procedures were desirable. The rework of those concepts, which is described in this report, provides major gains in accuracy, reliability, and speed. The computer program presented is internally structured for use as a part of a composite compressor design program. But, in the form presented, the program is set up to run as a separate entity so that it can be used in conjunction with different aerodynamic design programs. Thus, this program is presumed to start with velocity diagrams at fixed locations near the edges of the blades. These velocity diagrams are corrected to the edges of the blades as the edge locations are defined through the stacking iteration. Incidence- and deviation-angle prediction methods are included to establish the blade-element edge angles from the velocity diagrams.

DESCRIPTION OF BLADE DESIGN PROCEDURES

The general blade design system can be divided into four rather distinct parts: (1) blade-element definition, (2) blade-element stacking, (3) interfacing of the reference velocity diagrams to the blade-element edges, and (4) terminal calculations. The first three parts are used in an iterative procedure in the computer program to establish the blade for the terminal calculations. The iterative loop through these parts occurs because the blade-edge locations for the velocity diagrams are known only as accurately as the blade elements are stacked. Most of the computer program information of interest to the user is given in the section entitled DISCUSSION OF COMPUTER PROGRAM; but occasionally, computer subroutines are mentioned in this section when a procedure is the specific function of a subroutine. The following discussion covers the development of concepts that are used in the computer program.

Blade-Element Definition

It is desired that a blade element lie on the surface of revolution generated by revolving the flow streamline about the compressor axis. For the purposes of blade-element definition, this surface is simplified to the cone passing through the intersections of the streamline surface with the blade leading and trailing edges. (The conical coordinate system for blade-element layout is illustrated in fig. 1.) Since the difference of streamline slope from a blade-row inlet to an outlet is usually relatively low, the blade properties along the streamline of revolution will closely approximate those laid out on the cone. The advantage of the conic approximation is that a cone is a single curved surface which is undistorted when unwrapped for layout.

All centerline and surface curves used to lay out a blade element on a cone are based on the concept of constant rate of change of local blade angle with path distance; that is, the paths are defined as functions of the κ and s shown in figure 1. (All symbols are defined in appendix A.) At any point on one of these paths, the angle of the tangent to the path is defined with respect to the local conic ray to the point. Since κ is defined with respect to a conic ray, it is convenient to define the blade element in the conic coordinate system associated with that layout-cone half-angle α and leading-edge radius r_{le}. General equations for representing these conic coordinates, R and ϵ, as functions of κ and s were originally developed and presented in reference 1. For some ranges of parameters, these functions have computational accuracy problems caused by the subtraction of nearly equal numbers. In the following redevelopment of R and ϵ as functions of κ and s, a different mathematical approach was used to improve computational accuracy.

Conic radius R as a function of κ and s. - In the conic coordinate system shown in figure 1, the basic principle can be expressed as

$$\frac{d\kappa}{ds} = C \tag{1}$$

where C is a constant. Integration of equation (1) from a reference point to some general point gives

$$\kappa - \kappa_0 = C(s - s_0) \tag{2}$$

The differential relation for conic radius is

$$dR = \cos\kappa \, ds \tag{3}$$

Substitution of equation (2) and integration from a reference point to a general point gives

$$R - R_0 = \frac{1}{C}\int_{s_0}^{s} \cos\left[\kappa_0 + C(s - s_0)\right]C\, ds = \frac{1}{C}\sin\left[\kappa_0 + C(s - s_0)\right]\Big|_{s_0}^{s}$$

$$R - R_0 = \frac{1}{C}(\sin\kappa - \sin\kappa_0) \tag{4}$$

This form of equation has poor accuracy on a computer for small C (i.e., $\kappa \to \kappa_0$). And the computation fails for C equals zero. The following development illustrates how this problem can be eliminated: Substitute for C in equation (4) to give

$$R - R_0 = \frac{s - s_0}{\kappa - \kappa_0}(\sin \kappa - \sin \kappa_0) = \frac{s - s_0}{\kappa - \kappa_0} 2 \sin\left(\frac{\kappa - \kappa_0}{2}\right)\cos\left(\frac{\kappa + \kappa_0}{2}\right) \tag{5}$$

The series form for the sine function of x is

$$\sin x = x - \frac{x^3}{3!} + \frac{x^5}{5!} - \frac{x^7}{7!} + \ldots \tag{6}$$

which can be rewritten as

$$\sin x = x\left(1 - \frac{x^2}{3!} + \frac{x^4}{5!} - \frac{x^6}{7!} + \ldots\right) \tag{7}$$

For the present application, x is $(\kappa - \kappa_0)/2$. Thus, the substitution of equation (7) into equation (5) and the subsequent cancellation of the $(\kappa - \kappa_0)/2$ terms yields a form that is accurate for small and zero C values (low $\kappa - \kappa_0$).

The series form can also be accurate for relatively large $(\kappa - \kappa_0)/2$, provided enough series terms are used. If terms through $x^8/9!$ are used, the first term dropped is $x^{10}/11!$. If this term is to be kept to 10^{-8} as compared to the first term of the series (1.0), the limit on $(\kappa - \kappa_0)/2$ is ± 0.9122 radian. That is, $(\kappa - \kappa_0)/2$ would be limited to 52.27° and $\kappa - \kappa_0$ to 104.5° to satisfy the criterion. Thus, series terms through x^8 are sufficient for our turbomachinery application. Therefore, the form of the equation for $R - R_0$ that is used for computation can be expressed as

$$R - R_0 = (s - s_0)\cos\left(\frac{\kappa + \kappa_0}{2}\right)\left[1 - \frac{1}{6}\left(\frac{\kappa - \kappa_0}{2}\right)^2\left(1 - \frac{1}{20}\left(\frac{\kappa - \kappa_0}{2}\right)^2\left\{1 - \frac{1}{42}\left(\frac{\kappa - \kappa_0}{2}\right)^2\left[1 - \frac{1}{72}\left(\frac{\kappa - \kappa_0}{2}\right)^2\right]\right\}\right)\right] \tag{8}$$

Conic angular coordinate ϵ as a function of κ and s. - The differential form for the conic angular coordinate is

$$R\, d\epsilon = \sin \kappa\, ds$$

or

$$d\epsilon = \frac{\sin \kappa}{R} ds \tag{9}$$

With the substitution of equations (4) and (2), equation (9) becomes

$$d\epsilon = \frac{\sin\left[\kappa_0 + C(s - s_0)\right] C\, ds}{R_0 C - \sin \kappa_0 + \sin\left[\kappa_0 + C(s - s_0)\right]} \tag{10}$$

The integral of equation (10) is of the form

$$\int \frac{\sin x\, dx}{a + b \sin x} = \frac{x}{b} - \frac{a}{b} \int \frac{dx}{a + b \sin x} \tag{11}$$

where the solution of

$$\int \frac{dx}{a + b \sin x}$$

is dependent on the ratio of the constants a and b. The solutions of the latter integral and the subsequent treatments of them are given in appendix B because of the complexity.

The computational difficulty encountered with the direct use of equation (11) can be explained when our specific variables are substituted into the x/b term. The equation for ϵ can be expressed as

$$\epsilon - \epsilon_0 = \frac{\left[\kappa_0 + C(s - s_0)\right]_{s_0}^{s}}{1} - \frac{a}{b} \int \frac{dx}{a + b \sin x} = \kappa - \kappa_0 - \frac{a}{b} \int \frac{dx}{a + b \sin x} \tag{12}$$

From figure 1, it can be seen that $\epsilon - \epsilon_0$ must be very small for large R. However, $\kappa - \kappa_0$ usually is not small. With the mathematical form shown in equation (11), $\epsilon - \epsilon_0$ is obtained by subtraction of nearly equal numbers. This, of course, leads to poorer accuracy with increasing R and a totally inaccurate value for the degenerate case of a cone becoming a cylinder.

In appendix B, it is shown that the solutions of the integral term in equation (12) all reduce to the same infinite but convergent series. Computational accuracy with this form is improved because the first term of this series practically cancels the $\kappa - \kappa_0$ term in equation (12). The remaining terms are then of the order $\epsilon - \epsilon_0$. The resulting equations for ϵ as developed in appendix B are

$$\epsilon - \epsilon_0 = \frac{(\kappa - \kappa_0)\left[\sin \kappa_0 + \sin \frac{\kappa + \kappa_0}{2} + CR_0\left(\sqrt{\frac{R}{R_0}} - 1\right) - X_1 - 4(R_0C - \sin \kappa_0)\sin \frac{\kappa - \kappa_0}{2}\left(\frac{X_2^2}{3} + \frac{X_2^4}{5} + \frac{X_2^6}{7} + \cdots + \frac{X_2^{2n}}{2n+1}\right)\right]}{(R_0C - \sin \kappa_0)\cos \frac{\kappa - \kappa_0}{2} + \sin \frac{\kappa + \kappa_0}{2} + CR_0\sqrt{\frac{R}{R_0}}} \tag{13}$$

where

$$X_1 = (R_0C - \sin \kappa_0)\left(\frac{2}{3}\left(\frac{\kappa - \kappa_0}{4}\right)^2\left\{1 - \frac{3}{5}\left(\frac{\kappa - \kappa_0}{4}\right)^2\left[1 - \frac{10}{63}\left(\frac{\kappa - \kappa_0}{4}\right)^2\left(1 - \frac{7}{90}\left(\frac{\kappa - \kappa_0}{4}\right)^2\left\{- \frac{18}{385}\left(\frac{\kappa - \kappa_0}{4}\right)^2\left[1 - \frac{11}{351}\left(\frac{\kappa - \kappa_0}{4}\right)\right]\right\}\right)\right]\right\}\right) \tag{B32}$$

$$X_2^2 = \frac{\left[1 - (R_0C - \sin \kappa_0)^2\right]\sin^2 \frac{\kappa - \kappa_0}{2}}{\left[(R_0C - \sin \kappa_0)\cos \frac{\kappa - \kappa_0}{2} + \sin \frac{\kappa + \kappa_0}{2} + CR_0\sqrt{\frac{R}{R_0}}\right]^2} \tag{B26}$$

and

$$C = \frac{\kappa - \kappa_0}{s - s_0}$$

The number of terms in the converging X_2^2 series used to limit the relative error to a maximum of 10^{-8} is

$$n = 35\left|X_2^2\right| + 5 \tag{14}$$

For $|(R - R_0)/R_0| < 0.21$, the following series form should be used to calculate the $\sqrt{R/R_0} - 1$ term in equation (13)

$$\sqrt{\frac{R}{R_0}} = 1 + \frac{1}{2}\left(\frac{R - R_0}{R_0}\right)\left[1 - \frac{1}{4}\,\frac{R - R_0}{R_0}\left(1 - \frac{1}{2}\,\frac{R - R_0}{R_0}\left\{1 - \frac{5}{8}\,\frac{R - R_0}{R_0}\left[1 - \frac{7}{10}\,\frac{R - R_0}{R_0}\left(1 - \frac{3}{4}\,\frac{R - R_0}{R_0}\left\{1 - \frac{11}{14}\,\frac{R - R_0}{R_0}\left[1 - \frac{13}{16}\,\frac{R - R_0}{R_0}\left(1 - \frac{5}{6}\,\frac{R - R_0}{R_0}\right)\right]\right\}\right)\right]\right\}\right)\right] \tag{B30}$$

For the special case of very small $|C|$,

$$\epsilon - \epsilon_0 = \tan \kappa_0 \ln \frac{R}{R_0} \tag{B12}$$

Finally, for the special case of very small $|(R - R_0)/R_0|$,

$$\epsilon - \epsilon_0 = \frac{2(s - s_0)}{R + R_0} \sin \frac{\kappa + \kappa_0}{2}\left[1 - \frac{1}{6}\left(\frac{\kappa - \kappa_0}{2}\right)^2\left(1 - \frac{1}{20}\left(\frac{\kappa - \kappa_0}{2}\right)^2\left\{1 - \frac{1}{42}\left(\frac{\kappa - \kappa_0}{2}\right)^2\left[1 - \frac{1}{72}\left(\frac{\kappa - \kappa_0}{2}\right)^2\right]\right\}\right)\right] \tag{B36}$$

In the limiting case of a cone becoming a cylinder, the preceding equation breaks down even though there is a physically meaningful path component perpendicular to R. The problem can be eliminated by multiplying both sides of equation (B36) by R so that a physically meaningful component in the same units as R can be computed directly. Thus, in the general subroutine EPSILON the calculated components are always ΔR and $R\,\Delta\epsilon$, where the radius associated with $\Delta\epsilon$ is the conic radius at the terminal end of the path (end opposite the path reference or beginning).

Blade-element layout parameters. - Subroutine CONIC contains the logic for layout of a two-segment blade element on a cone. The information for a blade-element layout comes from input data and the velocity diagram interfacing calculations. The parameters specifically used for a layout are listed here and illustrated in figures 1 to 3:

(1) Layout-cone half-angle, α

(2) Blade-element chord c, where the chord line is tangent to the blade-edge circles on the pressure side and the chord length is measured to the outer tangency points of the edge circles

(3) Cylindrical coordinate radius at the most forward axial point on the leading-edge circle, r_{le}

(4) Leading-edge blade angle on the cone, κ_{le}

(5) Trailing-edge blade angle on the cone, κ_{te}

(6) Ratio of leading-edge-circle radius to chord, t_{le}/c

(7) Ratio of trailing-edge-circle radius to chord, t_{te}/c

(8) Ratio of maximum thickness to chord, t_m/c

(9) Chordwise coordinate location of element centerline transition point as a fraction of chord, c_t/c

(10) Chordwise coordinate location of element centerline maximum-thickness point as a fraction of chord, c_m/c

(11) Ratio of first- to second-segment path distance derivatives $(d\kappa/ds)$, C_1/C_2

Definition of blade-element centerline. - The objective of the first phase of layout is to establish the centerline between the edge-circle centers (figs. 2 and 3). The length of a blade element is only known initially through the input chord; so the centerline-path length to the transition point and the trailing-edge-circle center are not known. The chord could be expressed as a function of R and ϵ, but the angular coordinate ϵ is a complicated function of κ and s. Thus, there would be no direct way of solving for the desired centerline-path length s. So a different approach is required.

The approach used is to estimate the centerline-path lengths so that s becomes the independent variable in the computation of chord. Adjustments are then made in the s values to converge the chord and transition-point locations to the specified values. Thus, the general procedure, which is in subroutine CONIC, is an iterative predictor-corrector method on the first-segment and overall centerline paths to give the input transition-point location and chord for the specified κ_{le}, κ_{te}, and C_1/C_2.

The first estimate of the blade-element centerline-path length is essentially that of a circular arc laid on the cone to meet the specified end angles in this unwrapped state. The path length corrections for succeeding iterations are the transition-point-location and chord relative errors, which are simply linear corrections. Since the initial path length approximation is a good one, only three or four iterations are required to converge the computed chord to within the relative error tolerance of 10^{-6}.

Within the iterative procedure, some specialized computer subprograms are called. Subroutine EPSLON gives the conic coordinate changes ΔR and $R\,\Delta\epsilon$ associated with a path length s and the κ angles at the ends of the path. To relate the path distances to chordwise component distances, two other subroutines were used. One is TANKAP, which calculates the constant-angle path between two points in the conic coordinates R and ϵ. It is used here for the purpose of establishing the chordwise direction. The other subroutine is RPOINT, which finds the intersection of a constant-angle path through a point at a given slope with a perpendicular path line through a second point. This routine is used here to find the chordwise component of the element transition point.

When the centerline path is established, the next step is to locate the maximum-thickness point on the centerline with respect to the transition point (fig. 3). The relation of c_m/c with respect to c_t/c establishes on which segment the maximum-thickness point is located. In addition, it gives an approximation of the path distance to the maximum-thickness point. Subroutine RPOINT is used to locate the maximum-thickness point in an iterative setup similar to that used to locate the transition point. Convergence to the path distance which places the maximum-thickness point at the specified location takes about three iterations.

Definition of blade-element surfaces. - The first point to be established on either blade-element surface lies at the end of the maximum-thickness path. This point is one-half the element maximum thickness in length along a curved path of constant κ angle which is normal to the centerline at the maximum-thickness point (see fig. 3). A general thickness path is likewise perpendicular to the blade-element centerline and is a curved path of constant κ angle. Only at the maximum-thickness point, however, is the surface path angle perpendicular to the thickness path.

At the ends of a blade element, the surface curves are tangent to the end circles. The conditions of a known surface angle at a fixed point and tangency to a specified side of a given fixed circle are sufficient to establish a surface path. In this case, the particular path is the one from the surface maximum-thickness point to the end circle of the same segment.

The surface curve constants are established through an iterative procedure in subroutine SURF. In it, a good first approximation of the surface camber difference from that of the centerline is used. In essence, this approximation is a circular-arc representation of the change of thickness for the path. With a good first approximation of the surface curve end κ, the end-circle tangency point is usually located within a 10^{-6} relative error tolerance in three iterations.

The transition point on a surface lies on a thickness path through the centerline transition point. It is located at the intersection of a surface curve with this thickness path. Sufficient information exists to calculate the intersection coordinates and surface angle by using only the established surface curve through the surface maximum-thickness point. This calculation is made in subroutine TRAN. Since the segment end-point coordinates and angles are common to both segments at the transition point, sufficient information is then available to establish the surface curve for the other segment. Subroutine SURF is again called for this computation.

With appropriate signs on the thickness-path directions, these procedures are used to calculate both the suction- and pressure-surface curve constants $d\kappa/ds$ for each blade element. In each case, it is necessary to begin the surface calculations with the segment on which the maximum-thickness point is located to have sufficient definition conditions. When the maximum-thickness point is specified to be coincident with the transition point, the procedure simplifies because the surface transition-point calculation is not needed.

Stacking-line lean to balance stress. - The mechanical as well as aerodynamic aspects of design must be considered in blade-element design - and especially in stacking. The centrifugal force associated with the rotative speed of turbomachinery imposes significant tensile stress. Additional stresses are produced by bending and torsional moments with steady flow conditions. When bending and torsional oscillations are also considered, the combined stress is often too high for adequate life at some locations in turbomachinery blading. It behooves the designer to do what he can to generally lower any component of the combined stress to minimize the amount of aerodynamic configuration compromise for stress reduction in specific applications.

The one component of stress which can be changed with little or no aerodynamic compromise is the component from steady-state bending moments. These bending moments have two principal sources. A moment results from the blade forces associated with the change of angular momentum of flow acting with a lever arm in the spanwise direction. This moment, for the most part, is established by the weight flow and the change in momentum. So it cannot readily be changed to control bending moments. The other bending moment in rotors results from the centrifugal force on each element of blade mass acting with a lever arm, which is offset from the radial projection of the attachment or root area. Since the centrifugal forces are high, significant moments occur with small offset. Thus, by stacking to control an "average" centrifugal-force lever arm in rotors, it is possible to minimize either the bending moment from centrifugal forces or the combined centrifugal-force and gas bending moment for some operating point.

For moment calculation, it is convenient to have blade forces which are resultant components for a blade cross section. If the type of blade cross section selected is described by a constant cylindrical coordinate radius, the centrifugal force per unit of mass is constant. So the resultant radial force (centrifugal force) acts at the center of area of the blade section with an incremental but constant radial thickness. The moments resulting from the blade forces are then established by lever arms associated with the location of the blade-section center of area with respect to the reference stacking point at the blade-root attachment point. For a blade, the path or line through the reference stacking point and the blade-section centers of area is the stacking line.

Reference locations for blade sections in stacking. - The "stacking line" reference point is the center of area of the hub section. In the computer program, it is set by the input data. The radial line in the turbomachinery cylindrical coordinate system which passes through this stacking-line reference point is called the "stacking ray" for blade-section location. Notice that the stacking ray is always radial, while the stacking line can be leaned in both the z and θ directions.

The axial and tangential coordinate origins of the cylindrical coordinate system are on the stacking ray. The axial coordinate z is positive in the turbomachinery through-flow direction. The angular coordinate θ is positive in the same direction as $R\epsilon$ in the conic coordinate system used for blade-element definition.

In the blade-element-definition computer subroutines, the input angles are relative values for rotors and absolute values for stators. These blade-element-definition subroutines operate with no distinction between rotors and stators. So the conic coordinate ϵ is positive in the same direction as the blade input angles. Since the relative and absolute blade angles are defined to be positive in opposite directions from the axial reference, the ϵ values for rotors and stators are also positive in opposite directions. This difference must be recognized in stacking. For rotor blade elements, θ decreases in the direction of rotation; but for stator blade elements, θ increases in the direction of rotor rotation.

Blade-section points by interpolation across blade element. - The previously discussed blade sections of constant centrifugal force would be defined on cylinders. The actual blade sections used in the program are defined on planes perpendicular to the stacking ray. There are two reasons for this. First, the annular extent of axial-flow compressor blading is low enough so that the layout part of the cylinder is at most only an incremental distance from the tangential plane. Second, the output fabrication coordinates are desired on planes. So by using planes for stacking alinement too, only one type of blade section needs to be found.

The blade-section planes used for stacking alinement purposes pass through the intersection points of the blade elements with the stacking line. The blade-section shapes on these planes are described by interpolation across blade elements. The preparation steps for the interpolation are (1) conversion of the conic coordinates, which are normalized to chord, to actual size; (2) selection of points on the blade-element surfaces across which the interpolation will be made; and (3) conversion of the blade-element points from their defining conic coordinates to a common coordinate system for all blade elements. The coordinate system used is the cylindrical coordinate system with the stacking ray as the origin of the θ and z directions. The coordinate conversions to this system are the function of subroutine POINTS.

The blade-element points used for interpolation are located at the following fractions of surface distance from the tangency point of the leading-edge circle to the tangency point of the trailing-edge circle: 0.0, 0.05, 0.12, 0.2, 0.3, 0.4, 0.5, 0.6, 0.7, 0.8, 0.88, 0.95, and 1.0. The coordinates of the transition point between segments on each surface are also included. The interpolation curve used is a piecewise cubic across four blade elements. With the exception of the transition point, each curve fit is through points of the same fraction of surface distance. Thus, for each blade-section point, separate interpolations are made in the axial and tangential directions. In the interpolation process, the tangential coordinate is converted to a Cartesian coordinate on the blade-section plane.

The form of the cubic equation is specialized in the sense that one of the interior known points is used as a zero reference for the independent variable. The reason for it is that there is much better computational accuracy and much less change of computational difficulty when a curve-fit interpolation can be made near the independent variable origin. The development of this cubic interpolation equation is shown in appendix C.

A sequence of four adjacent blade elements is always used for each interpolation. Whenever possible the interpolation is between the center two points of the set of four for the cubic fit. Near the ends of the blade, it is necessary to interpolate between the outermost points and in some cases to extrapolate when the blade section is outside all blade elements. The interpolation routine is INTERP.

Spline fit of blade-section surface points. - A blade-section surface is defined by a complete set of 28 interpolated points on a plane normal to the stacking ray. One advantage of interpolation in both the z and θ directions is that the end points of a surface set on the blade-section plane can be considered as the intersections of the surface curve with the end circles. To determine good blade-section area and moment values, it is necessary to curve fit these points. A spline curve fit was selected for its characteristic smoothness at the junction points of the piecewise-fit curve through the points. The experience has been that the points are indeed smooth enough for a nonwavy spline fit of each surface individually. A number of things were done, however, to help ensure a good spline fit. A discussion of the concepts follows; but a more detailed discussion, along with the development of equations, is given in appendix D.

A spline fit maintains a linear second derivative between points, not a linear curvature. As long as the slope of the curve is reasonably low, the difference is not very significant. So to maintain nearly the linear relation on curvature too, it is desirable to spline curve fit only where slopes are low. To help facilitate this concept, before curve fitting, the blade-section coordinates are rotated to an independent axis which is parallel to the line which passes through the first and last pressure-surface points. At the same time, the blade-section coordinates are translated to the coordinate origin, which is at the stacking-line intersection. The blade-section coordinate systems are illustrated in figure 4.

The spline curve fit uses separate cubic equations between adjacent points of a set, with the joining condition being continuous slope and second derivative at the points. To have sufficient conditions to define a spline, it is necessary to specify a condition at each end. The blade elements have constant-curvature paths by definition. So unless the cone angle is quite large in magnitude, the blade sections will also have nearly constant curvature. Thus, it would seem reasonable to use constant curvature as the end conditions. The first and second derivatives were not available in a direct way from the matrix solution for the spline coefficients, so a relation was approximated beforehand. To set nearly constant-curvature ends for the spline, a circular-arc fit of the three end points in the rotated coordinates was used to establish the ratio of second derivatives between the last two increments. This is the function of subroutine ARCS.

In general, blade elements have a discontinuity in curvature at the surface transition point, so an interpolated blade section should have a corresponding discontinuity. The allowance for this capability with a spline curve fit requires a modification because a general spline has continuous curvature from beginning to end. The modification was accomplished by placing the transition point in its proper place in each of the surface arrays and then replacing the condition of continuous curvature at that point with a substitute condition. The resulting conditions imposed at the transition point are continuous slope and a curvature ratio based on a three-point finite difference calculation for each side of the transition point. The curvatures are for the adjacent points on either side of the transition point. Since the curvatures are relatively constant along a segment in the plane section, the situation of unequal distance from the adjacent points to the transition point is not of major consequence. The curvature ratio relation across the transition point by this technique is

$$C_R = \frac{y''_{k+1}}{y''_{k-1}} \left[\frac{1 + (y'_{k-1})^2}{1 + (y'_{k+1})^2} \right]^{3/2} = \frac{y''_{t(+)}}{y''_{t(-)}} \tag{15}$$

The ratio $y''_{t(+)}/y''_{t(-)}$ is also the curvature ratio since the slope is the same on both sides of the transition point. In actual usage in the program (subroutine SPITG), the value C_R was smoothed by using the 0.7 power with the same sign.

The imposition of this condition in the center of a spline makes the usual tridiagonal matrix solution more complicated. The usual Gauss elimination of variables from one end of the curve to the other end, followed by backward substitution to get the y'' array, is unsatisfactory for a general location of the transition point. A way to avoid most of the complication is to use the Gauss elimination from both ends to the transition point. Then equation (15) supplies the added condition needed to fix the two y'' values at the transition point. The rest of the y'' values can then be calculated by backward substitution in each direction from the transition point.

Once the spline coefficients are established, mathematical expressions exist for general surface-point definition. Areas and moments for the spline pieces can then be determined from the appropriate integrals of the surface equations. A separate integration is performed for each surface curve from $y = 0$ to the curve. The integrations and the resulting equations are presented in appendix D. The major part of a blade section's areas and moments are accounted for by subtracting all the pressure-surface integrals from the suction-surface ones. However, to get accurate section values, the end-circle contribution must be included. The specific pieces used in the end region are shown in figure 5. The twice-covered areas in the figure are areas cancelled in summation.

Lines perpendicular to the surfaces through their respective end points do not necessarily intersect at a point equidistant from the surface end points. For the purposes of describing an end-circle center, surface continuity, which implies the center point is equidistant from each of the surface points, is desired. Surface tangency to both surfaces at the end points, however, cannot then be satisfied. The compromise used is an equal-angle discrepancy between the end circle and each of the surface curves at the surface end points, as noted in figure 5.

The end adjustment consists of the sector of an end circle plus the two trapezoidal shapes which fill in the part between the spline segments and the end circle. Area and first-moment corrections for a blade-section end are made in subroutine ENDS. The routine gives positive numbers for the leading-edge correction but negative numbers for the trailing-edge correction. The equations used in the subroutine are developed in appendix E.

Stacking adjustments to blade elements on cone. - The blade-section area and first moments obtained from the piecewise summations are used to determine a new center of area for the blade section. The location of the center of area from the stacking-line intersection of the blade section is a stacking adjustment increment. The actual adjusting is done by translating blade elements on the surface of the cone. So it is necessary to relate the blade-section adjustment increment on the plane to the blade element on the cone. From the definition of a blade section, the blade-section plane and the associated blade-element surface are known to intersect the stacking line at a common point. The common stacking point simplifies the stacking adjustment relations to the application of direction derivatives to suitable components. The geometry associated with the stacking shift equations is shown in figure 6.

On a blade section, $\Delta\bar{x}$ and $\Delta\bar{y}$ (fig. 6) are directly known from the area and moment equations. The axial and normal components are

$$\Delta\bar{z} = \Delta\bar{x}\cos\gamma - \Delta\bar{y}\sin\gamma \tag{16}$$

$$\Delta\bar{n} = \Delta\bar{x}\sin\gamma + \Delta\bar{y}\cos\gamma \tag{17}$$

The axial blade-element shift is related to the similar blade-section shift in figure 6 by

$$\Delta\bar{z} = \Delta\bar{z}_e(1 - \tan\alpha\tan\lambda)$$

so that

$$\Delta \bar{z}_e = \frac{\Delta \bar{z}}{1 - \tan \alpha \tan \lambda} \tag{18}$$

In the tangential direction, the normal component on the blade section $\Delta \bar{n}$ is applied directly to the blade element ($r \Delta \bar{\theta}$ in fig. 6). This application is not mathematically correct, but it is sufficiently accurate to be used in an iterative adjustment procedure. One assumption in the tangential adjustment procedure is that a small distance along the tangent in the circumferential direction is the same as the projected distance in the θ direction on the blade element. A second and less satisfactory assumption is the neglect of tangential-stacking-axis lean. With such lean, the blade section will not be tangent to the blade element at the stacking point. However, because of high centrifugal force, the stacking-axis lean of rotors must be small; so this angular difference is small. Thus, for rotors for which good stacking control is desired, the tangential shift assumptions are always good. For stators, the main concern is the convergence of the iterative procedure for stacking adjustment. The shift increment is in the correct direction and is of satisfactory magnitude for at least moderate lean angles. One stator design with 45° tip-tangential-stacking-axis lean still had good stacking-axis convergence.

The stacking adjustments are used in two different ways. First, both the leading- and trailing-edge axial and radial coordinates are adjusted. The axial coordinates are shifted by $\Delta \bar{z}_e$, and the radial coordinates by $\Delta \bar{r}_e$ where

$$\Delta \bar{r}_e = \Delta \bar{z}_e \tan \alpha \tag{19}$$

The second shift application is to the blade-element chordwise and normal component distances from the leading-edge-circle center to the stacking point. These component distances normalized to chord are maintained during iteration. The reason for them is that the iteration loop between stacking includes several other blade-angle or stacking-axis-lean adjustments which influence the blade-element edge locations. The normalized chordwise and normal coordinates are useful for the next iteration location of a blade element on the cone because these shifts are relatively invariant with the other shifts.

The adjustment procedure is based on the assumption that the shift of a blade element has the dominant effect on its associated blade section. In general, this dominance exists to a high degree, and the iterative procedure is highly convergent. However, this dominance no longer exists when a blade section crosses the ends of neighboring blade elements since, through interpolation, the neighboring blade element controls the blade-section end. So when a neighboring blade element intersects a blade section, the stacking procedure is nonconvergent. Such a situation can exist if closely spaced streamlines with large slopes are used.

Since nonconvergence of a possible design case is not desirable, some effort was made to extend the range of convergence. The approach was to make the blade-element shifts a function of the local and neighboring blade-section shifts. The influence coefficients were based on blade-section piecewise area and relative distances to adjacent blade elements. For the most part, the effort was unsuccessful and, consequently, it is not used in the program.

Stacking convergence problems can generally be avoided by judicial spacing of the blade elements in the design. As long as the ends of blade elements do not extend more than approximately one-half the distance to the next blade section, there is good stacking convergence. Once the blade is stacked, however, coordinates for closely spaced blade sections can be calculated for terminal calculations.

Balancing of bending moments. - The blade-element stacking procedure is controlled in subroutine STACK. One other major function of STACK is the balancing of bending moments. If the balance option is exercised by the specification of a blade material density, the steady-state rotor gas bending moments in the axial and tangential directions will be balanced by a centrifugal-force-on-blade-mass moment which is induced by stacking-axis lean. (Moments in the meridional plane are illustrated in figure 7.) In the balancing procedure, the blade mass moment is set up as a functional relation of blade lean. The equations for this are developed in appendix F. The major moment contribution is usually the blade-section center-of-area offset from a radial line. However, with a tapered tip the wedge-shaped excess and decrement masses from the tip blade section make significant contributions because their centers are relatively much farther from the stacking axis.

The steady-state gas bending moments to be balanced are calculated in subroutine GASMNT. The approach used is the change-in-momentum principle. The momentum boundaries in the meridional plane are the edge of the blade and the nonattached end of the blade (fig. 7). The state conditions and velocities on the boundaries are drawn from the input and interfacing calculation. The moment arm for both the gas-bending and blade-mass-centrifugal-force moments is referenced to the blade-element midradius value r_h on the blade attachment end.

Interfacing to Blade Edges

Velocity diagram corrections to blade edges. - Input fluid-state properties and velocities are given for fixed locations near the edges of blade rows. Streamline slope and/or streamtube convergence cause flow conditions to change from the input reference locations to the blade edges. To maintain the desired degree of design control over specification of blade-element edge angles, it is necessary to account for the flow changes between locations. The two assumptions used for those velocity diagram corrections were (1) conservation of angular momentum along a streamline with local slope between a reference station and a blade edge and (2) flow continuity from local stream-tube convergence. The blade-edge locations are not firmly established until the final stacking iteration, so the velocity diagram corrections are made for every iteration. Velocity diagrams at the reference locations are used for the first iteration.

Incidence and deviation angles. - In subroutine BLADE the inlet blade-edge velocity diagram is related to the physical blade through an incidence angle, and similarly the outlet blade-edge velocity diagram is related to the blade trailing edge through a deviation angle. The incidence angle can be specified through input options in five different ways, and the deviation angle can be specified in four ways. Two of the respective incidence and deviation options are the two- and three-dimensional values of reference 2. The parametric curves in reference 2 that are used for the determination of the incidence and deviation values were fit with equations which yield values within at least 3 percent of those from the curve. The third incidence option is a specified zero incidence on the suction surface at the edge-circle tangency point. The remaining two incidence options are tabulated values which can be referenced to either the leading-edge centerline angle or the aforementioned suction-surface angle.

The input incidence angles in some cases can be overriden during iteration by choke-margin option considerations. Since the inlet area of the blade-to-blade channel is a function of incidence angle, a specified choke margin can sometimes be achieved through a reasonable variation of incidence. If the blade-to-blade channel inlet choke margin is less than a specified (greater than zero) value, the input incidence angles will be adjusted to a limit of $+2.0^{\circ}$ on the suction surface to achieve the specified choke margin.

The third deviation-angle option uses tabulated values referenced to the trailing-edge centerline angle. The remaining deviation-angle option is a modified application of Carter's rule

$$\delta = \frac{m}{\sqrt{\sigma}} \varphi \tag{20}$$

where φ is the camber of the blade element which has an exit axial velocity equal to the inlet axial velocity and an equivalent angular momentum change at a constant radius r_{le}. The definition of m is

$$m = (0.219 + 0.0008916\,\gamma + 0.00002708\,\gamma^2)\left(\frac{2c_a}{c}\right)^{2.175-0.03552\,\gamma+0.0001917\,\gamma^2} \tag{21}$$

where the blade setting angle γ is in degrees and the ratio c_a/c is the fraction of chordwise distance to the maximum camber height point. The modification of m accounts for the deviation-angle change associated with the different turning rates on the two segments of a blade element. For a double-circular-arc-type element, m has the same value as that determined by the classical Carter's rule.

Blade-edge-angle corrections to layout cone. - The last interfacing step relates a blade-edge angle at local streamline slope to a blade-edge angle on the layout cone at that same point. When the inlet and outlet streamline slopes differ significantly, the layout-cone slope must also differ significantly from at least one of the edge slopes. The angle difference can be properly accounted for through the use of two nonparallel direction derivatives. The selected directions as viewed in the meridional plane are the streamline meridional and the radial. The direction derivative in the streamline meridional direction is obtained directly from the blade angle. However, to get the radial derivative it is necessary to fit across adjacent blade elements. The desired derivative could have been calculated from a curve fit of points from interpolated and extrapolated blade-element definition curves for a common axial location, but the interpolations and extrapolations were avoided with another approach. The blade-end-circle centers are already calculated with a common reference in subroutine POINTS so that they can be curve fit directly and converted to the radial directional derivatives by the methods shown in appendix G. In the program, the curve fit for the edge derivative in the meridional plane was done in subroutine POINTS, and the conversion to the radial direction was done in MAIN. For the first iteration, the radial direction derivative is set to zero.

Terminal Calculations

Once the blade geometry is established, the terminal calculations convert the information into a more convenient form for further analysis and further application. First, the computed flow parameters at the blade edges can be analyzed by the user to judge the practicality of the obtained aerodynamic design. Second, the output gives good aerodynamic forces and geometry parameters for mechanical design analysis of stresses and natural frequencies. Finally, suitable coordinates for blade fabrication are given.

Aerodynamic parameters. - Most of the aerodynamic parameters of interest are available from the last blade design iteration. The design-point choke margin is the major terminal calculation of an aerodynamic nature. The choke margin at the blade-channel inlet has been calculated and possibly was adjusted during the iterations if the choke-margin option was exercised. Adjustments for better margin at other channel locations were not programmed because, in general, it was not obvious what adjustments the designer would have chosen. Thus, the minimum blade-element-channel choke margins along with their locations are calculated and printed as terminal calculations so that such evaluations and adjustments can be made external to the program.

A local choke margin is defined as the ratio of available flow area above the choke flow area to the choked flow area, or $(A/A^*) - 1$. Thus, the minimum choke margin for a blade element corresponds to the local minimum A/A^* for the covered channel formed by two adjacent blades. The local minimum A/A^* is calculated with an iterative procedure in subroutine MARGIN. The first two calculations for A/A^* and its derivative with meridional distance are at the channel ends. The next location for an A/A^* calculation is the minimum of a cubic curve fit to the conditions of two values A/A^* and the two slopes $d(A/A^*)/ds$ at the end points. Succeeding iterations use the value and slope of the last calculated point along with the corresponding values of an end point. An A/A^* value is accepted as a minimum when the magnitude of the slope is below a tolerance of 0.001.

The ratio A/A^* is obtained from three other area ratios.

$$\frac{A}{A^*} = \left(\frac{A}{A_{le}}\right)\left(\frac{A_{le}}{A^*_{le}}\right)\left(\frac{A^*_{le}}{A^*}\right) \tag{22}$$

The choke areas are based on relative flow conditions for rotors since the rotating channel is controlling the choke situation.

The term A/A_{le} is a ratio of physical areas. It is obtained from ratios of dimensions in two directions. The first dimension direction is normal to the flow direction on the blade-element layout cone. At the inlet it is the product of blade inlet spacing and the cosine of the relative flow angle. In the channel the distance is measured on the layout cone from the suction surface of a blade element to the pressure surface of the adjacent blade element. The path is normal to the average of the local blade-surface angles.

The second ratio of dimensions needed for A/A_{le} comes from the rate of streamline convergence. The ratio is obtained from the radial spacing of blade elements and the direction-angle differences of adjacent layout cones. The local application point for this ratio is the midpoint of the blade-to-blade distance path.

The second area ratio in equation (22), A_{le}/A^*_{le}, is obtained directly from the inlet relative Mach number and the associated equation for compressible gas flow (ref. 3).

$$\frac{A_{le}}{A^*_{le}} = \frac{1}{M'_{le}}\left[\frac{1 + \frac{\gamma - 1}{2}(M'_{le})^2}{\frac{\gamma + 1}{2}}\right]^{\frac{\gamma+1}{2(\gamma-1)}} \tag{23}$$

The approach to the value of the third area term of equation (22), A^*_{le}/A^*, is to begin with relative flow continuity

$$\rho V'A = \rho^* V'^* A^* = \rho^*_{le} V'^*_{le} A^*_{le} \tag{24}$$

with the result that

$$\frac{A^*_{le}}{A^*} = \frac{\rho^* V'^*}{\rho^*_{le} V'^*_{le}} = \frac{\left(\dfrac{p^*}{Rt^*}\right)\sqrt{\dfrac{2\gamma gRT'}{\gamma + 1}}}{\left(\dfrac{p^*_{le}}{Rt^*_{le}}\right)\sqrt{\dfrac{2\gamma gRT'_{le}}{\gamma + 1}}}$$

The next step is the introduction of stagnation-state values by multiplication and division, so that all static properties can be expressed as ratios of static to stagnation values. These ratios can then be expressed in terms of local Mach number, which is 1 for the choke values. After cancellation, the equation reduces to

$$\frac{A^*_{le}}{A^*} = \frac{P'}{P'_{le}}\sqrt{\frac{T'_{le}}{T'}} \tag{25}$$

From the definition of relative stagnation temperature, the temperature ratio is

$$\frac{T'}{T'_{le}} = 1 + \frac{(\gamma - 1)\omega^2\left(r^2 - r^2_{le}\right)}{2\gamma gRT'_{le}} \tag{26}$$

The pressure ratio can be expressed as

$$\frac{P'}{P'_{le}} = \frac{P'_i}{P'_{le}} - \frac{P'_i}{P'_{le}} + \frac{P'}{P'_{le}} = \left(\frac{T'}{T'_{le}}\right)^{\frac{\gamma}{\gamma - 1}} - 1 + \left(1 - \frac{P'_i - P'}{P'_{le}}\right) \tag{27}$$

The last term in parentheses represents the blade-element losses from the inlet to the local point.

The overall blade-element losses can be calculated from the input-data stagnation temperature and pressure values at the inlet and outlet. The accumulated loss from the inlet to a local point was presumed to be some part of the total. The approach used was to break the total loss into shock and profile components. The shock loss was applied at the blade-element channel entrance, and the profile loss was made a linear function of the distance along the blade element. The shock loss was calculated by methods similar to those of reference 4, but with a modification. The methods of reference 4 approximate normal shock strength at the channel inlet. At the higher transonic and supersonic Mach numbers, this model tends to overestimate the actual shock strength for two reasons. First, the actual shock often becomes somewhat oblique, and so its strength is lowered. And secondly, the blade-surface pressure gradient will not support a strong shock. So an apparent strong shock in real flow develops the weaker structure of a shock foot. Consequently, the relative stagnation pressure loss at the channel entrance would be expected to be less than that indicated by a normal shock. In an effort to partially spread the shock loss through the channel, the loss at the channel inlet was calculated as the shock loss reduced by the empirical factor $1/(M'_{sh})^2$. No effort was made to quantitatively verify this factor from experimental data. It can easily be changed by the user in subroutine LOSS.

Blade-section forces. - The blade forces, which are computed in the terminal calculations, are of interest for blade stress analysis. Blade forces are determined by the principle of change of momentum across the boundaries of the surface formed by the edges of a blade through one revolution. The principle is essentially the same as that used to calculate the gas forces in the section Balancing of bending moments. However, the calculation is slightly different in this case because a local value of force for a radial blade increment is desired rather than the contribution to a total force or moment. The radial blade increment is located at the average of the inlet and outlet blade-element radii. The change of momentum associated with a blade element is considered applicable for the radial blade increment, but the static pressures at the blade-element edges are interpolated to the radial blade increment radius. Blade force components in the axial and tangential directions are calculated in MAIN and are given in units of force per blade and per unit of radial height.

Location of output blade sections. - The terminal blade geometry calculations are either made in or controlled by subroutine COORD. In general, blade-section data can be requested by the user where information is desired. There are three optional methods available for this. With one option, the user tabulates the radial locations of the desired blade sections. With the other two options, the blade-section locations are selected within the program. With one the user chooses the number of blade sections desired, but with the other the number is selected within the program on the basis of aspect ratio. For either option, a blade section is located at the intersection of the stacking axis with the casing on the blade attachment end. The other blade sections are spread across the blade span.

Output blade-section coordinates. - The coordinates of blade sections for general radial locations are described with the use of subroutine INTERP in the same way as those at the specific locations used for stacking alinement purposes. However, coordinates for fabrication purposes are desired on a coordinate system with a length axis tangent to the end circles on the pressure side of the blade and a corresponding height axis tangent to the leading-edge circle. The coordinate values in this translated and rotated system are found directly from the appropriate spline-curve-fit segment of the blade-section definition points.

To ease fabrication layout, the suction- and pressure-surface height coordinates are given at rounded-number length increments. Height coordinates are also given at the end of the blade and for the end-circle centers. The height values are obtained by using the desired independent variable values in the appropriate surface-definition equation.

For fabrication, the blade sections are oriented with respect to the radial line, the stacking ray, through the hub stacking point. As noted earlier in the section Reference locations for blade sections in stacking, this ray is not necessarily the stacking line. The coordinates that are used for the alinement of blade sections during fabrication are those of the stacking-ray intersection with the blade-section plane. Those coordinates, along with the blade setting angle with respect to the axial direction, are the output given for blade-section alinement. The coordinates for the blade-section center of area, which is the stacking-line intersection of the blade-section plane, are also given because they are the reference point for the output moments of inertia.

For some applications a user may prefer coordinates for the blade sections in the turbomachinery orientation, so the original blade-section surface-definition points are also printed in subroutine BCOORD.

Output blade-section properties. - The blade geometry properties needed for stress analysis are computed from the blade-section coordinates. The blade-section area and first-moment values are calculated in subroutines SPLITG and EDGES as they were in the stacking iterations. The higher moments desired are the minimum moment of inertia and the section twist stiffness, which is defined in reference 5 as

$$B = \iint (x^2 + y^2 - k^2)(x^2 + y^2)dx\,dy \tag{28}$$

where k is the polar radius of gyration. Since x is the chordwise direction and y its normal on the blade section, the minimum moment of inertia can be found from I_{xx}, I_{yy}, and I_{xy} with

$$I_{min} = I_{xx} \cos^2\gamma_I + I_{yy} \sin^2\gamma_I - 2I_{xy} \sin\gamma_I \cos\gamma_I \tag{29}$$

where

$$\gamma_I = \frac{1}{2} \tan^{-1} \frac{2I_{xy}}{I_{yy} - I_{xx}} \tag{30}$$

By expansion of equation (28) into a sum of integrals, it is seen that B can be determined from the moments of inertia and I_{xxxx}, I_{yyyy}, and I_{xxyy}. The equations for these moments are developed in appendix D for the spline pieces. The values are calculated in subroutine IMOM. The corresponding end-circle moment corrections are calculated in subroutine ENDS with the equations developed in appendix E.

The other calculated blade geometry parameter is the torsion constant, which is defined in reference 6 as

$$K = \frac{\frac{1}{3} F}{1 + \frac{4}{3} \frac{F}{AU^2}} \tag{31}$$

where

$$F = \int_0^u t^3 \, du$$

The variable t is the blade-section thickness normal to the blade-section centerline path u. The equations for expressing t as a general function of u on a blade section are developed in appendix H. The calculation of F is done in subroutine TORSN.

DISCUSSION OF COMPUTER PROGRAM

The blade design computer program as presented in appendix I is run as a separate entity from a compressor aerodynamic design, but it is structured to be run in conjunction with a compressor aerodynamic design program. The point is made to explain, first, the double dimensioning where only one dimension is needed and, second, the failure to save many computed blade-element values. The need for doubly dimensioned variables arises when this program is run as a part of a composite multistage compressor design program. Enough information must be prescribed to define blade parameters for an array of blade elements within an array of blade rows. On the other hand the number of variables dimensioned was minimized because of computer storage limitations for the broader mode of operation. Just enough information to fully describe the blade elements is stored, and all other parameters are calculated from the basic information as needed.

The overall operation of this program is controlled in MAIN. The other subroutines of major control are CONIC for the blade-element design, STACK for blade-section definition and the stacking adjustment shift, and COORD for the terminal calculations and printing. The call sequences of the subroutines are detailed in figure 8. The program variables for the commons and the individual routines are described in appendix I. The core storage is about 29 500 words. The breakdown is 21 200 words for coding, 5000 words for undimensioned and dimensioned variable storage, and 3300 words for systems. On an IBM 7094 the running time is about 1 minute for a blade row with eight stacking iterations.

For the first few iterations the stacking shifts for each iteration decrease in size by almost an order of magnitude. Usually the stacking shifts for all blade elements are less than 10^{-5} of blade-element chord within five iterations. However, a specification of close blade elements with significant streamline slope (see section Stacking adjustments to blade elements on cone) can cause convergence difficulties. Even though the stacking process for a troublesome case may not end up convergent, the blade-element shifts in the beginning usually become smaller for the first few iterations and then diverge. The stacking shifts may be low enough after some iteration that the user may want to consider the stacking well enough converged. To give the user the freedom to make this judgement, the program is set up to always run eight iterations with the blade-element stacking shifts printed for each iteration. The shifts relative to the blade-element chord are DM in the meridional direction, which is along the ray of the layout cone, and DY in the tangential direction. If the user decides to terminate the iteration process at some other number of iterations, he can most easily do it in MAIN by changing ICONV to 2 on the desired ITER number. The particular statement lies between the statements with external formula numbers 900 and 920. When the logical parameter ICONV is set to 2, the terminal calculations are activated on the next iteration.

Input Data

The input data are read and processed in subroutine INPUT. The card format for the data is shown in appendix I. The input parameters and the options they represent are listed and described together as a group in appendix I, even though the parameters are mentioned again in the description of variables for the routines. The input data essentially consist of inlet and outlet station information for describing velocity diagrams and parameters for blade-element description. The velocity diagrams are located and described with radius, axial location, axial velocity, tangential velocity, streamline slope, stagnation temperature, stagnation pressure, and rotational speed. The molecular weight of the gas and the coefficients for a fifth-degree polynomial of specific heat as a function of temperature are input for the velocity diagram corrections to the blade edges.

The blade stacking axis is initially located by the user with coordinates at the hub and tip in the meridional plane and a tilt angle in the tangential direction. The stacking line may later be adjusted for rotors by using an option to balance gas bending moments with the bending moment induced by centrifugal force on a leaned blade. The blade chord at the tip is specified indirectly through the number of blades and the solidity at the tip radius. The chords at other radii are specified through a cubic polynomial of chord to tip chord as a function of the fraction of passage height. The blade-element leading- and trailing-edge radii and the maximum thickness are input as a fraction of chord. The radial distributions of these parameters are specified as cubic polynomial functions of the local fraction of passage height. The blade-element incidence angle, the deviation angle, the location of the segment transition point, the turning-rate ratio of the segments, and the location of the blade-element maximum point are controlled by input options. The available options for these variables are described in the discussion of input data parameters AA, AB, BB, CC, DD, EE, and EB in appendix I.

Printed Output Data

The printed output includes the input data with the associated options selected, the blade-element stacking shifts during iteration, and the results of the terminal calculations (see the example in appendix I). For the most part the information is printed shortly after the calculations are made, so the output data appear in the order of the program steps. The input data and the stacking shift information have previously been sufficiently discussed, so only the terminal calculation output is further explained.

The first page of terminal calculation data gives the blade-element edge locations in the meridional plane and the velocity component corrections at the blade edges. The second page of terminal calculation data gives blade-element parameters and blade force distributions. The blade-element parameters are listed here. Some of them are shown in figure 3.

(1) Ratio of leading-edge radius to chord, $r_{c,le}/c$

(2) Ratio of maximum thickness to chord, t_m/c

(3) Ratio of trailing-edge radius to chord, $r_{c,te}/c$

(4) Ratio of maximum-thickness location to chord, c_m/c

(5) Ratio of transition-point location to chord, c_t/c

(6) Ratio of segment inlet to outlet curvature, C_1/C_2

(7) Suction-surface change of angle of the first segment, $K_{1s} - K_{ts}$, deg

(8) Blade setting angle, γ, deg

(9) Blade-element solidity, σ

(10) Blade-element aerodynamic chord, c, in.

(11) Ratio of maximum-camber-point location to chord, c_a/c

(12) Incidence angle, i, deg

(13) Incidence angle to suction surface at leading edge, i_s, deg

(14) Inlet relative flow angle, β_{le}, deg

(15) Inlet blade angle on streamline, $\kappa_{le,st}$, deg

(16) Inlet blade angle corrected to layout cone, κ_{le}, deg

(17) Deviation angle, δ, deg

(18) Outlet relative flow angle, β_{te}, deg

(19) Outlet blade angle on streamline, $\kappa_{te,st}$, deg

(20) Outlet blade angle converted to layout cone, κ_{te}, deg

(21) Centerline blade angle at transition point, κ_t, deg

(22) Shock location as fraction of suction surface, f_s

(23) Covered channel as fraction of suction surface, f_c

(24) Minimum choke-area margin in covered channel, $\left(\frac{A}{A^*} - 1\right)_{min}$

(25) Location of minimum choke point as a fraction of covered-channel centerline path, f

(26) Blade force components (axial and tangential tabulated with radius), lbf/(radial in.)(blade)

The blade-section properties are given in two forms. First, blade-section coordinates in the chordwise and normal directions are listed in a form suitable for fabrication layouts. And second, the blade-section definition points are listed in the turbomachinery orientation. In the headings for the first set of coordinates the following blade-section properties are given. The coordinate system for the blade-section output data is illustrated in figure 9.

(1) Radial location of blade section, r_{sp}, in.

(2) Stacking-point coordinates

(a) Length along chord, L, in.

(b) Height from chord line, H, in.

(3) Blade setting angle from axial direction, γ, deg

(4) Center-of-area coordinates

(a) Length along chord, L_{ca}, in.

(b) Height from chord line, H_{ca}, in.

(5) Area, A, sq in.

(6) Minimum moment of inertia through center of area, I_{min}, in.^{4}

(7) Maximum moment of inertia through center of area, I_{max}, in.^{4}

(8) Minimum-moment-of-inertia setting angle with respect to axial direction, γ_I, deg

(9) Section torsion constant, K, in.^{4}

(10) Section twist stiffness, B, in.^{6}

In addition to printed output, it is sometimes convenient to get output in other forms with the use of available computer peripheral equipment. On the NASA Lewis computer the program is set up with output options through the input variable OPO to give the fabrication coordinates on punched cards and on microfilm. Subroutine BLUEPT has the coding which controls the microfilm plotting. It was originally developed for the program in reference 1 by David Janetzke and Gerald Lenhart. Since the system microfilm subroutines called will not be applicable on another computer, a discussion of the specific function of these systems library subroutines is given in appendix J to help in the conversion to another facility.

Lewis Research Center,
National Aeronautics and Space Administration,
Cleveland, Ohio, June 29, 1973,
501-24.

APPENDIX A

SYMBOLS

A blade-section area, sq in.; also channel cross-sectional area normal to flow, sq in.; also a constant during a mathematical operation

a constant during a mathematical operation; also acceleration, ft/sec^2

B blade-section twist stiffness, $in.^6$; also a constant during a mathematical operation

b constant during a mathematical operation

C segment blade angle with path distance derivative $d\kappa/ds$ or curvature which is constant for the segment, $in.^{-1}$; also a constant during a mathematical operation

c blade-element chord on layout cone (includes edge-circle radii), in.; also a constant during a mathematical operation

D constant during a mathematical operation

d constant during a mathematical operation

e development constant in appendix D

F blade-section property integral, $\int_0^U t^3 \, du$, $in.^4$; also force, lbf

f fraction of total suction-surface path; also constant expressed by eq. (D13)

f location of minimum choke point as fraction of covered-channel centerline path

g gravitation constant, 32.1740 $lbm\text{-}ft/lbf\text{-}sec^2$

H height (normal) coordinate on blade section, in.

h development constant in appendix D; also blade-section effective thickness for mass moment, in.

I moment of inertia, $in.^4$

i incidence angle, deg

J total number of streamlines

j streamline index

K blade-section torsion constant, $in.^4$

k radius of gyration, in.

L length (chordwise) coordinate on blade section, in.

l moment lever arm, in.; also path of stacked-blade-element end-circle centers, in.

M Mach number; also total moment, in.-lbf

m coefficient for Carter's rule for deviation angle; also mass, slugs; also meridional component distance, in.

n number of series terms; also coordinate in tangential direction, in.

P stagnation pressure, lbf/ft^2

p static pressure, lbf/ft^2

R radial coordinate on blade-element layout cone, in.; also gas constant, lbm-ft/lbf-^{o}R

r radius coordinate in cylindrical coordinate system, in.; also end-circle radius, in.

s path distance on blade-element layout cone, in.

T stagnation temperature, ^{o}R

t static temperature, ^{o}R; also blade-section local thickness, in.

U blade-section centerline length, in.

u increment along blade-section centerline, in.; also functional variable

V velocity, ft/sec

v functional variable

X functional variable expressed by eq. (B9); also a redefined independent variable

$\mathcal{X}$ functional variable expressed by eq. (B7)

X_1 value expressed by eq. (B31)

X_2 value expressed by eq. (B25)

x functional variable, usually the independent variable; also blade-section coordinate in chordwise direction, in.

y dependent functional variable; also blade-section coordinate normal to chordwise direction, in.

z axial coordinate in cylindrical coordinate system, in.

α layout-cone half-angle, deg; also functional angle variable, deg

β relative flow angle, deg

γ blade setting angle, deg; also ratio of specific heats

δ deviation angle, deg

ϵ angular coordinate on blade-element layout cone, rad

η stacking-axis lean in circumferential direction, deg

θ angular coordinate in cylindrical coordinate system, deg; also angular coordinate on end circle, deg

κ local blade angle with respect to conic ray on blade-element layout cone, deg

λ stacking-axis lean angle in meridional plane, deg; also angle of line through corresponding points on suction and pressure surfaces of a blade section with respect to normal to chord line (fig. 19)

ξ dummy angle variable, rad

ρ gas density, lbm/ft^3; also blade material density, lbm/ft^3

σ blade-element solidity

φ camber of blade element which has equivalent angular momentum change at constant radius, r_{1e}, deg

ω angular rate of rotation, rad/sec

Subscripts:

a moment associated with axial and radial forces acting with lever arms in meridional plane (fig. 7); also chordwise location of maximum camber point of blade-element centerline

ba moment produced by axial gas bending forces acting with radial lever arm from hub

bt moment produced by tangential gas bending forces acting with radial lever arm from hub

c end-circle center; also blade-element centerline on layout cone; also channel formed by adjacent blade elements

ca blade-section center of area

da moment correction (resulting from tip slope) to moment obtained by summation of centrifugal force acting at blade-section centers of area in meridional plane

dt moment correction (resulting from tip slope) to moment obtained by summation of centrifugal force acting at blade-section centers of area in r-θ plane

e blade-element, blade-section end

h hub

I minimum moment of inertia of blade section

i	isentropic flow process
k	local point in array
L	intersection of blade-section pressure surface with end circle
le	leading edge of blade element
m	maximum thickness point
max	maximum value
min	minimum value
n	next iteration
p	pressure surface
R	ratio
s	suction surface
sh	shock
sp	blade-section stacking point
st	streamline
t	transition point; also moment associated with tangential and radial forces acting with lever arms in r-θ plane
te	trailing edge of blade element
U	intersection of blade-section suction surface with end circle
x	axis about which a moment is taken
y	axis about which a moment is taken
0	initial or reference point
1	first segment; also first point in a set of sequence points
2	second segment; also second point in a set of sequence points
3	third point in a set of sequence points
4	fourth point in a set of sequence points
(-)	upstream side of transition point
(+)	downstream side of transition point

Superscripts:

'	first derivative; also relative to a rotating blade
''	second derivative

—	center-of-area shift increment; also average value
*	choke value

APPENDIX B

DEVELOPMENT OF EQUATIONS FOR CONIC ANGULAR COORDINATE

The differential form for the conic angular coordinate ϵ is

$$R\,d\epsilon = \sin\kappa\,ds$$

or

$$d\epsilon = \frac{\sin\kappa}{R}\,ds$$

$$= \frac{\sin\left[\kappa_0 + C(s - s_0)\right]ds}{R_0 + \frac{1}{C}\sin\left[\kappa_0 + C(s - s_0)\right] - \frac{1}{C}\sin\kappa_0} \tag{9}$$

$$d\epsilon = \frac{\sin\left[\kappa_0 + C(s - s_0)\right]C\,ds}{R_0C - \sin\kappa_0 + \sin\left[\kappa_0 + C(s - s_0)\right]} \tag{10}$$

The integral of equation (10) is of the form

$$\int\frac{\sin x\,dx}{a + b\sin x} = \frac{x}{b} - \frac{a}{b}\int\frac{dx}{a + b\sin x} \tag{11}$$

When equation (11) is applied to equation (10), note that $b = +1$. Also, the variable x is $\kappa_0 + C(s - s_0)$ and the constant a is $R_0C - \sin\kappa_0$.

The second integral in equation (11), $\int dx/(a + b\sin x)$, takes different forms dependent on the relation of a to b. If $a^2 = b^2 = 1$,

$$\int\frac{dx}{1 \pm \sin x} = \mp\tan\left(\frac{\pi}{4} \mp \frac{x}{2}\right) \tag{B1}$$

If $a^2 > b^2$,

$$\int \frac{dx}{a + b \sin x} = \frac{2}{\sqrt{a^2 - b^2}} \tan^{-1} \frac{a \tan \frac{x}{2} + b}{\sqrt{a^2 - b^2}} \tag{B2}$$

If $b^2 > a^2$,

$$\int \frac{dx}{a + b \sin x} = \frac{1}{\sqrt{b^2 - a^2}} \ln \left| \frac{a \tan\left(\frac{x}{2}\right) + b - \sqrt{b^2 - a^2}}{a \tan\left(\frac{x}{2}\right) + b + \sqrt{b^2 - a^2}} \right| \tag{B3}$$

or alternately,

$$\int \frac{dx}{a + b \sin x} = \frac{-2}{\sqrt{b^2 - a^2}} \tanh^{-1} \left[\frac{a \tan\left(\frac{x}{2}\right) + b}{\sqrt{b^2 - a^2}} \right] \quad \text{for} \quad \left| a \tan\left(\frac{x}{2}\right) + b \right| < \sqrt{b^2 - a^2} \tag{B3a}$$

and

$$\int \frac{dx}{a + b \sin x} = \frac{-2}{\sqrt{b^2 - a^2}} \coth^{-1} \left[\frac{a \tan\left(\frac{x}{2}\right) + b}{\sqrt{b^2 - a^2}} \right] \quad \text{for} \quad \left| a \tan\left(\frac{x}{2}\right) + b \right| > \sqrt{b^2 - a^2} \tag{B3b}$$

The next step is substitution of the turbomachinery nomenclature into the general integral forms. First, consider the case of $a = b = +1$.

Case of $a = b = +1$ in General Integral $\displaystyle\int \frac{\sin x\,dx}{a + b \sin x}$

$$\epsilon - \epsilon_0 = \left[\kappa_0 + C(s - s_0)\right]\Big|_{s_0}^{s} + (R_0 C - \sin \kappa_0)\tan\left[\frac{\pi}{4} - \frac{\kappa_0 + C(s - s_0)}{2}\right]\Bigg|_{s_0}^{s}$$

$$= \kappa_0 + C(s - s_0) - \kappa_0 + (1)\left\{\tan\left[\frac{\pi}{4} - \frac{\kappa_0 + C(s - s_0)}{2}\right] - \tan\left(\frac{\pi}{4} - \frac{\kappa_0}{2}\right)\right\}$$

$$= \kappa - \kappa_0 + \left[\tan\left(\frac{\pi}{4} - \frac{\kappa}{2}\right) - \tan\left(\frac{\pi}{4} - \frac{\kappa_0}{2}\right)\right]$$

$$= \kappa - \kappa_0 + \left(\frac{\tan\frac{\pi}{4} - \tan\frac{\kappa}{2}}{1 + \tan\frac{\pi}{4}\tan\frac{\kappa}{2}} - \frac{\tan\frac{\pi}{4} - \tan\frac{\kappa_0}{2}}{1 + \tan\frac{\pi}{4}\tan\frac{\kappa_0}{2}}\right)$$

$$= \kappa - \kappa_0 + \left(\frac{1 - \tan\frac{\kappa}{2}}{1 + \tan\frac{\kappa}{2}} - \frac{1 - \tan\frac{\kappa_0}{2}}{1 + \tan\frac{\kappa_0}{2}}\right)$$

$$= \kappa - \kappa_0 - \frac{2\left(\tan\frac{\kappa}{2} - \tan\frac{\kappa_0}{2}\right)}{1 + \tan\frac{\kappa}{2} + \tan\frac{\kappa_0}{2} + \tan\frac{\kappa}{2}\tan\frac{\kappa_0}{2}} \qquad \text{(B4)}$$

Case of $a - b = -1$ in General Integral $\int \frac{\sin x \, dx}{a + b \sin x}$

$$\epsilon - \epsilon_0 = \kappa - \kappa_0 - \frac{(-1)}{(1)} \int \frac{dx}{(-1) + (1)\sin x} = \kappa - \kappa_0 - \int \frac{dx}{1 - \sin x}$$

$$= \kappa - \kappa_0 - \tan\left(\frac{\pi}{4} + \frac{x}{2}\right)\Bigg|_{x_0}^{x} = \kappa - \kappa_0 - \tan\left[\frac{\pi}{4} + \frac{\kappa_0 + C(s - s_0)}{2}\right]_{s_0}^{s}$$

$$= \kappa - \kappa_0 - \left[\tan\left(\frac{\pi}{4} + \frac{\kappa}{2}\right) - \tan\left(\frac{\pi}{4} + \frac{\kappa_0}{2}\right)\right]$$

$$= \kappa - \kappa_0 - \left(\frac{\tan\frac{\pi}{4} + \tan\frac{\kappa}{2}}{1 - \tan\frac{\pi}{4}\tan\frac{\kappa}{2}} - \frac{\tan\frac{\pi}{4} + \tan\frac{\kappa_0}{2}}{1 - \tan\frac{\pi}{4}\tan\frac{\kappa_0}{2}}\right)$$

$$= \kappa - \kappa_0 - \left(\frac{1 + \tan\frac{\kappa}{2}}{1 - \tan\frac{\kappa}{2}} - \frac{1 + \tan\frac{\kappa_0}{2}}{1 - \tan\frac{\kappa_0}{2}}\right)$$

$$= \kappa - \kappa_0 - \frac{2\left(\tan\frac{\kappa}{2} - \tan\frac{\kappa_0}{2}\right)}{1 - \tan\frac{\kappa}{2} - \tan\frac{\kappa_0}{2} + \tan\frac{\kappa}{2}\tan\frac{\kappa_0}{2}} \qquad \text{(B5)}$$

Case of $a^2 > b^2$ in the General Integral $\int \frac{\sin x \, dx}{a + b \sin x}$

For the case $a^2 > b^2$ apply equation (B2), to give

$$s - s_0 = \kappa - \kappa_0 = \frac{2(R_0C - \sin\kappa_0)}{\sqrt{(R_0C - \sin\kappa_0)^2 - 1}}\left[\tan^{-1}\frac{(R_0C - \sin\kappa_0)\tan\frac{\kappa_0 + C(s - s_0)}{2} + 1}{\sqrt{(R_0C - \sin\kappa_0)^2 - 1}}\right]_{s_0}^{s}$$

$$= \kappa - \kappa_0 - \frac{2(R_0C - \sin\kappa_0)}{\sqrt{(R_0C - \sin\kappa_0)^2 - 1}}\left[\tan^{-1}\frac{(R_0C - \sin\kappa_0)\tan\frac{\kappa}{2} + 1}{\sqrt{(R_0C - \sin\kappa_0)^2 - 1}} - \tan^{-1}\frac{(R_0C - \sin\kappa_0)\tan\frac{\kappa_0}{2} + 1}{\sqrt{(R_0C - \sin\kappa_0)^2 - 1}}\right]$$

$$= \kappa - \kappa_0 - \frac{2(R_0C - \sin\kappa_0)}{\sqrt{(R_0C - \sin\kappa_0)^2 - 1}}\tan^{-1}\left\{\tan\left[\tan^{-1}\frac{(R_0C - \sin\kappa_0)\tan\frac{\kappa}{2} + 1}{\sqrt{(R_0C - \sin\kappa_0)^2 - 1}} - \tan^{-1}\frac{(R_0C - \sin\kappa_0)\tan\frac{\kappa_0}{2} + 1}{\sqrt{(R_0C - \sin\kappa_0)^2 - 1}}\right]\right\}$$

$$= \kappa - \kappa_0 - \frac{2(R_0C - \sin\kappa_0)}{\sqrt{(R_0C - \sin\kappa_0)^2 - 1}}\tan^{-1}\left\{\frac{\tan\left[\tan^{-1}\frac{(R_0C - \sin\kappa_0)\tan\frac{\kappa}{2} + 1}{\sqrt{(R_0C - \sin\kappa_0)^2 - 1}}\right] - \tan\left[\tan^{-1}\frac{(R_0C - \sin\kappa_0)\tan\frac{\kappa_0}{2} + 1}{\sqrt{(R_0C - \sin\kappa_0)^2 - 1}}\right]}{1 + \tan\left[\tan^{-1}\frac{(R_0C - \sin\kappa_0)\tan\frac{\kappa}{2} + 1}{\sqrt{(R_0C - \sin\kappa_0)^2 - 1}}\right]\tan\left[\tan^{-1}\frac{(R_0C - \sin\kappa_0)\tan\frac{\kappa_0}{2} + 1}{\sqrt{(R_0C - \sin\kappa_0)^2 - 1}}\right]}\right\}$$

$$= \kappa - \kappa_0 - \frac{2(R_0C - \sin\kappa_0)}{\sqrt{(R_0C - \sin\kappa_0)^2 - 1}}\tan^{-1}\left\{\frac{\frac{(R_0C - \sin\kappa_0)\tan\frac{\kappa}{2} + 1}{\sqrt{(R_0C - \sin\kappa_0)^2 - 1}} - \frac{(R_0C - \sin\kappa_0)\tan\frac{\kappa_0}{2} + 1}{\sqrt{(R_0C - \sin\kappa_0)^2 - 1}}}{1 + \left[\frac{(R_0C - \sin\kappa_0)\tan\frac{\kappa}{2} + 1}{\sqrt{(R_0C - \sin\kappa_0)^2 - 1}}\right]\left[\frac{(R_0C - \sin\kappa_0)\tan\frac{\kappa_0}{2} + 1}{\sqrt{(R_0C - \sin\kappa_0)^2 - 1}}\right]}\right\}$$

$$= \kappa - \kappa_0 - \frac{2(R_0C - \sin\kappa_0)}{\sqrt{(R_0C - \sin\kappa_0)^2 - 1}}\tan^{-1}\left\{\frac{(R_0C - \sin\kappa_0)\sqrt{(R_0C - \sin\kappa_0)^2 - 1}\left(\tan\frac{\kappa}{2} - \tan\frac{\kappa_0}{2}\right)}{(R_0C - \sin\kappa_0)^2 - 1 + \left[(R_0C - \sin\kappa_0)\tan\frac{\kappa}{2} + 1\right]\left[(R_0C - \sin\kappa_0)\tan\frac{\kappa_0}{2} + 1\right]}\right\}$$

$$= \kappa - \kappa_0 - \frac{2(R_0C - \sin\kappa_0)}{\sqrt{(R_0C - \sin\kappa_0)^2 - 1}}\tan^{-1}(\mathcal{Y}) \tag{B6}$$

where $\mathcal{Y}$ is defined as

$$\mathcal{X}' = \frac{\sqrt{(R_0C - \sin\kappa_0)^2 - 1}\left(\tan\frac{\kappa}{2} - \tan\frac{\kappa_0}{2}\right)}{(R_0C - \sin\kappa_0)\left(1 + \tan\frac{\kappa}{2}\tan\frac{\kappa_0}{2}\right) + \tan\frac{\kappa}{2} + \tan\frac{\kappa_0}{2}} \tag{B7}$$

Case of $b^2 > a^2$ and $\left|a\tan\left(\frac{x}{2}\right) + b\right| < \sqrt{b^2 - a^2}$

For $b^2 > a^2$, there is a choice of either equation (B3) or the alternate forms given by equations (B3a) and (B3b). The alternate forms were chosen because the results are equations similar to equations (B6) and (B7). This similarity will be used to further advantage later in the development. Equation (B3a), which is applicable for $b^2 > a^2$ and $\left|a\tan\left(\frac{x}{2}\right) + b\right| < \sqrt{b^2 - a^2}$, gives

$$\epsilon - \epsilon_0 = \kappa - \kappa_0 + \frac{2(R_0C - \sin\kappa_0)}{\sqrt{1 - (R_0C - \sin\kappa_0)^2}}\left\{\tanh^{-1}\frac{(R_0C - \sin\kappa_0)\tan\left[\frac{\kappa_0 + C(s - s_0)}{2}\right] + 1}{\sqrt{1 - (R_0C - \sin\kappa_0)^2}}\right\}_{s_0}^{s}$$

$$= \kappa - \kappa_0 + \frac{2(R_0C - \sin\kappa_0)}{\sqrt{1 - (R_0C - \sin\kappa_0)^2}}\left[\tanh^{-1}\frac{(R_0C - \sin\kappa_0)\tan\frac{\kappa}{2} + 1}{\sqrt{1 - (R_0C - \sin\kappa_0)^2}} - \tanh^{-1}\frac{(R_0C - \sin\kappa_0)\tan\frac{\kappa_0}{2} + 1}{\sqrt{1 - (R_0C - \sin\kappa_0)^2}}\right]$$

$$= \kappa - \kappa_0 + \frac{2(R_0C - \sin\kappa_0)}{\sqrt{1 - (R_0C - \sin\kappa_0)^2}}\tanh^{-1}\left\{\tanh\left[\tanh^{-1}\frac{(R_0C - \sin\kappa_0)\tan\frac{\kappa}{2} + 1}{\sqrt{1 - (R_0C - \sin\kappa_0)^2}} - \tanh^{-1}\frac{(R_0C - \sin\kappa_0)\tan\frac{\kappa_0}{2} + 1}{\sqrt{1 - (R_0C - \sin\kappa_0)^2}}\right]\right\}$$

$$= \kappa - \kappa_0 + \frac{2(R_0C - \sin\kappa_0)}{\sqrt{1 - (R_0C - \sin\kappa_0)^2}}\tanh^{-1}\left\{\frac{\tanh\left[\tanh^{-1}\frac{(R_0C - \sin\kappa_0)\tan\frac{\kappa}{2} + 1}{\sqrt{1 - (R_0C - \sin\kappa_0)^2}}\right] - \tanh\left[\tanh^{-1}\frac{(R_0C - \sin\kappa_0)\tan\frac{\kappa_0}{2} + 1}{\sqrt{1 - (R_0C - \sin\kappa_0)^2}}\right]}{1 - \tanh\left[\tanh^{-1}\frac{(R_0C - \sin\kappa_0)\tan\frac{\kappa}{2} + 1}{\sqrt{1 - (R_0C - \sin\kappa_0)^2}}\right]\tanh\left[\tanh^{-1}\frac{(R_0C - \sin\kappa_0)\tan\frac{\kappa_0}{2} + 1}{\sqrt{1 - (R_0C - \sin\kappa_0)^2}}\right]}\right\}$$

$$= \kappa - \kappa_0 + \frac{2(R_0C - \sin\kappa_0)}{\sqrt{1 - (R_0C - \sin\kappa_0)^2}}\tanh^{-1}\left[\frac{\sqrt{1 - (R_0C - \sin\kappa_0)^2}(R_0C - \sin\kappa_0)\left(\tan\frac{\kappa}{2} - \tan\frac{\kappa_0}{2}\right)}{1 - (R_0C - \sin\kappa_0)^2 - (R_0C - \sin\kappa_0)^2\tan\frac{\kappa}{2}\tan\frac{\kappa_0}{2} - (R_0C - \sin\kappa_0)\left(\tan\frac{\kappa}{2} + \tan\frac{\kappa_0}{2}\right) - 1}\right]$$

$$= \kappa - \kappa_0 - \frac{2(R_0C - \sin\kappa_0)}{\sqrt{1 - (R_0C - \sin\kappa_0)^2}}\tanh^{-1} X$$

where X is defined as

$$X = \frac{\sqrt{1 - (R_0C - \sin\kappa_0)^2}\left(\tan\frac{\kappa}{2} - \tan\frac{\kappa_0}{2}\right)}{(R_0C - \sin\kappa_0)\left(1 + \tan\frac{\kappa}{2}\tan\frac{\kappa_0}{2}\right) + \tan\frac{\kappa}{2}\tan\frac{\kappa_0}{2}} \tag{B9}$$

Investigation of $\tanh^{-1} X = \pm\infty$

Equation (B8) does not appear practical because $\tanh^{-1} X$ approaches $+\infty$ and $-\infty$ at $X = 1$ and $X = -1$, respectively. To investigate the conditions which lead to this result, solve for $\kappa/2$ at $X = \pm 1$.

$$X = \frac{\sqrt{1 - (R_0C - \sin\kappa_0)^2}\left(\tan\frac{\kappa}{2} - \tan\frac{\kappa_0}{2}\right)}{(R_0C - \sin\kappa_0)\left(1 + \tan\frac{\kappa}{2}\tan\frac{\kappa_0}{2}\right) + \tan\frac{\kappa}{2} + \tan\frac{\kappa_0}{2}} = \pm 1$$

$$\therefore \quad \pm\sqrt{1 - (R_0C - \sin\kappa_0)^2}\left(\tan\frac{\kappa}{2} - \tan\frac{\kappa_0}{2}\right) = (R_0C - \sin\kappa_0)\left(1 + \tan\frac{\kappa}{2}\tan\frac{\kappa_0}{2}\right) + \tan\frac{\kappa}{2} + \tan\frac{\kappa_0}{2}$$

Square both sides and solve for $\tan(\kappa/2)$. The result is

$$\tan\frac{\kappa}{2} = \frac{-1 \pm \sqrt{1 - (R_0C - \sin\kappa_0)^2}}{R_0C - \sin\kappa_0} \tag{B10}$$

By using equation (B10) in (B9) it can be shown that the plus sign in equation (B10) is the solution for $X = -1$ and that the minus sign in equation (B10) is the solution for $X = 1$.

Table I lists $\kappa/2$ values which make $\tanh^{-1} X$ equal to $\pm\infty$ over the hyperbolic function range $-1 < (R_0C - \sin\kappa_0) < 1$. The κ values associated with $X = -1$ are clearly in the turbomachinery range of interest. So there is a need to investigate what causes $\tanh^{-1} X$ to approach $-\infty$. Start with the equation for conic radius

$$R - R_0 = \frac{1}{C}(\sin\kappa - \sin\kappa_0) \tag{4}$$

$$RC = (R_0C - \sin\kappa_0) + \sin\kappa = (R_0C - \sin\kappa_0) + 2\sin\frac{\kappa}{2}\cos\frac{\kappa}{2}$$

$$= (R_0C - \sin\kappa_0) + 2\frac{\sin\frac{\kappa}{2}}{\cos\frac{\kappa}{2}}\cos^2\frac{\kappa}{2} = (R_0C - \sin\kappa_0) + 2\frac{\tan\frac{\kappa}{2}}{1 + \tan^2\frac{\kappa}{2}}$$

Substitute equation (B10) with the plus sign. The result is $RC = 0$. So, either $C = 0$ or $R = 0$.

First consider $C = 0$. Since $d\kappa/ds = C$, $\kappa = \kappa_0$ for all s when $C = 0$. Thus, equation (8) for the conic radius reduces to

$$R = R_0 + (s - s_0)\cos\kappa_0$$

When κ is constant, the equation for ϵ (eq. (9)) can be expressed as

$$d\epsilon = \frac{\sin\kappa_0\, ds}{R} = \frac{\sin\kappa_0\, ds}{R_0 + \cos\kappa_0(s - s_0)} \qquad \text{(B11)}$$

$$\epsilon - \epsilon_0 = \frac{\sin\kappa_0}{\cos\kappa_0}\ln\left[R_0 + \cos\kappa_0(s - s_0)\right]\Big|_{s_0}^{s}$$

$$= \tan\kappa_0(\ln R - \ln R_0) = \tan\kappa_0 \ln\left(\frac{R}{R_0}\right) \qquad \text{(B12)}$$

All κ_0 of interest lie inside the range $-\pi/2$ to $\pi/2$. So $\epsilon - \epsilon_0$ approaches $-\infty$ only as R approaches zero. Therefore, the conclusion is that $R = 0$ is the condition which makes $\tanh^{-1} X$ approach $-\infty$, whether or not $C = 0$. This, in essence, means the curve spirals infinite revolutions as R approaches zero for $\pi/2 < |\kappa_0| < 0$.

Fortunately, R never approaches zero in the turbomachinery application, so $\tanh^{-1} X$ remains finite. Thus, the $\tanh^{-1} X$ form of solution could be satisfactory, but it remains to be shown if and when the $\tanh^{-1} X$ form is usable. Basically, it is applicable only when $|X| < 1$ because the $\coth^{-1} X$ form of equation (B3b) is used when $|X| > 1$. Thus, the next consideration is an investigation of the possible range of X for the turbomachinery application.

Investigation of Range of X

Let us begin with equation (4), which in general can be expressed as

$$\text{Constant} = R_0C - \sin\kappa_0 = RC - \sin\kappa$$

As a convenience, define κ_c as the κ value in the range $-\pi/2$ to $\pi/2$ for $R = 0$. So the preceding equation can be extended to

$$\text{Constant} = R_0C - \sin\kappa_0 = RC - \sin\kappa = -\sin\kappa_c \tag{B13}$$

The defined value of κ_c and the other κ_c values which satisfy equation (B13) are the κ values which make $X = \pm 1$. (This can be shown by substituting $-\sin\kappa_c$ for $R_0C - \sin\kappa_0$ in equation (B10) and applying the tangent half-angle formula.) Thus, X can cross between the $|X| > 1$ and $|X| < 1$ regimes only when κ equals the κ_c values. Since X is a single-valued function of κ, all X values between consecutive κ_c values must be in the same $|X|$ regime. This characteristic is shown graphically in figure 10, which has plots of X against κ for the two sample κ_c values of 45° and -20°. On each example plot, curves for a spectrum of κ_0 values are shown to illustrate the nature of the function.

The κ range of interest for turbomachinery is from $-\pi/2$ to $\pi/2$. The defined κ_c is the only κ_c value in this range because $\sin\kappa_c$ is single valued between $-\pi/2$ and $\pi/2$. Thus, observations of whether regimes of $|X|$ are greater or less than 1 can be made with respect to this particular κ_c. A first observation from figure 10 is that the κ curves switch between the $|X| > 1$ and $|X| < 1$ regimes as κ_0 crosses κ_c. A study of the $X = 0$ points is an indirect way of showing that the X-against-κ curves switch regimes precisely at $\kappa_0 = \kappa_c$. From equation (B9), note that $X = 0$ when $\kappa = \kappa_0$. Thus, as κ_0 is moved closer and across κ_c, the $X = 0$ point moves with κ_0 and hence with κ. Since $X = 0$ is in the $|X| < 1$ regime and stays in that regime as κ_0 crosses κ_c, the direction of the $|X|$ regime crossover at κ_c has to switch when κ_0 crosses κ_c. Since no other κ_c can lie in the range $-\pi/2$ to $\pi/2$, only the one switch of regime can occur in the $-\pi/2$ to $\pi/2$ range of κ. So κ stays in the $|X| < 1$ regime when on the κ_0 side of κ_c. The preceding reasoning leads to the general conclusion that X is always in the $|X| < 1$ regime when κ and κ_0 are on the same side of κ_c within the $-\pi/2$ to $\pi/2$ range of κ.

So far it has been shown that the regime of $|X|$ is tied to the relation of κ and κ_0 to κ_c. To further investigate these κ relations in the turbomachinery application, rewrite equation (B13) to show κ and κ_0 as functions of κ_c, C, and R.

$$\sin\kappa = \sin\kappa_c + CR$$

$$\sin\kappa_0 = \sin\kappa_c + CR_0 \tag{B15}$$

By definition C is a constant for a curve, so the remaining information needed is the limits of the variation of R with respect to R_0. When the cone angle α of figure 1 is positive, R_0 is positive; but when α is negative, R_0 is defined as negative. However, whether the blade-element cone is defined by a positive or negative α, a blade element for turbomachinery is always completely defined on the cone without ever approaching $R = 0$. Thus, R always has the same sign as R_0. This means that, by equations (B14) and (B15), κ and κ_0 are always on the same side of κ_c. So $|X|$ is always less than 1 in the range $-\pi/2$ to $\pi/2$ for κ_0 and κ.

The conditions imposed along the way to the preceding conclusion can be summarized as follows: For $|R_0C - \sin\kappa_0| < 1$, the X defined by equation (B9) has an absolute value less than 1 when κ and κ_0 are in the range $-\pi/2$ to $\pi/2$ and R has the same sign as R_0. Since the turbomachinery application falls within these κ and R restrictions, the conclusion is rather significant because it is not necessary to consider the $\coth^{-1} X$ form of equation (B3b) at all. This means that the natural logarithm form of equation (B3) can be replaced with only the alternate form (B3a), which was developed to equations (B8) and (B9). The alternate form is selected because of the similarity of the arguments with those of equations (B6) and (B7). Later it will be shown that this similarity leads to further simplification.

Consideration of Accuracy of Computation

Equations (B4) to (B9) are a complete set of equations for $\epsilon - \epsilon_0$, which also is expressed as $\Delta\epsilon$ in the text. For a blade-element path Δs, $\Delta\epsilon$ is the conic angular coordinate in the circumferential direction; and $R\,\Delta\epsilon$ is the circumferential component distance in the units of s. As long as the conic half-angle α is several degrees from zero, R and $\Delta\epsilon$ can readily be calculated and used to accurately define a blade element. However, as α approaches zero, R approaches $\pm\infty$ and $\Delta\epsilon$ approaches zero. This means that conic coordinates cannot be directly used for the degenerate case of a cone to a cylinder or radius r. As α approaches zero the conic coordinate R approaches independence from Δs and κ (see fig. 1 and eq. (8)). So $R\,\Delta\epsilon$ approaches the circumferential component of Δs. Since R can be considered as a constant for the degenerate case of a cone to a cylinder, a simple equation for the circumferential component can, and later will be, derived from equation (9).

In the preceding discussion it was shown that, at some point in the α approach to zero, it is necessary to switch from the conic coordinate system to the cylindrical. The condition for a switch most logically comes from an accuracy criterion. From equation (8) it can be observed that the relative error by which R is not constant is approximately $\Delta s/R$. In general, this means that to keep an accuracy of more than a few significant figures in a computed circumferential component of Δs, the switch to the cylindrical coordinates must be made at α's very near zero. Thus, the mathematically accurate conic coordinate system is needed to nearly zero α's. The problem is that sufficient computational accuracy with conic coordinate systems is not always attained with normal procedures. The nature of the problem and its remedy are the subject of the following discussion.

Each of the equations for the computation of $\Delta\epsilon$ in the conic coordinate system is expressed as $\kappa - \kappa_0$ plus another term. As α approaches zero, $\Delta\epsilon$ also approaches zero; so in general, $|\Delta\epsilon|$ becomes much less than $|\Delta\kappa|$. When $|\Delta\epsilon| << |\Delta\kappa|$, the computational accuracy of $\Delta\epsilon$ becomes poor because $\Delta\epsilon$ is determined by the subtraction of a term nearly equal to $\Delta\kappa$ from $\Delta\kappa$. One way to improve accuracy is to reduce or eliminate the subtraction of nearly equal terms in the computation of a $\Delta\epsilon$ value. For the turbomachinery application, the computational accuracy of $\Delta\epsilon$ can be improved considerably with the application of infinite series forms for the functions of equations (B4), (B5), (B6), and (B8).

Series Forms for $\Delta\epsilon$ Equations

The series for $\tan^{-1} \mathscr{Y}'$ is

$$\tan^{-1} \mathscr{Y}' = \mathscr{Y}' - \frac{1}{3}\mathscr{Y}'^3 + \frac{1}{5}\mathscr{Y}'^5 - \frac{1}{7}\mathscr{Y}'^7 + \dots$$

$$= \mathscr{Y}'\left[1 - \frac{1}{3}\mathscr{Y}'^2 + \frac{1}{5}\mathscr{Y}'^4 - \frac{1}{7}\mathscr{Y}'^6 + \dots\right] \qquad \text{for } \mathscr{Y}'^2 < 1 \qquad \text{(B16)}$$

where $\mathscr{Y}'$ is defined by equation (B7) for application of equation (B16) to equation (B6). The absolute value of $\mathscr{Y}'$ can be greater than 1, but a rather easy way to handle that will be shown later. For equation (B6),

$$\epsilon - \epsilon_0 = \kappa - \kappa_0 - \frac{2(R_0C - \sin\kappa_0)}{\sqrt{(R_0C - \sin\kappa_0)^2 - 1}} \tan^{-1}\mathcal{Y}$$

$$= \kappa - \kappa_0 - \frac{2(R_0C - \sin\kappa_0)}{\sqrt{(R_0C - \sin\kappa_0)^2 - 1}}\,\mathcal{Y}\left(1 - \frac{\mathcal{Y}^2}{3} + \frac{\mathcal{Y}^4}{5} - \frac{\mathcal{Y}^6}{7} + \cdots\right)$$

$$= \kappa - \kappa_0 - \frac{2(R_0C - \sin\kappa_0)\sqrt{(R_0C - \sin\kappa_0)^2 - 1}\left(\tan\frac{\kappa}{2} - \tan\frac{\kappa_0}{2}\right)}{\sqrt{(R_0C - \sin\kappa_0)^2 - 1}\left[(R_0C - \sin\kappa_0)\left(1 + \tan\frac{\kappa}{2}\tan\frac{\kappa_0}{2}\right) + \tan\frac{\kappa}{2} + \tan\frac{\kappa_0}{2}\right]}\left(1 - \frac{\mathcal{Y}^2}{3} + \frac{\mathcal{Y}^4}{5} - \frac{\mathcal{Y}^6}{7} + \cdots\right)$$

$$= \kappa - \kappa_0 - \frac{2(R_0C - \sin\kappa_0)\left(\tan\frac{\kappa}{2} - \tan\frac{\kappa_0}{2}\right)}{(R_0C - \sin\kappa_0)\left(1 + \tan\frac{\kappa}{2}\tan\frac{\kappa_0}{2}\right) + \tan\frac{\kappa}{2} + \tan\frac{\kappa_0}{2}}\left(1 - \frac{\mathcal{Y}^2}{3} + \frac{\mathcal{Y}^4}{7} - \frac{\mathcal{Y}^6}{8} + \cdots\right) \qquad \text{(B17)}$$

At this point note that for $R_0C - \sin\kappa_0 = 1$, which is the special case covered by equation (B4), $\mathcal{Y} = 0$ and equation (B17) reduces to equation (B4). Likewise for $R_0C - \sin\kappa_0 = -1$, which is the special case covered by equation (B5), equation (B17) reduces to equation (B5). Thus, equation (B17) can be used in place of equations (B4) to (B6).

The remaining equation of the set for $\Delta\epsilon$ is (B8). The series form for $\tanh^{-1}X$ in it is

$$\tanh^{-1}X = X + \frac{X^3}{3} + \frac{X^5}{5} + \frac{X^7}{7} \cdots = X\left[1 + \frac{X^2}{3} + \frac{X^4}{5} + \frac{X^6}{7} + \cdots\right] \qquad \text{for } X^2 < 1 \qquad \text{(B18)}$$

where X is defined by equation (B9).

We have already shown that the absolute value of X is always less than 1 for the turbomachinery application, so this series is always applicable. For equation (B8)

$$\epsilon - \epsilon_0 = \kappa - \kappa_0 - \frac{2(R_0C - \sin\kappa_0)}{\sqrt{1 - (R_0C - \sin\kappa_0)^2}} \tanh^{-1} X = \kappa - \kappa_0 - \frac{2(R_0C - \sin\kappa_0)}{\sqrt{1 - (R_0C - \sin\kappa_0)^2}} X \left(1 + \frac{X^2}{3} + \frac{X^4}{5} + \frac{X^6}{7} + \cdots\right)$$

$$= \kappa - \kappa_0 - \frac{2(R_0C - \sin\kappa_0)\sqrt{1 - (R_0C - \sin\kappa_0)^2}\left(\tan\frac{\kappa}{2} - \tan\frac{\kappa_0}{2}\right)}{\sqrt{1 - (R_0C - \sin\kappa_0)^2}\left[(R_0C - \sin\kappa_0)\left(1 + \tan\frac{\kappa}{2}\tan\frac{\kappa_0}{2}\right) + \tan\frac{\kappa}{2} + \tan\frac{\kappa_0}{2}\right]}\left(1 + \frac{X^2}{3} + \frac{X^4}{5} + \frac{X^6}{7} + \cdots\right)$$

$$= \kappa - \kappa_0 - \frac{2(R_0C - \sin\kappa_0)\left(\tan\frac{\kappa}{2} - \tan\frac{\kappa_0}{2}\right)}{(R_0C - \sin\kappa_0)\left(1 + \tan\frac{\kappa}{2}\tan\frac{\kappa_0}{2}\right) + \tan\frac{\kappa}{2} + \tan\frac{\kappa_0}{2}}\left(1 + \frac{X^2}{3} + \frac{X^4}{5} + \frac{X^6}{7} \cdots\right) \qquad \text{(B19)}$$

Single-Series Form of Equation

Equations (B17) and (B19) look similar, and upon examination it can be determined that they are in fact the same. Note that the $\mathcal{Y}^2$ of equation (B7) is the negative of the X^2 of equation (B9). This difference of sign accounts for the sign differences of the series. Thus, equation (B19) can be used for all values of $R_0C - \sin\kappa_0$, so long as $X^2 < 1$. For $|R_0C - \sin\kappa_0| < 1$, which produced the $\tanh^{-1} X$ form of equation, it has been shown that $X^2 < 1$; but for $|R_0C - \sin\kappa_0| > 1$, which produced the $\tan^{-1}\mathcal{Y}$ form of equation, $\mathcal{Y}^2$ can be greater than 1. When $\mathcal{Y}^2$ is greater than 1, either an alternate series for $\tan^{-1}\mathcal{Y}$ needs to be used for convergence or a $\cot^{-1}\mathcal{Y}$ function can be used. However, with the use of half angles, it is possible to keep the argument in the convergent range so that only the one form of equation is retained.

Application of Half-Angle Formulas

An inverse function can be expressed in terms of a half-angle as follows:

$$\tan^{-1}\mathcal{Y} = \xi = 2\left(\frac{\xi}{2}\right)$$

The $\xi/2$ can be expressed in terms of $\mathcal{Y}$ as follows

$$\tan\frac{\xi}{2} = \frac{\sin\xi}{1+\cos\xi} = \frac{\dfrac{\sin\xi}{\cos\xi}}{\dfrac{1+\cos\xi}{\cos\xi}}$$

$$= \frac{\tan\xi}{1+\sec\xi} = \frac{\tan\xi}{1+\sqrt{1+\tan^2\xi}}$$

For $|\xi| < \pi/2$,

$$\tan\frac{\xi}{2} = \frac{y'}{1+\sqrt{1+y'^2}}$$

$$\frac{\xi}{2} = \tan^{-1}\tan\left(\frac{\xi}{2}\right) = \tan^{-1}\frac{y'}{1+\sqrt{1+y'^2}}$$

$$\therefore \qquad \tan^{-1} y' = 2\tan^{-1}\frac{y'}{1+\sqrt{1+y'^2}} = 2\tan^{-1} X_2 \tag{B20}$$

where by definition

$$X_2 = \frac{y'}{1+\sqrt{1+y'^2}} \tag{B21}$$

The maximum value of $|\xi|$ is $\pi/2$ for turbomachinery so the maximum value of $|\xi/2|$ is $\pi/4$. Therefore,

$$\left|\frac{y'}{1+\sqrt{1+y'^2}}\right| \leq 1$$

So the half-angle procedure reduces the argument of the series enough to make the $\tan^{-1} y'$ series always converge; thus, the series in equation (B19) always converges.

Before applying the half-angle procedure to the general equation, let us check the procedure with the hyperbolic functions to see if the procedure is completely general.

$$\tanh^{-1} X = \xi = 2\left(\frac{\xi}{2}\right) = 2 \tanh^{-1}\left(\tanh \frac{\xi}{2}\right)$$

$$= 2 \tanh^{-1} \frac{\sinh \xi}{\cosh \xi + 1} = 2 \tanh^{-1} \frac{\frac{\sinh \xi}{\cosh \xi}}{\frac{\cosh \xi + 1}{\cosh \xi}}$$

$$= 2 \tanh^{-1} \frac{\tanh \xi}{1 + \operatorname{sech} \xi} = 2 \tanh^{-1} \frac{\tanh \xi}{1 + \sqrt{1 - \tanh^2 \xi}}$$

For $|\xi| < \pi/2$,

$$\tanh^{-1} X = 2 \tanh^{-1} \frac{X}{1 + \sqrt{1 - X^2}} = 2 \tanh^{-1} X_2 \tag{B22}$$

where by definition

$$X_2 = \frac{X}{1 + \sqrt{1 - X^2}} \tag{B23}$$

Equations (B20) and (B22) are the same in application to the general equation when the X's are defined the same. Remember the X^2 in equations (B20) and (B21) is the negative of the X^2 in equations (B22) and (B23). Thus, the half-angle formulation in general can be substituted into the general equation (B19).

$$\epsilon - \epsilon_0 = \kappa - \kappa_0 - \frac{4(R_0C - \sin \kappa_0)\left(\tan \frac{\kappa}{2} - \tan \frac{\kappa_0}{2}\right)}{\left(1 + \sqrt{1 - X^2}\right)\left[(R_0C - \sin \kappa_0)\left(1 + \tan \frac{\kappa}{2} \tan \frac{\kappa_0}{2}\right) + \tan \frac{\kappa}{2} + \tan \frac{\kappa_0}{2}\right]}$$

$$\times \left(1 + \frac{X_2^2}{3} + \frac{X_2^4}{5} + \frac{X_2^6}{7} + \ldots\right) \tag{B24}$$

where X^2 is defined by equation (B9) and X_2^2 by equation (B23). The term $1 + \sqrt{1 - X^2}$ in turbomachinery nomenclature is

$$1 + \sqrt{1 - X^2} = 1 + \sqrt{1 - \left[1 - (R_0C - \sin\kappa_0)^2\right]\left[\frac{\tan\frac{\kappa}{2} - \tan\frac{\kappa_0}{2}}{(R_0C - \sin\kappa_0)\left(1 + \tan\frac{\kappa}{2}\tan\frac{\kappa_0}{2}\right) + \tan\frac{\kappa}{2} + \tan\frac{\kappa_0}{2}}\right]^2}$$

With some trigometric manipulation, the preceding equation becomes

$$1 + \sqrt{1 - X^2} = 1 + \frac{\sqrt{\left[R_0C + \frac{1}{2}(\sin\kappa - \sin\kappa_0)\right]^2 - \left[\frac{1}{2}(\sin\kappa_0 - \sin\kappa)\right]^2}}{\left[(R_0C - \sin\kappa_0)\left(1 + \tan\frac{\kappa}{2}\tan\frac{\kappa_0}{2}\right) + \tan\frac{\kappa}{2} + \tan\frac{\kappa_0}{2}\right]\cos\frac{\kappa}{2}\cos\frac{\kappa_0}{2}}$$

With the substitution of equation (4), the preceding equation becomes

$$1 + \sqrt{1 - X^2} = \frac{\left[(R_0C - \sin\kappa_0)\left(1 + \tan\frac{\kappa}{2}\tan\frac{\kappa_0}{2}\right) + \tan\frac{\kappa}{2} + \tan\frac{\kappa_0}{2}\right]\cos\frac{\kappa}{2}\cos\frac{\kappa_0}{2} + CR_0\sqrt{\frac{R}{R_0}}}{\left[(R_0C - \sin\kappa_0)\left(1 + \tan\frac{\kappa}{2}\tan\frac{\kappa_0}{2}\right) + \tan\frac{\kappa}{2} + \tan\frac{\kappa_0}{2}\right]\cos\frac{\kappa}{2}\cos\frac{\kappa_0}{2}} \tag{B25}$$

The term $CR_0\sqrt{R/R_0}$, as shown, yields the proper sign for the square root. The X for the half-angle form can be expressed as

$$X_2^2 = \left(\frac{X}{1 + \sqrt{1 - X^2}}\right)^2$$

$$= \frac{\left[\frac{\sqrt{1 - (R_0C - \sin\kappa_0)^2}\left(\tan\frac{\kappa}{2} - \tan\frac{\kappa_0}{2}\right)}{(R_0C - \sin\kappa_0)\left(1 + \tan\frac{\kappa}{2}\tan\frac{\kappa_0}{2}\right) + \tan\frac{\kappa}{2} + \tan\frac{\kappa_0}{2}}\right]^2}{\left\{\frac{\left[(R_0C - \sin\kappa_0)\left(1 + \tan\frac{\kappa}{2}\tan\frac{\kappa_0}{2}\right) + \tan\frac{\kappa}{2} + \tan\frac{\kappa_0}{2}\right]\cos\frac{\kappa}{2}\cos\frac{\kappa_0}{2} + CR_0\sqrt{\frac{R}{R_0}}}{\left[(R_0C - \sin\kappa_0)\left(1 + \tan\frac{\kappa}{2}\tan\frac{\kappa_0}{2}\right) + \tan\frac{\kappa}{2} + \tan\frac{\kappa_0}{2}\right]\cos\frac{\kappa}{2}\cos\frac{\kappa_0}{2}}\right\}^2}$$

$$= \frac{\left[1 - (R_0C - \sin\kappa_0)^2\right]\sin^2\frac{\kappa - \kappa_0}{2}}{\left[(R_0C - \sin\kappa_0)\cos\frac{\kappa - \kappa_0}{2} + \sin\frac{\kappa + \kappa_0}{2} + CR_0\sqrt{\frac{R}{R_0}}\right]^2} \tag{B26}$$

Now substitute equation (B25) into (B24) and reduce as follows:

[illegible]

[illegible]

[illegible]

[illegible] (B27)

After all the manipulation, the half-angle form of equation (B27) is no more complicated than equation (B19). It also has the advantage of the need of fewer series terms to converge to a desired precision in calculation. The half-angle procedure can be repeated to further reduce the number of series terms needed. However, a further reduction of the number of series terms complicates the coefficient term for the series to a much greater extent than the first application of half-angles. So it was not considered useful to carry it further. The number of series terms needed will be shown later when the operating form of the equation is finally established.

Use of a Sine Series to Effectively Cancel Large Terms

At this point, let us readdress ourselves to the problem of finding $\epsilon - \epsilon_0$ by the subtraction of two nearly equal numbers. The problem can, to a large extent, be eliminated by further series treatment and cancellation of the large terms. Begin by rewritting equation (B27) as

$$\epsilon - \epsilon_0 = \kappa - \kappa_0 - \frac{4(R_0C - \sin\kappa_0)\left(2\sin\frac{\kappa - \kappa_0}{4}\cos\frac{\kappa - \kappa_0}{4}\right)}{(R_0C - \sin\kappa_0)\cos\frac{\kappa - \kappa_0}{2} + \sin\frac{\kappa + \kappa_0}{2} + CR_0\sqrt{\frac{R}{R_0}}}$$

$$- \frac{4(R_0C - \sin\kappa_0)\sin\frac{\kappa - \kappa_0}{2}}{(R_0C - \sin\kappa_0)\cos\frac{\kappa - \kappa_0}{2} + \sin\frac{\kappa + \kappa_0}{2} + CR_0\sqrt{\frac{R}{R_0}}}\left(\frac{X_2^2}{3} + \frac{X_2^4}{5} + \frac{X_2^6}{7} + \ldots\right)$$

Application of equation (7) for the sine series gives

$$\epsilon - \epsilon_0 = \frac{(\kappa - \kappa_0)\left[(R_0C - \sin\kappa_0)\cos\frac{\kappa - \kappa_0}{2} + \sin\frac{\kappa + \kappa_0}{2} + CR_0\sqrt{\frac{R}{R_0}}\right] - 8(R_0C - \sin\kappa_0)\cos\frac{\kappa - \kappa_0}{4}\left\{\frac{\kappa - \kappa_0}{4}\left[1 - \frac{1}{3!}\left(\frac{\kappa - \kappa_0}{4}\right)^2 + \frac{1}{5!}\left(\frac{\kappa - \kappa_0}{4}\right)^4 - \ldots\right]\right\}}{D}$$

$$- \frac{4(R_0C - \sin\kappa_0)\sin\frac{\kappa - \kappa_0}{2}}{D}\left(\frac{X_2^2}{3} + \frac{X_2^4}{5} + \frac{X_2^6}{7} + \ldots\right)$$

where D is a temporary symbolic representation of the denominator.

$$\epsilon - \epsilon_0 = \frac{(\kappa - \kappa_0)\left\{(R_0C - \sin\kappa_0)\left(2\cos^2\frac{\kappa - \kappa_0}{4} - 1\right) + \sin\frac{\kappa + \kappa_0}{2} + CR_0\sqrt{\frac{R}{R_0}} - 2(R_0C - \sin\kappa_0)\cos\frac{\kappa - \kappa_0}{4}\left[1 - \frac{1}{3!}\left(\frac{\kappa - \kappa_0}{4}\right)^2 + \frac{1}{5!}\left(\frac{\kappa - \kappa_0}{4}\right)^4 - \ldots\right]\right\}}{D}$$

$$- \frac{4(R_0C - \sin\kappa_0)\sin\frac{\kappa - \kappa_0}{2}}{D}\left(\frac{X_2^2}{3} + \frac{X_2^4}{5} + \frac{X_2^6}{7} + \ldots\right)$$

$$\ldots \left\{ R_0 \ldots \right\} \ldots [illegible]$$

$$- \frac{4(R_0C - \sin\kappa_0)\sin\frac{\kappa - \kappa_0}{2}}{D}\left(\frac{x_2^2}{3} + \frac{x_2^4}{5} + \frac{x_2^6}{7} + \cdots\right)$$

$$= \frac{(\kappa - \kappa_0)\left\{\sin\kappa_0 + \sin\frac{\kappa + \kappa_0}{2} + CR_0\left(\sqrt{\frac{R}{R_0}} - 1\right) - 2(R_0C - \sin\kappa_0)\cos\frac{\kappa - \kappa_0}{4}\left[2\sin^2\frac{\kappa - \kappa_0}{8} - \frac{1}{3!}\left(\frac{\kappa - \kappa_0}{4}\right)^2 + \frac{1}{5!}\left(\frac{\kappa - \kappa_0}{4}\right)^4 - \frac{1}{7!}\left(\frac{\kappa - \kappa_0}{4}\right)^6 \cdots\right]\right\}}{(R_0C + \sin\kappa_0)\cos\frac{\kappa - \kappa_0}{2} + \sin\frac{\kappa + \kappa_0}{2} + CR_0\sqrt{\frac{R}{R_0}}}$$

$$- \frac{4(R_0C - \sin\kappa_0)\sin\frac{\kappa - \kappa_0}{2}}{(R_0C + \sin\kappa_0)\cos\frac{\kappa - \kappa_0}{2} + \sin\frac{\kappa + \kappa_0}{2} + CR_0\sqrt{\frac{R}{R_0}}}\left(\frac{x_2^2}{3} + \frac{x_2^4}{5} + \frac{x_2^6}{7} + \cdots\right) \tag{B28}$$

An example best illustrates the superiority of equation (B28) over (B27) for computational accuracy when R is relatively large. Let $R_0 = 1000$, $\Delta s = 2$, $\kappa_0 = 45^o$, and $\kappa = 35^o$. In equation (B27) the numbers combine as follows:

$$\epsilon - \epsilon_0 = (\kappa - \kappa_0) - \frac{4(R_0C - \sin\kappa_0)\sin\frac{\kappa - \kappa_0}{2}}{(R_0C + \sin\kappa_0)\cos\frac{\kappa - \kappa_0}{2} + \sin\frac{\kappa + \kappa_0}{2} + CR_0\sqrt{\frac{R}{R_0}}}\left(1 + \frac{x_2^2}{3} + \frac{x_2^4}{5} + \frac{x_2^6}{7} + \frac{x_2^8}{9}\right)$$

$$= -0.1745329252 - \frac{30.66960712}{-174.3292180}(0.9993560159)$$

$$= -0.1745329252 + 0.1758159460 = 0.00128302 \text{ radian}$$

Two orders of magnitude of precision are lost in the final operation, since the answer is obtained by subtraction of nearly equal numbers.

In equation (B28), the numbers combine better, as shown in the following:

$$\epsilon - \epsilon_0 = \frac{(\kappa - \kappa_0)(\sin \kappa_0) + \left(\sin \frac{[illegible]}{2}\right) \cdot [illegible]}{[illegible]} \quad [illegible]$$

$$\frac{\left[4 R_0 C [illegible] \frac{[illegible]}{2} \left(\frac{\chi^3}{3} + \frac{\chi^5}{5} + \frac{\chi^7}{7} + \frac{\chi^9}{9} \right) \right]}{(R_0 C - \sin \kappa_0 \cos \frac{[illegible]_0}{2} + \sin \frac{[illegible]_0}{2} + C R_0 \sqrt{\frac{R}{R_0}}}$$

$$= \frac{(-0.1745329252)[(0.7071067811) + (0.6427876096) + (-0.06673965183) + (-0.111531995)] + (-0.01975073743)}{-174.3292180}$$

$$= \frac{-0.2434187554 + 0.01975073743}{-174.3292180} = 0.00128302083$$

Series Representation of $\sqrt{\frac{R}{R_0}} - 1$

If the cone radius becomes larger than that given in the example, a point will be reached where computations by equation (B27) will not give a satisfactory engineering answer. While equation (B28) as shown is much better, it is not foolproof either. At large R the term $\sqrt{R/R_0} - 1$ is the subtraction of nearly equal numbers. A series representation can help this term too.

$$\sqrt{\frac{R}{R_0}} - 1 = \sqrt{\frac{R_0 + R - R_0}{R_0}} - 1 = \left(1 + \frac{R - R_0}{R_0}\right)^{1/2} - 1$$

Now using a binomial series expansion on the square-root term,

$$\sqrt{\frac{R}{R_0}} - 1 = \left[1 + \frac{1}{2}\left(\frac{R - R_0}{R_0}\right) + \frac{\frac{1}{2}\left(-\frac{1}{2}\right)}{2!}\left(\frac{R - R_0}{R_0}\right)^2 + \frac{\frac{1}{2}\left(-\frac{1}{2}\right)\left(-\frac{3}{2}\right)}{3!}\left(\frac{R - R_0}{R_0}\right)^3 + \frac{\frac{1}{2}\left(-\frac{1}{2}\right)\left(-\frac{3}{2}\right)\left(-\frac{5}{2}\right)}{4!}\left(\frac{R - R_0}{R}\right)^4 + \dots\right] - 1$$

$$= \left[\frac{1}{2}\left(\frac{R - R_0}{R_0}\right) + \frac{\frac{1}{2}\left(-\frac{1}{2}\right)}{2!}\left(\frac{R - R_0}{R_0}\right)^2 + \frac{\frac{1}{2}\left(-\frac{1}{2}\right)\left(-\frac{3}{2}\right)}{3!}\left(\frac{R - R_0}{R_0}\right)^3 + \frac{\frac{1}{2}\left(-\frac{1}{2}\right)\left(-\frac{3}{2}\right)\left(-\frac{5}{2}\right)}{4!}\left(\frac{R - R_0}{R_0}\right)^4 + \dots + \frac{\left(\frac{3 - 2n}{2}\right)!}{n!}\left(\frac{R - R_0}{R_0}\right)^n\right]$$

$$\text{for } \left|\frac{R - R_0}{R_0}\right| < 1 \qquad \text{(B29)}$$

In equation (B29) the factorial

$$\left(\frac{3 - 2n}{2}\right)!$$

is defined as the product of n terms which are represented by $(3 - 2n)/2$ for all integers n from 1 to n.

The ratio between series terms is

$$-\frac{2n - 3}{2n}\,\frac{R - R_0}{R_0}$$

so the series obviously has poor convergence properties as $(R - R_0)/R_0$ approaches 1. However, as $(R - R_0)/R_0$ approaches 1, the normal procedure of evaluating $\sqrt{R/R_0} - 1$ gives good precision, since $1.414 - 1 = 0.414$. Therefore, if a limit criterion on the loss of precision is set at one significant figure, the range of $\sqrt{R/R_0}$ is $0.9 \le \sqrt{R/R_0} \le 1.1$ to keep $(\sqrt{R/R_0} - 1) > 0.1$. This restriction on $\sqrt{R/R_0}$ corresponds to a maximum

$$\left|\frac{R - R_0}{R_0}\right| = 0.21$$

With a limit on the variable in the series, an evaluation of the number of series terms for a desired computational precision can be made. The series coefficients for the first nine terms are shown in table II. For $(R - R_0)/R_0 = 0.21$, the first term is $0.5\,(0.21) = 0.105$. The ninth term is $0.01091(0.21)^9 = 0.867\times10^{-8}$. This gives a ratio of about 10^7 between the first and last terms for the worst case. Therefore, an appropriate equation for the stated criterion on an eight-significant-figure computer is

$$\sqrt{\frac{R}{R_0}} - 1 = \frac{1}{2}\left(\frac{R - R_0}{R_0}\right)\left[1 - \frac{1}{4}\,\frac{R - R_0}{R_0}\left(1 - \frac{1}{2}\,\frac{R - R_0}{R_0}\left\{1 - \frac{5}{8}\,\frac{R - R_0}{R_0}\left[1 - \frac{7}{10}\,\frac{R - R_0}{R_0}\left(1 - \frac{3}{4}\,\frac{R - R_0}{R_0}\left\{1 - \frac{11}{14}\,\frac{R - R_0}{R_0}\left[1 - \frac{13}{16}\,\frac{R - R_0}{R_0}\left(1 - \frac{5}{6}\,\frac{R - R_0}{R_0}\right)\right]\right\}\right)\right]\right\}\right)\right]$$

$$\text{for } \left|\frac{R - R_0}{R_0}\right| < 0.21 \qquad \text{(B30)}$$

Combination of Terms with Further Use of Trigonometric Series

Equation (B28) is in a form that can give adequate precision provided we use enough terms in the series representations. Let us look at the sine series term

$$2(R_0C - \sin\kappa_0)\cos\frac{\kappa - \kappa_0}{4}\left[2\sin^2\frac{\kappa - \kappa_0}{8} - \frac{1}{3!}\left(\frac{\kappa - \kappa_0}{4}\right)^2 + \frac{1}{5!}\left(\frac{\kappa - \kappa_0}{4}\right)^4 - \frac{1}{7!}\left(\frac{\kappa - \kappa_0}{4}\right)^6 + \ldots\right] \tag{B31}$$

At no other place in equation (B28) are the trignometric functions of $(\kappa - \kappa_0)/4$ or $(\kappa - \kappa_0)/8$ used, so they can be expressed in series form too if they combine in a decent manner. Note that

$$2\sin^2\frac{\kappa - \kappa_0}{8} = 1 - \cos\frac{\kappa - \kappa_0}{4}$$

$$= 1 - \left[1 - \frac{1}{2}\left(\frac{\kappa - \kappa_0}{4}\right)^2 + \frac{1}{4!}\left(\frac{\kappa - \kappa_0}{4}\right)^4 - \frac{1}{6!}\left(\frac{\kappa - \kappa_0}{4}\right)^6 + \ldots\right]$$

$$= \left[\frac{1}{2}\left(\frac{\kappa - \kappa_0}{4}\right)^2 - \frac{1}{4!}\left(\frac{\kappa - \kappa_0}{4}\right)^4 + \frac{1}{6!}\left(\frac{\kappa - \kappa_0}{4}\right)^6 + \ldots\right]$$

Substituting this series into equation (B31) yields

$$2(R_0C - \sin\kappa_0)\cos\frac{\kappa - \kappa_0}{4}\left[\left(\frac{1}{2!} - \frac{1}{3!}\right)\left(\frac{\kappa - \kappa_0}{4}\right)^2 - \left(\frac{1}{4!} - \frac{1}{5!}\right)\left(\frac{\kappa - \kappa_0}{4}\right)^4 + \left(\frac{1}{6!} - \frac{1}{7!}\right)\left(\frac{\kappa - \kappa_0}{4}\right)^6 - \left(\frac{1}{8!} - \frac{1}{9!}\right)\left(\frac{\kappa - \kappa_0}{4}\right)^8 + \ldots\right]$$

$$= 2(R_0C - \sin\kappa_0)\cos\frac{\kappa - \kappa_0}{4}\left[\frac{3-1}{3!}\left(\frac{\kappa - \kappa_0}{4}\right)^2 - \frac{5-1}{5!}\left(\frac{\kappa - \kappa_0}{4}\right)^4 + \frac{7-1}{7!}\left(\frac{\kappa - \kappa_0}{4}\right)^6 - \frac{9-1}{9!}\left(\frac{\kappa - \kappa_0}{4}\right)^8 + \ldots\right]$$

Expressing $\cos(\kappa - \kappa_0)/4$ in series form too yields

$$2(R_0C - \sin\kappa_0)\left[1 - \frac{1}{2!}\left(\frac{\kappa - \kappa_0}{4}\right)^2 + \frac{1}{4!}\left(\frac{\kappa - \kappa_0}{4}\right)^4 - \frac{1}{6!}\left(\frac{\kappa - \kappa_0}{4}\right)^6 + \frac{1}{8!}\left(\frac{\kappa - \kappa_0}{4}\right)^8 + \cdots\right]\left[\frac{2}{3!}\left(\frac{\kappa - \kappa_0}{4}\right)^2 - \frac{4}{5!}\left(\frac{\kappa - \kappa_0}{4}\right)^4 + \frac{6}{7!}\left(\frac{\kappa - \kappa_0}{4}\right)^6 - \frac{8}{9!}\left(\frac{\kappa - \kappa_0}{4}\right)^8 + \cdots\right]$$

$$= 2(R_0C - \sin\kappa_0)\left[\frac{2}{3!}\left(\frac{\kappa - \kappa_0}{4}\right)^2 - \left(\frac{4}{5!} + \frac{2}{2!\,3!}\right)\left(\frac{\kappa - \kappa_0}{4}\right)^4 + \left(\frac{6}{7!} + \frac{4}{2!\,5!} + \frac{2}{4!\,3!}\right)\left(\frac{\kappa - \kappa_0}{4}\right)^6 - \left(\frac{8}{9!} + \frac{6}{2!\,7!} + \frac{4}{4!\,5!} + \frac{2}{6!\,3!}\right)\left(\frac{\kappa - \kappa_0}{4}\right)^8 + \cdots\right]$$

$$= 2(R_0C - \sin\kappa_0)\left[\frac{2}{3!}\left(\frac{\kappa - \kappa_0}{4}\right)^2 - \frac{24}{5!}\left(\frac{\kappa - \kappa_0}{4}\right)^4 + \frac{160}{7!}\left(\frac{\kappa - \kappa_0}{4}\right)^6 - \frac{896}{9!}\left(\frac{\kappa - \kappa_0}{4}\right)^8 + \cdots\right]$$

$$= 2(R_0C - \sin\kappa_0)\left[\frac{2}{3!}\left(\frac{\kappa - \kappa_0}{4}\right)^2 - \frac{3\cdot 2^3}{5!}\left(\frac{\kappa - \kappa_0}{4}\right)^4 + \frac{5\cdot 2^5}{7!}\left(\frac{\kappa - \kappa_0}{4}\right)^6 - \frac{7\cdot 2^7}{9!}\left(\frac{\kappa - \kappa_0}{4}\right)^8 + \cdots\right]$$

$$= 2(R_0C - \sin\kappa_0)\sum_{n=1}^{N}\left[(-1)^{n+1}\frac{(2n-1)\cdot 2^{(2n-1)}}{(2n+1)!}\left(\frac{\kappa - \kappa_0}{4}\right)^{2n}\right]$$

Number of Trignometric Series Terms Needed

The number of series terms needed for a desired computational precision is dependent on the magnitude of the series variable $(\kappa - \kappa_0)/4$. For a selected precision criterion, the maximum magnitude of $(\kappa - \kappa_0)/4$ can be computed for a specific number of series terms. For example, the sixth series term is

$$\frac{11\cdot 2^{11}}{13!}\left(\frac{\kappa - \kappa_0}{4}\right)^{12}$$

The ratio of the sixth series term to the first term

$$\frac{2}{3!}\left(\frac{\kappa - \kappa_0}{4}\right)$$

is

$$\frac{11\cdot 2^{10}\cdot 3!}{13!}\left(\frac{\kappa - \kappa_0}{4}\right)$$

For an eight-significant-figure computer, a maximum relative error of 10^{-7} should be a reasonable precision criterion. So for

$$\frac{11 \cdot 2^{10} \cdot 3!}{13!}\left(\frac{\kappa - \kappa_0}{4}\right)^{10} \leq 10^{-7}$$

$$\left|\frac{\kappa - \kappa_0}{4}\right| \leq 0.6258 \text{ rad}$$

that is, $|\kappa - \kappa_0| \leq 143.4^{\circ}$. For turbomachinery, $\kappa - \kappa_0$ will almost always be less than 140°, so fewer than six series terms usually will be needed for the selected precision criterion. However, the potential saving is hardly worth the extra logic, so six series terms are always used.

The nesting principle is used in calculation. A specific coefficient can be determined as the ratio of the n to $n - 1$ series terms

$$\frac{(-1)^{n+1}\dfrac{(2n - 1) \cdot 2^{(2n-1)}}{(2n + 1)!}\left(\dfrac{\kappa - \kappa_0}{4}\right)^{2n}}{(-1)^{n}\dfrac{(2n - 3) \cdot 2^{(2n-3)}}{(2n - 1)!}\left(\dfrac{\kappa - \kappa_0}{4}\right)^{2n-2}} = -\frac{(2n - 1) \cdot 2^{2}}{(2n - 3)(2n + 1)(2n)}\left(\frac{\kappa - \kappa_0}{4}\right)^{2}$$

The series can be expressed as

$$2(R_0C - \sin\kappa_0)\cos\frac{\kappa - \kappa_0}{4}\left[2\sin^2\left(\frac{\kappa - \kappa_0}{8}\right) - \frac{1}{3!}\left(\frac{\kappa - \kappa_0}{4}\right)^2 + \frac{1}{5!}\left(\frac{\kappa - \kappa_0}{4}\right)^4 - \frac{1}{7!}\left(\frac{\kappa - \kappa_0}{4}\right)^6 + \cdots\right]$$

$$= (R_0C - \sin\kappa_0)\ \frac{2}{3}\left(\frac{\kappa - \kappa_0}{4}\right)^2\left\{1 - \frac{3}{5}\left(\frac{\kappa - \kappa_0}{4}\right)^2\left[1 - \frac{10}{63}\left(\frac{\kappa - \kappa_0}{4}\right)^2\left(1 - \frac{7}{90}\left(\frac{\kappa - \kappa_0}{4}\right)^2\left\{1 - \frac{18}{385}\left(\frac{\kappa - \kappa_0}{4}\right)^2\left[1 - \frac{11}{351}\left(\frac{\kappa - \kappa_0}{4}\right)^2\right]\right\}\right)\right]\right\}$$

With the application of the preceding equation, the working equation for the sine series term of equation (B28) becomes

$$\sum_{n=1}^{6}\left[(-1)^{n+1}\frac{(2n - 1) \cdot 2^{(2n-1)}}{(2n + 1)!}x^{2n}\right] = \frac{2}{2 \cdot 3}x^2\left[1 - \frac{4 \cdot 3}{4 \cdot 5}x^2\left(1 - \frac{4 \cdot 5}{3 \cdot 6 \cdot 7}x^2\left\{1 - \frac{4 \cdot 7}{5 \cdot 8 \cdot 9}x^2\left[1 - \frac{4 \cdot 9}{7 \cdot 10 \cdot 11}x^2\left(1 - \frac{4 \cdot 11}{9 \cdot 12 \cdot 13}x^2\right)\right]\right\}\right)\right]$$

$$= \frac{x^2}{3}\left[1 - \frac{3}{5}x^2\left(1 - \frac{10}{63}x^2\left\{1 - \frac{7}{90}x^2\left[1 - \frac{13}{385}x^2\left(1 - \frac{11}{351}x^2\right)\right]\right\}\right)\right] \tag{B32}$$

Number of X_2 Series Terms Needed

The remaining series in equation (B28) to be investigated from a precision standpoint is the one containing the X_2^2 terms, where X_2^2 is defined by equation (B26). The series is of the form

$$\frac{X_2^2}{3} + \frac{X_2^4}{5} + \frac{X_2^6}{7} + \frac{X_2^8}{9} + \ldots + \frac{X_2^{2n}}{2n+1} \tag{B33}$$

The ratio of one term to the previous one is $(2n - 1)/(2n + 1)X_2^2$. At large values of n, the coefficient approaches 1. So for the series to converge to a finite value, $|X_2^2|$ must be less than 1. However, if $|X_2^2|$ is less than 1/2, the series converges to a value no larger than twice the magnitude of the first term. The number of terms needed in the series to meet a precision criterion depends upon how much less than 1/2 the magnitude of X_2^2 is. To get an idea of the magnitude of X_2^2 in turbomachinery, a search for a maximum value of $|X_2^2|$ can be made.

Since X_2^2 is a function of several variables, it would be helpful to have more information about the variation of X_2^2 in order to conduct an appropriate search for a maximum value of $|X_2^2|$. For a start, note that C always will be finite for turbomachinery. Then by equation (4), $\kappa = \kappa_0$ when $R = R_0$. When $\kappa = \kappa_0$, $X_2^2 = 0$ by equation (B26), so it is shown that $X_2^2 = 0$ when $R = R_0$. Thus, a maximum $|X_2^2|$ never occurs at $R = R_0$. Also, by implication, an effective way to search for maximum $|X_2^2|$ may be to differentiate X_2^2 with respect to R and inspect for the location of any zero slopes.

Before differentiation of X_2^2 with respect to R, note that κ is a function of R. A differential relation between them can be obtained from a combination of equations (1) and (3).

$$\frac{d\kappa}{dR} = \frac{C}{\cos \kappa} \tag{B34}$$

Now proceeding with the differentiation of X_2^2 as defined in equation (B26)

$$\frac{dK_2^2}{dR} = \left[1 - (R_0C - \sin\kappa_0)^2\right]\frac{d}{dR}\left[\frac{\sin\frac{\kappa-\kappa_0}{2}}{(R_0C - \sin\kappa_0)\cos\frac{\kappa-\kappa_0}{2} + \sin\frac{\kappa+\kappa_0}{2} + CR_0\sqrt{\frac{R}{R_0}}}\right]^2$$

$$= \frac{2\left[1 - (R_0C - \sin\kappa_0)^2\right]\sin\frac{\kappa-\kappa_0}{2}}{\left[(R_0C - \sin\kappa_0)\cos\frac{\kappa-\kappa_0}{2} + \sin\frac{\kappa+\kappa_0}{2} + CR_0\sqrt{\frac{R}{R_0}}\right]^3}$$

$$\cdot\left\{\cos\frac{\kappa-\kappa_0}{2}\,\frac{1}{2}\frac{d\kappa}{dR}\left[(R_0C - \sin\kappa_0)\cos\frac{\kappa-\kappa_0}{2} + \sin\frac{\kappa+\kappa_0}{2} + CR_0\sqrt{\frac{R}{R_0}}\right] - \sin\frac{\kappa-\kappa_0}{2}\left[-(R_0C - \sin\kappa_0)\sin\frac{\kappa-\kappa_0}{2}\,\frac{1}{2}\frac{d\kappa}{dR} + \cos\frac{\kappa+\kappa_0}{2}\,\frac{1}{2}\frac{d\kappa}{dR} + \frac{1}{2}\frac{CR_0}{\sqrt{RR_0}}\right]\right\}$$

$$= \frac{2\left[1 - (R_0C - \sin\kappa_0)^2\right]\sin\frac{\kappa-\kappa_0}{2}\left(\frac{1}{2}\right)}{\left[(R_0C - \sin\kappa_0)\cos\frac{\kappa-\kappa_0}{2} + \sin\frac{\kappa+\kappa_0}{2} + CR_0\sqrt{\frac{R}{R_0}}\right]^3}$$

$$\cdot\left\{\cos\frac{\kappa-\kappa_0}{2}\,\frac{C}{\cos\kappa}\left[(R_0C - \sin\kappa_0)\cos\frac{\kappa-\kappa_0}{2} + \sin\frac{\kappa+\kappa_0}{2} + CR_0\sqrt{\frac{R}{R_0}}\right] - \sin\frac{\kappa-\kappa_0}{2}\left[-(R_0C - \sin\kappa_0)\sin\frac{\kappa-\kappa_0}{2}\,\frac{C}{\cos\kappa} + \cos\frac{\kappa+\kappa_0}{2}\,\frac{C}{\cos\kappa} + \frac{CR_0}{\sqrt{R_0R}}\right]\right\}$$

$$= \frac{\left[1 - (R_0C - \sin\kappa_0)^2\right]\sin\frac{\kappa-\kappa_0}{2}\,\frac{C}{\cos\kappa}}{\left[(R_0C - \sin\kappa_0)\cos\frac{\kappa-\kappa_0}{2} + \sin\frac{\kappa+\kappa_0}{2} + CR_0\sqrt{\frac{R}{R_0}}\right]^3}$$

$$\cdot\left[(R_0C - \sin\kappa_0)\left(\cos^2\frac{\kappa-\kappa_0}{2} + \sin^2\frac{\kappa-\kappa_0}{2}\right) + \cos\frac{\kappa-\kappa_0}{2}\sin\frac{\kappa+\kappa_0}{2} - \sin\frac{\kappa-\kappa_0}{2}\cos\frac{\kappa+\kappa_0}{2} + \cos\frac{\kappa-\kappa_0}{2}CR_0\sqrt{\frac{R}{R_0}} - \sin\frac{\kappa-\kappa_0}{2}\cos\kappa\,\frac{R_0}{\sqrt{R_0R}}\right]$$

$$= \frac{\left[1 - (R_0C - \sin\kappa_0)^2\right]\sin\frac{\kappa-\kappa_0}{2}\,\frac{C}{\cos\kappa}}{\left[(R_0C - \sin\kappa_0)\cos\frac{\kappa-\kappa_0}{2} + \sin\frac{\kappa+\kappa_0}{2} + CR_0\sqrt{\frac{R}{R_0}}\right]^3}\left(R_0C - \sin\kappa_0 + \sin\kappa_0 + \cos\frac{\kappa-\kappa_0}{2}CR_0\sqrt{\frac{R}{R_0}} - \sin\frac{\kappa-\kappa_0}{2}\cos\kappa\,\frac{R_0}{\sqrt{R_0R}}\right)$$

$$= \frac{\left[1 - (R_0C - \sin\kappa_0)^2\right]\sin\frac{\kappa-\kappa_0}{2}\,\frac{CR_0}{\cos\kappa}\left[C\left(1 + \cos\frac{\kappa-\kappa_0}{2}\sqrt{\frac{R}{R_0}}\right) - \sin\frac{\kappa-\kappa_0}{2}\cos\kappa\,\frac{1}{\sqrt{R_0R}}\right]}{\left[R_0C\cos\frac{\kappa-\kappa_0}{2} - 2\sin\frac{\kappa_0}{2}\cos\frac{\kappa_0}{2}\left(\cos\frac{\kappa}{2}\cos\frac{\kappa_0}{2} + \sin\frac{\kappa}{2}\sin\frac{\kappa_0}{2}\right) + \sin\frac{\kappa}{2}\cos\frac{\kappa_0}{2} + \sin\frac{\kappa_0}{2}\cos\frac{\kappa}{2} + CR_0\sqrt{\frac{R}{R_0}}\right]^3}$$

$$= \frac{\left[1 - (R_0C - \sin\kappa_0)^2\right]\sin\frac{\kappa-\kappa_0}{2}\,\frac{CR_0}{\cos\kappa}\left[C\left(1 + \cos\frac{\kappa-\kappa_0}{2}\sqrt{\frac{R}{R_0}}\right) - \sin\frac{\kappa-\kappa_0}{2}\cos\kappa\,\frac{1}{\sqrt{R_0R}}\right]}{\left[R_0C\cos\frac{\kappa-\kappa_0}{2} + \left(\sin\frac{\kappa}{2}\cos\frac{\kappa_0}{2} - \sin\frac{\kappa_0}{2}\cos\frac{\kappa}{2}\right)\left(1 - 2\sin^2\frac{\kappa_0}{2}\right) + CR_0\sqrt{\frac{R}{R_0}}\right]^3}$$

$$= \frac{\left[1 - (R_0C - \sin\kappa_0)^2\right]\sin\frac{\kappa-\kappa_0}{2}\,\frac{CR_0}{\cos\kappa}\left[C\left(1 + \cos\frac{\kappa-\kappa_0}{2}\sqrt{\frac{R}{R_0}}\right) - \sin\frac{\kappa-\kappa_0}{2}\cos\kappa\,\frac{1}{\sqrt{R_0R}}\right]}{\left[\sin\frac{\kappa-\kappa_0}{2}\cos\kappa_0 + R_0C\left(\cos\frac{\kappa-\kappa_0}{2} + \sqrt{\frac{R}{R_0}}\right)\right]^3}$$

However, from equation (4)

$$C = \frac{\sin \kappa - \sin \kappa_0}{R - R_0} = \frac{2 \sin \frac{\kappa - \kappa_0}{2} \cos \frac{\kappa + \kappa_0}{2}}{R - R_0}$$

$$\therefore \frac{dX_2^2}{dR} = \frac{\left[1 - (R_0C - \sin \kappa_0)^2\right] \sin \frac{\kappa - \kappa_0}{2} \frac{2R_0 \sin \frac{\kappa - \kappa_0}{2} \cos \frac{\kappa + \kappa_0}{2}}{(R - R_0)\cos \kappa} \left[\frac{2 \sin \frac{\kappa - \kappa_0}{2} \cos \frac{\kappa + \kappa_0}{2}}{R - R_0}\left(1 + \cos \frac{\kappa - \kappa_0}{2} \sqrt{\frac{R}{R_0}}\right) - \sin \frac{\kappa - \kappa_0}{2} \cos \kappa \frac{1}{\sqrt{R_0 R}}\right]}{\left[\sin \frac{\kappa - \kappa_0}{2} \cos \kappa_0 + \frac{2R_0}{R - R_0} \sin \frac{\kappa - \kappa_0}{2} \cos \frac{\kappa + \kappa_0}{2}\left(\cos \frac{\kappa - \kappa_0}{2} + \sqrt{\frac{R}{R_0}}\right)\right]^3}$$

$$= \frac{\left[1 - (R_0C - \sin \kappa_0)^2\right] \sin^3 \frac{\kappa - \kappa_0}{2} \frac{2R_0 \cos \frac{\kappa + \kappa_0}{2}}{(R - R_0)\cos \kappa} \left[\frac{2 \cos \frac{\kappa + \kappa_0}{2}}{R - R_0}\left(1 + \cos \frac{\kappa - \kappa_0}{2} \sqrt{\frac{R}{R_0}}\right) - \frac{\cos \kappa}{\sqrt{R_0 R}}\right]}{\sin^3 \frac{\kappa - \kappa_0}{2} \left[\cos \kappa_0 + \frac{2R_0}{R - R_0} \cos \frac{\kappa + \kappa_0}{2}\left(\cos \frac{\kappa - \kappa_0}{2} + \sqrt{\frac{R}{R_0}}\right)\right]^3}$$

$$= 2R_0(R - R_0)\left[1 - (R_0C - \sin \kappa_0)^2\right]\left(\frac{\cos \frac{\kappa + \kappa_0}{2}}{\cos \kappa}\right) \frac{\left[2 \cos \frac{\kappa + \kappa_0}{2}\left(1 + \cos \frac{\kappa - \kappa_0}{2} \sqrt{\frac{R}{R_0}}\right) - \frac{R - R_0}{\sqrt{R_0 R}} \cos \kappa\right]}{\left[(R - R_0)\cos \kappa_0 + 2R_0 \cos \frac{\kappa + \kappa_0}{2}\left(\cos \frac{\kappa - \kappa_0}{2} + \sqrt{\frac{R}{R_0}}\right)\right]^3} \qquad \text{(B35)}$$

When R is within the practical turbomachinery limits of $R_0/2 < R < 2R_0$, the values of the group of terms in either the numerator or the denominator of the last term in equation (B35) will never be zero. The conditions $R = R_0$ and $|R_0C - \sin \kappa_0| = 1$ yield zeros for dX_2^2/dR, but these both occur at $X_2^2 = 0$. Therefore, the conclusion is that the variation of X_2^2 with R has no maximum or minimum at $R \neq R_0$. Since X_2^2 is also zero at $R = R_0$, the maximum $|X_2^2|$ occurs at minimum or maximum R. This means that the maximum magnitude X_2^2 can always be found at minimum or maximum R for any combination of the two constants R_0C and κ_0.

In table III, maximum values of $|X_2^2|$ are shown over the complete spectrum of $R_0C - \sin \kappa_0$ for a κ_0 of 70°. The constant C is negative, as it usually is in turbomachinery, because κ normally decreases with path distance from the inlet reference. At the lower magnitude values of $R_0C - \sin \kappa_0$, the radius ratio reaches a limit first; so $\Delta\kappa$ is less than the imposed limit of 140°. At the higher magnitude values of $R_0C - \sin \kappa_0$, the $\Delta\kappa$ limit is reached before the radius ratio limits. The use of such a large $\Delta\kappa$ limit requires the choice of a relatively high κ_0 to keep both κ_0 and κ within the $|\pi/2|$ limit. It turns out, however, that the choice of κ_0 is not important.

The overall maximum value of $|X_2^2|$ occurs at the very large $|R_0C - \sin \kappa_0|$ values. And at these very large $|R_0C - \sin \kappa_0|$ values, the R_0C term completely dominates the trigonometric functions of κ_0. So the overall maximum value of $|X_2^2|$ is 0.4903 for any value of κ_0 that can give a $\kappa - \kappa_0$ of -140°.

Since the maximum value of $|X_2^2|$ is less than 1/2, the series (B33) is known to always converge to a finite value which is less than twice the magnitude of the first series term. The number of series terms needed for a specified precision, of course, depends on the magnitude of X_2^2. The number of terms needed to give a relative error of about 10^{-8} is shown in table IV for the range of X_2^2.

For normal usage, $|X_2^2|$ usually will be quite low; so not many series terms are needed. However, as many as 23 may be desirable for special cases. For good program efficiency, the number of series terms used was made a function of the magnitude of X_2^2.

Range of Applicability for the ϵ Equations

Equation (B28) is a satisfactory form to use for the vast majority of $\epsilon - \epsilon_0$ calculations. However, it eventually becomes plagued with the subtraction-of-nearly-equal-numbers problem for certain parameter combinations. Fortunately, this occurs as very simple solution forms are approached. The first of these is $|C| << 1$, for which equation (B12) is the solution. The second is

$$\left|\frac{R - R_0}{R_0}\right| << 1$$

In this case, equation (9) becomes

$$d\epsilon \cong \frac{\sin \kappa}{R_m} ds$$

$$= \sin \frac{\kappa_0 + C(s - s_0)}{R_m} ds$$

where

$$R_m = \frac{R + R_0}{2}$$

$$\epsilon - \epsilon_0 = \int_{s_0}^{s} \frac{\sin\left[\kappa_0 + C(s - s_0)\right] C\, ds}{CR_m} = - \left. \frac{\cos\left[\kappa_0 + C(s - s_0)\right]}{CR_m} \right|_{s_0}^{s}$$

$$= - \frac{\cos\left[\kappa_0 + C(s - s_0)\right] - \cos \kappa_0}{CR_m} = - \frac{\cos(\kappa_0 + \kappa - \kappa_0) - \cos \kappa_0}{CR_m}$$

$$= \frac{2 \sin\left(\frac{\kappa - \kappa_0}{2}\right) \sin\left(\frac{\kappa + \kappa_0}{2}\right)}{CR_m}$$

Using the sine series of equation (7) yields

$$\epsilon - \epsilon_0 = \frac{2 \sin\left(\frac{\kappa + \kappa_0}{2}\right)}{\frac{\kappa - \kappa_0}{s - s_0} R_m} \left(\frac{\kappa - \kappa_0}{2}\right)\left[1 - \frac{1}{3!}\left(\frac{\kappa - \kappa_0}{2}\right)^2 + \frac{1}{5!}\left(\frac{\kappa - \kappa_0}{2}\right)^4 - \frac{1}{7!}\left(\frac{\kappa - \kappa_0}{2}\right)^6 + \frac{1}{9!}\left(\frac{\kappa - \kappa_0}{2}\right)^8\right]$$

$$= \frac{s - s_0}{R_m} \sin \frac{\kappa + \kappa_0}{2}\left[1 - \frac{1}{6}\left(\frac{\kappa - \kappa_0}{2}\right)^2\left(1 - \frac{1}{20}\left(\frac{\kappa - \kappa_0}{2}\right)^2\left\{1 - \frac{1}{42}\left(\frac{\kappa - \kappa_0}{2}\right)^2\left[1 - \frac{1}{72}\left(\frac{\kappa - \kappa_0}{2}\right)^2\right]\right\}\right)\right] \tag{B36}$$

The approach used to establish when to use equations (B12) or (B36) in place of equation (B28) was simply to set up a computer program and calculate $\epsilon - \epsilon_0$ with each of the equations over the spectrum of constants. The reference value at each point was equation (B28) calculated in double precision with the necessary extra terms in the series. Equation (B28) gives the best accuracy except for very low $\Delta\kappa$ and very high $R_0/\Delta s$. However, enough points were used in these questionable regimes to reasonably well define parameter values at which a switch of equation should be made for better accuracy of computation. The study showed that by the choice of the best accuracy form of equation, $\epsilon - \epsilon_0$ can always be calculated with a relative error of 10^{-6} or less on an eight-significant-figure computer. The specific parametric values for the switches are shown in table V. In the program the computation is for $R\,\Delta\epsilon$ rather than $\Delta\epsilon$. Thus, even though R approaches infinity, a physically meaningful and accurate value of the circumferential component of a path can be obtained from equation (B36) with R_m

transferred to the left side of the equation. The computation of the conic radial (meridional) and circumferential ([illegible]) components for a Δs path are made in subroutine EPSLON.

APPENDIX C

DEVELOPMENT OF CUBIC INTERPOLATION EQUATION

Let y be the dependent variable at some independent variable location x. The general cubic polynomial for y is

$$y = a + bx + cx^2 + dx^3 \tag{C1}$$

To keep the cubic coefficients small in applications, redefine the independent variable as

$$X = \frac{x}{x_2} - 1 \tag{C2}$$

where x_2 is the independent variable at the second point of the four-point sequence to be curve fit. Thus, the general equation used becomes

$$y = A + BX + CX^2 + DX^3 \tag{C3}$$

The dependent variable y is known at the four points, so there are four equations in the four unknown coefficients. At the second point, when $x = x_2$, $X_2 = 0$; so

$$A = y_2 \tag{C4}$$

The other equations are

$$y_1 = A + BX_1 + CX_1^2 + DX_1^3 \tag{C5}$$

$$y_3 = A + BX_3 + CX_3^2 + DX_3^3 \tag{C6}$$

$$y_4 = A + BX_4 + CX_4^2 + DX_4^3 \tag{C7}$$

Subtraction of equation (C4) from each equation (C5) to (C7) gives

$$\frac{y_1 - y_2}{X_1} = B + CX_1 + DX_1^2 \tag{C8}$$

$$\frac{y_3 - y_2}{X_3} = B + CX_3 + DX_3^2 \tag{C9}$$

$$\frac{y_4 - y_2}{X_4} = B + CX_4 + DX_4^2 \tag{C10}$$

Using equation (C9) for each B elimination gives

$$\left(\frac{y_1 - y_2}{X_1} - \frac{y_3 - y_2}{X_3}\right)\frac{1}{X_1 - X_3} = C + D(X_1 + X_3)$$

$$\left(\frac{y_3 - y_2}{X_3} - \frac{y_4 - y_2}{X_4}\right)\frac{1}{X_3 - X_4} = C + D(X_3 + X_4)$$

The equations for the cubic coefficients can be expressed as

$$D = \frac{\left(\frac{y_1 - y_2}{X_1} - \frac{y_3 - y_2}{X_3}\right)\frac{1}{X_1 - X_3} - \left(\frac{y_3 - y_2}{X_3} - \frac{y_4 - y_2}{X_4}\right)\frac{1}{X_3 - X_4}}{X_1 - X_4}$$

$$C = \left(\frac{y_1 - y_2}{X_1} - \frac{y_3 - y_2}{X_3}\right)\frac{1}{X_1 - X_3} - D(X_1 + X_3)$$

$$B = \frac{y_3 - y_2}{X_3} - (C + DX_3)X_3$$

$$A = y_2$$

APPENDIX D

DEVELOPMENT OF INTEGRATION EQUATIONS FOR A CUBIC SPLINE FIT OF BLADE-SECTION POINTS

Development of Spline Equations

The spline curve fit used in this application is a specialized form of that presented in reference 7. For completeness, this particular development begins with a summary of the basics from reference 7. The knowns are x_k and y_k for k systematically spaced points on a blade surface, where x_k is a coordinate approximately along the blade-segment chord and y_k is the normal coordinate. The coordinates of the transition point, x_t and y_t, are also known. The transition point is used in its proper place in the surface array if its relative distance to the nearest surface point is greater than 10 percent of the corresponding increment between the systematically spaced points.

The surface points are fit with piecewise cubics between the points. The joining conditions between cubics at the points are continuous first and second derivatives, except at the transition point, where the second derivative is allowed to be discontinuous. Between points the second derivative is varied linearly so that a general y'' can be expressed as

$$y'' = y''_{k-1} \frac{x_k - x}{x_k - x_{k-1}} + y''_k \frac{x - x_{k-1}}{x_k - x_{k-1}} \qquad \text{for } x_{k-1} \le x \le x_k \tag{D1}$$

Integration of equation (D1) gives

$$y' = \frac{1}{x_k - x_{k-1}} \left[y''_{k-1}\left(xx_k - \frac{x^2}{2}\right) + y''_k\left(\frac{x^2}{2} - xx_{k-1}\right)\right] + C_1 \tag{D2}$$

Integration of (D2) gives

$$y = \frac{1}{x_k - x_{k-1}} \left[y''_{k-1}\left(\frac{x^2}{2} x_k - \frac{x^3}{6}\right) + y''_k\left(\frac{x^3}{6} - \frac{x^2}{2} x_{k-1}\right)\right] + C_1 x + C_2 \tag{D3}$$

In equation (D3) $y = y_{k-1}$ at $x = x_{k-1}$ and $y = y_k$ at $x = x_k$. Substitution of these values in equation (D3) and subtraction of the resulting equations yields

$$C_1 = \frac{1}{x_k - x_{k-1}} \left[y_k - y_{k-1} - y''_{k-1} \left(\frac{x_k^3}{3} + \frac{x_k x_{k-1}}{3} - \frac{x_{k-1}^2}{6} \right) - y''_k \left(\frac{x_k^2}{6} - \frac{x_k x_{k-1}}{3} - \frac{x_{k-1}^2}{3} \right) \right] \tag{D4}$$

and

$$C_2 = \frac{1}{x_k - x_{k-1}} \left\{ x_k y_{k-1} - x_{k-1} y_k + \frac{x_k x_{k-1}}{3} \left[y''_{k-1} \left(x_k - \frac{x_{k-1}}{2} \right) + y''_k \left(\frac{x_k}{2} - x_{k-1} \right) \right] \right\} \tag{D5}$$

Substitution of equation (D4) into (D2) yields the general equation for y'

$$y' = \frac{1}{x_k - x_{k-1}} \left[y_k - y_{k-1} - y''_{k-1} \frac{(x_k - x)^2}{2} + y''_k \frac{(x - x_{k-1})^2}{2} \right] + (x_k - x_{k-1}) \frac{y''_{k-1} - y''_k}{6} \tag{D6}$$

Substitution of equations (D4) and (D5) into (D3) yields the general equation for y

$$y = \frac{y''_{k-1}(x_k - x)^3 + y''_k (x - x_{k-1})^3}{6(x_k - x_{k-1})} + \left[\frac{y_k}{x_k - x_{k-1}} - \frac{y''_k (x_k - x_{k-1})}{6} \right] (x - x_{k-1})$$

$$+ \left[\frac{y_{k-1}}{x_k - x_{k-1}} - \frac{y''_{k-1}(x_k - x_{k-1})}{6} \right] (x_k - x) \tag{D7}$$

Joining Conditions for Curve Segments

At the junctions between the cubic pieces, the slopes are the same; that is, $y'(x_{k(-)}) = y'(x_{k(+)})$. Also $y''(x_{k(-)}) = y''(x_{k(+)})$, except at the transition point. So at a point x_k other than the transition point,

$$y'_k = \frac{1}{x_k - x_{k-1}} \left[y_k - y_{k-1} - y''_{k-1} \frac{(x_k - x_k)^2}{2} + y''_k \frac{(x_k - x_{k-1})^2}{2} \right] + (x_k - x_{k-1}) \frac{y''_{k-1} - y''_k}{6}$$

$$= \frac{1}{x_{k+1} - x_k} \left[y_{k+1} - y_k - y''_k \frac{(x_{k+1} - x_k)^2}{2} + y''_{k+1} \frac{(x_k - x_k)^2}{2} \right] + (x_{k+1} - x_k) \frac{y''_k - y''_{k+1}}{6}$$

Therefore,

$$\left(\frac{x_k - x_{k-1}}{6}\right)y''_{k-1} + \left(\frac{x_{k+1} - x_{k-1}}{3}\right)y''_k + \left(\frac{x_{k+1} - x_k}{6}\right)y''_{k+1} = \left(\frac{y_{k+1} - y_k}{x_{k+1} - x_k} - \frac{y_k - y_{k-1}}{x_k - x_{k-1}}\right)$$

$$a_{k-1}y''_{k-1} + b_{k-1}y''_k + c_{k-1}y''_{k+1} = d_{k-1} \tag{D8}$$

When the transition point is considered as one of the points of the array k, the equation for the cubic junction at the transition point is

$$\left(\frac{x_t - x_{k-1}}{6}\right)y''_{k-1} + \left(\frac{x_t - x_{k-1}}{3}\right)y''_{t(-)} + \left(\frac{x_{k+1} - x_t}{3}\right)y''_{t(+)} + \left(\frac{x_{k+1} - x_t}{6}\right)y''_{k+1} = \left(\frac{y_{k+1} - y_t}{x_{k+1} - x_t} - \frac{y_t - y_{k-1}}{x_t - x_{k-1}}\right)$$

$$a_t y''_{k-1} + 2a_t y''_{t(-)} + 2b_t y''_{t(+)} + b_t y''_{k+1} = d_t \tag{D9}$$

Additional Conditions Imposed

The unknowns in equations (D8) and (D9) are the second derivatives at the known points. For the k points, there are k - 2 cubic equations. Also at the transition point, there are two y'' values at one point; so three more equations are needed for a solvable set. The normal procedure is to specify end restrictions for two of the equations. For this application, it is probably best to specify a curvature relation. Since the blade elements are circular-arc-type segments, the blade sections normally also will be nearly circular arcs. Thus, a reasonable end condition should be specification of end-point curvature equal to that of the adjacent point. However, curvature is $y''/\left[1 + (y')^2\right]^{3/2}$, where y' is an unknown too. So a direct solution, if possible, is a little more complicated than is justifiable. Alternatively, a three-point circular-arc fit of the end points was used initially to determine a factor relation between the end two y'' values so that the set of equations could be solved with the direct approach.

The equation for a circle is

$$(x - a)^2 + (y - b)^2 = R^2 \tag{D10}$$

From differentiation of equation (D10), the slope is

$$y' = -\frac{x - a}{y - b} \tag{D11}$$

Since only the equation for y' is needed, it is not necessary to solve for R. However, the known conditions are coordinates of the three points, so R must be eliminated from the three equations in the three unknowns a, b, and R. When the squared terms in equation (D10) are expanded, R, a^2, and b^2 are eliminated by subtraction of the equations applied at the three points. If the equation for the center point of the set is used in both subtractions, the resulting equations for the desired constants can be expressed as

$$2b = \frac{\left(x_3^2 - x_2^2\right)(x_1 - x_2) - \left(x_1^2 - x_2^2\right)(x_3 - x_2) + \left(y_3^2 - y_2^2\right)(x_1 - x_2) - \left(y_1^2 - y_2^2\right)(x_3 - x_2)}{(y_3 - y_2)(x_1 - x_2) - (y_1 - y_2)(x_3 - x_2)}$$

$$2a = \frac{x_1^2 - x_2^2 + y_1^2 - y_2^2 - 2b(y_1 - y_2)}{x_1 - x_2}$$

When the constants are substituted into equation (D11), the general slope equation can be expressed as

$$y' = \frac{(x_2 - x_1)(y_3 - y_2)(2x - x_1 - x_2) - (x_3 - x_2)(y_2 - y_1)(2x - x_3 - x_2) + (y_3 - y_1)(y_2 - y_1)(y_3 - y_2)}{(x_3 - x_2)(y_2 - y_1)(2y - y_1 - y_2) - (x_2 - x_1)(y_3 - y_2)(2y - y_2 - y_3) + (x_3 - x_1)(x_2 - x_1)(x_3 - x_2)} \tag{D12}$$

The application of y' is in the factor relation between y'' values which yields constant curvature. So for $C_1 = C_2$

$$\frac{y_1''}{\left[1 + (y_1')^2\right]^{3/2}} = \frac{y_2''}{\left[1 + (y_2')^2\right]^{3/2}}$$

and

$$y_1'' = y_2''\left[f_1\right]$$

where

$$f_1 = \left[\frac{1 + (y_1')^2}{1 + (y_2')^2}\right]^{3/2} \tag{D13}$$

The same procedure, of course, is used at each end of the surface curve.

The third additional equation is needed at the transition point, where there is a different curvature on each side of the point. The condition is imposed through a curvature ratio at the transition point. The particular curvature ratio is calculated from a three-point finite difference calculation on each side of the transition point.

$$C_R = \frac{C_{k+1}}{C_{k-1}} = \frac{y''_{k+1}}{y''_{k-1}}\left[\frac{1 + (y'_{k-1})^2}{1 + (y'_{k+1})^2}\right]^{3/2}$$

$$C_R = \frac{\dfrac{\dfrac{y_t - y_{k+1}}{x_t - x_{k+1}} - \dfrac{y_{k+1} - y_{k+2}}{x_{k+1} - x_{k+2}}}{x_t - x_{k+2}}}{\dfrac{\dfrac{y_{k-1} - y_{k-2}}{x_{k-1} - x_{k-2}} - \dfrac{y_t - y_{k-1}}{x_t - x_{k-1}}}{x_{k-2} - x_t}} \left(\frac{1.0 + \left\{\left[\dfrac{y_t - y_{k-1}}{x_t - x_{k-1}}(x_{k-1} - x_{k-2}) + \dfrac{y_{k-1} - y_{k-2}}{x_{k-1} - x_{k-2}}(x_t - x_{k-1})\right]\dfrac{1.0}{x_t - x_{k-2}}\right\}^2}{1.0 + \left\{\left[\dfrac{y_{k+1} - y_t}{x_{k+1} - x_t}(x_{k+2} - x_{k+1}) + \dfrac{y_{k+2} - y_{k+1}}{x_{k+2} - x_{k+1}}(x_{k+1} - x_t)\right]\dfrac{1.0}{x_{k+2} - x_t}\right\}^2}\right)^{3/2} = \frac{y''_{t(+)}}{y''_{t(-)}} \tag{D14}$$

The curvature ratio is equal to $y''_{t(+)}/y''_{t(-)}$ because the slope is the same on both sides of the transition point. Since this curvature discontinuity is computed by finite difference methods for interpolated points, it was judged that a better overall surface curve representation of a blade section is obtained with some smoothing of the discontinuity. In the program, the magnitude of the C_R used is the 0.7 power of the C_R obtained from equation (D14).

Method of Solving for Unknown y''

There are now enough equations to determine all the unknown y''. Usually, the tridiagonal matrix is solved by Gauss elimination of variables from one end of the curve to the other end, followed by backward substitution. However, the imposition of the unusual condition at the transition point of the curve can cause some complication. To allow for some versatility for each change of the transition-point condition, a modified approach was used. With the modified approach, Gauss elimination is used from both ends to the transition point, the transition condition is applied, and backward substitution is used to each end. In parametric equation form, the equations from an end are

$$y_1'' = f_1 y_2''$$

$$a_1 y_1'' + b_1 y_2'' + c_1 y_3'' = d_1$$

$$a_2 y_2'' + b_2 y_3'' + c_2 y_4'' = d_2$$

$$a_3 y_3'' + b_3 y_4'' + c_3 y_5'' = d_3$$

$$a_k y_k'' + b_k y_{k+1}'' + c_k y_{k+2}'' = d_k \tag{D15}$$

For the Gauss elimination, it is desirable to set up a standard form. Let it be

$$y_k'' + e_k y_{k+1}'' = h_k \tag{D16}$$

Therefore, for $k = 1$, $e_1 = -f_1$ and $h_1 = 0$. Application of equation (D16) to (D15) gives

$$a_k(h_k - e_k y_{k+1}'') + b_k y_{k+1}'' + c_k y_{k+2}'' = d_k$$

So,

$$(b_k - a_k e_k) y_{k+1}'' + c_k y_{k+2}'' = d_k - a_k h_k$$

$$y_{k+1}'' + \left(\frac{c_k}{b_k - a_k e_k}\right) y_{k+2}'' = \frac{d_k - a_k h_k}{b_k - a_k e_k}$$

$$y_{k+1}'' + (e_{k+1}) y_{k+2}'' = h_{k+1}$$

So,

$$e_{k+1} = \frac{c_k}{b_k - a_k e_k}$$

and

$$h_{k+1} = \frac{d_k - a_k h_k}{b_k - a_k e_k}$$

The same procedure is used from each end, so at the transition point the equations are

$$y''_{k-1} + e_{k-1} y''_{t(-)} = h_{k-1} \tag{D17}$$

and

$$y''_{k+1} + e_{k+1} y''_{t(+)} = h_{k+1} \tag{D18}$$

Using equations (D17) and (D18) in equation (D9) gives

$$a_t(2 - e_{k-1})y''_{t(-)} + b_t(2 - e_{k+1})y''_{t(+)} = d_t - a_t h_{k-1} - b_t h_{k+1} \tag{D19}$$

Equations (D14) and (D19) are two linear equations in the unknowns $y''_{t(-)}$ and $y''_{t(+)}$, so they can be readily calculated. The other y'' values are found by back substitution through the (D16) sets.

Area and Moments Integrals

Once the spline-curve coefficients, y'' values, are established, general surface points then can be located by using equation (D7) for the appropriate interval. The general equation can also be integrated to give areas and moments for the piecewise segments. These can then be summed to locate the blade-section center of area. The developments for the following integrals are for a segment with the y distance being from the $y = 0$ axis to the curve.

$$A = \int_{x_{k-1}}^{x_k} \int_0^y dy\, dx = \int_{x_{k-1}}^{x_k} y\, dx$$

$$= \int_{x_{k-1}}^{x_k} \left\{ \frac{y''_{k-1}(x_k - x)^3 + y''_k(x - x_{k-1})^3}{6(x_k - x_{k-1})} + \left[\frac{y_k}{x_k - x_{k-1}} - \frac{y''_k(x_k - x_{k-1})}{6} \right](x - x_{k-1}) + \left[\frac{y_{k-1}}{x_k - x_{k-1}} - \frac{y''_{k-1}(x_k - x_{k-1})}{6} \right](x_k - x) \right\} dx$$

$$= \left\{ \frac{-y''_{k-1}(x_k - x)^4 + y''_k(x - x_{k-1})^4}{24(x_k - x_{k-1})} + \left[\frac{y_k}{x_k - x_{k-1}} - \frac{y''_k(x_k - x_{k-1})}{6} \right] \frac{(x - x_{k-1})^2}{2} - \left[\frac{y_{k-1}}{x_k - x_{k-1}} - \frac{y''_{k-1}(x_k - x_{k-1})}{6} \right] \frac{(x_k - x)^2}{2} \right\}_{x_{k-1}}^{x_k}$$

$$= \left[\frac{y_k + y_{k-1}}{2} - \frac{y''_k + y''_{k-1}}{24} (x_k - x_{k-1})^2 \right](x_k - x_{k-1}) \qquad \text{(D20)}$$

$$A\bar{x} = \int_{x_{k-1}}^{x_k} \int_0^y x\, dy\, dx = \int_{x_{k-1}}^{x_k} yx\, dx$$

$$= \int_{x_{k-1}}^{x_k} \left\{ \frac{y''_{k-1}(x_k - x)^3 + y''_k(x - x_{k-1})^3}{6(x_k - x_{k-1})} + \left[\frac{y_k}{x_k - x_{k-1}} - \frac{y''_k(x_k - x_{k-1})}{6} \right](x - x_{k-1}) + \left[\frac{y_{k-1}}{x_k - x_{k-1}} - \frac{y''_{k-1}(x_k - x_{k-1})}{6} \right](x_k - x) \right\} x\, dx$$

$$= \left\{ \frac{y''_{k-1}\left[4(x_k - x)^5 - 5x_k(x_k - x)^4\right] + y''_k\left[4(x - x_{k-1})^5 + 5x_{k-1}(x - x_{k-1})^4\right]}{120(x_k - x_{k-1})} + \left[\frac{y_k}{x_k - x_{k-1}} - \frac{y''_k(x_k - x_{k-1})}{6} \right]\left(\frac{x^3}{3} - \frac{x^2}{2} x_{k-1} \right) + \left[\frac{y_{k-1}}{y''_k - y_{k-1}} - \frac{y''_{k-1}(x_k - x_{k-1})}{6} \right]\left(\frac{x^2}{2} x_k - \frac{x^3}{3} \right) \right\}_{x_{k-1}}^{x_k}$$

$$= \frac{x_k - x_{k-1}}{6} \left\{ y_k(2x_k + x_{k-1}) + y_{k-1}(x_k + 2x_{k-1}) - \frac{(x_k - x_{k-1})^2}{60} \left[y''_k(8x_k + 7x_{k-1}) + y''_{k-1}(7x_k + 8x_{k-1}) \right] \right\}$$

$$A\bar{y} = \int_{x_{k-1}}^{x_k} \int_0^y y\, dy\, dx = \int_{x_{k-1}}^{x_k} \frac{y^2}{2}\, dx$$

$$= \frac{1}{2} \int_{x_{k-1}}^{x_k} \left\{ \frac{y''_{k-1}(x_k - x)^3 + y''_k(x - x_{k-1})^3}{6(x_k - x_{k-1})} + \left[\frac{y_k}{x_k - x_{k-1}} - \frac{y''_k(x_k - x_{k-1})}{6} \right](x - x_{k-1}) + \left[\frac{y_{k-1}}{x_k - x_{k-1}} - \frac{y''_{k-1}(x_k - x_{k-1})}{6} \right](x_k - x) \right\}^2 dx$$

$$= \frac{x_k - x_{k-1}}{6} \left(y_k^2 + y_k y_{k-1} + y_{k-1}^2 - \left[8(y_k y''_k + y_{k-1} y''_{k-1}) + 7(y_k y''_{k-1} + y_{k-1} y''_k) \right] \frac{(x_k - x_{k-1})^2}{60} + \frac{1}{7} \left\{ 16\left[(y''_k)^2 + (y''_{k-1})^2 \right] + 31 y''_k y''_{k-1} \right\} \frac{(x_k - x_{k-1})^4}{360} \right)$$

$$\text{(D22)}$$

Other spline segment integrals that are needed for the terminal calculations are

$$I_{yy} = \int_{x_{k-1}}^{x_k} \int_0^y x^2 \, dy \, dx = \int_{x_{k-1}}^{x_k} yx^2 \, dx$$

$$= (x_k - x_{k-1}) \left[y_{k-1} \left(\frac{x_k^2}{12} + \frac{x_k x_{k-1}}{6} + \frac{x_{k-1}^2}{4} \right) + y_k \left(\frac{x_k^2}{4} + \frac{x_k x_{k-1}}{6} + \frac{x_{k-1}^2}{12} \right) \right]$$

$$- \frac{(x_k - x_{k-1})^3}{6} \left[y''_{k-1} \left(\frac{x_k^2}{15} + \frac{x_k x_{k-1}}{10} + \frac{x_{k-1}^2}{12} \right) + y''_k \left(\frac{x_k^2}{12} + \frac{x_k x_{k-1}}{10} + \frac{x_{k-1}^2}{15} \right) \right] \qquad \text{(D23)}$$

$$I_{xx} = \int_{x_{k-1}}^{x_k} \int_0^y y^2 \, dy \, dx = \int_{x_{k-1}}^{x_k} \frac{y^3}{3} \, dx$$

$$= \frac{x_k - x_{k-1}}{12} \Bigg\{ y_{k-1}^3 + y_k \left[y_{k-1}^2 + y_k (y_{k-1} + y_k) \right] - \frac{(x_k - x_{k-1})^3}{30} \Bigg[y''_{k-1} \left[5y_{k-1}^2 + y_k (6y_{k-1} + 4y_k) \right]$$

$$+ y''_k \left[4y_{k-1}^2 + y_k (6y_{k-1} + 5y_k) \right] - \frac{(x_k - x_{k-1})^2}{84} \Bigg(y_{k-1} \left[35(y''_{k-1})^2 + y''_k (62y''_{k-1} + 29y''_k) \right] \qquad \text{(D24)}$$

$$+ y_k \left[29(y''_{k-1})^2 + y''_k (62y''_{k-1} + 35y''_k) \right] - \frac{(x_k - x_{k-1})^2}{6} \left\{ 7(y''_{k-1})^3 + y''_k \left[20(y''_{k-1})^2 + y''_k (20y''_{k-1} + 7y''_k) \right] \right\} \Bigg) \Bigg] \Bigg\}$$

$$I_{xy} = \int_{x_{k-1}}^{x_k} \int_0^y xy \, dy \, dx = \int_{x_{k-1}}^{x_k} \frac{y^2}{2} x \, dx$$

$$= \frac{x_k - x_{k-1}}{24} \Bigg[y_{k-1}^2 (3x_{k-1} + x_k) + y_k \left[2(x_{k-1} + x_k) y_{k-1} + y_k (x_{k-1} + 3x_k) \right] - \frac{(x_k - x_{k-1})^2}{15} \Bigg(y_{k-1} \left[x_{k-1} (5y''_{k-1} + 4y''_k) + 3x_k (y''_{k-1} + y''_k) \right]$$

$$+ y_k \left[3x_{k-1} (y''_{k-1} + y''_k) + x_k (4y''_{k-1} + 5y''_k) \right] - \frac{(x_k - x_{k-1})^2}{168} \left\{ (y''_{k-1})^2 (35x_{k-1} + 29x_k) + y''_k \left[62y''_{k-1} (x_{k-1} + x_k) + y''_k (29x_{k-1} + 35x_k) \right] \right\} \Bigg) \Bigg]$$

$$\text{(D25)}$$

$$I_{yyxx} = \int_{x_{k-1}}^{x_k} \int_0^{y} x^4 \, dy \, dx = \int_{x_{k-1}}^{x_k} y x^4 \, dx$$

$$= \frac{x_k - x_{k-1}}{30} \Bigg\{ y_k \left(5x_k^4 + 4x_k^3 x_{k-1} + 3x_k^2 x_{k-1}^2 + 2x_k x_{k-1}^3 + x_{k-1}^4\right) + y_{k-1}\left(x_k^4 + 2x_k^3 x_{k-1} + 3x_k^2 x_{k-1}^2 + 4x_k x_{k-1}^3 + 5x_{k-1}^4\right)$$

$$- \frac{(x_k - x_{k-1})^2}{168} \left[y''_{k-1}\left(25x_k^4 + 44x_k^3 x_{k-1} + 54x_k^2 x_{k-1}^2 + 52x_k x_{k-1}^3 + 35x_{k-1}^4\right) + y''_k\left(35x_k^4 + 52x_k^3 x_{k-1} + 54x_k^2 x_{k-1}^2 + 44x_k x_{k-1}^3 + 25x_{k-1}^4\right)\right]\Bigg\}$$

(D26)

$$I_{xxyy} = \int_{x_{k-1}}^{x_k} \int_0^{y} y^2 x^2 \, dy \, dx = \int_{x_{k-1}}^{x_k} \frac{y^3}{3} x^2 \, dx$$

$$= \frac{x_k - x_{k-1}}{180} \Bigg[y_{k-1}^3 \left(x_k^2 + 4x_k x_{k-1} + 10x_{k-1}^2\right) + y_{k-1}^2 y_k \left(3x_k^2 + 6x_k x_{k-1} + 6x_{k-1}^2\right) + y_{k-1} y_k^2 \left(6x_k^2 + 6x_k x_{k-1} + 3x_{k-1}^2\right) + y_k^3 \left(10x_k^2 + 4x_k x_{k-1} + x_{k-1}^2\right)$$

$$- \frac{(x_k - x_{k-1})^2}{26} \Bigg(y_{k-1}^2 y''_{k-1}\left(9x_k^2 + 26x_k x_{k-1} + 35x_{k-1}^2\right) + y_{k-1}^2 y''_k\left(9x_k^2 + 22x_k x_{k-1} + 25x_{k-1}^2\right) + y_{k-1} y_k y''_{k-1}\left(22x_k^2 + 36x_k x_{k-1} + 26x_{k-1}^2\right)$$

$$+ y_{k-1} y_k y''_k \left(26x_k^2 + 36x_k x_{k-1} + 22x_{k-1}^2\right) + y_k^2 y''_{k-1}\left(25x_k^2 + 22x_k x_{k-1} + 9x_{k-1}^2\right) + y_k^2 y''_k\left(35x_k^2 + 26x_k x_{k-1} + 9x_{k-1}^2\right)$$

$$- \frac{(x_k - x_{k-1})^2}{18} \Bigg\{ y_{k-1}(y''_{k-1})^2\left(19x_k^2 + 44x_k x_{k-1} + 42x_{k-1}^2\right) + y_k (y''_{k-1})^2\left(27x_k^2 + 38x_k x_{k-1} + 22x_{k-1}^2\right) + y_{k-1} y''_{k-1} y''_k\left(40x_k^2 + 80x_k x_{k-1} + 66x_{k-1}^2\right)$$

$$+ y_k y''_{k-1} y''_k\left(66x_k^2 + 80x_k x_{k-1} + 40x_{k-1}^2\right) + y_{k-1}(y''_k)^2\left(22x_k^2 + 33x_k x_{k-1} + 27x_{k-1}^2\right) + y_k (y''_k)^2\left(42x_k^2 + 44x_k x_{k-1} + 19x_{k-1}^2\right)$$

$$- \frac{(x_k - x_{k-1})^2}{66} \Big[(y''_{k-1})^3\left(52x_k^2 + 102x_k x_{k-1} + 77x_{k-1}^2\right) + (y''_{k-1})^2 y''_k\left(171x_k^2 + 294x_k x_{k-1} + 195x_{k-1}^2\right) + y''_{k-1}(y''_k)^2\left(195x_k^2 + 294x_k x_{k-1} + 171x_{k-1}^2\right)$$

$$+ (y''_k)^3\left(77x_k^2 + 102x_k x_{k-1} + 52x_{k-1}^2\right)\Big]\Bigg\}\Bigg)\Bigg]$$

(D27)

$$I_{xxxx} = \int_{x_{k-1}}^{x_k} \int_0^{y} y^4 \, dy \, dx = \int_{x_{k-1}}^{x_k} \frac{y^5}{5} \, dx$$

where

$$
y = \frac{y''_{k-1}(x_k - x)^3 + y''_k(x - x_{k-1})^3}{6(x_k - x_{k-1})} + \left[\frac{y_k}{x_k - x_{k-1}} - \frac{y''_k(x_k - x_{k-1})}{6}\right](x - x_{k-1})
$$

$$
+ \left[\frac{y_{k-1}}{x_k - x_{k-1}} - \frac{y''_{k-1}(x_k - x_{k-1})}{6}\right](x_k - x) \tag{D7}
$$

Since expansion and integration of this equation is very complicated, a simplification was used. Note that for axial-flow compressor blade sections, the maximum value of x (chordwise direction) with respect to the center-of-area reference is always greater than the maximum magnitude of y. So $x^4\,dx\,dy$ will be larger than $y^4\,dy\,dx$. Consequently, $\iint x^4\,dx\,dy$ over the blade will always be greater than $\iint y^4\,dx\,dy$. Thus, the integral under consideration is essentially a second-order term for the blade-section twist stiffness calculation. The use of a reasonable approximation in the computation of a second-order term should not significantly lower the accuracy of the computed twist stiffness. The approximation used is an average y'' for the increment.

$$
y'' = \frac{1}{2}(y''_{k-1} + y''_k)
$$

The general equation for y by substituting y'' for y''_{k-1} and y''_k in equation (D7) then reduces to

$$
y = \frac{y_k(x - x_{k-1}) + y_{k-1}(x_k - x)}{x_k - x_{k-1}} - \frac{y''(x - x_{k-1})(x_k - x)}{2}
$$

Integration for I_{xxxx} gives

$$
\begin{aligned}
I_{xxxx} = \frac{x_k - x_{k-1}}{30}\Bigg\{ & y_k^5 + y_k^4 y_{k-1} + y_k^3 y_{k-1}^2 + y_k^2 y_{k-1}^3 + y_k y_{k-1}^4 + y_{k-1}^5 - \frac{y''(x_k - x_{k-1})^2}{14}\Bigg[5y_k^4 + 8y_k^3 y_{k-1} + 9y_k^2 y_{k-1}^2 + 8y_k y_{k-1}^3 + 5y_{k-1}^4 \\
& - \frac{y''(x_k - x_{k-1})^2}{4}\Bigg(5y_k^3 + 9y_k^2 y_{k-1} + 9y_k y_{k-1}^2 + 5y_{k-1}^3 - \frac{y''(x_k - x_{k-1})^2}{6}\Bigg\{5y_k^2 + 8y_k y_{k-1} + 5y_{k-1}^2 - \frac{y''(x_k - x_{k-1})^2}{2}\Bigg[y_k + y_{k-1} - \frac{y''(x_k - x_{k-1})^2}{22}\Bigg]\Bigg\}\Bigg)\Bigg]\Bigg\}
\end{aligned}
\tag{D28}
$$

APPENDIX E

DEVELOPMENT OF EQUATIONS FOR BLADE-SECTION END AREA AND MOMENT CORRECTIONS

The spline integrals properly summed give the major part of the moment values for a blade section. The remaining parts needed are obtained from end-circle corrections. The geometric shapes used for the end corrections are the sector of a circle and two trapezoids (fig. 5).

Area and Moments of End-Circle Sector

The blade-end-circle size and location are determined from the blade-section surface end-point coordinates and slopes, which are known from the spline curve fit of the interpolated surface points. In general, the four conditions of two points and the slopes at the points are an overspecification for a circle, which is a second-degree equation with three constants. Since preservation of surface continuity is of first-order priority, the compromise is made with slope. The condition imposed is equal slope difference between the end circle and the surface at the suction- and pressure-surface end points. The geometric placement of the blade-section end circle is shown in figure 11.

To give $r_L = r_U$, the equations for the end-circle center coordinates are

$$x_c = x_U + r_U \sin(\kappa_U + \Delta\kappa)$$

$$y_c = y_U - r_U \cos(\kappa_U + \Delta\kappa)$$

and

$$x_c = x_L - r_L \sin(\kappa_L + \Delta\kappa)$$

$$y_c = y_L + r_L \cos(\kappa_L + \Delta\kappa)$$

Eliminate x_c and y_c by subtraction:

$$x_U - x_L = -r_U\left[\sin(\kappa_U + \Delta\kappa) + \sin(\kappa_L + \Delta\kappa)\right]$$

$$y_U - y_L = r_U\left[\cos(\kappa_U + \Delta\kappa) + \cos(\kappa_L + \Delta\kappa)\right]$$

Eliminate r_U by division:

$$(x_U - x_L)\left[\cos(\kappa_U + \Delta\kappa) + \cos(\kappa_L + \Delta\kappa)\right] = -(y_U - y_L)\left[\sin(\kappa_U + \Delta\kappa) + \sin(\kappa_L + \Delta\kappa)\right]$$

Expand the trigonometric function to get the solution for $\Delta\kappa$:

$$(x_U - x_L)(\cos\kappa_U \cos\Delta\kappa - \sin\kappa_U \sin\Delta\kappa + \cos\kappa_L \cos\Delta\kappa - \sin\kappa_L \sin\Delta\kappa)$$

$$= -(y_U - y_L)(\sin\kappa_U \cos\Delta\kappa + \cos\kappa_U \sin\Delta\kappa + \sin\kappa_L \cos\Delta\kappa + \cos\kappa_L \sin\Delta\kappa)$$

$$\left[(y_U - y_L)(\cos\kappa_U + \cos\kappa_L) - (x_U - x_L)(\sin\kappa_U + \sin\kappa_L)\right]\sin\Delta\kappa$$

$$= -\left[(x_U - x_L)(\cos\kappa_U + \cos\kappa_L) + (y_U - y_L)(\sin\kappa_U + \sin\kappa_L)\right]\cos\Delta\kappa$$

$$\tan\Delta\kappa = \frac{\sin\Delta\kappa}{\cos\Delta\kappa} = \frac{(x_U - x_L)(\cos\kappa_U + \cos\kappa_L) + (y_U - y_L)(\sin\kappa_U + \sin\kappa_L)}{(x_U - x_L)(\sin\kappa_U + \sin\kappa_L) - (y_U - y_L)(\cos\kappa_U + \cos\kappa_L)} \tag{E1}$$

For computing purposes, the more appropriate equation for r_U is

$$r = r_U = \frac{y_U - y_L}{(\cos\kappa_U + \cos\kappa_L)\cos\Delta\kappa - (\sin\kappa_U + \sin\kappa_L)\sin\Delta\kappa} \tag{E2}$$

because y_U is never equal to y_L, whereas x_U may equal x_L.

The area of the leading-edge end-circle sector, which is shown in figure 31, is

$$A = \int_{\theta_U}^{\pi+\theta_L} \int_0^r r\,dr\,d\theta = \int_{\theta_U}^{\pi+\theta_L} \frac{r^2}{2}\,d\theta = \frac{r^2}{2}(\pi + \theta_L - \theta_U) \tag{E3}$$

where $\theta_L = \kappa_L + \Delta\kappa$ and $\theta_U = \kappa_U + \Delta\kappa$. The first moments of the end-circle sector are

$$A\bar{x} = \int_{\theta_U}^{\pi+\theta_L} \int_0^r (x_c - r \sin \theta) r \, dr \, d\theta = \int_{\theta_U}^{\pi+\theta_L} \frac{r^2}{2} \left(x_c - \frac{2r}{3} \sin \theta \right) d\theta$$

$$= x_c \frac{r^2}{2} \theta \Bigg|_{\theta_U}^{\pi+\theta_L} + \frac{r^3}{3} \cos \theta \Bigg|_{\theta_U}^{\pi+\theta_L} = Ax_c - \frac{r^3}{3} (\cos \theta_U + \cos \theta_L) \tag{E4}$$

$$A\bar{y} = \int_{\theta_U}^{\pi+\theta_L} \int_0^r (y_c + r \cos \theta) r \, dr \, d\theta = \int_{\theta_U}^{\pi+\theta_L} \frac{r^2}{2} \left(y_c + \frac{2}{3} r \cos \theta \right) d\theta$$

$$= y_c \frac{r^2}{2} \theta \Bigg|_{\theta_U}^{\pi+\theta_L} + \frac{r^3}{3} \sin \theta \Bigg|_{\theta_U}^{\pi+\theta_L} = Ay_c - \frac{r^3}{3} (\sin \theta_U + \sin \theta_L) \tag{E5}$$

A similar development for the trailing edge gives slightly different results. However, a general similarity is restored by using the negative of the trailing-edge area,

$$A = \frac{r^2}{2} (\theta_L - \theta_U - \pi) \tag{E6}$$

in the preceding and following moment equations. This procedure gives negative values for all trailing-edge area and moment values, but it is a convenience in the program to use the same coding for both ends.

For the terminal calculations, higher moments are also used. Such equations for the end circle follow:

$$I_{yy} = \int_{\theta_U}^{\pi+\theta_L} \int_0^r (x_c - r \sin \theta)^2 r \, dr \, d\theta$$

$$= \int_{\theta_U}^{\pi+\theta_L} \left(\frac{x_c^2 r^2}{2} - \frac{2x_c r^3 \sin \theta}{3} + \frac{r^4 \sin^2 \theta}{4} \right) d\theta$$

$$= \left(\frac{x_c^2 r^2}{2} \theta \right)_{\theta_U}^{\pi+\theta_L} + \left(\frac{2x_c r^3}{3} \cos \theta \right)_{\theta_U}^{\pi+\theta_L} + \frac{r^2}{4} \left(\frac{\theta}{2} - \frac{\sin 2\theta}{4} \right)_{\theta_U}^{\pi+\theta_L}$$

$$= \left(x_c^2 + \frac{r^2}{4} \right) A - \frac{2r^3 x_c}{3} (\cos \theta_U + \cos \theta_L) - \frac{r^4}{8} \sin (\theta_L - \theta_U) \cos(\theta_U + \theta_L) \qquad \text{(E7)}$$

$$I_{xx} = \int_{\theta_U}^{\pi+\theta_L} \int_0^r (y_c + r \cos \theta)^2 r \, dr \, d\theta$$

$$= \int_{\theta_U}^{\pi+\theta_L} \left(\frac{y_c^2 r^2}{2} + \frac{2r^3 y_c}{3} \cos \theta + \frac{r^4}{4} \cos^2 \theta \right) d\theta$$

$$= \left(\frac{y_c^2 r^2}{2} \theta \right)_{\theta_U}^{\pi+\theta_L} + \left(\frac{2r^3 y_c}{3} \sin \theta \right)_{\theta_U}^{\pi+\theta_L} + \frac{r^4}{4} \left(\frac{\theta}{2} + \frac{\sin 2\theta}{4} \right)_{\theta_U}^{\pi+\theta_L}$$

$$= \left(y_c + \frac{r^2}{4} \right) A - \frac{2r^3 y_c}{3} (\sin \theta_U + \sin \theta_L) + \frac{r^4}{8} \sin(\theta_L - \theta_U) \cos(\theta_U + \theta_L) \qquad \text{(E8)}$$

$$I_{xy} = \int_{\theta_U}^{\pi+\theta_L} \int_0^r (x_c - r \sin \theta)(y_c + r \cos \theta) r \, dr \, d\theta$$

$$= \int_{\theta_U}^{\pi+\theta_L} \left[\frac{x_c y_c r^2}{2} + \frac{(x_c \cos \theta - y_c \sin \theta) r^3}{3} - \frac{r^4}{4} \sin \theta \cos \theta \right] d\theta$$

$$= \left(\frac{x_c y_c r^2}{2} \theta \right)_{\theta_U}^{\pi+\theta_L} + \left(\frac{x_c r^3}{3} \sin \theta \right)_{\theta_U}^{\pi+\theta_L} + \left(\frac{y_c r^3 \cos \theta}{3} \right)_{\theta_U}^{\pi+\theta_L} - \left(\frac{r^4}{4} \frac{\sin^2 \theta}{2} \right)_{\theta_U}^{\pi+\theta_L} \tag{E9}$$

$$= x_c y_c A - \frac{r^3}{3} \left[x_c (\sin \theta_L + \sin \theta_U) + y_c (\cos \theta_L + \cos \theta_U) \right] - \frac{r^4}{8} (\sin \theta_L - \sin \theta_U)(\sin \theta_L + \sin \theta_U)$$

(E10)

$$I_{yyyy} = \int_{\theta_U}^{\pi+\theta_L} \int_0^r (x_c - r \sin \theta)^4 \, r \, dr \, d\theta$$

$$= \int_{\theta_U}^{\pi+\theta_L} \left(x_c^4 \frac{r^2}{2} - 4x_c^3 \frac{r^3}{3} \sin \theta + 6x_c^2 \frac{r^4}{4} \sin^2 \theta - 4x_c \frac{r^5}{5} \sin^3 \theta + \frac{r^6}{6} \sin^4 \theta \right) d\theta$$

$$= \left(x_c^4 \frac{r^2}{2} \theta \right)_{\theta_U}^{\pi+\theta_L} + 4 \left(x_c^3 \frac{r^3}{3} \cos \theta \right)_{\theta_U}^{\pi+\theta_L} + 6x_c^2 \frac{r^4}{4} \left(\frac{\theta}{2} - \frac{\sin 2\theta}{4} \right)_{\theta_U}^{\pi+\theta_L} + 4x_c \frac{r^5}{5} \left[\frac{\cos \theta}{3} (2 + \sin^2 \theta) \right]_{\theta_U}^{\pi+\theta_L} + \frac{r^6}{6} \left(\frac{3\theta}{8} - \frac{\sin 2\theta}{4} + \frac{\sin 4\theta}{32} \right)_{\theta_U}^{\pi+\theta_L}$$

$$= \left(x_c^4 + \frac{3}{2} x_c^2 r^2 + \frac{r^4}{8} \right) A - r^3 \left\{ \frac{2x_c}{15} \left[\left(10x_c^2 + 4r^2 \right) (\cos \theta_U + \cos \theta_L) + r^2 (\sin 2\kappa_L \sin \kappa_L + \sin \kappa_U \sin 2\kappa_U) \right] \right.$$

$$\left. + \frac{r}{8} \left[\left(3x_c^2 + \frac{r^2}{3} \right) (\sin 2\theta_L - \sin 2\theta_U) - \frac{r}{24} (\sin 4\theta_L - \sin 4\theta_U) \right] \right\}$$

$$I_{xxxx} = \int_{\theta_U}^{\pi+\theta_L} \int_0^r (y_c + r\cos\theta)^4\, r\, dr\, d\theta$$

$$= \int_{\theta_U}^{\pi+\theta_L} \left(y_c^4 \frac{r^2}{2} + 4y_c^3 \frac{r^3}{3}\cos\theta + 6y_c^2 \frac{r^4}{4}\cos^2\theta + 4y_c \frac{r^5}{5}\cos^3\theta + \frac{r^6}{6}\cos^4\theta \right) d\theta$$

$$= \left(y_c^4 \frac{r^2}{2}\theta \right)_{\theta_U}^{\pi+\theta_L} + \frac{4}{3} y_c^3 r^3 (\sin\theta)_{\theta_U}^{\pi+\theta_L} + \frac{3}{2} y_c^2 r^4 \left(\frac{\theta}{2} + \frac{\sin 2\theta}{4} \right)_{\theta_U}^{\pi+\theta_L} + \frac{4}{5} y_c r^5 \left[\frac{\sin\theta}{3}(\cos^2\theta + 2) \right]_{\theta_U}^{\pi+\theta_L} + \frac{r^6}{6}\left(\frac{3\theta}{8} + \frac{\sin 2\theta}{4} + \frac{\sin 4\theta}{32} \right)_{\theta_U}^{\pi+\theta_L}$$

$$= \left(y_c^4 + \frac{3}{2} y_c^2 r^2 + \frac{r^4}{8} \right) A - r^3 \left\{ \frac{2y_c}{15} \left[(10y_c^2 + 4r^2)(\sin\theta_L + \sin\theta_U) + r^2(\sin 2\theta_L \cos\theta_L + \sin 2\theta_U \cos\theta_U) \right] \right.$$
$$\left. - \frac{r}{8} \left[\left(3y_c^2 + \frac{r^2}{3} \right)(\sin 2\theta_L - \sin 2\theta_U) + \frac{r^2}{24}(\sin 4\theta_L - \sin 4\theta_U) \right] \right\} \qquad \textbf{(E11)}$$

$$I_{xxyy} = \int_{\theta_U}^{\pi+\theta_L} \int_0^r (x_c - r\sin\theta)^2 (y_c + r\cos\theta)^2\, r\, dr\, d\theta$$

$$= \int_{\theta_U}^{\pi+\theta_L} \left[x_c^2 y_c^2 \frac{r^2}{2} + 2x_c^2 y_c \frac{r^3}{3}\cos\theta - 2x_c y_c^2 \frac{r^3}{3}\sin\theta + x_c^2 \frac{r^4}{4}\cos^2\theta + y_c^2 \frac{r^4}{4}\sin^2\theta \right.$$
$$\left. - x_c y_c r^4 \sin\theta\cos\theta + \frac{2}{5} r^5 \left(y_c \sin^2\theta\cos\theta - x_c\cos^2\theta\sin\theta \right) + \frac{r^6}{6}\sin^2\theta\cos^2\theta \right] d\theta$$

$$= x_c^2 y_c^2 \frac{r^2}{2}(\theta)_{\theta_U}^{\pi+\theta_L} + \frac{2}{3} x_c^2 y_c r^3 (\sin\theta)_{\theta_U}^{\pi+\theta_L} + \frac{2}{3} x_c y_c^2 r^3 (\cos\theta)_{\theta_U}^{\pi+\theta_L} + \frac{x_c^2 r^4}{4}\left(\frac{\theta}{2} + \frac{\sin 2\theta}{4} \right)_{\theta_U}^{\pi+\theta_L} + \frac{y_c r^4}{4}\left(\frac{\theta}{2} - \frac{\sin 2\theta}{4} \right)_{\theta_U}^{\pi+\theta_L}$$

$$- \frac{x_c y_c r^4}{2}(\sin^2\theta)_{\theta_U}^{\pi+\theta_L} + \frac{2}{15} y_c r^5 (\sin^3\theta)_{\theta_U}^{\pi+\theta_L} + \frac{2}{15} x_c r^5 (\cos^3\theta)_{\theta_U}^{\pi+\theta_L} + \frac{r^6}{48}\left(\frac{2\theta}{2} - \frac{\sin 4\theta}{4} \right)_{\theta_U}^{\pi+\theta_L}$$

$$= \left[x_c^2 y_c^2 + \frac{r^2}{4}\left(x_c^2 + y_c^2 + \frac{r^2}{6} \right) \right] A - r^3 \left(x_c y_c \left\{ \frac{2}{3}\left[x_c(\sin\theta_L + \sin\theta_U) + y_c(\cos\theta_L + \cos\theta_U) \right] + \frac{r}{2}(\sin 2\theta_L - \sin 2\theta_U) \right\} \right.$$
$$\left. + \frac{2}{15} r^2 \left[x_c\left(\cos^3\theta_L + \cos^3\theta_U \right) + y_c\left(\sin^3\theta_L + \sin^3\theta_U \right) \right] - \frac{r}{16}\left[\left(x_c^2 - y_c^2 \right)\left(\sin^2\theta_L - \sin^2\theta_U \right) - \frac{r^2}{12}(\sin 4\theta_L - \sin 4\theta_U) \right] \right)$$

$$\textbf{(E12)}$$

Area and Moments of Trapezoids

In addition to the end circles, values for the two trapezoidal pieces (as shown in fig. 5) are also needed to properly account for the blade-section ends left from the spline integrals. The following equations for the trapezoids use the nomenclature of figure 11:

$$A = \frac{1}{2}(x_c - x_U)(y_U + y_c) + \frac{1}{2}(x_L - x_c)(y_L + y_c)$$

$$= \frac{1}{2}(x_c - x_U)(y_U - y_L) + \frac{1}{2}(x_L - x_U)(y_L + y_c) \tag{E13}$$

$$A\bar{x} = (x_c - x_U)y_c \frac{x_c + x_U}{2} + \frac{1}{2}(x_c - x_U)(y_U - y_c)\frac{2x_U + x_c}{3} + (x_L - x_c)y_L \frac{x_c + x_L}{2}$$

$$+ \frac{1}{2}(x_L - x_c)(y_c - y_L)\frac{2x_c + x_L}{3}$$

$$= \frac{x_c - x_U}{6}\left[y_c(2x_c + x_U) + y_U(2x_U + x_c)\right] + \frac{x_L - x_c}{6}\left[y_L(x_c + 2x_L) + y_c(2x_c + x_L)\right] \tag{E14}$$

$$A\bar{y} = (x_c - x_U)y_c \frac{y_c}{2} + \frac{1}{2}(x_c - x_U)(y_U - y_c)\frac{y_U + 2y_c}{3} + (x_L - x_c)y_L \frac{y_L}{2} + \frac{1}{2}(x_L - x_c)$$

$$\times (y_c - y_L)\frac{y_c + 2y_L}{3}$$

$$= \frac{x_c - x_U}{6}\left(y_U^2 + y_U y_c + y_c^2\right) + \frac{x_L - x_c}{6}\left(y_L^2 + y_c y_L + y_c^2\right) \tag{E15}$$

Higher moments for the trapezoidal-shaped pieces are needed in the terminal calculations. The values of these higher moments were found by integration. For the trapezoid with a corner at the suction-surface-curve end point,

$$y = y_c + (x - x_c)\frac{y_U - y_c}{x_U - x_c}$$

The form of this equation for integration is $a + bx$ where

$$a = y_c - x_c \frac{y_U - y_c}{x_U - x_c}$$

and

$$b = \frac{y_U - y_c}{x_U - x_c}$$

$$
\begin{aligned}
I_{yy} &= \int_{x_U}^{x_c} \int_0^y x^2 \, dy \, dx + \int_{x_c}^{x_L} \int_0^y x^2 \, dy \, dx = \int_{x_U}^{x_c} y x^2 \, dx + \int_{x_c}^{x_L} y x^2 \, dx \\
&= \int_{x_U}^{x_c} \left(y_c - x_c \frac{y_U - y_c}{x_U - x_c}\right) x^2 \, dx + \int_{x_U}^{x_c} \left(\frac{y_U - y_c}{x_U - x_c}\right) x^3 \, dx + \int_{x_c}^{x_L} \left(y_c - x_c \frac{y_L - y_c}{x_L - x_c}\right) x^2 \, dx + \int_{x_c}^{x_L} \frac{y_L - y_c}{x_L - x_c} x^3 \, dx \\
&= \left[\left(y_c - x_c \frac{y_U - y_c}{x_U - x_c}\right)\frac{x^3}{3}\right]_{x_U}^{x_c} + \left(\frac{y_U - y_c}{x_U - x_c} \frac{x^4}{4}\right)_{x_U}^{x_c} + \left[\left(y_c - x_c \frac{y_L - y_c}{x_L - x_c}\right)\frac{x^3}{3}\right]_{x_c}^{x_L} + \left(\frac{y_L - y_c}{x_L - x_c} \frac{x^4}{4}\right)_{x_c}^{x_L} \\
&= (x_c - x_U)\left\{\frac{1}{3}\left(y_c - x_c \frac{y_U - y_c}{x_U - x_c}\right)\left(x_c^2 + x_c x_U + x_U^2\right) + \frac{1}{4}\frac{y_U - y_c}{x_U - x_c}\left[x_c\left(x_c^2 + x_c x_U + x_U^2\right) + x_U^3\right]\right\} \\
&\quad + (x_L - x_c \left\{\frac{1}{3}\left(y_c - x_c \frac{y_L - y_c}{x_L - x_c}\right)\left(x_L^2 + x_L x_c + x_c^2\right) + \frac{1}{4}\frac{y_L - y_c}{x_L - x_c}\left[x_L^3 + \left(x_L^2 + x_L x_c + x_c^2\right)x_c\right]\right\} \\
&= \frac{(x_c - x_U)y_c}{3}\left(x_c^2 + x_c x_U + x_U^2\right) + \frac{x_c(y_U - y_c)}{12}\left(x_c^2 + x_c x_U + x_U^2\right) - \frac{y_U - y_c}{4} x_U^3 \\
&\quad + \frac{(x_L - x_c)y_c}{3}\left(x_c^2 + x_c x_L + x_L^2\right) - \frac{x_c(y_L - y_c)}{12}\left(x_c^2 + x_c x_L + x_L^2\right) + \frac{y_L - y_c}{4} x_L^3 \qquad \text{(E16)}
\end{aligned}
$$

$$I_{xx} = \int_{x_U}^{x_c} \int_0^{y} y^2\, dy\, dx + \int_{x_c}^{x_L} \int_0^{y} y^2\, dy\, dx = \int_{x_U}^{x_c} \frac{y^3}{3}\, dx + \int_{x_c}^{x_L} \frac{y^3}{3}\, dx$$

$$= \int_{x_U}^{x_c} \frac{(a_U + b_U x)^3}{3}\, dx + \int_{x_c}^{x_L} \frac{(a_L + b_L x)^3}{3}\, dx = \left[\frac{(a_U + b_U x)^4}{12b}\right]_{x_U}^{x_c} + \left[\frac{(a_L + b_L x)^4}{12b}\right]_{x_c}^{x_L}$$

$$= \left\{\frac{\left[y_c + (x - x_c)\dfrac{y_U - y_c}{x_U - x_c}\right]^4}{12\dfrac{y_U - y_c}{x_U - x_c}}\right\}_{x_U}^{x_c} + \left\{\frac{\left[y_c + (x - x_c)\dfrac{y_L - y_c}{x_L - x_c}\right]^4}{12\dfrac{y_L - y_c}{x_L - x_c}}\right\}_{x_c}^{x_L} \qquad \text{(E17)}$$

$$= \frac{(x_U - x_c)\left(y_c^4 - y_U^4\right)}{12(y_U - y_c)} + \frac{(x_L - x_c)\left(y_L^4 - y_c^4\right)}{12(y_L - y_c)} = -\frac{x_U - x_c}{12}\left(y_c^3 + y_c^2 y_U + y_c y_U^2 + y_U^3\right) + \frac{x_L - x_c}{12}\left(y_c^3 + y_c^2 y_L + y_c y_L^2 + y_L^3\right)$$

$$I_{xy} = \int_{x_U}^{x_c} \int_0^{y} xy\, dy\, dx + \int_{x_c}^{x_L} \int_0^{y} xy\, dy\, dx$$

$$= \int_{x_U}^{x_c} \frac{(a_U + b_U x)^2}{2}\, x\, dx + \int_{x}^{x_L} \frac{(a_L + b_L x)^2}{2}\, x\, dx = \left[\frac{(a_U + b_U x)^4}{8b^2} - \frac{a(a_U + b_U x)^3}{6b^2}\right]_{x_U}^{x_c} + \left[\frac{(a_L + b_L x)^4}{8b^2} - \frac{a(a_L + b_L x)^3}{6b^2}\right]_{x_c}^{x_L}$$

$$= \left\{\frac{\left[y_c + (x - x_c)\dfrac{y_U - y_c}{x_U - x_c}\right]^4}{8\left(\dfrac{y_U - y_c}{x_U - x_c}\right)^2} - \frac{\left(y_c - x_c\dfrac{y_U - y_c}{x_U - x_c}\right)\left[y_c + (x - x_c)\dfrac{y_U - y_c}{x_U - x_c}\right]^3}{6\left(\dfrac{y_U - y_c}{x_U - x_c}\right)^2}\right\}_{x_U}^{x_c} + \left\{\frac{\left[y_c + (x - x_c)\dfrac{y_L - y_c}{x_L - x_c}\right]^4}{8\left(\dfrac{y_L - y_c}{x_L - x_c}\right)^2} - \frac{\left(y_L - x_c\dfrac{y_L - y_c}{x_L - x_c}\right)\left[y_c + (x - x_c)\dfrac{y_L - y_c}{x_L - x_c}\right]^3}{6\left(\dfrac{y_L - y_c}{x_L - x_c}\right)^2}\right\}_{x_c}^{x_L}$$

$$= -\frac{x_U - x_c}{24}\left[x_U\left(3y_U^2 + 2y_U y_c + y_c^2\right) + x_c\left(y_U^2 + 2y_U y_c + 3y_c^2\right)\right] + \frac{x_L - x_c}{24}\left[x_L\left(3y_L^2 + 2y_L y_c + y_c^2\right) + x_c\left(y_L^2 + 2y_L y_c + 3y_c^2\right)\right]$$

(E18)

$$I_{yyyy} = \int_{x_U}^{x_c} \int_0^{y} x^4 \, dy \, dx + \int_{x_c}^{x_L} \int_0^{y} x^4 \, dy \, dx$$

$$= \int_{x_U}^{x_c} (a_U + b_U x) x^4 \, dx + \int_{x_c}^{x_L} (a_L + b_L x) x^4 \, dx = \frac{a_U}{5}\left(x_c^5 - x_U^5\right) + \frac{b_U}{6}\left(x_c^6 - x_U^6\right) + \frac{a_L}{5}\left(x_L^5 - x_c^5\right) + \frac{b_L}{6}\left(x_L^6 - x_c^6\right)$$

$$= \frac{y_c}{5}(x_c - x_U)\left(x_c^4 + x_c^3 x_U + x_c^2 x_U^2 + x_c x_U^3 + x_U^4\right) + \frac{y_U - y_c}{30} x_c\left(x_c^4 + x_c^3 x_U + x_c^2 x_U^2 + x_c x_U^3 + x_U^4\right)$$

$$- \frac{y_U - y_c}{6} x_U^5 + \frac{y_c}{5}(x_L - x_c)\left(x_L^4 + x_L^3 x_c + x_L^2 x_c^2 + x_L x_c^3 + x_L^4\right) - \frac{y_L - y_c}{30} x_c\left(x_L^4 + x_L^3 x_c + x_L^2 x_c^2 + x_L x_c^3 + x_c^4\right) + \frac{y_L - y_c}{6} x_L^5 \tag{E19}$$

$$I_{xxxx} = \int_{x_U}^{x_c} \int_0^{y} y^4 \, dy \, dx + \int_{x_c}^{x_L} \int_0^{y} y^4 \, dy \, dx = \int_{x_U}^{x_c} \frac{(a_U + b_U x)^5}{5} \, dx + \int_{x_c}^{x_L} \frac{(a_L + b_L x)^5}{5} \, dx$$

$$= \left[\frac{(a_U + b_U x)^6}{30b}\right]_{x_U}^{x_c} + \left[\frac{(a_L + b_L x)^6}{30b}\right]_{x_c}^{x_L} = \left\{\frac{\left[y_c + (x - x_c)\dfrac{y_U - y_c}{x_U - x_c}\right]^6}{30\,\dfrac{y_U - y_c}{x_U - x_c}}\right\}_{x_U}^{x_c} + \left[\frac{y_c + (x - x_c)\dfrac{y_L - y_c}{x_L - x_c}}{30\,\dfrac{y_L - y_c}{x_L - x_c}}\right]_{x_c}^{x_L}$$

$$= -\frac{(x_U - x_c)\left(y_c^5 + y_c^4 y_U + y_c^3 y_U^2 + y_c^2 y_U^3 + y_c y_U^4 y_U^5\right)}{30} + \frac{(x_L - x_c)\left(y_L^5 + y_L^4 y_c + y_L^3 y_c^2 + y_L^2 y_c^3 + y_L y_c^4 + y_c^5\right)}{30} \tag{E20}$$

$$I_{xxyy} = \int_{x_U}^{x_c} \int_0^{y} x^2 y^2 \, dy \, dx + \int_{x_c}^{x_L} \int_0^{y} x^2 y^2 \, dy \, dx \; [illegible]$$

$$= \frac{1}{3b_U^3} \left[\frac{(a_U + b_U x)^6}{6} - 2a \frac{(a_U + b_U x)^5}{5} + a^2 \frac{(a_U + b_U x)^4}{4} \right]_{x_U}^{x_c} + \frac{1}{3b_L^3} \left[[illegible] \frac{(a_L + b_L x)^4}{4} \right]_{x_c}^{x_L}$$

$$= \frac{(x_U - x_c)^3}{3(y_U - y_c)^3} \left\{ \frac{y_c^6 - y_U^6}{6} - \frac{2}{5}\left(y_c - x_c \frac{y_U - y_c}{x_U - x_c} \right)\left(y_c^5 - y_U^5 \right) + \frac{1}{4}\left[y_c^2 - 2x_c y_c \frac{y_U - y_c}{x_U - x_c} + x_c^2 \left(\frac{y_U - y_c}{x_U - x_c} \right)^2 \right] [illegible] \right.$$

$$+ \frac{(x_L - x_c)^3}{3(y_L - y_c)^3} \left\{ \frac{y_L^6 - y_c^6}{6} - \frac{2}{5}\left(y_c - x_c \frac{y_L - y_c}{x_L - x_c} \right)\left(y_L^5 - y_c^5 \right) + \frac{1}{4}\left[y_c^2 - 2x_c y_c \frac{y_L - y_c}{x_L - x_c} + x_c^2 \left(\frac{y_L - y_c}{x_L - x_c} \right)^2 \right] [illegible] \right.$$

$$= -\frac{x_U - x_c}{180} \left[x_U^2 \left(10y_U^3 + 6y_U^2 y_c + 3y_U y_c^2 + y_c^3 \right) + x_U x_c \left(4y_U^3 + 6y_U^2 y_c + 6y_U y_c^2 + 4y_c^3 \right) + x_c^2 \left(y_U^3 + 3y_U^2 y_c + 6y_U y_c^2 + 10y_c^3 \right) \right]$$

$$+ \frac{x_L - x_c}{180} \left[x_L^2 \left(10y_L^3 + 6y_L^2 y_c + 3y_L y_c^2 + y_c^3 \right) + x_L x_c \left(4y_L^3 + 6y_L^2 y_c + 6y_L y_c^2 + 4y_c^3 \right) + x_c^2 \left(y_L^3 + 3y_L^2 y_c + 6y_L y_c^2 + 10y_c^3 \right) \right]$$

(E21)

APPENDIX F

DEVELOPMENT OF BLADE BENDING MOMENT EQUATIONS

The centrifugal force on a blade mass element dm is

$$dF = dm \cdot a$$

$$dF = dm \cdot \omega^2 \cdot r \qquad \text{(F1)}$$

For a thin blade section, this force is approximated by

$$dF = \frac{\rho A\, dr}{12g}\omega^2 r \qquad \text{(F2)}$$

A corresponding bending moment on this blade element is

$$dM = dF \cdot l \qquad \text{(F3)}$$

Bending Moment from Centrifugal Force Acting with a Meridional Plane Lever

The net effect of centrifugal force on a thin blade section can be considered as a summed force acting at the center of area of the blade section. This force acting with a lever arm in the meridional plane can be expressed as

$$dM = dF \frac{r - r_h}{12} \tan \lambda$$

where λ is the stacking-axis lean shown in figure 12.

$$M_a = \int_{r_h}^{r_t} \frac{\rho\omega^2 \tan \lambda}{144g} Ar(r - r_h)dr = \left[\frac{\rho\omega^2}{144g} \sum_{j=1}^{J} Ar(r - r_h)h\right] \tan \lambda = (C_a)\tan \lambda \qquad \text{(F4)}$$

Definition of Tip Volume Element for Moment Corrections

When the end streamlines are sloped, the previous summation is not complete. The wedge-shaped excess and decrement masses from the tip blade section should be accounted for because their centers of mass are far from the stacking axis (fig. 7). The material at the hub, for practical purposes, can be considered as part of the blade base; so no moment correction is made for the offset hub material.

The reference plane for excess volume definition passes through the stacking-line intersection of the end of the blade at the tip (fig. 12). The height of an element of excess volume is the radial distance from the local tip edge of the blade to the reference plane. The side surfaces of an element of volume are approximated by radial projection of the reference section shape. In the tip region, the blade camber is usually quite small; so a simple linear fit between the blade-section definition points was used. The resulting equation for the path between surface points is a line

$$y = \frac{y_k(x - x_{k-1}) + y_{k-1}(x_k - x)}{x_k - x_{k-1}} \tag{F5}$$

The moments are needed in the axial and tangential directions. Since the wedge elements are also more naturally defined in an axial-normal coordinate system, the surface definition equations are redefined in the rotated coordinates shown in figure 13.

$$z = x \cos \gamma - y \sin \gamma \tag{F6}$$

$$n = x \sin \gamma + y \cos \gamma \tag{F7}$$

The coordinate z is the new independent variable, and n is the new dependent variable. To get a relation between x and z, use equation (F5) in (F6). The result is

$$x = \frac{z(x_k - x_{k-1}) - (y_k x_{k-1} - y_{k-1} x_k)\sin \gamma}{(x_k - x_{k-1})\cos \gamma - (y_k - y_{k-1})\sin \gamma} \tag{F8}$$

Substitution of equations (F5) and (F8) into (F7) gives the rotated form for n in terms of knowns and the independent variable

$$n = \frac{\left[(x_k - x_{k-1})\sin \gamma + (y_k - y_{k-1})\cos \gamma\right] z + y_{k-1}x_k - y_k x_{k-1}}{(x_k - x_{k-1})\cos \gamma - (y_k - y_{k-1})\sin \gamma} \tag{F9}$$

For integration purposes, equation (F9) is expressed as

$$n = Az + B$$

where

$$A = \frac{(x_k - x_{k-1})\sin\gamma + (y_k - y_{k-1})\cos\gamma}{(x_k - x_{k-1})\cos\gamma - (y_k - y_{k-1})\sin\gamma}$$

and

$$B = \frac{y_{k-1}x_k - y_k x_{k-1}}{(x_k - x_{k-1})\cos\gamma - (y_k - y_{k-1})\sin\gamma}$$

Tip Correction Moment for Centrifugal Force Acting in Meridional Plane

The bending moment associated with forces acting in the meridional plane is defined as positive in the counterclockwise direction in figure 12. The differential moment for the tip correction can be expressed as

$$dM = dm\ \omega^2\bar{r}l$$

where $\bar{r}$ is the average element radius

$$\therefore \qquad dM\ \frac{\rho}{g}\ d(Vol)\omega^2\bar{r}l$$

$$dM = \frac{\rho}{144g}(n_s - n_p)z \tan\alpha\ dz\ \omega^2\bar{r}\left[z + (r_t - r_h)\tan\lambda\right] \qquad \text{(F10)}$$

The tip correction from the center of the leading-edge circle to the center of the trailing-edge circle is

$$M_{da} = \int_{z_{le}}^{z_{te}} \frac{\rho\omega^2}{144g} \tan\alpha (n_s - n_p)\bar{r} z \left[z + (r_t - r_h)\tan\lambda\right] dz$$

$$= \frac{\rho\omega^2 \tan\alpha}{144g} \sum_{n=1}^{N} \bar{r} \int_{z_{n-1}}^{z_n} \left[A_s z + B_s - (A_p z + B_p)\right] z \left[z + (r_t - r_h)\tan\lambda\right] dz$$

The integral is applicable between surface points after the equations for line segments have been substituted. Since the constants change for a point on either surface, the number of summation terms is 2k - 2, where k is the number of points on each surface. The term $\bar{r}$ was removed from the integral because it is relatively independent of z for the integration increment between surface points.

$$M_{da} = \frac{\rho\omega^2 \tan\alpha}{144g} \sum_{n=1}^{N} \bar{r} \left\{ \int_{z_{n-1}}^{z_n} \left[(A_s - A_p)z^3 + (B_s - B_p)z^2\right] dz + (r_t - r_h)\tan\lambda \int_{z_{n-1}}^{z_n} \left[(A_s - A_p)z^2 + (B_s - B_p)z\right] dz \right\}$$

$$= \frac{\rho\omega^2 \tan\alpha}{144g} \sum_{n=1}^{N} \bar{r} \left\{ \left[(A_s - A_p)\frac{z^4}{4}\right]_{z_{n-1}}^{z_n} + \left[(B_s - B_p)\frac{z^3}{3}\right]_{z_{n-1}}^{z_n} + (r_t - r_h)\tan\lambda \left[(A_s - A_p)\frac{z^3}{3} + (B_s - B_p)\frac{z^2}{2}\right]_{z_{n-1}}^{z_n} \right\}$$

$$= \frac{\rho\omega^2 \tan\alpha}{144g} \sum_{n=1}^{N} \left(r_t + \frac{z_n + z_{n-1}}{4}\tan\alpha\right)(z_n - z_{n-1})$$

$$\cdot \left\{\frac{A_s - A_p}{4}\left(z_n^3 + z_n^2 z_{n-1} + z_n z_{n-1}^2 + z_{n-1}^3\right) + \frac{B_s - B_p}{3}\left(z_n^2 + z_n z_{n-1} + z_{n-1}^2\right) + (r_t - r_h)\tan\lambda\left[\frac{A_s - A_p}{3}\left(z_n^2 + z_n z_{n-1} + z_{n-1}^2\right) + \frac{B_s - B_p}{2}\left(z_n + z_{n-1}\right)\right]\right\}$$

$$= D_a + C_{da}\tan\lambda \qquad \text{(F11)}$$

The previous summation carried from the leading-edge-circle center to the trailing-edge-circle center. The edge circles have the largest element height, so they are accounted for too. The approximations used are illustrated in figure 14. An end semicircle is used, with the shaded areas considered to approximately compensate each other. The center of area of the end semicircle is $4r_e/3\pi$ from the circle center. The end-circle moment additions are expressed as

$$M_{da} = \frac{\rho\omega^2\bar{r}}{144g}\,\frac{\pi r_e^2}{2}\,(z_e \tan\alpha)\left[z_e \pm \frac{4r_e}{3\pi} + (r_t - r_h)\tan\lambda\right] \qquad \text{(F12)}$$

The minus sign is used for the leading-edge circle, and the plus sign for the trailing-edge circle.

Stacking-Axis Lean Angle from a Moment Balance in Meridional Plane

When equations (F4), (F11), and (F12) are summed, the bending moment due to centrifugal force of the blade mass is expressed in terms of the lean angle λ as

$$M_a = D_a + C_a \tan \lambda \tag{F13}$$

The lean angle which will balance the axial component of the steady-state gas bending moment M_{ba} is then readily available from the moment balance

$$M_{ba} + M_a = 0$$

$$M_{ba} + D_a + C_a \tan \lambda = 0$$

so

$$\tan \lambda = - \frac{M_{ba} + D_a}{C_a} \tag{F14}$$

Stacking-Axis Lean Angle from a Moment Balance in r-θ Plane

The procedure of determining a stacking-axis lean angle in the r-θ plane is similar to that used in the meridional plane. The bending moment produced in the r-θ plane by centrifugal force acting at the center of area of blade sections has the same form as equation (F4),

$$M_t = (C_t)\tan \eta \tag{F15}$$

where C_t is equal to the C_a of equation (F4). The moment is positive in the counter-rotational direction.

For the tip correction moment, the differential moment arm is expressed with a different equation; so it is necessary to go through a separate development.

$$dM = \frac{\rho}{144g} (n_s - n_p) z \tan \alpha \, dz \, \omega^2 \bar{r} \left[- \frac{n_s + n_p}{2} + (r_t - r_h) \tan \eta \right]$$

$$M_{dt} = \frac{\rho \omega^2 \tan \alpha}{144g} \sum_{n=1}^{N} \bar{r} \int_{z_{n-1}}^{z_n} \left[A_s z + B_s - (A_p z + B_p) \right] z \left[- \frac{A_s z + B_s + A_p z + B_p}{2} + (r_t - r_h) \tan \eta \right] dz$$

$$= - \frac{\rho \omega^2 \tan \alpha}{144g} \sum_{n=1}^{N} \left(r_t + \frac{z_n + z_{n-1}}{4} \tan \alpha \right) (z_n - z_{n-1}) \left\{ \frac{A_s^2 - A_p^2}{8} (z_n^3 + z_n^2 z_{n-1} + z_n z_{n-1}^2 + z_{n-1}^3) + \frac{A_s B_s - A_p B_p}{3} (z_n^2 + z_n z_{n-1} + z_{n-1}^2) \right.$$

$$\left. + \frac{B_s^2 - B_p^2}{4} (z_n + z_{n-1}) - \left[\frac{A_s - A_p}{3} (z_n^2 + z_n z_{n-1} + z_{n-1}^2) + \frac{B_s - B_p}{2} (z_n + z_{n-1}) \right] (r_t - r_h) \tan \eta \right\}$$

$$= D_t + C_{dt} \tan \eta \qquad \text{(F16)}$$

For the end semicircles, the equation is

$$M_{dt} = \frac{\rho \omega^2 \bar{r}}{144g} \frac{\pi r_e^2}{2} z_e \tan \alpha \left[- n_e + (r_t - r_h) \tan \eta \right] \qquad \text{(F17)}$$

When equations (F15), (F16), and (F17) are summed, the moment equation in terms of the tangential lean angle is

$$M_t = D_t + C_t \tan \eta$$

The gas bending mom nt M_{bt} is calculated with the opposite sign convention of the moment produced by centrifugal force. Thus, the moment balancing equation in the r-θ plane is

$$M_t - M_{bt} = 0$$

$$D_t + C_t \tan \eta = M_{bt}$$

$$\tan \eta = \frac{M_{bt} - D_t}{C_t} \qquad \text{(F18)}$$

Blade-Element Coordinate Adjustments Associated with Stacking-Axis Lean Adjustments

The blade-edge coordinates change with changes in stacking-axis lean. These changes can be approximated by blade-element translations on the cone. Thus, the shift of blade-edge coordinates for a blade element is assumed to be the same as the shift of the stacking-axis intersection with the blade element. The geometry associated with the shifts is shown in figure 15, where λ_n is the new stacking-axis lean in the meridional plane and λ_0 is the stacking-axis lean from the previous iteration. The equations for the three lines are

$$r_n - r_0 = (z_n - z_0)\tan \alpha \tag{F19}$$

$$z_0 - z_h = (r_0 - r_h)\tan \lambda_0 \tag{F20}$$

$$z_n - z_h = (r_n - r_h)\tan \lambda_n \tag{F21}$$

To eliminate z_h, subtract equation (F20) from (F21).

$$z_n - z_0 = (r_n - r_h)\tan \lambda_n - (r_0 - r_h)\tan \lambda_0$$

Then, to eliminate r_n, use equation (F19) in the preceding equation. The z shift can be expressed as

$$z_n - z_0 = \frac{(r_0 - r_h)(\tan \lambda_n - \tan \lambda_0)}{1 - \tan \alpha \tan \lambda_n} \tag{F22}$$

The r shift from the use of equation (F22) in (F19) is

$$r_n - r_0 = \frac{(r_0 - r_h)(\tan \lambda_n - \tan \lambda_0)}{1 - \tan \alpha \tan \lambda_n} \tan \alpha \tag{F23}$$

The blade stacking-axis lean angle λ is not directly stored in the program. It is calculated from stacking reference points at the hub and tip. Since the hub point is the fixed reference stacking point, it is necessary to relocate a point at the tip to conform with the new λ. The new tip reference point will be assumed to lie on a line which passes through the old reference point with the slope of the tip blade-element cone.

Since the tip casing wall may be curved, the new tip reference point may be slightly off the physical wall; but this is of no consequence since the point is only used for a stacking-point reference. The equation used for $z_n - z_0$ in the program appears different from equation (F22), but it is the one obtained by using equation (F20) in (F22) to eliminate λ_0.

APPENDIX G

BLADE-ANGLE CORRECTION FROM LOCAL STREAMLINE SLOPE TO LAYOUT-CONE SLOPE

The differential blade-element-edge angle correction from a local direction α to the layout-cone direction α_c is illustrated in figure 16. The equation used to express the relation is

$$\tan \kappa_c = \frac{r\, d\theta_c}{dm_c} = \frac{r\, d\theta - r \frac{\partial \theta}{\partial r}(dr - dr_c)}{dm_c}$$

$$= \frac{r\, d\theta}{dm}\left(\frac{dm}{dm_c}\right) - r\frac{\partial \theta}{\partial r}\,\frac{(dm)\sin \alpha - (dm_c)\sin \alpha_c}{dm_c}$$

$$= \frac{r\, d\theta}{dm}\left(\frac{\dfrac{dz}{\cos \alpha}}{\dfrac{dz}{\cos \alpha_c}}\right) - r\frac{\partial \theta}{\partial r}\,\frac{\left(\dfrac{dz}{\cos \alpha}\right)\sin \alpha - \left(\dfrac{dz}{\cos \alpha_c}\right)\sin \alpha_c}{\dfrac{dz}{\cos \alpha_c}}$$

$$= \tan \kappa_{st}\frac{\cos \alpha_c}{\cos \alpha} - r\frac{\partial \theta}{\partial r}\,\frac{\cos \alpha_c \sin \alpha - \cos \alpha \sin \alpha_c}{\cos \alpha}$$

$$= \tan \kappa_{st}\frac{\cos \alpha_c}{\cos \alpha} - r\frac{\partial \theta}{\partial r}\,\frac{\sin(\alpha - \alpha_c)}{\cos \alpha} \qquad \text{(G1)}$$

In equation (G1) the blade angle on the layout cone is expressed in terms of the α direction angles, the blade-edge angle on the local streamline, and $r(\partial\theta/\partial r)$. The only unknown is $r(\partial\theta/\partial r)$, which must be determined from a fit of blade-element end points across stacked adjacent blade elements. Since the blade-element end points were set up in a common coordinate system in subroutine POINTS, the end points are curve fit directly for the slope $r(d\theta/d\ell)$. Since for normal blading the slope is relatively low, a simple three-point parabolic curve fit was considered adequate.

The curve-fit value, $r(d\theta/d\ell)$, can be related to $r(\partial\theta/\partial r)$ through the directional derivatives associated with the geometry shown in figure 17.

$$r \frac{d\theta}{dl} = r \frac{\partial\theta}{\partial r} \frac{dr}{dl} + r \frac{\partial\theta}{\partial z} \frac{dz}{dl} = r \frac{\partial\theta}{\partial r} \cos \lambda + r \frac{\partial\theta}{\partial z} \sin \lambda \tag{G2}$$

Another equation in terms of the known partials is the one for the definition of the blade angle on the cone.

$$\tan \kappa_c = r \frac{d\theta}{dm_c} = r \frac{\partial\theta}{\partial r} \frac{dr}{dm_c} + r \frac{\partial\theta}{\partial z} \frac{dr}{dm_c} = r \frac{\partial\theta}{\partial r} \sin \alpha_c + r \frac{\partial\theta}{\partial z} \cos \alpha_c \tag{G3}$$

The elimination of $\partial\theta/\partial z$ between equations (G2) and (G3) yields an expression for $r(\partial\theta/\partial r)$. After some trigonometric manipulation, the equation can be expressed as

$$r \frac{\partial\theta}{\partial r} = r \frac{d\theta}{dl} \frac{\cos \alpha_c}{\cos(\alpha_c + \lambda)} - \tan \kappa_c \frac{\lambda}{\cos(\alpha_c + \lambda)} \tag{G4}$$

Now there is a choice either of substituting equation (G4) into (G1) so that $r(d\theta/dl)$ is stored and used directly or of using these equations separately so that $r(d\theta/dr)$ is stored. The latter approach was used in the program because of procedural considerations. First, note that it is not desirable to compute $r(d\theta/dl)$ as needed when calculating successive streamlines because a different level of iteration would have been made on the ends of the curve used for the fit. So instead, curve fits for $r(d\theta/dl)$ are made after the same level of iterative adjustments has been made for all blade elements. Secondly, the direction of l changes during stacking-axis lean adjustments, so it was considered fundamentally better to save $r(d\theta/dr)$ between iterations since the derivative direction is constant. Thus, the procedure in the program is to obtain $r(d\theta/dr)$ values from equation (G4) with the curve-fit value of $r(d\theta/dl)$. These $r(d\theta/dr)$ values are stored between stacking iterations so that they can be used in equation (G1) when needed.

APPENDIX H

DEVELOPMENT OF EQUATIONS FOR TORSION CONSTANT

The torsion constant is a geometry parameter which is used for both stress and blade untwist deflection calculations. It is defined in reference 6 as

$$K = \frac{\frac{1}{3} F}{1 + \frac{4}{3} \frac{F}{AU^2}} \tag{31}$$

where

$$F = \int_0^U t^3 \, dU$$

A is the section area, t is the thickness normal to the blade-section median line, and U is the length of the blade-section median line. The blade-section geometry parameters are illustrated in figure 18.

Unfortunately, the blade sections are not defined in terms of a median line and thickness. They are defined by 13 points on each surface. These points, however, have already been curve fit for the purposes of determining blade-section areas and moments. The surface curves provide sufficient information to calculate a blade-section thickness everywhere. The trace of the median points of these thickness paths defines the median line.

While this approach is good in principle, it is difficult to apply in the full differential form because the general equation for t is too complicated for the subsequent integrations. So instead, the principles are applied in a piecewise way from the surface definition points. Specific thickness paths are calculated at the surface definition points. The median path passes through the midpoints of these thickness paths. The slope of the median line at these points is the average of the surface curve slopes at the end points of the thickness path. Then using the centerline path as the independent variable, a general thickness is defined by a cubic curve fit of the end thicknesses and the slope differences between the suction and pressure slopes at the ends of the segment-end thickness paths. A more detailed description of the procedure follows.

Definition of Blade-Section Thickness at Pressure-Surface Points

Let the piecewise segment junctions be at the pressure-surface definition points. At these points, the thickness path t, which is shown in figure 19, satisfies the angle condition

$$\alpha_a = \frac{\alpha_s + \alpha_p}{2} \tag{H1}$$

On the suction surface, the point which satisfies this condition will generally be offset from the corresponding suction-surface definition point. The suction-surface point which satisfies the angle condition is found with a simple iterative procedure. For the first trial, the suction-surface point corresponding to the current pressure-surface point is used. The angle λ is defined from a trial suction-surface point as

$$\tan \lambda = \frac{x_p - x_s}{y_s - y_p} \tag{H2}$$

The convergence criterion is then expressed as $|\alpha_a - \lambda| < 0.0001$.

When the convergence criterion is not satisfied, the point adjustment mechanism is derived from an assumption of negligible suction-surface slope change for the adjustment increment. An equation for the new point along the suction surface is

$$\tan \alpha_s = \frac{y_s - y_{sn}}{x_s - x_{sn}} \tag{H3}$$

An equation for the new point along the thickness path is

$$\tan \alpha_a = \frac{x_p - x_{sn}}{y_{sn} - y_p} \tag{H4}$$

Upon elimination of y_{sn} between equations (H3) and (H4), the equation for x_{sn} is

$$x_{sn} = x_s + \frac{(y_p - y_s)\tan \alpha_a + (x_p - x_s)}{1 + \tan \alpha_a \tan \alpha_s} \tag{H5}$$

This value of x_{sn} is used in the spline equation for the appropriate suction-surface segment to get y_{sn} and α_s for the new point.

When the convergence criterion is satisfied, t is expressed as

$$t = \sqrt{(x_{sn} - x_p)^2 + (y_{sn} - y_p)^2} \tag{H6}$$

Median Line Length of a Segment

The thicknesses and their associated directions at the end points of a segment are used to define the segment centerline-path length shown in figure 20. The centerline path passes through the midpoints of the segment-end thicknesses. The straightline length between the points is

$$l = \frac{\sqrt{(x_{p,k} + x_{s,k} - x_{p,k-1} - x_{s,k-1})^2 + (y_{p,k} + y_{s,k} - y_{p,k-1} - y_{s,k-1})^2}}{2} \tag{H7}$$

The path u_k has an angle difference of $\alpha_{a,k-1} - \alpha_{a,k}$ between the ends. If it is assumed that the path is a circular arc, the path u_k is expressed as

$$u_k = 2R\,\frac{\alpha_{a,k-1} - \alpha_{a,k}}{2} = 2\,\frac{\frac{l}{2}}{\sin\frac{\alpha_{a,k-1} - \alpha_{a,k}}{2}}\,\frac{\alpha_{a,k-1} - \alpha_{a,k}}{2}$$

$$= l\,\frac{\frac{\alpha_{a,k-1} - \alpha_{a,k}}{2}}{\frac{\alpha_{a,k-1} - \alpha_{a,k}}{2} - \frac{1}{6}\left(\frac{\alpha_{a,k-1} - \alpha_{a,k}}{2}\right)^3 + \frac{1}{120}\left(\frac{\alpha_{a,k-1} - \alpha_{a,k}}{2}\right)^5 + \ldots}$$

$$\approx \frac{l}{1 - \frac{1}{6}\left(\frac{\alpha_{a,k-1} - \alpha_{a,k}}{2}\right)^2 + \frac{1}{120}\left(\frac{\alpha_{a,k-1} - \alpha_{a,k}}{2}\right)^4} \tag{H8}$$

Definition of a General Blade-Section Thickness

A general cubic equation for the thickness of a segment is

$$t = a + bu + cu^2 + du^3 \tag{H9}$$

Two conditions for the evaluation of the four constants are known thickness at the ends, or

$$t = t_{k-1} \quad \text{at} \quad u = 0 \tag{H10}$$

and

$$t = t_k \quad \text{at} \quad u = u_k \tag{H11}$$

The other two conditions come from the slope difference between the surfaces at the segment ends.

$$s_k = \tan(\alpha_{s,k} - \alpha_{p,k}) = \frac{\tan \alpha_{s,k} - \tan \alpha_{p,k}}{1 + \tan \alpha_{s,k} \tan \alpha_{p,k}} \tag{H12}$$

They are expressed as

$$s = s_{k-1} \quad \text{at} \quad u = 0 \tag{H13}$$

$$s = s_k \quad \text{at} \quad u = u_k \tag{H14}$$

Application of the condition expressed by equation (H10) directly gives

$$a = t_{k-1} \tag{H15}$$

The derivative of equation (H9) is

$$\frac{dt}{du} = b + 2cu + 3du^2 \tag{H16}$$

Application of the condition expressed by equation (H13) directly gives

$$b = s_{k-1} \tag{H17}$$

When the other two conditions are applied, the equations for the other two constants are

$$c = -\frac{2s_{k-1} + s_k}{u_k} - \frac{3(t_{k-1} - t_k)}{u_k^2} \tag{H18}$$

and

$$d = \frac{s_{k-1} + s_k}{u_k^2} + \frac{2(t_{k-1} - t_k)}{u_k^3} \tag{H19}$$

The general equation for t, therefore, is expressed as

$$t = t_{k-1} + s_{k-1}\,u - \left[\frac{2s_{k-1} + s_k}{u_k} + \frac{3(t_{k-1} - t_k)}{u_k^2}\right]u^2 + \left[\frac{s_{k-1} + s_k}{u_k^2} + \frac{2(t_{k-1} - t_k)}{u_k^3}\right]u^3 \tag{H20}$$

Integrals of t with Respect to du

For the area of a segment, the integral is

$$A = \int_0^{u_k} t\,du = \left(\frac{t_{k-1} + t_k}{2}\right)u_k + \left(\frac{s_{k-1} - s_k}{12}\right)u_k^2 \tag{H21}$$

The integral for F for a segment is

$$\int_0^{u_k} t^3\,du = \int_0^{u_k} \left(a + bu + cu^2 + du^3\right)^3 du$$

Some of the integration bookkeeping can be reduced by use of integration by parts.

$$\int w\,dv = wv - \int v\,dw$$

Let $w = t^3$

$$dw = 3t^2\,dt = 3t^2(b + 2cu + 3du^2)du$$

$v = u$, and $dv = du$. Therefore,

$$\int_0^{u_k} t^3\,du = \left(t^3u\right)_0^{u_k} - \int_0^{u_k} 3t^2(bu + 2cu^2 + 3du^3)du$$

The same procedure could be used on the remaining integral; however, at some point an integral has to be evaluated. The resulting equation is

$$\int_0^{u_k} t^3\,du = \left(43t_{k-1}^3 + 27t_{k-1}^2t_k + 27t_{k-1}t_k^2 + 43t_k^3\right)\frac{u_k}{140}$$

$$+ \left[\left(97t_{k-1}^2 + 70t_{k-1}t_k + 43t_k^2\right)s_{k-1} - \left(43t_{k-1}^2 + 70t_{k-1}t_k + 97t_k^2\right)s_k\right]\frac{u_k^2}{840}$$

$$+ \left[(16t_{k-1} + 8t_k)s_{k-1}^2 - 18(t_{k-1} + t_k)s_{k-1}s_k + (8t_{k-1} + 16t_k)s_k^2\right]\frac{u_k^3}{840}$$

$$+ \left[\left(s_{k-1}^2 - s_{k-1}s_k + s_k^2\right)(s_{k-1} - s_k)\right]\frac{u_k^4}{840} \qquad \text{(H22)}$$

End-Circle Contributions to Integral F

The major part of F for a blade section is obtained from a summation of the segment contributions as determined from equation (H22). A minor addition is made for the end circles. The geometry for this is shown in figure 21. The independent variable for the end-circle integration u is referenced from the end-circle center. The limits of the integration are from $r \sin(\alpha_s - \alpha_p)/2$ to r. The local thickness is

$$t = 2\sqrt{r^2 - u^2}$$

So the integral for an end-circle contribution to F is

$$\int_{r \sin \frac{\alpha_s - \alpha_p}{2}}^{r} t^3\,du = 8 \int_{r \sin \frac{\alpha_s - \alpha_p}{2}}^{r} (r^2 - u^2)^{3/2}\,du$$

Let $u = r \sin\theta$, so $du = r \cos\theta\, d\theta$ and

$$\int_{r \sin \frac{\alpha_s - \alpha_p}{2}}^{r} t^3 \, du = 8 \int_{\frac{\alpha_s - \alpha_p}{2}}^{\frac{\pi}{2}} \left[r^2 - (r \sin \theta)^2\right]^{3/2} r \cos \theta \, d\theta = 8r^4 \int_{\frac{\alpha_s - \alpha_p}{2}}^{\frac{\pi}{2}} \cos^4\theta \, d\theta$$

$$= \frac{r^4}{8} \left\{3(\pi - \alpha_s + \alpha_p) - \sin(\alpha_s - \alpha_p)\left[4 + \cos(\alpha_s - \alpha_p)\right]\right\} \qquad \text{(H23)}$$

APPENDIX I

PROGRAM INFORMATION

The program information presented is (1) a description of the input parameters, (2) a description of the variables in the program commons, and (3) a listing of the program.

Description of Input Parameters for Blade Design Program

The format for the input data described below is given in figure 22.

Parameter symbol	Description	Format
AA	Incidence-angle option for blade design purposes. Interpretable options are 2-D, 3-D, SUCTION, and TABLE. A noninterpretable incidence option word is set to the 2-D option. The 2-D and 3-D options mean incidence angles are determined by reference 2 procedures for the respective option. The SUCTION option gives zero incidence to the suction surface of the blade at the leading edge. The TABLE option means the blade incidence angles for the blade element will be input in tabular form, INC(IROW, J), at the end of the data set.	A4
AB	Completes the incidence TABLE option. To reference incidence to the suction surface at the leading edge, the eight columns of the card for AA and AB must read $\underbrace{\text{TABL}}_{AA}\underbrace{\text{E SS}}_{AB}$. (If AB is anything other than E SS, the incidence angles will be referenced to the leading-edge centerline.)	A4
BB	Deviation-angle option for blade design purposes. Interpretable options are 2-D, 3-D, TABLE, CARTER, and MODIFY. Noninterpretable input is set to the 2-D option. For the 2-D and 3-D options, deviation angles are determined by reference 2 procedures for the corresponding option. The CARTER and MODIFY options are now the same in the program. They indicate the use of	A4

Parameter symbol	Description	Format
	Carter's rule with a modification when blade elements have different camber rates on the front and rear segments of a blade element (eq. (21)). The TABLE option means the blade deviation angles for the blade elements will be input in tabular form, DEV(ROW, J), at the end of the data set.	
BMATL(IROTOR)	Rotor material density, lbm/in.^{3}. If a positive nonzero number is input, the blade will be stacked so as to balance gas bending moments with the centrifugal force moment for the material density (see section Balancing of Bending Moments on p. 31). The hub stacking point stays fixed, so the tip location is moved if necessary.	F10.4
BLADES(IROW)	Number of blades in each rotor or stator blade row	F10.4
CC	Blade-element geometry option for blade design purposes. Interpretable options are CIRCULAR, OPTIMUM, and TABLE. The CIRCULAR option gives equal segment turning rates. Noninterpretable input will be set to the CIRCULAR option. The OPTIMUM option means that the ratio of blade-element segment turning rates will be set by an empirical function of inlet relative Mach number M_1'. Below a M_1' of 0.8, the blade element will be a circular arc. As M_1' is increased, the ratio of front-segment turning rate to rear-segment turning rate is reduced. A limit of zero camber on the suction surface of the front segment is approached at a M_1' of about 1.60. The TABLE option means the ratio of blade-segment turning rates will be input in tabular form, PHI(IROW, J), at the end of the data set.	A4
CHORDA(IROW) CHORDB(IROW) CHORDC(IROW)	Constants to define ratio of blade-element chord to tip chord on projected plane. $\frac{c}{c_t} = 1.0 + R \cdot \mathrm{CHORDA(IROW)} + R^2 \cdot \mathrm{CHORDB(IROW)} + R^3 \cdot \mathrm{CHORDC(IROW)}$ where $R = (r_t - r)/(r_t - r_h)$ or a fraction of the annulus height at the blade mean.	F10.4

Parameter symbol	Description	Format
CHOKE(IROW)	Desired minimum ratio of excess area to choke area within a blade passage. If zero is input, no adjustment will be attempted within the program. For input values greater than zero, incidence angle will be increased as necessary to a maximum of $+2.0^{0}$ on the leading edge of the suction surface in an attempt to give the specified choke margin at the covered channel entrance.	F10.4
CPCO(I) for I=1, 6	Constants for the specific-heat polynomial function of temperature. $C_p = CPCO(1) + CPCO(2) \cdot T + CPCO(3) \cdot T^2 + CPCO(4) \cdot T^3 + CPCO(5) \cdot T^4 + CPCO(6) \cdot T^5$	E20.8
DD	Option control of location of transition point between segments of a blade element. The interpretable options are CIRCULAR, SHOCK, and TABLE. The SHOCK option locates the transition point on the suction surface at the normal shock impingement point from the leading edge of the adjacent blade. The TABLE option means the location of the transition point will be input in tabular form, TRANS(IROW, J), at the end of the data set. The CIRCULAR option and noninterpretable data put the transition point at midchord.	A4
DEV(IROW, J)	Deviation angle (deg), which may be specified by option. If the tabular option is used, a value is expected for each streamline starting from the tip.	F10.4
EE	Option control of location of maximum-thickness point of a blade element. The interpretable options are TRAN and TABLE. The TRAN option and noninterpretable options will set the maximum-thickness point at the transition point. The TABLE option means the maximum-thickness-point location will be input in tabular form, ZMAX(IROW, J), at the end of the data set.	A4
EB	Completes the TABLE option of the maximum-thickness location. If the eight format spaces in figure 22 appear as $\underbrace{\text{TABL}}_{EE}\underbrace{\text{E LE}}_{EB}$, the input values of ZMAX(IROW, J) will	A4

Parameter symbol	Description	Format
	be used as the fraction of chord distance from the leading edge. If EB is not as shown, the values of ZMAX(IROW, J) will be used as the fraction of chord distance behind the transition point.	
I	Calculating station index. Each blade row accounts for two calculating stations, one at the leading edge of the blade and the other at the trailing edge.	(not input)
INC(IROW, J)	Incidence angle (deg), which may be input by option. If the tabular option is used, a value is expected for each streamline starting from the tip.	F10.4
IROW	Blade-row index	(not input)
J	Streamline index. Streamlines are numbered from 1 at the tip.	(not input)
MOLE	Molecular weight of gas (28.97 for dry air).	F10.4
NXCUT(IROW)	Number of sections across a blade for which fabrication coordinates are desired. If zero, the program will set the number of XCUT's on the basis of aspect ratio. For all positive values, the program will set appropriate locations to represent the blade. Negative values of NXCUT(IROW) activate an option to read cards for the XCUT values. The number of values expected for a blade row is the absolute value of NXCUT(IROW).	I10
NSTRM	Number of streamlines (maximum of 21)	
OP	Option controlling amount of output information desired. Interpretable options are APPROX., VEL. DIA., DESIGN, COOR., PUNCH, and ALL. The program as presented in this report is not run in conjunction with an aerodynamic design; so it essentially always uses the COORD option, which gives the printout of blade-section properties and coordinates for fabrication.	A4
OPO	Option controlling output from systems peripheral equipment. Options to get blade-section coordinates on punched cards and on microfilm exist for the NASA	A4

Parameter symbol	Description	Format
	Lewis System. The option is specified by only a single letter in card column 18 of the 17-20 column field for OPO. M gives microfilm coordinates. P gives punched cards. B gives both microfilm and punched cards. Anything else gives neither.	
PHI(IROW, J)	Ratio of inlet-segment turning to outlet-segment turning (ratio of $d\kappa/ds$'s) for a blade element. If input values are expected by use of the tabular option, the data cards go within the optional cards at the end of the data set for each blade row (fig. 22). A value is expected for each streamline beginning from the tip.	F10.4
PO(I, J)	Stagnation pressure for each streamline starting from the tip, psia	F10.4
	When blade edge coordinates are input, PO(I, J) is a temporary storage location for the radial coordinate of the points.	F8.4
R(I, J)	Radius of each streamline at blade-edge reference stations, in.	F10.4
RBHUB(IROW)	Radius coordinate of hub stacking point, in.	F10.4
RBTIP(IROW)	Radius coordinate of tip stacking point, in.	F10.4
ROT	Compressor rotational speed, rpm	F10.4
SLOPE(I, J)	Streamline slope angle at blade-edge stations, deg	F10.4
SOLID(IROW)	Tip solidity of a blade row (chord/circumferential spacing)	F10.4
TALE(IROW) TBLE(IROW) TCLE(IROW) TDLE(IROW)	Polynomial coefficients for ratio of blade-element leading-edge radius to chord $$\frac{t_{le}}{c} = \mathrm{TALE} + \mathrm{TBLE} \cdot R + \mathrm{TCLE} \cdot R^2 + \mathrm{TDLE} \cdot R^3$$ where R is $(r_t - r)/(r_t - r_h)$ or the fraction of passage height at blade leading edge	F10.4

Parameter symbol	Description	Format
TAMAX(IROW) TBMAX(IROW) TCMAX(IROW) TDMAX(IROW)	Polynomial coefficients for ratio of blade-element maximum thickness to chord $\frac{t_{max}}{c} = TAMAX + TBMAX \cdot R + TCMAX \cdot R^2 + TDMAX \cdot R^3$	F10.4
TATE(IROW) TBTE(IROW) TCTE(IROW) TDTE(IROW)	Polynomial coefficients for ratio of blade-element trailing-edge radius to chord $\frac{t_{te}}{c} = TATE + TBTE \cdot R + TCTE \cdot R^2 + TCTE \cdot R^3$ where R is $(r_t - r)/(r_t - r_h)$ at the blade trailing edge	F10.4
TILT(IROW)	Circumferential direction angle of stacking-axis tilt at hub, deg. The angle is positive in the direction of rotor rotation. If |TILT(IROW)| is greater than 100.0, a curved stacking line is specified according to $r - r_h = C \sin \gamma$, where γ is the local stacking-line slope with respect to a local radial line. The code of the digits of TILT(IROW) is -x<u>xx</u> <u>xx.xx</u>, where <u>xx</u> is the γ angle at the hub in degrees with the sign of the overall TILT(IROW) number, and <u>xx.xx</u> is γ at the tip in degrees.	F10.4
TITLE(I)	Description of blade row for printout and later identification	18A4
TO(I, J)	Total temperature for each streamline starting from the tip, ^{o}R	F10.4
TRANS(IROW, J)	Location of transition point on blade-element centerline as a fraction of the blade-element chord. If input values are expected by use of the tabular option, the data cards go with the optional cards at the end of the data set for each blade row (fig. 22). A value is expected for each streamline beginning from the tip.	F10.4
VTH(IROW, J)	Tangential velocity component at blade-edge stations, ft/sec	F10.4
VZ(IROW, J)	Axial velocity component at blade-edge stations, ft/sec	F10.4
XCUT(IC)	Radial location of blade-section planes. Whether or not data cards are read for values of XCUT(IC) for a blade row is controlled by the value of NXCUT(IROW). Any XCUT(IC) cards are read in an output routine so they	F10.4

Parameter symbol	Description	Format
	must follow all cards read in subroutine INPUT. It is preferable, but not necessary, to list the XCUTS(IC) for a blade row in order starting from the tip.	
Z(I, J)	Axial location of blade-edge reference velocity diagrams, in.	F10. 4
ZBHUB(IROW)	Axial location of hub stacking point, in.	F10. 4
ZBTIP(IROW)	Initial axial location of tip stacking point, in.	F10. 4
ZMAX(IROW, J)	Location of maximum-thickness point on the centerline as a fraction of blade-element chord. If input values are expected by use of the tabular options, the data cards go with the optional cards at the end of the data set for each blade row (fig. 22). A value is expected for each streamline beginning from the tip with a leading-edge or transition-point reference according to option (see EB). With a transition point reference, the values input are $(c_m - c_t)/c$	F10. 4

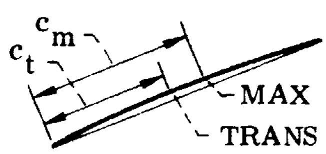

Description of Program Variables in Commons

Symbol	Common	Description
AC	RCUT	Area of blade-section end-circle sector
AL	MARG	AOAS value for some other location in blade-element channel
AMACH	BLADES	Average inlet relative Mach number for shock at a blade-element channel entrance
AOAS	MARG	Ratio of blade-element area to choke area at some channel location
AOA1	MARG	Ratio of a local blade-element channel area to blade-element inlet relative flow area

Symbol	Common	Description
AOC	BLADES	Fraction of chord location of blade-element maximum camber point
A1SOAS	BLADES	Ratio of blade-element inlet to local choke areas
A1SOA1	BLADES	Ratio of blade-element inlet choke to actual areas
BETA	SCALAR	Blade-section setting angle
BETAS(IROW, J)	VECTOR	Relative flow angle at blade-element channel entrance shock
BETA1(J)	Blank	Blade-element-inlet relative flow angle
BETA2(J)	Blank	Blade-element-outlet relative flow angle
BINC	BLADES	Streamline incidence angle to blade centerline
BLADES(IROW)	VECTOR	Number of blades in a rotor or stator
BMATL(IROTOR)	VECTOR	Rotor blade material density
CALP	BLADES	Cosine of blade-element layout-cone angle
CCC	BLADES	Ratio of distance between edge-circle centers to overall blade-element chord
CCHORD	MARG	Product of CALP and CHORD
CEPE	BLADES	Cosine of angle that line between blade-element edge-circle centers makes with chord line
CGBL	BLADES	Cosine of blade-element setting angle for chord
CHD(J)	EQUIV	Blade-element chord as measured along a constant-angle path tangent to end circles on pressure side. The chord length is measured from the outer tangency points to the end circles.
CHK(J)	EQUIV	Ratio of the minimum blade-element-channel-area margin to choke area
CHOKE(IROW)	VECTOR	Desired minimum blade-element-channel-area choke margin
CHORD	BLADES	CHD(J) for local element
CHORDA(IROW)	VECTOR	Coefficient for linear term of a polynomial representation of radial variation of blade-element chord projected to a blade-section plane

Symbol	Common	Description
CHORDB(IROW)	VECTOR	Coefficient for quadratic term of chord polynomial
CHORDC(IROW)	VECTOR	Coefficient for cubic term of chord polynomial
CINC	BLADES	Streamline incidence angle without influence of incidence on deviation
CKTC	BLADES	Cosine of blade-element centerline angle at transition point of segments
CKTS	BLADES	Cosine of blade-element surface angle at transition point of segments
COSA(J)	Blank	Cosine of blade-element streamline inlet slope angle
COSA2(J)	EQUIV	Cosine of blade-element streamline outlet slope angle
COSKL	RCUT	Cosine of blade-section edge-circle angle at joining point with pressure (lower) surface
COSKU	RCUT	Cosine of blade-section edge-circle angle at joining point with suction (upper) surface
COSL(J)	Blank	Cosine of blade-edge angle in meridional plane with reference to radial direction
CP	SCALAR	Specific heat at constant pressure
CPCO(6)	VECTOR	Polynomial coefficients for specific-heat function of temperature
CPH2	SCALAR	CPCO(2)/2.0 — Polynomial coefficients for an enthalpy change as derived from integration of specific-heat polynomial c_p dt
CPH3	SCALAR	CPCO(3)/3.0
CPH4	SCALAR	CPCO(4)/4.0
CPH5	SCALAR	CPCO(5)/5.0
CPH6	SCALAR	CPCO(6)/6.0
CPP3	SCALAR	CPCO(3)/2.0 — Polynomial coefficient for an isentropic pressure change as derived from integration of specific-heat polynomial $c_p(dt/t)$
CPP4	SCALAR	CPCO(4)/3.0
CPP5	SCALAR	CPCO(5)/4.0
CPP6	SCALAR	CPCO(6)/5.0
CP1	SCALAR	Approximation to $\gamma/(\gamma - 1)$ with use of only first term of specific-heat polynomial
CV	SCALAR	Specific heat at constant volume

Symbol	Common	Description
C1	BLADES	Chordwise component distance of leading-edge center circle to centerline transition point as a fraction of blade-element chord
C2	BLADES	Chordwise component distance of centerline transition point to trailing-edge center circle as a fraction of blade-element chord
DAL	MARG	DAOAS value for some other location in blade-element channel
DAOAS	MARG	Derivative of AOAS in blade-element channel throughflow direction
DCP	SCALAR	Specific-heat difference, CP - CV
DEV(IROW, J)	VECTOR	Blade-element deviation angle on streamline-of-revolution surface
DF	SCALAR	Diffusion factor, a blade-element aerodynamic loading parameter
DHC	SCALAR	Compressor enthalpy rise
DHCI	SCALAR	Compressor enthalpy rise required by an isentropic process
DKAPPA	BLADES	Inlet- to outlet-blade-angle change on streamline-of-revolution surface
DKLE(IROW)	Blank	Blade-element angle difference between suction surface and centerline at leading edge
DL(J)	Blank	Meridional plane distance between end-circle centers of adjacent blade elements
DLOSC	SCALAR	The part of the pressure loss correlated with diffusion factor
DPW	MARG	Normalized-to-chord distance of a point on blade-element pressure surface from pressure-surface transition point
DPWL	MARG	DPW value for some other location in blade-element channel

Symbol	Common	Description
DRCE	BLADES	Normalized-to-chord conic radius component from a blade-element end-circle center to the tangency point of the edge circle with a surface curve
DRCGI	BLADES	Normalized-to-chord conic radius component from the leading-edge end-circle center to the blade-element stacking reference point
DRCLEP	MARG	DRCE for leading-edge circle to the pressure surface
DRCM	MARG	Normalized-to-chord conic radius component for maximum-thickness path from centerline to surface; also used as the same type of radius component from the leading edge to a mid-channel point
DRCMST	BLADES	Normalized-to-chord conic radius component from centerline transition point to surface maximum-thickness point
DRCMT	BLADES	Normalized-to-chord conic radius component from transition point to maximum-thickness point on the centerline
DRCOI	BLADES	Normalized-to-chord conic radius component from leading-edge circle center to trailing-edge circle center
DRCT	BLADES	Normalized-to-chord conic radius component of transition-point thickness path which is perpendicular to the centerline and which goes from the centerline to a surface
DRCTI	BLADES	Normalized-to-chord conic radius component from leading-edge circle center to transition point on the centerline
DRCTPI	MARG	Normalized-to-chord conic radius component from leading-edge circle center to pressure-surface transition point
DRCTSI	MARG	Normalized-to-chord conic radius component from leading-edge circle center to suction-surface transition point

Symbol	Common	Description
DRCWT	MARG	Normalized-to-chord conic radius component from suction-surface transition point to a point on the pressure surface of the blade element on the other side of the flow channel
DR1	BLADES	Reference streamtube thickness at leading edge of a blade element
DSA	MARG	Average of two blade-surface path distances normalized to chord
DSME	BLADES	Normalized-to-chord centerline-path distance from the end-circle center on which maximum thickness occurs to the maximum-thickness point
DSMT	BLADES	Normalized-to-chord centerline-path distance from the transition point to the maximum-thickness point
DSOI	BLADES	Normalized-to-chord centerline-path distance from the leading-edge circle center to the trailing-edge circle center
DSOT	BLADES	Normalized-to-chord centerline-path distance from the transition point to the trailing-edge circle center
DSP	MARG	Normalized-to-chord pressure-surface path length
DSP1	MARG	Normalized-to-chord pressure-surface path length of first segment
DSP2	MARG	Normalized-to-chord pressure-surface path length of second segment
DSS	MARG	Normalized-to-chord suction-surface path length
DSSE	BLADES	Normalized-to-chord surface path distance from either the maximum-thickness point or the transition point to the surface end which is in the opposite direction of the other point
DSS1	MARG	Normalized-to-chord suction-surface path length of the first segment
DSS2	MARG	Normalized-to-chord suction-surface path length of the second segment

Symbol	Common	Description
DST	BLADES	Normalized-to-chord transition-point blade thickness path from the centerline to a surface
DSTI	BLADES	Normalized-to-chord centerline-path distance from the leading-edge circle center to the transition point
DSW	MARG	Normalized-to-chord distance of a point on the blade-element suction surface from the suction-surface transition point
DX(K)	RCUT	Chordwise increment between blade-section surface points
EB	MARG	Conic angle between repeated blade elements of a blade row
EM(K)	RCUT	Second derivatives of a spline-fit blade-section surface curve
EMT	BLADES	Conic angular component from centerline transition point to a surface maximum-thickness point
EMTM	RCUT	EM(K) value for the transition point on the first-segment side
EWC	MARG	Conic angular component of a channel width path
F	MARG	Fraction of total suction-surface distance
FSB(K)	PTS	Blade-element surface distance fractions at which points are obtained for blade-section definition
FSM(J)	EQUIV	Fraction of covered-channel through-flow distance at which minimum choke margin occurs
F1	BLADES	F at the covered-channel entrance
F2	BLADES	F at the covered-channel exit
G	SCALAR	Gravitational acceleration conversion constant, 32.1740 lbm-ft/lbf-sec^2
GAMM(J)	Blank	Ratio of specific heats, CP/CV
GAMMA	SCALAR	Local value of GAMM(J), γ
GBL	BLADES	Angle of a blade-element chord line with respect to a conic ray
GJ	SCALAR	Product of G and the mechanical equivalent of heat, 25035.24 ft^2-lbm/sec^2-Btu

Symbol	Common	Description
GJ2	SCALAR	$2.0 \cdot GJ = 50070.47$ ft^2-lbm/sec^2-Btu
GR1	SCALAR	Combination of specific-heat terms, $(\gamma + 1)/(\gamma - 1)$
GR2	SCALAR	Combination of specific-heat terms, $\gamma/(\gamma - 1)$
GR3	SCALAR	Combination of specific-heat terms, $1/(\gamma - 1)$
GR4	SCALAR	Combination of specific-heat terms, $(\gamma + 1)/2$
GR5	SCALAR	Combination of specific-heat terms, $(\gamma - 1)/2$
H	SCALAR	General enthalpy change
HC	MARG	Ratio of a local channel to inlet streamtube thickness
I	SCALAR	Calculating station index
ICHOKE	MARG	Index for location in blade-element channel
ICL	BLADES	Integer routing device used in blade-element centerline iteration
ICONV	SCALAR	Integer parameter for highest level program routing
ICOUNT	SCALAR	Line counter for printout of input data
IDEV(IROW)	VECTOR	Integer designation of the deviation angle option: 1 for 2-D value of reference 2 2 for 3-D value of reference 2 3 for Carter's rule 4 for Carter's rule modified by equation (21) 5 tabular
IERROR	SCALAR	Integer parameter which controls the exit when incompatible input data are discovered
IGEO(IROW)	VECTOR	Integer designation of the option for PHI(IROW, J): 1 for midpoint 2 for optimum (see CC of input parameter list) 3 for tabulated
IGO	BLADES	Integer routing parameter
IIN	SCALAR	Temporary storage location of an index

Symbol	Common	Description
IINC(IROW)	VECTOR	Integer designation of the incidence [illegible]: 1 for 2-D value of reference 1 2 for 3-D value of reference 2 3 for zero incidence to leading-edge suction surface 4 for tabular with centerline reference 5 for tabular with suction-surface reference
ILOSS(IROW)	VECTOR	Integer designation of loss data set associated with a blade row
IMAX(IROW)	VECTOR	Integer designation of option for blade-element maximum-thickness-point location: 1 for midpoint 2 for tabular with transition-point reference 3 for tabular with leading-edge reference
INC(IROW)	VECTOR	Blade-element incidence angle on streamline-of-revolution surface (a real variable)
IOUT	RCUT	Counter of number of variables of an array eliminated for a particular calculation (not used in this setup of program)
IPASS	BLADES	Integer routing parameter used for blade-element centerline calculation
IPR	SCALAR	Temporary storage location of an index
IR	SCALAR	Read tape number of computer facility
IROTOR	SCALAR	Rotor index
IROW	SCALAR	Blade-row index
ISTN(I)	VECTOR	Integer designation of calculating station type: 1 for rotor inlet 2 for rotor outlet -1 for stator inlet -2 for stator outlet 0 for annular
IT	RCUT	Counter of blade-section surface points
ITER	SCALAR	Iteration counter

Symbol	Common	Description
ITRANS(IROW)	VECTOR	Integer designation of the option for the blade-element transition point: 1 for midpoint 2 for covered-channel inlet point on suction surface 3 for tabular
IW	SCALAR	Write tape number of computer facility
J	SCALAR	Streamline index
JM	SCALAR	Index for mean streamline
KIC(J)	EQUIV	Centerline blade inlet angle on layout cone (a real variable)
KIP	MARG	Blade-element pressure-surface blade angle at inlet (a real variable)
KIS	BLADES	Blade-element suction-surface blade angle at inlet (a real variable)
KM	BLADES	Centerline and surface blade angle at blade-element maximum-thickness point (a real variable)
KOC(J)	EQUIV	Centerline blade outlet angle on layout cone (a real variable)
KOP	MARG	Blade-element pressure-surface blade angle at outlet (a real variable)
KOS	MARG	Blade-element suction-surface blade angle at outlet (a real variable)
KP	MARG	Blade angle at some general pressure-surface point (a real variable)
KS	MARG	Blade angle at some general suction-surface point (a real variable)
KTC	BLADES	Blade-element centerline angle at segment transition point (a real variable)
KTP	MARG	Pressure-surface blade angle at transition point (a real variable)
KTS	BLADES	Suction-surface blade angle at transition point (a real variable)

Symbol	Common	Description
KWC	MARG	Angle of the path across a blade-element channel with respect to the tangential direction (a real variable)
MACH	SCALAR	Relative Mach number (a real variable)
NAL	SCALAR	Number of input blade rows and annular stations (not used in this setup of the program)
NBROWS	SCALAR	Number of blade rows (not relevant in this setup of the program)
NHUB	SCALAR	Number of hub contour definition points (not used in this setup of the program)
NOPT(IROW)	VECTOR	Index designation of the option which controls the program output. In this program setup, the coordinate option is essentially always in effect.
NP	RCUT	Number of blade-section points that are spline curve fit
NROTOR	SCALAR	Number of rotors (not used in this setup of the program)
NSTN	SCALAR	Total number of calculating stations, I (not used in this setup of the program)
NSTRM	SCALAR	Total number of streamlines, J
NTIP	SCALAR	Number of tip contour definition points (not used in this setup of the program)
NTUBES	SCALAR	Number of streamtubes (NSTRM - 1)
NXCUT(IC)	VECTOR	Number of blade sections desired in the terminal calculation
OBAR(J)	Blank	Relative pressure-loss coefficient for the losses correlated with DF, $(P'_{2i} - P'_2)/(P'_1 - p_1)$
OMEGA	SCALAR	Rotational speed, rad/sec
P	BLADES	Specific PHI(IROW, J) in current use
PFLOS	BLADES	Relative pressure-loss coefficient for the losses correlated with DF, $(P'_{2i} - P'_2)/P'_1$
PHI(IROW, J)	VECTOR	Ratio of inlet-segment turning rate to outlet-segment turning rate (ratio of $d\kappa/ds$) for a blade element
PI	SCALAR	$\pi = 3.1415927$
PI2	MARG	One-half pi, $\pi/2$

Symbol	Common	Description
PO(I, J)	VECTOR	Total pressure at blade-edge stations (input and output in psia, but converted to lbf/ft^2 for internal calculations)
POA1	SCALAR	Average inlet total pressure (not used in this setup of the program)
PR	SCALAR	Pressure ratio (not used in this setup of the program)
R(I, J)	VECTOR	Cylindrical-coordinate radius at blade-edge stations, in.
RADIAN	SCALAR	Conversion factor from radians to degrees, 57.29578
RBHUB(IROW)	VECTOR	Radius coordinate of hub stacking point, in.
RBTIP(IROW)	VECTOR	Radius coordinate of tip stacking point, in.
RCA(J)	EQUIV	Cylindrical-coordinate radius of a blade-element stacking point
RCG	BLADES	Normalized-to-chord conic radius of a blade-element stacking point
RCI	MARG	Normalized-to-chord conic radius of a blade-element leading-edge circle center
RCM	BLADES	Normalized-to-chord conic radius of the maximum-thickness point on the centerline of a blade element
RCMS	BLADES	Normalized-to-chord conic radius of the maximum-thickness point on the surface of a blade element
RCO	MARG	Normalized-to-chord conic radius of a blade-element trailing-edge circle center
RCP	MARG	Normalized-to-chord conic radius of a point on the pressure surface of a blade element
RCS	MARG	Normalized-to-chord conic radius of a point on the suction surface of a blade element
RCT	BLADES	Normalized-to-chord conic radius of the transition point on the centerline of a blade element
RCTP	MARG	Normalized-to-chord conic radius of the transition point on the pressure surface of a blade element
RCTS	MARG	Normalized-to-chord conic radius of the transition point on the suction surface of a blade element

Symbol	Common	Description
RD1	BLADES	Inlet station radius difference of the blade elements which define the local channel convergence
REC(I, J)	EQUIV	Cylindrical-coordinate radius coordinate of the blade-element end-circle centers
RECGI	BLADES	Circumferential direction coordinate from the inlet circle center to the blade-element stacking point (RCG times the conic angle difference)
REE	BLADES	Circumferential direction coordinate from an end-circle center to the end-circle tangency point with a surface (RCS times the conic angle difference)
RELEP	MARG	Special REE value, the one to the pressure surface at the leading edge
RELM(J)	Blank	Blade-element inlet relative Mach number
REMT	MARG	Circumferential direction coordinate from the transition point to the maximum-thickness point along the centerline (RCM times the conic-angle difference)
REOI	MARG	Circumferential direction coordinate from the leading-edge circle center to the trailing-edge circle center (RCO times the conic-angle difference)
REP	MARG	Circumferential direction coordinate from the leading-edge circle center to a point on the pressure surface of the following blade (RCP times the conic-angle difference)
RES	MARG	Circumferential direction coordinate of a point on the suction surface referenced to the suction-surface transition point (RCS times the conic-angle difference)
RET	BLADES	Circumferential direction coordinate from the centerline transition point to a surface transition point (RCTS times the conic-angle difference)
RETI	BLADES	Circumferential direction coordinate from the leading-edge circle center to the centerline transition point (RCT times the conic-angle difference)

Symbol	Common	Description
RETP	MARG	Circumferential direction coordinate from the leading-edge circle center to the pressure-surface transition point (RCTP times the conic-angle difference)
RETS	MARG	Circumferential direction coordinate from the leading-edge circle center to the suction-surface transition point (RCTS times the conic-angle difference)
REWT	MARG	Circumferential direction coordinate from the suction-surface transition point to a point on the pressure surface of the next blade (RCP times the conic-angle difference)
RE1(J)	Blank	Temporary storage location for an array
RE2(J)	Blank	Temporary storage location for an array
RE3(J)	Blank	Temporary storage location for an array
RE4(J)	Blank	Temporary storage location for an array
RE5(J)	Blank	Temporary storage location for an array
RF	SCALAR	Gas constant for the fluid, lbf-ft/lbm-^{o}R
RG	SCALAR	Product of G and RF, ft^2/sec^2-^{o}R
RMSJ	BLADES	Product of blade-element solidity with the mean radius normalized to chord
ROT	SCALAR	Rotational speed, rpm
RPR1(J)	Blank	Relative total pressure ratio, $(P_1' - p_1)/P'$ (not used in this setup of the program)
RPTE(I, J)	EQUIV	$r(\partial\theta/\partial l)$ at a blade-element end-circle center
RTR	MARG	Ratio of a local relative total temperature to the blade-element inlet relative total temperature
RTRC	BLADES	Constant for computing RTR, $\left[(\gamma - 1)\omega^2 c^2/144\gamma g R_f T_1'\right]$
RTRD	MARG	Constant used for estimation of the derivative of RTR with blade-element path distance, RTRC $\times$ sin α $\times$ (Blade-element path distance)
RTRQ	MARG	Square root of RTR
RVTH(J)	Blank	rV_θ (not used in this setup of the program)
R1	BLADES	Particular value of R(I, J) at blade-element inlet

Symbol	Common	Description
R1C	BLADES	R1 normalized to chord
R2	BLADES	Particular value of R(I, J) at blade-element exit
SALP	BLADES	Sine of blade-element layout-cone angle
SECGBL	MARG	Secant of blade-element setting angle for chord
SEPE	BLADES	Sine of angle that the line between the blade-element edge-circle centers makes with the chord line
SGAM	BLADES	Sine of blade-element setting angle for the line between the edge-circle centers
SGBL	BLADES	Sine of blade-element setting angle for the chord
SINA(J)	Blank	Sine of blade-element streamline inlet slope angle
SINA2(J)	EQUIV	Sine of the blade-element streamline outlet slope angle
SINKL	RCUT	Sine of blade-section edge-circle angle at the joining point with the pressure (lower) surface
SINKU	RCUT	Sine of blade-section edge-circle angle at the joining point with the suction (upper) surface
SINL(J)	Blank	Sine of blade-edge angle in meridional plane with reference to the radial direction
SJ	BLADES	Blade-element solidity (chord/tangential spacing)
SKIC(J)	EQUIV	Blade inlet angle on a streamline of revolution
SKOC(J)	EQUIV	Blade outlet angle on a streamline of revolution
SKTC	BLADES	Sine of blade-element centerline angle at the transition point of the segments
SKTS	BLADES	Sine of blade-element surface angle at the transition point of the segments
SLJD	BLADES	Difference of slope between the neighboring cones used to define changes of streamtube thickness
SLOPE(I, J)	VECTOR	Streamline slope at the blade-edge stations
SLOS(J)	Blank	Ratio of relative total pressures behind a shock to that ahead of the shock
SOLID(IROW)	VECTOR	Tip solidity of a blade row

Symbol	Common	Description
SONIC(J)	Blank	Square of the local speed of sound (not used in this program setup)
T	BLADES	Specific TRANS(IROW, J) in current use
TALE(IROW)	VECTOR	Constant term in the polynomial representation of the normalized-to-chord leading-edge radius function of fraction of passage height
TALP(J)	EQUIV	Tangent of the blade-element layout-cone angle
TAMAX(IROW)	VECTOR	Constant term in polynomial representation of the normalized-to-chord maximum-thickness function of fraction of passage height
TATE(IROW)	VECTOR	Constant term in polynomial representation of the normalized-to-chord trailing-edge radius function of fraction of passage height
TBLE(IROW)	VECTOR	Constant for linear term in the polynomial associated with TALE(IROW)
TBMAX(IROW)	VECTOR	Constant for linear term in the polynomial associated with TAMAX(IROW)
TBTE(IROW)	VECTOR	Constant for linear term in the polynomial associated with TATE(IROW)
TCA(J)	EQUIV	Angular cylindrical coordinate displacement of a blade-element stacking point from the reference hub element (positive in direction of rotor rotation)
TCGI	MARG	Angular cylindrical coordinate from a blade-element leading-edge circle center to the stacking point
TCLE(IROW)	VECTOR	Constant for quadratic term in the polynomial associated with TALE(IROW)
TCMAX(IROW)	VECTOR	Constant for quadratic term in the polynomial associated with TAMAX(IROW)
TCTE(IROW)	VECTOR	Constant for quadratic term in the polynomial associated with TATE(IROW)
TDLE(IROW)	VECTOR	Constant for cubic term in the polynomial associated with TALE(IROW)

Symbol	Common	Description
TDMAX(IROW)	VECTOR	Constant for cubic term in the polynomial associated with TAMAX(IROW)
TDTE(IROW)	VECTOR	Constant for cubic term in the polynomial associated with TATE(IROW)
TEC(I, J)	EQUIV	Angular cylindrical coordinate of an end-circle center referenced to the hub-element stacking point
TEPE	BLADES	Tangent of angle that the line between the blade-element edge-circle centers makes with the chord line
TGB(J)	EQUIV	Tangent of blade-element setting angle for the chord
TGBL	MARG	Same as TGB(J) for the current blade element
TGBLL	BLADES	Value of TGBL on the previous iteration
THD	BLADES	Normalized-to-chord radius difference of trailing-edge circle from leading-edge circle
THETAP(J, K)	Blank	Angular cylindrical coordinate of point on the pressure surface of a blade element referenced to the hub-element stacking point
THETAS(J, K)	Blank	Angular cylindrical coordinate of point on the suction surface of a blade element referenced to the hub-element stacking point
THLE	BLADES	Ratio of blade-element leading-edge circle radius to chord
THMAX	BLADES	Ratio of blade-element maximum thickness to chord
THTE	BLADES	Ratio of blade-element trailing-edge circle radius to chord
TILT(IROW)	VECTOR	Stacking-axis lean angle in the circumferential direction (complete description given in input variable list)
TITLE(I)	LABEL	Input alphanumeric title of the data set
TKTN	BLADES	Tangent of angle for the transition thickness path which is normal to the local centerline
TL	SCALAR	Lower temperature for a thermodynamic-change-of-state calculation

Symbol	Common	Description
TLS	BLADES	Tangent of stacking-axis lean from radial direction in meridional (r, z) plane
TO(I, J)	VECTOR	Total temperature at blade-edge stations, ^{O}R
TOA1	SCALAR	Average inlet total temperature (not used in this setup of the program)
TRANS(IROW, J)	VECTOR	Chordwise component of centerline transition-point location normalized by the chord
TREL1(J)	Blank	Blade-element inlet relative total temperature, ^{O}R
TSTAT(J)	Blank	Static temperature, ^{O}R
TTRP(J)	EQUIV	Angular cylindrical coordinate of transition point on pressure surface of a blade element (hub stacking-point reference)
TTRS(J)	EQUIV	Angular cylindrical coordinate of transition point on suction surface of a blade element (hub stacking-point reference)
TU	SCALAR	Upper temperature for a thermodynamic-change-of-state calculation
VM(J)	Blank	Meridional component of velocity, ft/sec
VTH(I, J)	VECTOR	Circumferential (θ) component of velocity, ft/sec
VTSQ(J)	Blank	VTH(I, J) squared at a station, ft^2/sec^2
VZ(I, J)	VECTOR	Axial (z) component of velocity, ft/sec
WC	MARG	Ratio of a local blade-to-blade channel width to chord
WC1	BLADES	Inlet streamline channel width in the blade-to-blade plane
XBAR(IROW, J)	Blank	Normalized-to-chord chordwise component of the distance from the leading-edge circle center to the blade-element stacking point
YBAR(IROW, J)	Blank	Corresponding perpendicular component to XBAR(IROW, J)
YBP(K)	RCUT	Pressure-surface blade-section coordinate normal to chord, in.
YBS(K)	RCUT	Suction-surface blade-section coordinate normal to chord, in.

Symbol	Common	Description
YB1	BLADES	Average of the two blade-element end-circle radii normalized to chord
YB2	BLADES	Constant for first approximation calculation of YBAR(IROW, J)
YCCLE(J)	EQUIV	Tangential-direction coordinate of blade-section leading-edge circle center, in.
YCCTE(J)	EQUIV	Tangential-direction coordinate of blade-section trailing-edge circle center, in.
Z(I, J)	VECTOR	Axial location of blade-edge stations, in.
ZBHUB(IROW)	VECTOR	Axial location of hub stacking point, in.
ZBP(K)	RCUT	Chordwise blade-section coordinate on pressure surface, in.
ZBS(K)	RCUT	Chordwise blade-section coordinate on suction surface, in.
ZBTIP(IROW)	VECTOR	Axial location of tip stacking point, in.
ZCCLE(J)	EQUIV	Axial coordinate of blade-section leading-edge circle center, in.
ZCCTE(J)	EQUIV	Axial coordinate of blade-section trailing-edge circle center, in.
ZCDA(J)	EQUIV	Axial displacement of blade-element stacking points from hub-element stacking point
ZEC(I, J)	EQUIV	Axial location of blade-element end-circle centers
ZM		Chordwise component of centerline maximum-thickness-point location normalized by the chord
ZMAX(IROW, J)	VECTOR	General array of ZM, but referenced either to blade-element leading edge or transition point
ZMT	MARG	Location of maximum-thickness point with respect to transition point normalized to chord
ZP(J, K)	Blank	Axial coordinate of blade-element pressure-surface points, in.
ZS(J, K)	Blank	Axial coordinate of blade-element suction-surface points, in.

Symbol	Common	Description
[illegible]	EQUIV	Axial location of blade-section transition point on pressure surface, in.
[illegible]RS(J)	EQUIV	Axial location of blade-section transition point on suction surface, in.

Listing of Computer Program

```
C *** THIS ROUTINE SERVES AS A CENTRAL CONTROL
      REAL INC, KIC, KIP, KIS, KM, KOC, KOP, KOS, KP, KS, KTC, KTP, KTS,
     X KWC, MACH
      COMMON /VECTOR/
     1 BETAS(1,21), BMATL(1), BLADES(1), CHOKE(1), CHORDA(1), CHORDB(1),
     2 CHORDC(1), CPCO(6), DEV(1,21), IDEV(1), IGEO(1), IINC(1),
     3 ILOSS(1), IMAX(1), INC(1,21), ISTN(2), ITRANS(1), NOPT(1),
     4 NXCUT(1), PHI(1,21), PO(2,21), R(2,21), RBHUB(1), RBTIP(1),
     5 SLOPE(2,21), SOLID(1), TALE(1), TAMAX(1), TATE(1), TBLE(1),
     6 TBMAX(1), TBTE(1), TCLE(1), TCMAX(1), TCTE(1), TDLE(1), TDMAX(1),
     7 TDTE(1), TILT(1), TO(2,21), TRANS(1,21), VTH(2,21), VZ(2,21),
     8 Z(2,21), ZBHUB(1), ZBTIP(1), ZMAX(1,21)
      COMMON /SCALAR/
     1 BETA, CP, CPH2, CPH3, CPH4, CPH5, CPH6, CPP3, CPP4, CPP5, CPP6,
     2 CP1, CV, DCP, DF, DHC, DHCI, DLOSC, G, GAMMA, GJ, GJ2, GR1, GR2,
     3 GR3, GR4, GR5, H, I, ICONV, ICOUNT, IERROR, IIN, IPR, IROTOR, IR,
     4 IROW, ITER, IW, J, JM, MACH, NAB, NBROWS, NHUB,NROTOR,NSTN,NSTRM,
     5 NTIP, NTUBES, OMEGA, PI, POA1, PR, RADIAN, RF, RG, ROT,TL,TOA1,TU
      COMMON
     1 BETA1(21), BETA2(21), COSA(21), COSL(21), DKLE(1,21), DL(21),
     2 GAMM(21), OBAR(21), RELM(21), RPR1(21), RE1(21), RE2(21),
     3 RE3(21), RE4(21), RE5(21), RVTH(21), SINA(21), SINL(21), SLOS(21)
     4,SONIC(21), THETAP(21,13), THETAS(21,13), TREL1(21), TSTAT(21),
     5 VM(21), VTSC(21), XBAR(1,21), YBAR(1,21), ZP(21,13), ZS(21,13)
      COMMON /EQUIV/
     1 CHD(21), CHK(21), COSA2(21), FSM(21), KIC(21), KOC(21), RCA(21),
     2 REC(2,21), RPTE(2,21), SINA2(21), SKIC(21), SKOC(21), TALP(21),
     3 TCA(21), TEC(2,21), TGB(21),TTRP(21),TTRS(21),YCCLE(25),YCCTE(25)
     4,ZCCLE(25), ZCCTE(25), ZCDA(21), ZEC(2,21), ZTRP(21), ZTRS(21)
      COMMON /BLADES/
     1 AMACH, ACC, A1SOAS, A1SCA1, BINC, CALP, CCC, CEPE, CGBL, CHORD,
     2 CINC, CKTC, CKTS, C1, C2, DKAPPA, DRCE, DRCGI, DRCMST, DRCMT,
     3 DRCCI, DRCT, DRCTI, DR1, DSME, DSMT, DSOI, DSOT, DSSE, DST, DSTI,
     4 EMT, F1, F2, GBL, ICL, IGO, IPASS, KIS, KM, KTC, KTS, P, PFLOS,
     5 RCG, RCM, RCMS, RCT, RD1, RECGI, REE, REMT, RET, RETI, RMSJ, RTRC
     6,R1, R1C, R2, SALP, SEPE, SGAM, SGBL, SJ, SKTC, SKTS, SLJD, T,
     7 TEPE, TGBLL, THD, THLE, THMAX, THTE, TKTN, TLS, WC1, YB1, YB2, ZM
      COMMON /MARG/
     1 AL, AOAS, AOA1, CCHORD, DAL, DAOAS, DPW, DPWL, DRCLEP, DRCM,
     2 DRCTPI, DRCTSI, DRCWT, DSA, DSP, DSP1, DSP2, DSS, DSS1, DSS2, DSW
     3,EB, EWC, F, HC, ICHCKE, KIP, KOP, KOS, KP, KS, KTP, KWC, PI2, RCI
     4,RCL, RCP, RCS, RCTP, RCTS, RELEP, REOI, REP, RES, RETP, RETS,
     5 REWT, RTR, RTRO, RTRC, SECGBL, TCGI, TGBL, WC, ZMT
      DIMENSION BI(21), BKTC(21), CF(21), FA(21), FT(21), PS1(21),
     1 PS2(21), RBF(21), SF(21), SMACH(21), TLOS(21), ZEL(2,21)
```

```
C *** DERIVATIVE OF A FUNCTION FROM A PARABOLIC FIT
      DFDR(R,F1,F2,F3,R1,R2,R3) = ((F3- F2)*(R1 + R2 - 2.0*R)/(R2 - R3)
     X + (F2 - F1)*(R2 + R3 - 2.0*R)/(R2 - R1))/(R3 - R1)
C *** LOCAL VALUE OF A FUNCTION FROM A PARABOLIC FIT OF NEARBY POINTS
      PRESS(R,P1,P2,P3,R1,R2,R3) = P2 + (R - R2)/(R1 - R3)*((P1 - P2)*
     X (R - R3)/(R1 - R2) - (P2 - P3)*(R - R1)/(R2 - R3))
      IR = 5
      IW = 6
      IROW = 1
      ILOSS(IROW) = 1
      IROTOR = 1
   10 CALL INPUT
      ICONV = 0
      ITER = 0
      NTUBES = NSTRM -1
      JM = NTUBES/2 + 1
      PI2 = PI/2.0
C *** CALCULATE PARAMETERS THAT ARE NOT ITERATION DEPENDENT
      RTA = R(I,1) + R(I-1,1)
      RHTA = RTA - (R(I,NSTRM) + R(I-1,NSTRM))
      CHD(1) = PI*RTA*SOLID(IROW)/BLADES(IROW)
      DO 690 J=1,NSTRM
      SINA(J) = SLOPE(I-1,J)/SQRT(1.0 + SLOPE(I-1,J)**2)
      COSA(J) = SQRT(1.0 - SINA(J)**2)
      SINA2(J) = SLOPE(I,J)/SQRT(1.0 + SLOPE(I,J)**2)
      COSA2(J) = SQRT(1.0 - SINA2(J)**2)
      RPTE(I-1,J) = 0.0
  690 RPTE(I,J) = 0.0
C *** THE MAIN OPERATING LOOP
  700 ITER = ITER + 1
      IF (ICONV.NE.2) GO TO 708
C *** COMPUTE STATIC PRESSURES ON STREAMLINES AT THE BLADE EDGES
      WRITE (IW,2540)
      DO 701 JI = 1,3
      HR = ((VZ(I-1,JI)/COSA(JI))**2 + VTH(I-1,JI)**2)/GJ2
      TU = TO(I-1,JI)
      TL = TEMP(HR)
      TSTAT(JI) = TL
      PS1(JI) = PO(I-1,JI)/144.0/PRATIO(TU)
      HR = ((VZ(I,JI)/COSA2(JI))**2 + VTH(I,JI)**2)/GJ2
      TU = TO(I,JI)
      TL = TEMP(HR)
  701 PS2(JI) = PO(I,JI)/144.0/PRATIO(TU)
      JJ = 2
      IFIN = 0
      DO 705 J=1,NSTRM
      RBF(J) = (R(I-1,J) + R(I,J))/2.0
  702 IF (JJ.EQ.NTUBES) GO TO 704
      IF (RBF(J).GE.(R(I-1,JJ) + R(I-1,JJ+1))/2.0) GO TO 704
  703 JJ = JJ + 1
      HR = ((VZ(I-1,JJ+1)/COSA(JJ+1))**2 + VTH(I-1,JJ+1)**2)/GJ2
      TU = TO(I-1,JJ+1)
      TL = TEMP(HR)
      TSTAT(JJ+1) = TL
      PS1(JJ+1) = PO(I-1,JJ+1)/144.0/PRATIO(TU)
      HR = ((VZ(I,JJ+1)/COSA2(JJ+1))**2 + VTH(I,JJ+1)**2)/GJ2
      TU = TO(I,JJ+1)
      TL = TEMP(HR)
      PS2(JJ+1) = PO(I,JJ+1)/144.0/PRATIO(TU)
      IF (IFIN.EQ.1) GO TO 705
      GO TO 702
```

```
704 PA(J) = PRESS(RBF(J),PS1(JJ-1),PS1(JJ),PS1(JJ+1),R(I-1,JJ-1),
   X R(I-1,JJ),R(I-1,JJ+1))
    IF (J.NE.NSTRM.OR.JJ.EQ.NTUBES) GO TO 705
    IFIN = 1
    GO TO 703
705 WRITE (IW,2550) R(I-1,J), Z(I-1,J), VZ(I-1,J), VTH(I-1,J), R(I,J),
   X Z(I,J), VZ(I,J), VTH(I,J)
    WRITE (IW,2560)
    JJ = 2
    ORATIO = PI*(PS1(1)/TSTAT(1)*VZ(I-1,1)*R(I-1,1) + PS1(2)/TSTAT(2)*
   X VZ(I-1,2)*R(I-1,2))/RF*(R(I-1,1) - R(I-1,2))/(RBF(1) - RBF(2))
708 DO 900 J=1,NSTRM
    IF (ICONV.GE.2) GO TO 895
    IF (ITER.EQ.1) GO TO 780
C *** CORRECT THE VELOCITY DIAGRAMS TO THE EDGES OF THE BLADE
    IF (J.EQ.1) GO TO 710
    JU = J - 1
    J1 = J - 1
    J2 = J
    J3 = J + 1
    IF (J.NE.NSTRM) GO TO 720
    JL = J
    JU = J - 1
    J1 = J - 2
    J2 = J - 1
    J3 = J
    GO TO 730
710 JU = J
    J1 = J
    J2 = J + 1
    J3 = J + 2
720 JL = J + 1
730 DO 770 I=1,2
    IF (I.GT.1) GO TO 740
    TANKE = TAN(KIC(J))
    COSAE = COSA(J)
    GO TO 750
740 TANKE = TAN(KOC(J))
    COSAE = COSA2(J)
750 DRI = (Z(I,J) - ZEL(I,J))*SLOPE(I,J)
    VTH(I,J) = VTH(I,J)*(1.0 - DRI/R(I,J))
    DADR = (SLOPE(I,JU) - SLOPE(I,JL))/(1.0 + SLOPE(I,JU)*SLOPE(I,JL))
   1 /(R(I,JU) - R(I,JL) + (Z(I,JU) - Z(I,J))*SLOPE(I,JU) - (Z(I,JL) -
   2 Z(I,J))*SLOPE(I,JL))
    ARATIO = (1.0 + DRI/R(I,J))*(1.0 - DADR*(Z(I,J) - ZEL(I,J)))
    HR = ((VZ(I,J)/COSAE)**2 + VTH(I,J)**2)/GJ2
    TU = TO(I,J)
    TL = TEMP(HR)
    RHC = PC(I,J)/(TL*RF*PRATIO(TU))
    RVZC = RHC*VZ(I,J)/ARATIO
    VZ(I,J) = VZ(I,J)*(1.0 + (1.0/ARATIO - 1.0)/(1.0 - (VZ(I,J)/
   X COSAE)**2/(GAMM(J)*RG*TL)))
760 HR = ((VZ(I,J)/COSAE)**2 + VTH(I,J)**2)/GJ2
    TL = TEMP(HR)
    RVZ = VZ(I,J)*PO(I,J)/(TL*RF*PRATIO(TU))
    IF (ABS(RVZ/RVZC - 1.0).LT.0.0001) GO TO 765
    VZ(I,J) = VZ(I,J)*(1.0 + (1.0 - RVZ/RVZC)/(1.0 - (VZ(I,J)/COSAE)**
   X 2/(GAMM(J)*RG*TL)))
    GO TO 760
```

```
C *** SET THE EDGE DERIVATIVE, R*PARTIAL OF THETA WITH RESPECT TO R
  765 TANLD = DFDR(REC(I,J),ZEC(I,J1),ZEC(I,J2),ZEC(I,J3),REC(I,J1),
     X REC(I,J2),REC(I,J3))
      SINLD = TANLD/SQRT(1.0 + TANLD**2)
      TANLA = (TANLD + TALP(J))/(1.0 - TANLD*TALP(J))
      COSLA = 1.0 /SQRT(1.0 + TANLA**2)
      CALP = 1.0/SQRT(1.0 + TALP(J)**2)
      RPTE(I,J) = DFDR(REC(I,J),TEC(I,J1),TEC(I,J2),TEC(I,J3),REC(I,J1),
     X REC(I,J2),REC(I,J3))
  770 RPTE(I,J) = (REC(I,J)*RPTE(I,J)*CALP - TANKE*SINLD)/COSLA
      I = 2
  780 ZEL(I-1,J) = Z(I-1,J)
      ZEL(I,J) = Z(I,J)
C *** VELOCITY DIAGRAM PARAMETERS FOR THE BLADE ELEMENT DESIGN
      VM(J) = VZ(I-1,J)/COSA(J)
      W1 = SQRT(VM(J)**2 + VTH(I-1,J)**2)
      HR = W1**2/GJ2
      TU = TO(I-1,J)
      TL = TEMP(HR)
      CP = CPF(TL)
      GAMM(J) = CP/(CP - DCP)
      SONIC(J) = RG*GAMM(J)*TL
      VMO = VZ(I,J)/COSA2(J)
      IF (ISTN(I).GT.0) GO TO 790
      TREL1(J) = TO(I-1,J)
      WTH1 = VTH(I-1,J)
      WTH2 = VTH(I,J)
      TLOS(J) = 1.0 - PO(I,J)/PO(I-1,J)
      GO TO 800
  790 U = OMEGA*R(I-1,J)/12.0
      HR = U*(2.0*VTH(I-1,J) - U)/GJ2
      TU = TO(I-1,J)
      TREL1(J) = TEMP(HR)
      WTH1 = U - VTH(I-1,J)
      W1 = SQRT(VM(J)**2 + WTH1**2)
      WTH2 = R(I,J)*OMEGA/12.0 - VTH(I,J)
      GR2 = GAMM(J)/(GAMM(J) - 1.0 )
      TLOS(J) = (1.0 - PO(I,J)/PO(I-1,J)/(TO(I,J)/TO(I-1,J))**GR2)*(1.0
     1 + (OMEGA*R(I,J))**2/(288.0*GR2*RG*TREL1(J))*(1.0 - (R(I-1,J)/
     2 R(I,J))**2))**GR2
  800 W2 = SQRT(VMO**2 + WTH2**2)
      BETA1(J) = ATAN(WTH1/VM(J))
      BETA2(J) = ATAN(WTH2/VMO)
      RELM(J) = W1/SQRT(SONIC(J))
      RJA = R(I,J) + R(I-1,J)
      DR = (R(I,J) - R(I-1,J))**2
      CR = SQRT(1.0 - (1.0 + (VM(J)*VMO - WTH1*WTH2)/(W1*W2))*DR/(2.0*
     X (DR + (Z(I,J) - Z(I-1,J))**2)))
      RRA = (RTA - RJA)/RHTA
      IF (J.NE.1) GO TO 810
      CRT = CR
      GO TO 820
  810 CR = CRT*(1.0 + RRA*(CHORDA(IROW) + RRA*(CHORDB(IROW) + RRA*
     X CHORDC(IROW))))/CR
      CHD(J) = CHD(1)*CR
  820 IF (ITER.NE.1) GO TO 825
      BETAS(IROW,J) = 0.8*BETA1(J) + 0.2*BETA2(J)
      IF (ITRANS(IROW).NE.2) GO TO 825
      TRANS(IROW,J) = SIN(BETA1(J))*RJA/(RTA*SOLID(IROW)*(1.0 + RRA*
     X (CHORDA(IROW) + RRA*(CHORDB(IROW) + RRA*CHORDC(IROW)))))
      IF (TRANS(IROW,J).GT.0.9) TRANS(IROW,J) = 0.9
```

```
C *** CALCULATE THE SHOCK LOSS PARAMETER
  825 GP1 = GAMM(J) + 1.0
      GM1 = GAMM(J) - 1.0
      GR1 = SQRT(GP1/GM1)
      GR2 = GAMM(J)/GM1
      GR3 = 1.0/GM1
      GR4 = GP1/2.0
      GR5 = GM1/2.0
      SSBETA= BETA1(J) - BETAS(IROW,J)
C *** TEST FOR SUPERSONIC VELOCITY
      IF (RELM(J).LT.1.0) GO TO 830
      SMM = SQRT(RELM(J)**2 - 1.0)
      PMEYER = GR1*ATAN(SMM/GR1) - ATAN(SMM)
      GO TO 840
  830 PMEYER = 0.0
  840 PMEYER = PMEYER + SSBETA
      IF (PMEYER.LE.0.0) GO TO 860
C *** ITERATE FOR THE SUCTION SURFACE MACH NUMBER
      TEMPM = 1.0 + 3.0*PMEYER
  850 SM = SQRT(TEMPM**2 - 1.0)
      SMG = SM/GR1
      VV = GR1*ATAN(SMG) - ATAN(SM)
      DIFF = PMEYER - VV
      TEMPM = TEMPM + DIFF*SM/(TEMPM/(1.0 + SMG**2) - 1.0/TEMPM)
      IF (ABS(DIFF).LE.0.001) GO TO 870
      GO TO 850
  860 TEMPM = 1.0
  870 AMACH = (RELM(J) + TEMPM)/2.0
      IF (AMACH.GT.1.0) GO TO 880
      SLOS(J) = 1.0
      GO TO 890
  880 AMSQ = AMACH**2
      SLOS(J) = ((GR4*AMSQ/(1.0 + GR5*AMSQ))**GR2)*(GR4/(GAMM(J)*AMSQ -
     X GR5))**GR3
      SLOS(J) = 1.0 - (1.0 - SLOS(J))/AMSQ
  890 OBAR(J) = (TLOS(J) - 1.0 + SLOS(J))/(1.0 - (1.0 + GM1/2.0*RELM(J)
     X **2)**(-GR2))
  895 CALL BLADE
      IF (IERROR.EQ.1.AND.ICONV.LT.2) GO TO 10
      CALL SBETA
      IF (ICONV.LT.2) GO TO 900
      IF (IGO.NE.2) CALL MARGIN
C *** COMPUTE THE BLADE FORCES
  896 IF (JJ.EQ.NTUBES) GO TO 897
      IF (RBF(J).GE.(R(I,JJ) + R(I,JJ+1))/2.0) GO TO 897
      JJ = JJ + 1
      GO TO 896
  897 FA(J) = 2.0*PI*RBF(J)*(PRESS(RBF(J),PS2(JJ-1),PS2(JJ),PS2(JJ+1),
     X R(I,JJ-1),R(I,JJ),R(I,JJ+1)) -FA(J))/BLADES(IROW)
      IF (J.NE.NSTRM) GO TO 898
      RATIO = ORATIO
      GO TO 899
  898 RATIO = PI*(PS1(J)/TSTAT(J)*VZ(I-1,J)*R(I-1,J) + PS1(J+1)/
     X TSTAT(J+1)*VZ(I-1,J+1)*R(I-1,J+1))/RF*(R(I-1,J) - R(I-1,J+1))/
     2 (RBF(J) - RBF(J+1))
  899 FT(J) = (RATIO + ORATIO)/(2.0*C*BLADES(IROW))
      FA(J) = FA(J) + FT(J)*(VZ(I,J) - VZ(I-1,J))
      FT(J) = FT(J)*(VTH(I-1,J) - VTH(I,J))
      ORATIO = RATIO
```

```
C *** SET UP CALCULATED BLADE ELEMENT PARAMETERS FOR PRINTOUT
      THMAX = 2.0*THMAX
      SSCAMB = (KIS - KTS)*RADIAN
      GBL = GBL*RADIAN
      INC(IROW,J) = BINC
      BI(J) = BINC*RADIAN
      DEV(IROW,J) = BETA2(J) - SKOC(J)
      BKTC(J) = KTC*RADIAN
      SF(J) = F1
      CF(J) = F2 - F1
      WRITE (IW,2570) THLE, THMAX, THTE, ZM, T, P, SSCAMB, GBL, SJ,
     X CHC(J), ACC, RBF(J), FA(J), FT(J)
  900 CALL POINTS
      CALL STACK
      IF (ICONV.EQ.2) GO TO 920
      IF (ITER.EQ.8) ICONV = 2
      GO TO 700
  920 WRITE(IW,2580)
      DO 930 J=1,NSTRM
      B1 = BETA1(J)*RADIAN
      B2 = BETA2(J)*RADIAN
      SSI = BI(J) - DKLE(IROW,J)*RADIAN
      KIC(J) = KIC(J)*RADIAN
      DV = DEV(IROW,J)*RADIAN
      KOC(J) = KOC(J)*RADIAN
      SKIC(J) = SKIC(J)*RADIAN
      SKOC(J) = SKOC(J)*RADIAN
  930 WRITE (IW,2590) BI(J), SSI, B1, SKIC(J), KIC(J), DV, B2
     X,SKOC(J), KOC(J), BKTC(J), SF(J), CF(J), CHK(J), FSM(J)
      CALL COCRC
      GO TO 10
 2540 FORMAT (1H1 //// 40X,52H*** TERMINAL CALCULATIONS WITH THE STACKED
     1 BLADE *** ///   43X,45H** INPUT DATA CORRECTED TO THE BLADE EDGES
     2 ** // 9X,23(1H-),7H INLET ,22(1H-), 9X,22(1H-),8H OUTLET ,22(1H-)
     3 // 7X,2(2X,10HSTREAMLINE,7X,5HAXIAL,9X,5HAXIAL,5X,10HTANGENTIAL,
     4 8X) /7X,2(4X,6HRADIUS,7X,8HLOCATION,6X,8HVELOCITY,6X,8HVELOCITY,
     5 9X) / 7X,2(3X,8H(INCHES),6X,8H(INCHES),6X,8H(FT/SEC),6X,
     6 8H(FT/SEC),9X) // )
 2550 FORMAT (3X,2F14.4,1X,2F14.3,5X,2F14.4,1X,2F14.3)
 2560 FORMAT (1H1 /// 2X,8HL.E.RAD.,2X,7HMAX.TH.,1X,8HT.E.RAD.,2X,
     1 7HMAX.TH.,1X,8HTRAN.PT.,1X,7HSEGMENT,2X,8H1ST SEG.,1X,7HBLD.SET,
     2 2X,7HELEMENT,3X,5HAERO.,2X,10HLOC.OF MAX,6X,18HLOCAL BLADE FORCES
     3 / 3X,6H/CHORD,2(3X,6H/CHORD),3X,7HPT.LOC.,1X,8HLOCATION,2X,
     4 6HIN/OUT,2X,8HS.S.CAM.,2X,5HANGLE,3X,8HSOLIDITY,2X,5HCHORD,3X,
     5 8HCAMB.PT.,3X,6HRADIUS,2X,9HFOR.AXIAL,3X,5HTANG. / 27X,2(3X,
     6 6H/CHORD),2X,9HTURN.RATE,1X,5H(DEG),4X,5H(DEG),13X,5H(IN.),4X,
     7 6H/CHORD,4X,5H(IN.),3X,8H(LBS/IN),2X,8H(LBS/IN) // )
 2570 FORMAT (2X,F7.4,5F9.4,F8.2,F9.2,F10.4,2F9.4,F10.3,2F10.4)
 2580 FORMAT (/// 4X,4HINC.,1X,8HS.S.INC.,1X,7HIN.FLOW,2X,
     1 8HIN.BLADE,2X,8HIN.ANGLE,3X,4HDEV.,1X,8HOUT.FLOW,2X,9HOUT.BLADE,
     2 2X,8HOUT.ANG.,2X,8HTRAN.PT.,2X,7HSH.LOC.,2X,
     3 9HCOV.CHAN.,2X,8HMIN.CHK.,2X,8HMIN.CHK. / 3X,5HANGLE,3X,5HANGLE,
     4 3X,5HANGLE,4X,5HANGLE,4X,7HON CONE,3X,5HANGLE,3X,5HANGLE,5X,
     5 5HANGLE,4X,7HON CONE,2X,8HBL.ANGLE,2X,8HAS FRACT,
     6 2X,8HAS FRACT,4X,4HAREA,3X,9HPT.LOC.IN / 3X,5H(DEG),3X,5H(DEG),
     7 3X,5H(DEG),4X,5H(DEG),5X,5H(DEG),4X,5H(DEG),3X,5H(DEG),5X,5H(DEG)
     8,5X,5H(DEG),5X,5H(DEG),4X,7HOF S.S.,3X,7HOF S.S.,3X,
     9 6HMARGIN,3X,9HCOV.CHAN. // )
 2590 FORMAT (2X,F6.2,2F8.2,F9.2,F10.2,F9.2,F8.2,3F10.2,4F10.4 )
      END
```

```
      SUBROUTINE INPUT
C *** READ AND PROCESS THE INPUT DATA
      REAL INC, MACH, MOLE
      COMMON /VECTOR/
     1 BETAS(1,21), BMATL(1), BLADES(1), CHOKE(1), CHORDA(1), CHORDB(1),
     2 CHORDC(1), CPCO(6), DEV(1,21), IDEV(1), IGEO(1), IINC(1),
     3 ILOSS(1), IMAX(1), INC(1,21), ISTN(2), ITRANS(1), NOPT(1),
     4 NXCUT(1), PHI(1,21), PL(2,21), R(2,21), RBHUB(1), RBTIP(1),
     5 SLOPE(2,21), SOLID(1), TALE(1), TAMAX(1), TATE(1), TBLE(1),
     6 TBMAX(1), TBTE(1), TCLE(1), TCMAX(1), TCTE(1), TDLE(1), TDMAX(1),
     7 TDTE(1), TILT(1), TL(2,21), TRANS(1,21), VTH(2,21), VZ(2,21),
     8 Z(2,21), ZBHUB(1), ZBTIP(1), ZMAX(1,21)
      COMMON /SCALAR/
     1 BETA, CP, CPH2, CPH3, CPH4, CPH5, CPH6, CPP3, CPP4, CPP5, CPP6,
     2 CP1, CV, DCP, DF, DFC, DHCI, DLOSC, G, GAMMA, GJ, GJ2, GR1, GR2,
     3 GR3, GR4, GR5, H, I, ICONV, ICOUNT, IERROR, IIN, IPR, IROTOR, IR,
     4 IROW, ITER, IW, J, JM, MACH, NAB, NBROWS, NHUB,NROTOR,NSTN,NSTRM,
     5 NTIP, NTUBES, OMEGA, PI, POA1, PR, RADIAN, RF, RG, ROT,TL,TOA1,TU
      DIMENSION WORD(20)
      COMMON /LABEL/ TITLE(18)
      DATA WORD / 4HVEL., 4HDESI, 4HCOOR, 4HPUNC, 4HALL , 4H2-D , 4H3-D
     X, 4HTABL, 4HSUCT, 4HCART, 4HMODI, 4HCIRC, 4HOPTI, 4HSHOC, 4HAPPR,
     X 4HESS, 4HELF, 4H B  , 4H M  , 4H P   /
   10 READ (IR,1000) (TITLE(I),I=1,18)
      WRITE (IW,2000) (TITLE(I),I=1,18)
C *** READ THE SPECIFIC HEAT COEFFICIENTS
      READ (IR,1020) (CPCO(I),I=1,6)
      WRITE (IW,2060) (CPCO(I),I=1,6)
      READ (IR,1010) NSTRM, MOLE, ROT, ZBTIP(IROW), RBTIP(IROW),
     X ZBHUB(IROW), RBHUB(IROW), NXCUT(IROW)
      I = 2
      PI = 3.1415927
      RADIAN =57.29578
      G = 32.1740
      GJ = 25035.24
      GJ2 = 50070.47
      OMEGA = ROT*6.2831854/60.0
      RF = 1545.44/MOLE
      RG = RF*G
      DCP = RF/778.12
      CPH2 = CPCO(2)/2.0
      CPH3 = CPCO(3)/3.0
      CPH4 = CPCO(4)/4.0
      CPH5 = CPCO(5)/5.0
      CPH6 = CPCO(6)/6.0
      CPP3 = CPCO(3)/2.0
      CPP4 = CPCO(4)/3.0
      CPP5 = CPCO(5)/4.0
      CPP6 = CPCO(6)/5.0
      CP1 = CPCO(1)/DCP
      CP = 0.24
      READ (IR,1030) BLADES(IROW), SOLID(IROW), TILT(IROW),
     X BMATL(IROTOR), CHOKE(IROW)
      IF (ROT.GT.0.0) GO TO 20
      ISTN(I) = -2
      GO TO 30
   20 ISTN(I) = 2
   30 READ (IR,1030) TALE(IROW), TBLE(IROW), TCLE(IROW), TDLE(IROW),
     X TATE(IROW), TBTE(IROW), TCTE(IROW), TDTE(IROW)
      READ (IR,1030) TAMAX(IROW), TBMAX(IROW), TCMAX(IROW),
```

```
     X TOMAX(IROW), CHORDA(IROW), CHORDB(IROW), CHORDC(IROW)
      READ (IR,1040) OP, OPO, AA, AB, BB, CC, DD, EE, EB
      WRITE (IW,2010) NSTRM, MOLE, ROT, ZRTIP(IROW), RRTIP(IROW),
     1 ZRHUB(IROW), RRHUB(IROW), BLADES(IROW), SOLID(IROW), TILT(IROW)
      WRITE (IW,2020) TALE(IROW), TATE(IROW), TAMAX(IROW), TBLE(IROW),
     1 TBTE(IROW), TBMAX(IROW), CHORDA(IROW), TCLE(IROW), TCTE(IROW),
     2 TCMAX(IROW), CHORDB(IROW), TDLE(IROW), TDTE(IROW), TDMAX(IROW),
     3 CHORDC(IROW)
C *** SET OPTION WHICH CONTROLS THE AMOUNT OF INFORMATION DESIRED
      IF (OP.NE.WORD(5)) GO TO 40
      NOPT(IROW) = 6
      GO TO 60
   40 IF (OP.NE.WORD(4)) GO TO 50
      NOPT(IROW) = 5
      GO TO 120
   50 IF (OP.NE.WORD(3)) GO TO 90
      NOPT(IROW) = 4
   60 IF (OPO.NE.WORD(18)) GO TO 70
      NOPT(IROW) = NOPT(IROW) + 30
      GO TO 120
   70 IF (OPO.NE.WORD(20)) GO TO 80
      NOPT(IROW) = NOPT(IROW) + 20
      GO TO 120
   80 IF (OPO.NE.WORD(19)) GO TO 120
      NOPT(IROW) = NOPT(IROW) + 10
      GO TO 120
   90 IF (OP.NE.WORD(2)) GO TO 100
      NOPT(IROW) = 3
      GO TO 120
  100 IF (OP.NE.WORD(1)) GO TO 110
      NOPT(IROW) = 2
      GO TO 120
  110 NOPT(IROW) = 1
  120 IF (ABS(TILT(IROW)).LT.1.0.0) TILT(IROW) = TILT(IROW)/RADIAN
      IF (ISTN(I).LT.0) GO TO 140
      WRITE (IW,2355)
      IF (CHOKE(IROW).LE.0.0) GO TO 130
      WRITE (IW,2360) CHOKE(IROW), BMATL(IROTOR)
      GO TO 160
  130 WRITE (IW,2370) BMATL(IROTOR)
      GO TO 160
  140 IF (CHOKE(IROW).LE.0.0) GO TO 150
      WRITE (IW,2360) CHOKE(IROW)
      GO TO 160
  150 WRITE (IW,2370)
  160 IF (NOPT(IROW).LT.3) GO TO 620
      ITABLE = 0
C *** SET BLADE ELEMENT DESIGN CONTROL OPTIONS AND READ NECESSARY INPUT
  410 IF (AA.EQ.WORD(7)) GO TO 420
      IF (AA.EQ.WORD(9)) GO TO 430
      IF (AA.EQ.WORD(8)) GO TO 440
      IINC(IROW) = 1
      WRITE (IW,2375)
      GO TO 434
  420 IINC(IROW) = 2
      WRITE (IW,2380)
      GO TO 434
  430 IINC(IROW) = 3
      WRITE (IW,2390)
  434 DO 436 J=1,NSTRM
```

```
436 INC(IROW,J) = -0.0
    GO TO 450
440 READ (IR,1030) (INC(IROW,J),J=1,NSTRM)
    ITABLE = 1
    IF (AB.EQ.WORD(16)) GC TC 445
    IINC(IROW) = 4
    WRITE (IW,2392)
    GC TC 450
445 IINC(IROW) = 5
    WRITE (IW,2394)
450 IF (BB.EC.WORD(7)) GO TC 460
    IF (BB.EQ.WORD(10)) GC TC 470
    IF (BB.EQ.WORD(11)) CC TC 48C
    IF (BB.EQ.WORD(8)) GO TO 490
    IDEV(IROW) = 1
    WRITE (IW,2400)
    GC TO 484
460 IDEV(IROW) = 2
    WRITE (IW,2410)
    GC TC 484
470 IDEV(IROW) = 3
    WRITE (IW,2420)
    GC TC 484
480 IDEV(IROW) = 4
    WRITE (IW,2430)
484 DC 486 J=1,NSTRM
486 DEV(IROW,J) = -0.0
    GC TO 500
490 IDEV(IROW) = 5
    WRITE (IW,2435)
    READ (IR,1030) (DEV(IROW,J),J=1,NSTRM)
    ITABLE = 1
500 IF (CC.EQ.WCRD(13)) GC TC 510
    IF (CC.EQ.WORD(8)) GC TO 520
    IGEC(IROW) = 1
    DC 505 J=1,NSTRM
505 PHI(IROW,J) = 1.0
    WRITE (IW,2440)
    GC TC 530
510 IGEC(IROW) = 2
    WRITE (IW,2450)
514 DC 516 J=1,NSTRM
516 PHI(IROW,J) = -0.0
    GC TO 530
520 IGEC(IROW) = 3
    READ (IR,1030) (PHI(IROW,J),J=1,NSTRM)
    ITABLE = 1
    WRITE (IW,2455)
530 IF (DD.EQ.WORD(14).ANC.IGEO(IROW).NE.1) GO TO 540
    IF (DD.EQ.WORC(8)) GC TO 550
    ITRANS(IRCW) = 1
    DC 535 J=1,NSTRM
535 TRANS(IRCW,J) = 0.5
    WRITE (IW,2458)
    GC TC 560
540 ITRANS(IRCW) = 2
    WRITE (IW,2460)
    DC 545 J=1,NSTRM
545 TRANS(IRCW,J) = -0.0
    GC TC 560
```

```
550 ITRANS(IROW) = 3
    READ (IR,1030) (TRANS(IROW,J),J=1,NSTRM)
    ITABLE = 1
    WRITE (IW,2462)
    DO 552 J=1,NSTRM
    IF (TRANS(IROW,J).LT.0.0.OR.TRANS(IROW,J).GT.1.0) GO TO 554
552 CONTINUE
    GO TO 560
554 WRITE (IW,2465) IROW, J
    IERROR = 1
    RETURN
560 IF (EE.EQ.WORD(8)) GO TO 570
    IMAX(IROW) = 1
    DO 565 J=1,NSTRM
565 ZMAX(IROW,J) = 0.0
    WRITE (IW,2470)
    GO TO 580
570 READ (IR,1030) (ZMAX(IROW,J),J=1,NSTRM)
    ITABLE = 1
    IF (E8.EQ.WORD(17)) GO TO 572
    IMAX(IROW) = 2
    WRITE (IW,2472)
    GO TO 574
572 IMAX(IROW) = 3
    WRITE (IW,2474)
574 IF (ITRANS(IROW).EQ.2.AND.IMAX(IROW).EQ.2) GO TO 580
    DO 576 J=1,NSTRM
    ZT = ZMAX(IROW,J)
    IF (IMAX(IROW).EQ.2) ZT = ZT + TRANS(IROW,J)
    IF (ZT.LT.0.1.OR.ZT.GT.0.9) GO TO 578
576 CONTINUE
    GO TO 580
578 WRITE (IW,2475) IROW, J
    IERROR = 1
    RETURN
580 IF (ITABLE.EQ.0) GO TO 620
    WRITE (IW,2480)
    IF (IINC(IROW).EQ.5) WRITE(IW,2482)
    IF (IMAX(IROW).EQ.3) GO TO 582
    WRITE (IW,2484)
    GO TO 584
582 WRITE (IW,2486)
584 WRITE (IW,2488)
    DO 590 J=1,NSTRM
    WRITE (IW,2490) J, INC(IROW,J), DEV(IROW,J), PHI(IROW,J),
   X TRANS(IROW,J), ZMAX(IROW,J)
    INC(IROW,J) = INC(IROW,J)/RADIAN
590 DEV(IROW,J) = DEV(IROW,J)/RADIAN
C *** READ IN BLADE ELEMENT INLET AND OUTLET CONDITIONS
620 DO 630 J=1,NSTRM
630 READ (IR,1030) R(I-1,J), Z(I-1,J), VZ(I-1,J), VTH(I-1,J),
   X SLOPE(I-1,J), TO(I-1,J), PO(I-1,J)
    DO 640 J=1,NSTRM
640 READ (IR,1030) R(I,J), Z(I,J), VZ(I,J), VTH(I,J), SLOPE(I,J),
   X TO(I,J), PO(I,J)
    WRITE (IW,2500)
    WRITE (IW,2520)
    DO 650 J=1,NSTRM
```

```
650 WRITE (IW,2530) J, R(I-1,J), Z(I-1,J), VZ(I-1,J), VTH(I-1,J),
   X SLOPE(I-1,J), TO(I-1,J), PO(I-1,J)
    WRITE (IW,2510)
    WRITE (IW,2520)
    DO 660 J=1,NSTRM
    WRITE (IW,2530) J, R(I,J), Z(I,J), VZ(I,J), VTH(I,J), SLOPE(I,J),
   X TO(I,J), PO(I,J)
    PO(I-1,J) = PO(I-1,J)*144.0
    PO(I,J) = PO(I,J)*144.0
    SLOPE(I-1,J) = TAN(SLOPE(I-1,J)/RADIAN)
660 SLOPE(I,J) = TAN(SLOPE(I,J)/RADIAN)
    WRITE (IW,2540)
    RETURN
1000 FORMAT (18A4)
1010 FORMAT (I5,5X,6F10.4,I10)
1020 FORMAT (3E20.8)
1030 FORMAT (8F10.4)
1040 FORMAT (A4,2X,A4,2A4,2X,3(A4,6X),2A4,2X)
2000 FORMAT (1H1 ///// 41X,48H*** INPUT DATA FOR COMPRESSOR DESIGN PROG
    1RAM *** //// 30X,18A4 )
2010 FORMAT (3X,9HNUMBER OF,4X,9HMOLECULAR,4X,10HROTATIONAL,3X,
   1 9HTIP AXIAL,4X,10HTIP RADIAL,3X,9HHUB AXIAL,4X,10HHUB RADIAL,3X,
   2 9HNUMBER OF,7X,3HTIP,6X,10HSTACK LINE / 2X,11HSTREAMLINES,5X,
   3 6HWEIGHT,7X,5HSPEED,6X,4(10HSTACK LOC.,3X),2X,6HBLADES,6X,
   4 8HSOLIDITY,3X,10HTANG. TILT / 31X,5H(RPM),7X,4(8H(INCHES),5X),
   5 25X,9H(DEGREES) // 7X,I2,F15.3,F13.1,4F13.4,F12.1,F14.4,F12.3 )
2020 FORMAT (// 22X,91H* POLYNOMIAL CONSTANTS FOR THE FOLLOWING FUNCTIO
   1NS OF RADIUS WITH  TIP = 0  AND  HUB = 1  * // 25X,17HL.E. RADIUS/
   2CHORD,8X,17HT.E. RADIUS/CHORD,6X,20HMAX. THICKNESS/CHORD,8X,
   3 15HCHORD/TIP CHORD // 11X,8HCONSTANT, 10X,3(F10.4,15X) / 11X,
   4 6HLINEAR,12X,4(F10.4,15X) / 11X,9HQUADRATIC,9X,4(F10.4,15X) /
   5 11X,5HCUBIC,13X,4(F10.4,15X) /// )
2060 FORMAT (///39X,53HTHE SPECIFIC HEAT POLYNOMIAL IS IN THE FOLLOWING
   1 FORM ,// 9X,4HCP =,E12.5,3H + ,E12.5,5H*T + ,E12.5,8H*T**2 + ,
   2 E12.5,8H*T**3 + ,E12.5,8H*T**4 + ,E12.5,5H*T**5 ////)
2355 FORMAT (/ 45X,42H* INPUT BLADE ELEMENT DEFINITION OPTIONS * //
   1 8X,9HINCIDENCE,9X,9HDEVIATION,7X,12HTURNING RATE,7X,10HTRANSITION
   2,6X,14HMAX. THICKNESS,9X,5HCHOKE,4X,22HBLADE MATERIAL DENSITY /
   3 10X,2(5HANGLE,13X),5HRATIO,2(13X,5HPOINT),12X,6HMARGIN,10X,
   4 10HLB/(IN)**3 // )
2356 FORMAT (/ 45X,42H* INPUT BLADE ELEMENT DEFINITION OPTIONS * //
   1 8X,9HINCIDENCE,9X,9HDEVIATION,7X,12HTURNING RATE,7X,10HTRANSITION
   2,6X,14HMAX. THICKNESS,9X,5HCHOKE / 10X,2(5HANGLE,13X),5HRATIO,
   3 2(13X,5HPOINT),12X,6HMARGIN,10X // )
2360 FORMAT (98X,F7.4,10X,F8.5)
2370 FORMAT (100X,4HNONE,12X,F8.5)
2375 FORMAT (1H+,10X,3H2-D)
2380 FORMAT (1H+,10X,3H3-D)
2390 FORMAT (1H+,8X,7HSUCTION)
2392 FORMAT (1H+,9X,5HTABLE)
2394 FORMAT (1H+,4X,16HTABLE (S.S.REF.))
2400 FORMAT (1H+,28X,3H2-D)
2410 FORMAT (1H+,28X,3H3-D)
2420 FORMAT (1H+,23X,12HCARTERS RULE)
2430 FORMAT (1H+,21X,16HMODIFIED CARTERS)
2435 FORMAT (1H+,27X,5HTABLE)
2440 FORMAT (1H+,41X,12HCIRCULAR ARC)
2450 FORMAT (1H+,44X,7HOPTIMUM)
2455 FORMAT (1H+,45X,5HTABLE)
2458 FORMAT (1H+,59X,12HCIRCULAR ARC)
2460 FORMAT (1H+,60X,10HS.S. SHOCK)
2462 FORMAT (1H+,63X,5HTABLE)
```

```
2465 FORMAT (/// 12X,53HTHE INPUT TRANSITION POINT LOCATION OF BLADE RO
    1W NO.,I2,20H, ON STREAMLINE NO.,I2,30H, IS NOT ON THE BLADE ELEMEN
    2T. )
2470 FORMAT (1H+,78X,10HTRANS. PT.)
2472 FORMAT (1H+,74X,18HTABLE (TRANS.REF.))
2474 FORMAT (1H+,75X,16HTABLE (L.E.REF.))
2475 FORMAT (///  3X,55HTHE INPUT MAX. THICKNESS PT. LOCATION OF BLADE
    1ROW NO.,I2,20H, ON STREAMLINE NO.,I2,49H, IS NOT WITHIN THE REQUIR
    2ED 10 TO 90 PCT. CHORD. )
2480 FORMAT (1H1 ///// 41X,49H* TABLE OF BLADE SECTION DESIGN VARIABLES
    1 INPUT * //26X,80H(VARIABLES CONTROLLED BY OTHER OPTIONS WILL APPE
    2AR AS MINUS ZEROS IN THE TABLE.) // )
2482 FORMAT (29X,15HSUCTION SURFACE )
2484 FORMAT (11X,10HSTREAMLINE,8X,15HINCIDENCE ANGLE,5X,
    1 15HDEVIATION ANGLE,2X,20HINLET/OUTLET TURNING,2X,
    2 16HTRANSITION/CHORD,3X,18H(MAX - TRANSITION) )
2486 FORMAT (11X,10HSTREAMLINE,8X,15HINCIDENCE ANGLE,5X,
    1 15HDEVIATION ANGLE,2X,20HINLET/OUTLET TURNING,2X,
    2 16HTRANSITION/CHORD,5X,14HMAX. THICKNESS )
2488 FORMAT (13X,6HNUMBER,2X,2(11X,9H(DEGREES)),10X,10HRATE RATIO,11X,
    1 8HLOCATION,9X,14HLOCATION/CHORD // )
2490 FORMAT (15X,I2,2X,5(12X,F8.4))
2500 FORMAT (1H1 //    51X,30H** INLET STATION INPUT DATA ** )
2510 FORMAT ( //    51X,31H** OUTLET STATION INPUT DATA ** )
2520 FORMAT ( / 1X,2(3X,10HSTREAMLINE),9X,5HAXIAL,11X,5HAXIAL,8X,
    1 10HTANGENTIAL,6X,10HSTREAMLINE,2(6X,10HSTAGNATION) / 6X,6HNUMBER,
    2 7X,6HRADIUS,9X,8HLOCATION,2(8X,8HVELOCITY),10X,5HSLOPE,8X,
    3 11HTEMPERATURE,6X,8HPRESSURE / 18X,2(8H(INCHES),8X),2(8H(FT/SEC),
    4 8X),9H(DEGREES),7X,8H(DEG.R.),9X,6H(PSIA) // )
2530 FORMAT (7X,I3,5X,F10.4,F16.4,F17.3,F16.3,F16.5,F15.2,F16.3)
2540 FORMAT (1H1 // 49X,35H*** PRINTOUT FOR EACH ITERATION ***)
     END
```

```
      FUNCTION CPF(TL)
C***  CALCULATES CP(T) OF THE FLUID AT TEMPERATURE,T
      REAL INC
      COMMON /VECTOR/
     1 BETAS(1,21), BMATL(1), BLADES(1), CHOKE(1), CHORDA(1), CHORDB(1),
     2 CHORDC(1), CPCO(6), DEV(1,21), IDEV(1), IGEO(1), IINC(1),
     3 ILOSS(1), IMAX(1), INC(1,21), ISTN(2), ITRANS(1), NOPT(1),
     4 NXCUT(1), PHI(1,21), PO(2,21), R(2,21), RBHUB(1), RBTIP(1),
     5 SLOPE(2,21), SOLID(1), TALE(1), TAMAX(1), TATE(1), TBLE(1),
     6 TBMAX(1), TBTE(1), TCLE(1), TCMAX(1), TCTE(1), TDLE(1), TDMAX(1),
     7 TDTE(1), TILT(1), TO(2,21), TRANS(1,21), VTH(2,21), VZ(2,21),
     8 Z(2,21), ZBHUB(1), ZBTIP(1), ZMAX(1,21)
      CPF = CPCO(1)+(CPCO(2)+(CPCO(3)+(CPCO(4)+(CPCO(5)+ CPCO(6)*TL)*TL)
     X *TL)*TL)*TL
      RETURN
      END
```

```
      FUNCTION TEMP(HD)
C***  CALCULATES TEMPERATURE ASSOCIATED WITH AN ENTHALPY CHANGE, HD.
      REAL INC, MACH
      COMMON /VECTOR/
     1 BETAS(1,21), BMATL(1), BLADES(1), CHOKE(1), CHORDA(1), CHORDB(1),
     2 CHORDC(1), CPCO(6), DEV(1,21), IDEV(1), IGEO(1), IINC(1),
     3 ILOSS(1), IMAX(1), INC(1,21), ISTN(2), ITRANS(1), NOPT(1),
     4 NXCUT(1), PHI(1,21), PO(2,21), R(2,21), RBHUB(1), RBTIP(1),
     5 SLOPE(2,21), SOLID(1), TALE(1), TAMAX(1), TATE(1), TBLE(1),
     6 TBMAX(1), TBTE(1), TCLE(1), TCMAX(1), TCTE(1), TDLE(1), TDMAX(1),
     7 TDTE(1), TILT(1), TO(2,21), TRANS(1,21), VTH(2,21), VZ(2,21),
     8 Z(2,21), ZBHUB(1), ZBTIP(1), ZMAX(1,21)
      COMMON /SCALAR/
     1 BETA, CP, CPH2, CPH3, CPH4, CPH5, CPH6, CPP3, CPP4, CPP5, CPP6,
     2 CPI, CV, DCP, DF, DHC, DHCI, DH    , G, GAMMA, GJ, GJ2, GR1, GR2,
     3 GR3, GR4, GR5, H, I, ICONV, IC    , IERROR, IIN, IPR, IROTOR, IR,
     4 IROW, ITER, IW, J, JM, MACH, NAB, NBROWS, NHUB,NROTOR,NSTN,NSTRM,
     5 NTIP, NTUBES, OMEGA, PI, POA1, PR, RADIAN, RF, RG, ROT,TL,TOA1,TU
      IF (ABS(HD/TU).LT.0.001) GO TO 15
      IC = 0
      CVC = 5.0E-09/ABS(HD/TU)
      IF (CVC.LT.0.00001) CVC = 0.00001
   10 TEMP = TU - HD/CP
      TSUM = TU+TEMP
      SUM = CPCO(1) + CPH2*TSUM
      PROD = TEMP*TEMP
      TSUM = TSUM*TU+PROD
      SUM = SUM+CPH3*TSUM
      PROD = PROD*TEMP
      TSUM = TSUM*TU+PROD
      SUM = SUM+CPH4*TSUM
      PROD = PROD*TEMP
      TSUM = TSUM*TU+PROD
      DT= TU-TEMP
      HN=  DT*(SUM+CPH5*TSUM+CPH6*(TSUM*TU+PROD*TEMP))
      IF (ABS(1.0 - HN/HD).LT.CVC) GO TO 20
      IC = IC + 1
      IF (IC.GT.10) WRITE (IW,2000) J, TU, HD, HN
      IF (IC.GT.15) GO TO 18
      CP = HN/DT
      GO TO 10
   15 TEMP = TU - HD/CP
      GO TO 20
   18 IERROR = 1
   20 RETURN
 2000 FORMAT (//14X,34HINSTABILITY IN FUNCTION TEMP    J =,I3,15H   UPPER
     1 TEMP =,F8.2,13H   INPUT DH =,F8.4,12H   PRES.DH =,F8.4 )
      END
```

```
      FUNCTION PRATIO(TH)
C***  CALCULATES PRESSURE RATIO BY ISENTROPIC PROCESS FOR A
C     TEMPERATURE DIFFERENCE
      REAL INC, MACH
      COMMON /VECTOR/
     1 BETAS(1,21), BMATL(1), BLADES(1), CHOKE(1), CHORDA(1), CHORDB(1),
     2 CHORDC(1), CPCO(6), DEV(1,21), IDEV(1), IGEO(1), IINC(1),
     3 ILOSS(1), IMAX(1), INC(1,21), ISTN(2), ITRANS(1), NOPT(1),
```

```
4 NXCUT(1), PHI(1,21), PO(2,21), R(2,21), RBHUB(1), RBTIP(1),
5 SLOPE(2,21), SOLID(1), TALE(1), TAMAX(1), TATE(1), TBLE(1),
6 TBMAX(1), TBTE(1), TCLE(1), TCMAX(1), TCTE(1), TDLE(1), TDMAX(1),
7 TDTE(1), TILT(1), TO(2,21), TRANS(1,21), VTH(2,21), VZ(2,21),
8 Z(2,21), ZBHUB(1), ZBTIP(1), ZMAX(1,21)
 COMMON /SCALAR/
1 BETA, CP, CPH2, CPH3, CPH4, CPH5, CPH6, CPP3, CPP4, CPP5, CPP6,
2 CP1, CV, DCP, DF, DHC, DHCI, DLOSC, G, GAMMA, GJ, GJ2, GR1, GR2,
3 GR3, GR4, GR5, H, I, ICONV, ICOUNT, IERROR, IIN, IPR, IROTOR, IR,
4 IROW, ITER, IW, J, JM, MACH, NAB, NBROWS, NHUB,NROTOR,NSTN,NSTRM,
5 NTIP, NTUBES, OMEGA, PI, POA1, PR, RADIAN, RF, RG, ROT,TL,TOA1,TU
 TSUM = TH + TL
 SUM = CPCO(2) + CPP3*TSUM
 PROD = TL*TL
 TSUM = TSUM*TH + PROD
 SUM = SUM + CPP4*TSUM
 PROD = PROD*TL
 TSUM = TSUM*TH + PROD
 PRATIO = (TH/TL)**CP1*EXP((TH-TL)/DCP*(SUM+CPP5*TSUM+CPP6*(TSUM*TH
X + PROD*TL)))
 RETURN
 END
```

```
 BLOCK DATA
 COMMON /PTS/ FSB(13)
 DATA (FSB(K),K=1,13) /.0,.05,.12,.2,.3,.4,.5,.6,.7,.8,.88,.95,1.0/
 END
```

```
     SUBROUTINE BLADE
***      THIS ROUTINE SERVES AS A CONTROL OF THE BLADE ELEMENT DESIGN.
*** INCIDENCE AND DEVIATION ANGLES ARE SET IN THIS SUBROUTINE.
     REAL INC,I2D10,I3D,KC,KI,KIC,KIS,KM,KOC,KTC,KTS,MACH,MD,NI
     COMMON /VECTOR/
   1 BETAS(1,21), BMATL(1), BLADES(1), CHOKE(1), CHORDA(1), CHORDB(1),
   2 CHORDC(1), CPCO(6), DEV(1,21), IDEV(1), IGEO(1), IINC(1),
   3 ILOSS(1), IMAX(1), INC(1,21), ISTN(2), ITRANS(1), NOPT(1),
   4 NXCUT(1), PHI(1,21), PO(2,21), R(2,21), RBHUB(1), RBTIP(1),
   5 SLOPE(2,21), SOLID(1), TALE(1), TAMAX(1), TATE(1), TBLE(1),
   6 TBMAX(1), TBTE(1), TCLE(1), TCMAX(1), TCTE(1), TDLE(1), TDMAX(1),
   7 TDTE(1), TILT(1), TO(2,21), TRANS(1,21), VTH(2,21), VZ(2,21),
   8 Z(2,21), ZBHUB(1), ZBTIP(1), ZMAX(1,21)
     COMMON /SCALAR/
   1 BETA, CP, CPH2, CPH3, CPH4, CPH5, CPH6, CPP3, CPP4, CPP5, CPP6,
   2 CP1, CV, DCP, DF, DHC, DHCI, DLOSC, G, GAMMA, GJ, GJ2, GR1, GR2,
   3 GR3, GR4, GR5, H, I, ICONV, ICOUNT, IERROR, IIN, IPR, IROTOR, IR,
   4 IROW, ITER, IW, J, JM, MACH, NAB, NBROWS, NHUB,NROTOR,NSTN,NSTRM,
   5 NTIP, NTUBES, OMEGA, PI, POA1, PR, RADIAN, RF, RG, ROT,TL,TOA1,TU
     COMMON
   1 BETA1(21), BETA2(21), COSA(21), COSL(21), DKLE(1,21), DL(21),
   2 GAMM(21), GPAR(21), RELM(21), RPR1(21), RE1(21), RE2(21),
   3 RE3(21), RE4(21), RE5(21), RVTH(21), SINA(21), SINL(21), SLOS(21)
   4,SONIC(21), THETAP(21,13), THETAS(21,13), TREL1(21), TSTAT(21),
```

```
 5 VM(21), VTSC(21), XBAR(1,21), YBAR(1,21), ZP(21,13), ZS(21,13)
  COMMON /EQUIV/
 1 CHC(21), CHK(21), CCSA2(21), FSM(21), KIC(21), KOC(21), RCA(21),
 2 REC(2,21), RPTE(2,21), SINA2(21), SKIC(21), SKOC(21), TALP(21),
 3 TCA(21), TEC(2,21), TCB(21),TTRP(21),TTRS(21),YCCLE(25),YCCTE(25)
 4,ZCCLE(25), ZCCTE(25), ZCDA(21), ZEC(2,21), ZTRP(21), ZTRS(21)
  COMMON /BLADES/
 1 AMACH, ACC, A1SCAS, A1SCA1, BINC, CALP, CCC, CEPE, CGBL, CHORD,
 2 CINC, CKTC, CKTS, C1, C2, DKAPPA, DRCE, DRCGI, DRCMST, DRCMT,
 3 DRCOI, DRCT, DRCTI, DR1, DSME, DSMT, DSOI, DSOT, DSSE, DST, DSTI,
 4 EMT, F1, F2, GBL, ICL, IGC, IPASS, KIS, KM, KTC, KTS, P, PFLOS,
 5 RCG, RCM, RCMS, RCT, RD1, RECGI, REE, REMT, RET, RETI, RMSJ, RTRC
 6,R1, R1C, R2, SALP, SEPE, SGAM, SGBL, SJ, SKTC, SKTS, SLJD, T,
 7 TEPE, TGBLL, THD, THLE, THMAX, THTE, TKTN, TLS, WC1, YB1, YB2, ZM
  IGC = 0
  RT1 = R(I-1,1)
  RT2 = R(I,1)
  RCI = RT1 - R(I-1,NSTRM)
  RC2 = RT2 - R(I,NSTRM)
  CHCRDT = CHC(1)
  TLS= (ZBTIP(IROW) - ZBHUB(IROW))/(RBTIP(IROW) - RBHUB(IROW))
  IF (ABS(TILT(IROW)).GE.100.0) GO TO 4
  STILT = SIN(TILT(IROW))
  CTILT= SQRT(1.0- STILT**2)
  GO TO 6
4 HUBT = TILT(IROW)/100.0
  IH = HUBT
  TIPT = TAN((TILT(IROW) - 100.0*FLOAT(IH))/RADIAN)
  IH = IH - (IH/100)*100
  HUBT = TAN(FLOAT(IH)/RADIAN)
6 R1 = R(I-1,J)
  R2 = R(I,J)
  RR1 = (RT1 - R1)/RCI
  RR2 = (RT2 - R2)/RC2
  THLE= TALE(IROW)+(TBLE(IROW)+(TCLE(IROW)+TDLE(IROW)*RR1)*RR1)*RR1
  THMAX = (TAMAX(IROW) + (TBMAX(IROW) + (TCMAX(IROW) + TDMAX(IROW)*
 X RR1)*RR1)*RR1)/2.0
  THTE= TATE(IROW)+(TBTE(IROW)+(TCTE(IROW)+TDTE(IROW)*RR2)*RR2)*RR2
  CHCRD = CHC(J)
  R1C = R1/CHCRD
10 P = PHI(IROW,J)
  T =TRANS(IROW,J)
  ZM = ZMAX(IROW,J)
  IF (IMAX(IROW).NE.3) ZM = ZM + T
  B1 = BETA1(J)
  B2 = BETA2(J)
  B2EQ = R2*VTH(I,J)/R1
  IF (ISTN(I).GT.0) B2EQ = R1*OMEGA/12.0 - B2EQ
  B2EQ = ATAN(B2EQ/(VZ(I-1,J)*SQRT(1.0 + SLOPE(I-1,J)**2)))
  SJ = SOLID(IROW)*(RT1 + RT2)/(R1 + R2)*CHORD/CHORDT
  CCC= 1.0 - THLE - THTE
  C1 = T- THLE
  C2 = 1.0 - T - THTE
  THD = THLE - THTE
  TALP(J)= (R2-R1)/(Z(I,J)- Z(I-1,J))
  CALP = SQRT(1.0/(TALP(J)**2+1.0))
  SALP = TALP(J)*CALP
  TEPE = THD/CCC
  CEPE = 1.0/SQRT(1.0+TEPE**2)
  SEPE = TEPE*CEPE
```

```
C ***       LOCATE THE BLADE ELEMENT STACKING POINT REFERENCE WITH
C     RESPECT TO THE HUB WALL STACKING POINT.
      RCA(J)= (R1-RBHUB(IROW) + (ZBHUB(IROW) - Z(I-1,J))*TALP(J))/
     X (1.0 - TALP(J)*TLS)
      ZCDA(J) = RCA(J)*TLS
      RCA(J)= RCA(J) + RBHUB(IROW)
      RR= RBHUB(IROW)/RCA(J)
      IF (ABS(TILT(IROW)).GE.100.0) GO TO 12
      TCA(J)= ARSIN(STILT*(SQRT(1.0 - (RR*STILT)**2 ) -RR*CTILT))
      GO TO 14
   12 TCA(J) = (RCA(J) - RBHUB(IROW))/(RBTIP(IROW) - RBHUB(IROW))*(TIPT
     X - HUBT) + (HUBT - RBHUB(IROW)/(RBTIP(IROW) - RBHUB(IROW))*(TIPT -
     X HUBT))*ALOG(RCA(J)/RBHUB(IROW))
   14 IF (ISTN(I).LT.0) TCA(J) = -TCA(J)
      IF (ITER.GT.1) GO TO 15
C ***       AN APPROXIMATION OF THE LOCATION OF THE STACKING POINT WITH
C     RESPECT TO THE BLADE ELEMENT LEADING EDGE CENTER FOR INITIAL STACK
      AREA = (2.0*THMAX + THTE + ZM*THD)/3.0
      A = ZM*(2.0*THMAX - 2.0*THTE + ZM*THD)/12.0 + (THMAX + THTE)/4.0
      XBAR(IROW,J) = A/AREA - THLE
      YB1 = (THLE + THTE)/2.0
      YB2 = CCC*(4.0 - ( 4.0+ 1.0/THMAX)*YB1)/10.0
   15 IF (CHOKE(IROW).EQ.0.0.AND.ICONV.NE.2) GO TO 60
      IF (ICONV.GT.2) GO TO 60
C *** CALCULATE STREAMTUBE CONVERGENCE CONSTANTS
      IF (J.GT.1) GO TO 20
      RJM= R1
      ZJM= Z(I-1,J)
      SLJM= TALP(1)
      GO TO 40
   20 RJM= R(I-1,J-1)
      ZJM= Z(I-1,J-1)
      SLJM= TALP(J-1)
   30 IF (J.LT.NSTRM) GO TO 40
      RJP= R1
      ZJP= Z(I-1,NSTRM)
      SLJP= TALP(NSTRM)
      GO TO 50
   40 RJP= R(I-1,J+1)
      ZJP= Z(I-1,J+1)
      SLJP= (R(I,J+1) - R(I-1,J+1))/(Z(I,J+1) - Z(I-1,J+1))
   50 RD1 = RJM - RJP
      DR1 = RD1 - ZJM*SLJM + ZJP*SLJP
      SLJD= SLJP - SLJM
      GM1 = GAMM(J) - 1.0
      GR2 = GAMM(J)/GM1
      GR4 = (GAMM(J) + 1.0)/2.0
      GR1 = GR4/GM1
      RMR= 1.0 + GM1/2.0*RELM(J)**2
      A1SCA1 = RELM(J) *(GR4/RMR)**GR1
      PFLOS= OEAR(J)*(1.0 - RMR**(-GR2))
      RTRC = 0.0
      IF (ISTN(I).LT.0) GO TO 60
      RTRC = (OMEGA*CHORD)**2/(GR2*RG*TREL1(J)*144.0)
   60 IF (IINC(IROW) .GT.2) GO TO 90
C ***       IF INCIDENCE AND DEVIATION ANGLES ARE TO BE DETERMINED BY THE
C     METHODS OF NASA SP-36, VALUES FROM SEVERAL PARAMETRIC CURVES ARE
C     NEEDED. ALGEBRAIC EQUATIONS WHICH MATCH THE PARAMETER CURVES
C     WITHIN A FEW PERCENT ARE USED.
      IF (IINC(IROW).EQ.1) GO TO 70
```

```
*** CALCULATE THE 3-D INCIDENCE CORRECTION FACTOR.
    I3D = (2.55*RR1 - 2.8 + ((7.5 - 2.5*RR1)*RR1 +5.275)*RELM(J)**(((
   X 0.1563*RR1 - 0.344)*RR1 + 1.0828)/RELM(J))**((0.4375*RR1 - 1.1375
   X )*RR1 + 2.7094)))/RADIAN
*** CALCULATE SLOPE OF DEVIATION  WITH 2-D INCIDENCE FACTOR.
    A = 3.35 - B1*(0.71+ 0.29*B1)
    B = (0.0446*B1 - 0.0405)*B1+ 0.0070
    C = SIN(PI*SJ/1.2)
    DDEVDI = EXP(-A*SJ) + B*(C/SJ)**2
    GO TO 80
 70 I3D= 0.0
*** CALCULATE KI, THE BLADE THICKNESS FACTOR ON INCIDENCE.
 80 KI = ((1514.4*THMAX - 312.24)*THMAX + 26.0)*THMAX
*** CALCULATE 2-D INCIDENCE FACTOR FOR 10 PERCENT THICK AIRFOIL
    I2D10 = SJ*B1*(0.080 - B1**5*0.001442)
    CINC= I3D + KI*I2D10
*** CALCULATE, NI, INCIDENCE FACTOR ON BLADE CAMBER.
    AA = (0.1959 - 0.03757*SJ)*SJ - 0.2205 - 0.02638/SJ
    BB = ( 0.08833*(1.2 - SJ)**2 - 0.55653)*0.1882
    CC = 1.427 + 7.288 * (SJ - 0.4)/SJ**5.2
    DD = (0.00625*SJ - 0.0438)*SJ + 0.0165
    EE = ABS(B1*RADIAN - 40.0)/30.0
    NI = -0.025*(2.4 - SJ) + (AA+BB*B1**2) *B1 + (0.5+(ATAN(B1*
   X RADIAN- 40.0))/PI)*(0.0278*EE**1.65 + DD*EE**CC)
    GO TO 150
 90 IF (IINC(IROW).EQ.4) GO TO 130
    IF (ITER.GT.1) GO TO 120
    DKLE(IROW,J) = 2.0*ATAN((THMAX - THLE)/ZM)
120 CINC= DKLE(IROW,J)
    IF (IINC(IROW).EQ.5) CINC = CINC + INC(IROW,J)
    GO TO 140
130 CINC= INC(IROW,J)
140 NI= 0.0
    I3D = 0.0
150 IPASS = 0
    IF (IDEV(IROW).GT.2) GO TO 180
    IF (IDEV(IROW).EQ.1) GO TO 160
*** CALCULATE D3D, THE 3-D DEVIATION CORRECTION FACTOR
    A = -1.75 + 2.5*RR2 + RR2**6.58
    B = ((60.2 - RR2*46.25)*RR2 - 5.558)*RR2
    C= 5.0*(ABS(RR2 - 0.05))**0.166667
    D3D = (A + B*(RELM(J) - 0.45 + RR2/6.0)**C)/RADIAN
    GO TO 170
160 D3D= 0.0
*** CALCULATE D2D10, THE 2-D DEVIATION FACTOR FOR 10 PERCENT THICKNESS
170 D2D10 = ((((0.6812*SJ + 1.325)*SJ - 0.3895)*B1 + (0.4937- SJ*(
   X 0.837 + 1.0185*SJ)))*B1 + ((0.00825*SJ + 1.473)*SJ - 0.1049))*B1/
   X RADIAN
*** CALCULATE KD, THE BLADE THICKNESS FACTOR ON DEVIATION.
    KD = THMAX*(9.333 + 97.8*THMAX)
*** CALCULATE MD, DEVIATION FACTOR ON BLADE CAMBER.
    MD= ((0.05842*B1 -0.04221)*B1 + 0.04046)*B1 + 0.25
*** CALCULATE B, THE SOLIDITY EXPONENT.
    B = 0.966 + B1*(-0.17475 + B1*(0.2034 - B1*0.2781))
    CDEV = KD*D2D10 + I3D*DDEVDI + D3D
    GO TO 240
180 IF (IDEV(IROW).NE.5) GO TO 190
    MD= 0.0
    B = 1.0
    CDEV = DEV(IROW,J)
    GO TO 240
```

```
*** DEVIATION [illegible] BY CARTERS RULE.
190 B = 0.5
    GBL = 0.37*B1 + 0.63*B2
    IF (IGO.EQ.2.OR IGEO(IROW).NE.2) GO TO 195
    DK = 2.0*(THMAX - THLE)/ZM/(B1 - B2)
    CM = (RELM(J) - 1.0)*RELM(J)**6
    P = (1.0 - DK*CM*(1.0 - T)/T)/(1.0 + (1.0 + DK)*CM)
195 GAMPHI = 0.5*(P*C2**2/C1 - C1)/CCC
    IF (GAMPHI) 200,220,210
200 ACC = T + C1*GAMPHI
    GO TO 230
210 ACC = T + C1*GAMPHI/P
    GO TO 230
220 ACC = T
230 MD = (0.[illegible] + GBL*(0.[illegible] + 0.088915*GBL))*(2.0*ACC)**(2.175 -
   X GBL*(2.0354 - 0.62922*GBL))
    CDEV= 0.0
    IPASS = IPASS + 1
240 CN = B1 - B2EQ + CDEV - CINC
    DVC = MD/SJ**B
    CD = 1.0 - DVC + NI
    DKAPPA = CN/CD
    BINC = CINC + NI*DKAPPA
    SKIC(J) = B1 - BINC
    SKOC(J) = B2 - CDEV - DVC*DKAPPA
    KIC(J) = ATAN((TAN(SKIC(J))*CALP - (SINA(J)*CALP - SALP*COSA(J))*
   X RPTE(I-1,J))/COSA(J))
    KOC(J) = ATAN((TAN(SKOC(J))*CALP - (SINA2(J)*CALP - SALP*COSA2(J))
   X *RPTE(I,J))/COSA2(J))
    DKAPPA = KIC(J) - KOC(J)
    SGAM = SIN((KIC(J) + KOC(J))/2.0)
    IF (IGEO(IROW).NE.2) GO TO 250
***       SET SEGMENT TURNING RATE RATIO FOR OPTIMUM OPTION
    IF (RELM(J).GT.0.8) GO TO 242
    P = 1.0
    GO TO 248
242 IF (ITER.GT.1) GO TO 244
    DK = 2.0*(THMAX - THLE)/ZM
    GO TO 246
244 DK = DKLE(IROW,J)
246 CM = 0.75*(RELM(J) - 0.8)*RELM(J)**6
    DKT = KIC(J) - KOC(J)
    P = (DKT - DK*CM*(1.0 - T)/T)/(DKT + (DKT + DK)*CM)
248 PHI(IROW,J) = P
250 CALL CONIC
    IF (IERROR.EQ.1.AND.ICONV.LT.2) RETURN
    IF (IGO-1) 280,230,140
280 RETURN
    END
```

```
    SUBROUTINE CONIC
***      THIS IS THE MAIN BLADE ELEMENT LAYOUT ROUTINE.  BLADE ELEMENTS
*** ARE LAID OUT ON A CONE SUCH THAT THE CIRCULAR ARC CHARACTERISTIC
*** OF CONSTANT RATE OF ANGLE CHANGE WITH PATH DISTANCE IS MAINTAINED.
    REAL INC, KIC, KIP, KIS, KM, KOC, KOP, KOS, KP, KS, KT, KTC, KTP,
   1 KTS, KWC, MACH
    COMMON /VECTOR/
```

```
     1 BETAS(1,21), BMATL(1), BLADES(1), CHOKE(1), CHORDA(1), CHORDB(1),
     2 CHORDC(1), CPCO(6), DEV(1,21), IDEV(1), IGEO(1), IINC(1),
     3 ILOSS(1), IMAX(1), INC(1,21), ISTN(2), ITRANS(1), NOPT(1),
     4 NXCUT(1), PHI(1,21), PO(2,21), R(2,21), RBHUB(1), RBTIP(1),
     5 SLOPE(2,21), SOLID(1), TALE(1), TAMAX(1), TATE(1), TBLE(1),
     6 TBMAX(1), TBTE(1), TCLE(1), TCMAX(1), TCTE(1), TDLE(1), TDMAX(1),
     7 TDTE(1), TILT(1), TO(2,21), TRANS(1,21), VTH(2,21), VZ(2,21),
     8 Z(2,21), ZBHUB(1), ZBTIP(1), ZMAX(1,21)
      COMMON /SCALAR/
     1 BETA, CP, CPH2, CPH3, CPH4, CPH5, CPH6, CPP3, CPP4, CPP5, CPP6,
     2 CP1, CV, DCP, DF, DHC, DHCI, DLOSC, G, GAMMA, GJ, GJ2, GR1, GR2,
     3 GR3, GR4, GR5, H, I, ICONV, ICOUNT, IERROR, IIN, IPR, IROTOR, IR,
     4 IROW, ITER, IW, J, JM, MACH, NAB, NBROWS, NHUB,NROTOR,NSTN,NSTRM,
     5 NTIP, NTUBES, OMEGA, PI, POA1, PR, RADIAN, RF, RG, ROT,TL,TOA1,TU
      COMMON
     1 BETA1(21), BETA2(21), COSA(21), COSL(21), DKLE(1,21), DL(21),
     2 GAMM(21), OBAR(21), RELM(21), RPR1(21), RE1(21), RE2(21),
     3 RE3(21), RE4(21), RE5(21), RVTH(21), SINA(21), SINL(21), SLOS(21)
     4,SONIC(21), THETAP(21,13), THETAS(21,13), TREL1(21), TSTAT(21),
     5 VM(21), VTSQ(21), XBAR(1,21), YBAR(1,21), ZP(21,13), ZS(21,13)
      COMMON /EQUIV/
     1 CHD(21), CHK(21), COSA2(21), FSM(21), KIC(21), KOC(21), RCA(21),
     2 REC(2,21), RPTE(2,21), SINA2(21), SKIC(21), SKOC(21), TALP(21),
     3 TCA(21), TEC(2,21), TGB(21),TTRP(21),TTRS(21),YCCLE(25),YCCTE(25)
     4,ZCCLE(25), ZCCTE(25), ZCDA(21), ZEC(2,21), ZTRP(21), ZTRS(21)
      COMMON /BLADES/
     1 AMACH, ACC, A1SOAS, A1SCA1, BINC, CALP, CCC, CEPE, CGBL, CHORD,
     2 CINC, CKTC, CKTS, C1, C2, DKAPPA, DRCE, DRCGI, DRCMST, DRCMT,
     3 DRCOI, DRCT, DRCTI, DR1, DSME, DSMT, DSOI, DSOT, DSSE, DST, DSTI,
     4 EMT, F1, F2, GBL, ICL, IGO, IPASS, KIS, KM, KTC, KTS, P, PFLOS,
     5 RCG, RCM, RCMS, RCT, RD1, RECGI, REE, REMT, RET, RETI, RMSJ, RTRC
     6,R1, R1C, R2, SALP, SEPE, SGAM, SGBL, SJ, SKTC, SKTS, SLJD, T,
     7 TEPE, TGBLL, THD, THLE, THMAX, THTE, TKTN, TLS, WC1, YB1, YB2, ZM
      COMMON /MARG/
     1 AL, AOAS, ACA1, CCHORD, DAL, DAOAS, DPW, DPWL, DRCLEP, DRCM,
     2 DRCTPI, DRCTSI, DRCWT, DSA, DSP, DSP1, DSP2, DSS, DSS1, DSS2, DSW
     3,EB, EWC, F, HC, ICHOKE, KIP, KOP, KOS, KP, KS, KTP, KWC, PI2, RCI
     4,RCC, RCP, RCS, RCTP, RCTS, RELEP, REOI, REP, RES, RETP, RETS,
     5 REWT, RTR, RTRD, RTRC, SECGBL, TCGI, TGBL, WC, ZMT
      IGO=0
***       ESTABLISH BLADE ELEMENT CENTERLINE TO SATISFY CAMBER, CHORD
*** AND TRANSITION POINT REQUIREMENTS.
      CGAM= SQRT(1.0 - SGAM**2)
      DK2 = DKAPPA/(1.0 + P*C1/C2)
      CCHORD = CALP*CHORD
      IF (IPASS.GT.1) GO TO 30
      ICL = 1
      EPS= CCC*SGAM*SALP/(R1C + (THLE + CCC*CGAM)*SALP)
      DPHI = DKAPPA - EPS
      DPHI4 = DPHI/4.0
      DPHIHS = DPHI*DPHI4
      DSOI = CCC/(1.0 - DPHIHS/6.0*(1.0 - DPHIHS/20.0))
      DSTI= C1/CCC*DSOI
      DSOT= DSOI - DSTI
      IF (ITER.GT.1) GO TO 10
      SINDP4 = DPHI4*SRS(DPHI4)
      YBAR(IROW,J) = YB1 + YB2*SINDP4/SQRT(1.0 - SINDP4**2) - THLE
   10 IF (ABS(SALP/R1C).LT.1.0E-08)  GO TO 20
      RCI= R1C/SALP + THLE
      GO TO 25
   20 RCI= 1.0E+08
```

```
   25 RCG = RCI - THLE + (ZCCA(J) + ZBHUB(IROW) - Z(I-1,J))/CCHORD
   30 DK1 = DKAPPA - DK2
      CALL EPSLCN(KIC(J),-DK1,RCI,DSTI,DRCTI,RETI)
      KTC = KTC(J) - DK1
      RCT= RCI + DRCTI
   35 CALL EPSLCN(KTC,-DK2,RCT,DSOT,DRCOT,REOT)
      RCO= RCT + DRCOT
      REOI= RCO/RCT*RETI + REOT
      DRCOI= DRCTI + DRCOT
      CALL TANKAP(RCI,DRCOI,REOI,TANCCO)
      TGBL= (TANCCO + TEPE)/(1.0 - TANCCO*TEPE)
      CALL RPCINT(RCI,DRCTI,RETI,TGBL,DRCTP)
      SECGBL= SQRT(1.0 + TGBL**2)
      DC1= DRCTP*SECGBL - C1
      DC2 = DRCOI*SQRT(1.0 + TANCCO**2)*CEPE - CCC
      IF (ICL.GT.1.AND.ABS(TGBL - TGBLL).LT.1.0E-04) GO TO 45
      GBL= ATAN(TGBL)
      CALL EPSLCN(GBL,0.0,RCI,XBAR(IROW,J),DRCMT,REMT)
      RCM = RCI + DRCMT
      CALL EPSLCN(GBL+PI2,0.0,RCM,YBAR(IROW,J),DRCGI,RECGI)
      DRCGI = DRCGI + DRCMT
      RCI = RCG - DRCGI
      ICL = 2
      TGBLL = TGBL
   45 IF (ABS(DC1).LT.1.0E-05) GO TO 40
      DS1= DSTI*DC1/(C1 + DC1)
      DSTI= DSTI - DS1
      DSOT= DSOT - DSOI*DC2/(CCC + DC2) + DS1
      DSOI = DSTI + DSOT
      DK2 = DKAPPA/(1.0 + P*DSTI/DSOT)
      GO TO 30
   40 IF (ABS(DC2).LT.1.0E-06)  GO TO 50
      DSOT= DSOT - DSOI*DC2/(CCC + DC2)
      DSOI = DSTI + DSOT
      GO TO 35
   50 IF (IPASS.EQ.2) GO TO 100
      IF (ICONV.EQ.2) GO TO 55
      IF (IDEV(IROW).LE.2.OR.IDEV(IROW).GE.5)  GO TO 100
C ***        CALCULATION OF A BETTER VALUE OF MAXIMUM CAMBER HEIGHT ABOVE
C *** THE CONSTANT ANGLE LINE CONNECTING BLADE ELEMENT EDGE CIRCLE
C *** CENTERS.  IT IS USED FOR A MORE REFINED VALUE OF DEVIATION ANGLE
C *** BY MODIFIED CARTERS RULE.
   55 IF (ABS(DKAPPA).LT.0.001) GO TO 80
      GCCO= ATAN(TANCCO)
      DGAM= KTC - GCCO
      IF (ABS(DGAM/DKAPPA).LT.0.001)  GO TO 90
      IF (DGAM/DKAPPA.GT.0.0)  GO TO 60
      DSAT= DSTI*DGAM/DK1
      GO TO 70
   60 DSAT= DSOT*DGAM/DK2
   70 CALL EPSLCN(KTC,-DGAM,RCT,DSAT,DRCAT,REAT)
      CALL RPCINT(RCT,DRCAT,REAT,TGBL,DRCAP)
      ACC= T + DRCAP*SECGBL
      GO TO 95
   80 ACC= 0.5
      GO TO 95
   90 ACC= T
   95 IF (IDEV(IROW).LT.3.OR.IDEV(IROW).GT.4) GO TO 100
      IGC=1
      RETURN
  100 RECGI = RECGI + (1.0 + DRCGI/RCM)*REMT
```

```
C ***      RESET BLADE EDGE COORDINATES
      R(I-1,J) = RCA(J) - (DRCGI + THLE)*SALP*CHORD
      R(I,J) = R(I-1,J) + (DRCGI + THLE + THTE)*SALP*CHORD
      Z(I-1,J) = ZBHUB(IROW) + ZCDA(J) - (DRCGI + THLE)*CCHORD
      Z(I,J) = Z(I-1,J) + (DRCGI + THLE + THTE)*CCHORD
      R1C = R(I-1,J)/CHORD
      TCGI = RECGI/(R1C + (DRCGI + THLE)*SALP)
C ***      CONIC COORDINATES OF THE MAXIMUM THICKNESS POINT
      ZMT = ZM - T
      IF (ZMT.NE.0.0)  GO TO 120
      DRCMT= 0.0
      REMT= 0.0
      DK= 0.0
      DSMT = 0.0
      DSME= DSTI
      GO TO 150
  120 HKTC= KTC/2.0
      SHKTC= HKTC*SRS(HKTC)
      SHKTCQ= SHKTC**2
      SKTC= 2.0*SHKTC*SQRT(1.0 - SHKTCQ)
      IF (ABS(SKTC).LT.1.0E-07) SKTC = 1.0E-07
      CKTC= 1.0 - 2.0*SHKTCQ
      TKTN= -CKTC/SKTC
      IF (ZMT.GT.0.0)  GO TO 130
      DSMT= DSTI*ZMT/C1
      DKDS= DK1/DSTI
      DSME= DSTI
      GO TO 140
  130 DSMT= DSCT*ZMT/C2
      DKDS = DK2/DSCT
      DSME= -DSCT
  140 DK= -DSMT*DKDS
      CALL EPSLON(KTC,DK,RCT,DSMT,DRCMT,REMT)
      CALL RPOINT(RCT,DRCMT,REMT,TCBL,DRCMP)
      ZMTCAL= DRCMP*SECGBL
      IF (ABS(ZMTCAL - ZMT).LT.1.0E-05)  GO TO 150
      DSMT = DSMT*ZMT/ZMTCAL
      GO TO 140
  150 RCM= RCT + DRCMT
      REMI= (1.0 + DRCMT/RCT)*RETI + REMT
      KM= KTC  + DK
      HKM= KM/2.0
      SHKM= HKM*SRS(HKM)
      SHKMQ= SHKM**2
      CHKM= SQRT(1.0 - SHKMQ)
      SKM= 2.0*SHKM*CHKM
      CKM= 1.0 - 2.0*SHKMQ
      DSME= DSME + DSMT
C ***      DEFINITION OF SUCTION SURFACE MAX. THICKNESS POINT
      CALL EPSLON(KM+PI2,0.0,RCM,THMAX,DRCM,REM)
      RCMS= RCM + DRCM
      IF (ZMT.GT.0.0)  GO TO 180
C ***      DEFINITION OF SUCTION SURFACE CURVE FOR MAXIMUM THICKNESS
C *** POINT ON OR AHEAD OF THE TRANSITION POINT
      DK= 2.0*(THMAX - THLE)/DSME
      KIS= KIC(J) + DK
      KIP= KIC(J) - DK
      DRCIM= -DRCTI - DRCMT - DRCM
      EMSI= REMI/RCM + REM/RCMS
      CALL SURF(KIS,KM,SKM,CKM,RCI,DRCIM,THLE,EMSI,DSSE)
      IF (ZMT.EQ.0.0)  GO TO 160
```

```
      DRCMST= DRCMT + DRCM
      EMT= REM/RCMS + REMT/RCM
      CALL TRAN(KIS,THLE,THMAX,KTS,RCTS,RETS,DSS1)
      DHKT= (KTC - KTS)/2.0
      DK= 2.0*(DST - THTE - DSCT*DHKT)/(DSCT + (DST - THTE)*DHKT)
      DRCCTS= DRCCT - DRCT
      EMSC= RET/RCTS - REOT/RCC
      DRCTSI = DRCTI + DRCT
      GO TO 170
  160 RCTS= RCMS
      KTS= KM
      RETS = RCMS*EMSI
      DSS1 = -DSSE
      SKTS= SKM
      CKTS= CKM
      DK= 2.0*(THMAX - THTE)/DSOT
      DRCCTS= DRCOT - DRCM
      EMSC= REM/RCMS - REOT/RCC
      DRCTSI = DRCTI + DRCM
  170 KOS= KOC(J) - DK
      KOP= KOC(J) + DK
      CALL SURF(KOS,KTS,SKTS,CKTS,RCO,DRCOTS,THTE,EMSO,DSS2)
      GO TO 190
C ***      DEFINITION OF SUCTION SURFACE CURVE FOR MAXIMUM THICKNESS
C *** POINT BEHIND THE TRANSITION POINT
  180 DK= 2.0*(THMAX - THTE)/DSME
      KOS = KOC(J) + DK
      KOP = KOC(J) - DK
      DRCOM= DRCOT - DRCMT - DRCM
      EMSO= REMT/RCM - REOT/RCO + REM/RCMS
      CALL SURF(KOS,KM,SKM,CKM,RCO,DRCOM,THTE,EMSO,DSSE)
      DRCMST= DRCMT + DRCM
      EMT= REM/RCMS + REMT/RCM
      CALL TRAN(KOS,THTE,THMAX,KTS,RCTS,RETS,DSS2)
      DHKT= (KTS- KTC)/2.0
      DK= 2.0*(DST - THLE - DSTI*DHKT)/(DSTI + (DST - THLE)*DHKT)
      KIS= KIC(J) + DK
      KIP= KIC(J) - DK
      DRCTSI = DRCTI + DRCT
      EMSI= RETI/RCT + RET/RCTS
      CALL SURF(KIS,KTS,SKTS,CKTS,RCI,-DRCTSI,THLE,EMSI,DSSE)
      DSS1 = -DSSE
C ***      DEFINITION OF PRESSURE SURFACE MAXIMUM THICKNESS POINT
  190 CALL EPSLON(KM+PI2,0.0,RCM,-THMAX,DRCM,REM)
      RCMS= RCM + DRCM
      IF (ZMT.GT.0.0)  GO TO 220
C ***      DEFINITION OF PRESSURE SURFACE CURVE FOR MAXIMUM THICKNESS
C *** POINT ON OR AHEAD OF THE TRANSTION POINT
      DRCIM= -DRCTI - DRCMT - DRCM
      EMSI= REMI/RCM + REM/RCMS
      CALL SURF(KIP,KM,SKM,CKM,RCI,DRCIM,-THLE,EMSI,DSSE)
      DRCLEP = DRCE
      RELEP = REE
      IF (ZMT.EQ.0.0)  GO TO 200
      DRCMST= DRCMT + DRCM
      EMT = REM/RCMS + REMT/RCM
      CALL TRAN(KIP,-THLE,-THMAX,KTP,RCTP,RETP,DSP1)
      DRCCTS= DRCCT - DRCT
      EMSC = RET/RCTP - RECT/RCO
      DRCTPI = DRCTI + DRCT
      GO TO 210
```

```
  200 RCTP = RCMS
      KTP= KM
      RETP= RCMS * EMSI
      DSP1 = -DSSE
      DRCCTS= DRCCT - DRCM
      EMSC = REM/RCMS - RECT/RCO
      DRCTPI = DRCTI + DRCM
  210 CALL SURF(KOP,KTP,SKTS,CKTS,RCO,DRCOTS,-THTE,EMSC,DSP2)
      GO TO 230
C ***      DEFINITION OF PRESSURE SURFACE CURVE FOR THE MAXIMUM
C *** THICKNESS POINT BEHIND THE TRANSITION POINT
  220 DRCCM= DRCCT - DRCMT - DRCM
      EMSC = REMT/RCM - RECT/RCO + REM/RCMS
      CALL SURF(KOP,KM,SKM,CKM,RCO,DRCOM,-THTE,EMSO,DSSE)
      DRCMST= DRCMT + DRCM
      EMT = REM/RCMS + REMT/RCM
      CALL TRAN(KOP,-THTE,-THMAX,KTP,RCTP,RETP,DSP2)
      DRCTPI = DRCTI + DRCT
      EMSI = RETI/RCT + RET/RCTP
      CALL SURF(KIP,KTP,SKTS,CKTS,RCI,-DRCTPI,-THLE,EMSI,DSSE)
      DRCLEP = DRCE
      RELEP = REE
      DSP1 = -DSSF
  230 DSS = DSS1 + DSS2
      DSP = DSP1 + DSP2
      EB = 1.0/(SJ*(RCI + DRCCI/2.0))
      IF (ICONV.GT.2) RETURN
      DSA = (DSS + DSP)/2.0
      DKLE(IROW,J) = KIS - KIC(J)
      IF (DKLE(IROW,J).GE.0.0) GO TO 232
      WRITE (IW,2000) J, IROW, ITER
      GO TO 233
  232 IF ((KOS - KCC(J)).LE.0.0) GO TO 234
      WRITE (IW,2010) J, IROW, ITER
  233 THMAX = 2.0*THMAX
      WRITE (IW,2020) THLE, THMAX, THTE, ZM
      IERROR = 1
      IF (ICONV.LT.2) RETURN
  234 RTRC = RTRC*SALP*DSA
      RMSJ = (R1C + R2/CHORD)*SJ/2.0
      WC1 = R1C*COS(BETA1(J))/RMSJ
      ICHCKE = 1
      KP = KIP
      DPW = -DSP1
      RCP = RCI + DRCLEP
      REP = RCP*EB + RELEP
      DRCWT = DRCLEP - DRCTSI
      REWT = REP - RETS*RCP/RCTS
      CALL CHAN
      RETURN
 2000 FORMAT (/// 6X,74HTHE BLADE ELEMENT THICKNESS DECREASES FROM THE L
     1EADING EDGE OF ELEMENT NO.,I3,17H OF BLADE ROW NO.,I3,17H ON ITERA
     2TION NO.,I3 )
 2010 FORMAT (/// 6X,75HTHE BLADE ELEMENT THICKNESS DECREASES FROM THE T
     1RAILING EDGE OF ELEMENT NO.,I3,17H OF BLADE ROW NO.,I3,17H ON ITER
     2ATION NO.,I3 )
 2020 FORMAT (// 1X,47HADJUST SOME OF THIS INPUT DATA  L.E.RAD/CHORD =,
     1 F7.4,17H  MAX.TH./CHORD =,F7.4,17H  T.E.RAD/CHORD =,F7.4,
     2 21H  MAX.TH.LOC./CHORD =,F7.4 )
      END
```

```
      SUBROUTINE EPSLON(KO,DK,RO,DS,DR,RE)
C ***       CALCULATION OF CONIC RADIAL AND CIRCUMFERENTIAL COMPONENTS OF
C *** A BLADE ELEMENT SEGMENT WITH GIVEN PATH DISTANCE AND END ANGLES
      REAL KO
      IF (DS.EQ.0.0) GO TO 70
      HDK= DK/2.0
      SR= SRS(HDK)
      SHDK= HDK*SR
      SHDKQ= SHDK**2
      CHDK= SQRT(1.0 - SHDKQ)
      HKO= KO/2.0
      IF (HKO.GT.0.78539816) GO TO 4
      SHKO= HKO*SRS(HKO)
      SHKOQ= SHKO**2
      CHKO= SQRT(1.0 - SHKOQ)
      SKO= 2.0*SHKO*CHKO
      CKO= 1.0 - 2.0*SHKOQ
      GO TO 6
    4 HKO = 0.78539816 - HKO
      SHKO = HKO*SRS(HKO)
      SHKOQ = SHKO**2
      CHKO = SQRT(1.0 - SHKOQ)
      SKO = 1.0 - 2.0*SHKOQ
      CKO = 2.0*SHKO*CHKO
    6 SKA= SHDK*CKO + SKO*CHDK
      CKA= CHDK*CKO - SKO*SHDK
C ***       CONIC RADIAL COMPONENT OF THE PATH
      DR= DS*CKA*SR
      IF (ABS(DK).GT.0.00001) GO TO 10
      IF (ABS(RO).GT.100.0*DS) GO TO 60
C ***       CIRCUMFERENTIAL COMP. WHEN PATH ANGLE IS ESSENTIALLY CONSTANT
      RE= (RO + DR)*SKA/CKA*ALOG(1.0 + DR/RO)
      RETURN
   10 IF (ABS(RO).GT.10000.0*DS) GO TO 60
      RS= RO/DS
      IF (RS**2/ABS(DK).GT.1.7E+09) GO TO 60
C ***       CONIC CIRCUMFERENTIAL COMPONENT OF PATH BY GENERAL EQUATION
      RCK= RS*DK - SKO
      QDKS= HDK**2/4.0
      SES = 0.66666667*RCK*QDKS*(1.0 - 0.6*QDKS*(1.0 - 0.15873016*QDKS*
     X (1.0 - 0.077777778*QDKS*(1.0 - 0.046753247*QDKS*(1.0 - .031330903
     X *QDKS)))))
      DRR= DR/RO
      IF (ABS(DRR).GT.0.21)  GO TO 20
      RRM = 0.5*DRR*(1.0 - 0.25*DRR*(1.0 - 0.5*DRR*(1.0 - 0.625*DRR*(1.0
     X - 0.7*DRR*(1.0 - 0.75*DRR*(1.0 - 0.78571429*DRR*(1.0 - 0.8125*DRR
     X *(1.0 - 0.83333333*DRR))))))))
      RRO = RRM  + 1.0
      GO TO 30
   20 RRO= SQRT(1.0 + DRR)
      RRM= RRO - 1.0
   30 RM= RRO*RS
      D = RCK*CHDK + SKA + DK*RM
      XS= SHDKQ*(1.0 -RCK**2)/D**2
      XSN= 35.0*ABS(XS)
      NXS= XSN
      N= 5 + NXS
      SXS= 0.0
      XPS= 1.0
      DKN= 1.0
      DO 40  KN=1,N
```

```
      IF (ABS(XPS).LT.1.CE-12.ANC.KN.NE.1) GO TO 50
      XPS= XPS*XS
      DKN= DKN + 2.0
   40 SXS= SXS + XPS/DKN
   5C RE= (RO + DR)*(DK*(SKC + SKA + DK*RS*RRM - SES) - 4.0*RCK*SHDK*
     X SXS)/D
      RETURN
C ***       CCNIC CIRCUMFERENTIAL CCMPONENT WHEN PATH DISTANCE IS A VERY
C *** SMALL FRACTICN CF THE CISTANCE TO THE CONE VERTEX.
   6C DRR= DR/RC
      RE = (1.0 + DRR)/(1.0 + C.5*DRR*(1.0 - 0.25*DRR*(1.C - 0.5*DRR*
     X (1.0 - 0.625*DRR))))*CS*SKA*SR
      RETURN
   7C DR = 0.0
      RE = 0.0
      RETURN
      END
```

```
      FUNCTICN SRS(ANG)
C ***       SERIES FOR (SIN(ANG))/ANG WHEN THE MAGNITUDE OF ANG IS LESS
C *** THAN PI/4
      IF (ABS(ANG).LT.1.0E-C5) GC TO 10
      AC = ANG**2
      SRS = 1.0 - AQ/6.0*(1.C - AQ/20.0*(1.0 - AQ/42.0*(1.0 - AQ/72.0)))
      RETURN
   1C SRS = 1.0
      RETURN
      END
```

```
      SUBRCUTINE TANKAP(RO,CR,RE,TK)
C ***       CALCULATION CF THE SLOPE OF THE CONSTANT ANGLE PATH BETWEEN
C *** TWO POINTS IN CONIC RACIUS AND EPSILON COORDINATES
      R = DR/RO
      IF (ABS(R).LT.0.1) GC TC 20
      TK = RE/((RO + DR)*ALCG(1.0 + R))
      RETURN
   2C SUM = 1.0
      IF (ABS(R).GT.1.0E-08) GC TO 25
      IF (ABS(DR/RE).GT.1.0E-08) GC TO 35
      TK = 1.0E+08
      RETURN
   25 PRCC = 1.0
      DN = 8.0/(-ALCG10(ABS(R)))
      NT = DN
      DC 30 I=1,NT
      N = I + 1
      CN = N
      PRCC = -PRCC*R
   3C SUM = SUM + PROD/DN
   35 TK = RE/((RC + CR)*R*SUM)
      RETURN
      END
```

```
      SUBROUTINE RPOINT(RO,DR,RE,TK,DRP)
C ***       THIS SUBROUTINE CALCULATES THE CONIC RADIAL COORDINATE AT THE
C *** INTERSECTION OF PERPENDICULAR CONSTANT ANGLE LINES FROM TWO KNOWN
C *** POINTS ON A CONE.  THE LINE THROUGH THE REFERENCE POINT HAS THE
C *** INPUT SLOPE TK.
      R = DR/RC
      CK = SQRT(1.0/(1.0 + TK**2))
      SK = TK*CK
      IF (ABS(R).LT.0.01) GO TO 20
      DRP = RC*(EXP((RE*SK/(RC + DR) + ALOG(1.0 + R)*CK)*CK) - 1.0)
      RETURN
   20 C = (RE*SK/(RC + DR) + R*(1.0 - 0.5*R*(1.0 - 0.66666667*R*(1.0 -
     X 0.75*R))))*CK)*CK
      DRP = C
   30 CS = DRP*(1.0 - 0.5*DRP*(1.0 - 0.66666667*DRP*(1.0 - 0.75*DRP)))
      IF (ABS((CS - C)/C).LT.1.0E-06) GO TO 40
      DRP = DRP*C/CS
      GO TO 30
   40 DRP = DRP*RC
      RETURN
      END
```

```
      SUBROUTINE TRAN(KE,TE,TM,KT,RT,RE,DS)
C ***       THIS SUBROUTINE CALCULATES THE BLADE ELEMENT SURFACE CURVE
C *** TRANSITION POINT COORDINATES FROM THE INTERSECTION OF THE
C *** ESTABLISHED SURFACE CURVE OVER THE MAXIMUM THICKNESS POINT WITH A
C *** PATH PERPENDICULAR TO THE CENTERLINE AT THE TRANSITION POINT.
      REAL KE, KIS, KM, KT, KTC, KTS
      COMMON /BLADES/
     1 AMACH, ACC, AISOAS, AISCAI, BINC, CALP, CCC, CEPE, CGBL, CHORD,
     2 CINC, CKTC, CKTS, C1, C2, DKAPPA, DRCE, DRCGI, DRCMST, DRCMT,
     3 DRCCI, DRCI, DRCTI, DR1, DSME, DSMT, DSOI, DSOT, DSSE, DST, DSTI,
     4 EMT, F1, F2, GBL, ICL, IGO, IPASS, KIS, KM, KTC, KTS, P, PFLOS,
     5 RCC, RCM, RCMS, RCT, RCI, RECGI, REE, REMT, RET, RETI, RMSJ, RTRC
     6,RI, RIC, R2, SALP, SEPE, SGAM, SGBL, SJ, SKTC, SKTS, SLJD, T,
     7 TEPE, TGBLL, THO, THLE, THMAX, THTE, TKTN, TLS, WC1, YB1, YB2, ZM
      DST = TM - (TM - TE)*(DSMT/DSME)**2
      DSS = DST*(KM - KTC) - DSMT
      CS = (KE - KM)/DSSE
   10 DK = CS*DSS
      CALL EPSLON(KM,DK,RCMS,DSS,DRCS,RES)
      DRCT = DRCMST + DRCS
      RT = RCMS + DRCS
      RET = RES + RT*EMT
      CALL TANKAP(RCT,DRCT,RET,TK)
      TKD = (TK - TKTN)/(1.0 + TK*TKTN)
      IF (ABS(DST*TKD).LT.1.0E-06) GO TO 20
      DST = RET/(CKTC - SKTC*TKD)
      DSS = DSS + DST*TKD*SQRT(1.0 + TKD**2)/(1.0 -(DK +KM -KTC)**2/2.0)
      GO TO 10
   20 KT = KM + DK
      RE = RT*RETI/RCT + RET
      DS = DSS - DSSE
      IF (DSSE.GT.0.0) DS = -DS
      HKTS = KT/2.0
      SHKTS = HKTS*SRS(HKTS)
```

```
      SHKTSQ = SHKTS**2
      CHKTS = SQRT(1.0 - SHKTSQ)
      SKTS = 2.0*SHKTS*CHKTS
      CKTS = 1.0 - 2.0*SHKTSQ
      RETURN
      END
```

```
      SUBROUTINE SURF(KE,KMM,SKM,CKM,RO,DRC,TE,EMS,DSS)
C ***       THIS SUBROUTINE CALCULATES THE BLADE ELEMENT SURFACE CURVE
C *** END POINT COORDINATES.  THE SURFACE CURVE IS NORMAL TO THE END
C *** POINT THICKNESS PATH AND TANGENT TO A SURFACE REFFERENCE POINT
C *** WHICH IS EITHER THE TRANSITION OR MAXIMUM THICKNESS POINT.
      REAL KE, KE1, KIS, KM, KMM, KTC, KTS
      COMMON /BLADES/
     1 AMACH, AOC, AISOAS, AISOA1, BINC, CALP, CCC, CEPE, CGBL, CHORD,
     2 CINC, CKTC, CKTS, C1, C2, DKAPPA, DRCE, DRCGI, DRCMST, DRCMT,
     3 DRCOI, DRCT, DRCTI, DR1, DSME, DSMT, DSOI, DSOT, DSSE, DST, DSTI,
     4 EMT, F1, F2, GBL, ICL, IGO, IPASS, KIS, KM, KTC, KTS, P, PFLOS,
     5 RCG, RCM, RCMS, RCT, RD1, RECGI, REE, REMT, RET, RETI, RMSJ, RTRC
     6,R1, R1C, R2, SALP, SEPE, SGAM, SGBL, SJ, SKTC, SKTS, SLJD, T,
     7 TEPE, TGBLL, THD, THLE, THMAX, THTE, TKTN, TLS, WC1, YB1, YB2, ZM
      RMS = RO - DRC
      IT = 1
   10 CALL EPSLON(KE + 1.5707963,0.0,RO,TE,DRCE,REE)
      DRCS = DRC + DRCE
      DK = KE - KMM
      HDK = DK/2.0
      SR = SRS(HDK)
      SHDK = HDK*SR
      CHDK = SQRT(1.0 - SHDK**2)
      DSS = DRCS/(SR*(CHDK*CKM - SHDK*SKM))
      CALL EPSLON(KMM,DK,RMS,DSS,DRCS,RES)
      DRE = (RO + DRCE)*EMS + RES - REE
      IF (ABS(DRE).LT.1.0E-06) RETURN
      IF (IT.EQ.2) GO TO 20
      KE1 = KE
      DRE1 = DRE
      KE = KE - 2.0*DRE*(CKM*(1.0 -2.0*SHDK**2) -2.0*SKM*SHDK*CHDK)/DSS
      IT = 2
      GO TO 10
   20 KE = KE + (KE1 - KE)*DRE/(DRE - DRE1)
      GO TO 10
      END
```

```
      SUBROUTINE CHAN
C ***       CALCULATION OF CHANNEL AREA TO CHOKE AREA
      REAL INC, KIC, KIP, KIS, KM, KOC, KOP, KOS, KP, KS, KTC, KTP,
     1 KTS, KWC, MACH
      COMMON /VECTOR/
     1 BETAS(1,21), BMATL(1), BLADES(1), CHOKE(1), CHORDA(1), CHORDB(1),
     2 CHORDC(1), CPCC(6), DEV(1,21), IDEV(1), IGEO(1), IINC(1),
```

```
     3 ILOSS(1), IMAX(1), INC(1,21), ISTN(2), ITRANS(1), NOPT(1),
     4 NXCUT(1), PHI(1,21), PO(2,21), R(2,21), RBHUB(1), RBTIP(1),
     5 SLOPE(2,21), SOLID(1), TALE(1), TAMAX(1), TATE(1), TBLE(1),
     6 TBMAX(1), TBTE(1), TCLE(1), TCMAX(1), TCTE(1), TDLE(1), TDMAX(1),
     7 TDTE(1), TILT(1), TO(2,21), TRANS(1,21), VTH(2,21), VZ(2,21),
     8 Z(2,21), ZBHUB(1), ZBTIP(1), ZMAX(1,21)
      COMMON /SCALAR/
     1 BETA, CP, CPH2, CPH3, CPH4, CPH5, CPH6, CPP3, CPP4, CPP5, CPP6,
     2 CP1, CV, DCP, DF, DHC, DHCI, DLOSC, G, GAMMA, GJ, GJ2, GR1, GR2,
     3 GR3, GR4, GR5, H, I, ICONV, ICOUNT, IERROR, IIN, IPR, IROTOR, IR,
     4 IROW, ITER, IW, J, JM, MACH, NAB, NBROWS, NHUB,NROTOR,NSTN,NSTRM,
     5 NTIP, NTUBES, OMEGA, PI, POA1, PR, RADIAN, RF, RG, ROT,TL,TOA1,TU
      COMMON
     1 BETA1(21), BETA2(21), COSA(21), COSL(21), DKLE(1,21), DL(21),
     2 GAMM(21), OBAR(21), RELM(21), RPR1(21), RE1(21), RE2(21),
     3 RE3(21), RE4(21), RE5(21), RVTH(21), SINA(21), SINL(21), SLOS(21)
     4,SONIC(21), THETAP(21,13), THETAS(21,13), TREL1(21), TSTAT(21),
     5 VM(21), VTSQ(21), XBAR(1,21), YBAR(1,21), ZP(21,13), ZS(21,13)
      COMMON /EQUIV/
     1 CHD(21), CHK(21), COSA2(21), FSM(21), KIC(21), KOC(21), RCA(21),
     2 REC(2,21), RPTE(2,21), SINA2(21), SKIC(21), SKOC(21), TALP(21),
     3 TCA(21), TEC(2,21), TGB(21),TTRP(21),TTRS(21),YCCLE(25),YCCTE(25)
     4,ZCCLE(25), ZCCTE(25), ZCDA(21), ZEC(2,21), ZTRP(21), ZTRS(21)
      COMMON /BLADES/
     1 AMACH, ACC, A1SOAS, A1SOA1, BINC, CALP, CCC, CEPE, CGBL, CHORD,
     2 CINC, CKTC, CKTS, C1, C2, DKAPPA, DRCE, DRCGI, DRCMST, DRCMT,
     3 DRCOI, DRCT, DRCTI, DR1, DSME, DSMT, DSOI, DSOT, DSSE, DST, DSTI,
     4 EMT, F1, F2, GBL, ICL, IGO, IPASS, KIS, KM, KTC, KTS, P, PFLOS,
     5 RCG, RCM, RCMS, RCT, RD1, RECGI, REE, REMT, RET, RETI, RMSJ, RTRC
     6,R1, R1C, R2, SALP, SEPE, SGAM, SGBL, SJ, SKTC, SKTS, SLJD, T,
     7 TEPE, TGBLL, THD, THLE, THMAX, THTE, TKTN, TLS, WC1, YB1, YB2, ZM
      COMMON /MARG/
     1 AL, AOAS, AOA1, CCHORD, DAL, DAOAS, DPW, DPWL, DRCLEP, DRCM,
     2 DRCTPI, DRCTSI, DRCWT, DSA, DSP, DSP1, DSP2, DSS, DSS1, DSS2, DSW
     3,EB, EWC, F, HC, ICHCKE, KIP, KOP, KOS, KP, KS, KTP, KWC, PI2, RCI
     4,RCO, RCP, RCS, RCTP, RCTS, RELEP, REOI, REP, RES, RETP, RETS,
     5 REWT, RTR, RTRD, RTRC, SECGBL, TCGI, TGBL, WC, ZMT
      IF (IGO.EQ.2) GO TO 310
C ***       CALCULATION OF CHANNEL WIDTH
      ICL = 1
      DSW = 0.0
      DRCWC = DRCWT
      REWC = REWT
      RCS = RCTS
      KS = KTS
  250 CALL TANKAP(RCS,DRCWC,REWC,TK)
      WC = SQRT(1.0 + TK**2)
      IF (ABS(TK).GT.100.0) GO TO 260
      WC = WC*ABS(DRCWC)
      GO TO 270
  260 WC = WC*ABS(REWC/TK)
  270 KWC = ATAN(-1.0/TK)
      IF (REWC.GT.0.0) GO TO 275
      IF (DRCWC.GT.0.0) GO TO 272
      KWC = PI + KWC
      GO TO 275
  272 KWC = KWC - PI
  275 DK = KS + KP - 2.0*KWC
      IF (ABS(DK).LT.0.0001) GO TO 300
      IF (ICL.GT.1) GO TO 290
      ICL = 2
```

```
      IF (DK.GT.0.0) GO TO 280
      DKDS = (KTS - KIS)/DSS1
      GO TO 290
  280 DKDS = (KCS - KTS)/DSS2
  290 DSW = DK*WC/(2.0 - DKDS*WC) + DSW
      DK = DKDS*DSW
      CALL EPSLON(KTS,DK,RCTS,DSW,DRCS,RES)
      KS = KTS + DK
      DRCWC = DRCWT - DRCS
      RCS = RCTS + DRCS
      REWC = REWT - RES*RCP/RCS
      GO TO 250
  300 IF (CHOKE(IROW).EQ.0.0.AND.ICONV.NE.2) RETURN
      EWC = REWC/RCP
      DRCM = DRCLEP + THLE - DRCWC/2.0
  310 HC = 1.0 - DRCM*SLJD*CCHORD/(DR1 - Z(I-1,J)*SLJD)
      ACA1 = WC/WC1*HC
      F = (DSS1 + DSW)/DSS
      PLOSS = SLOS(J) - (F + (DSP1 + DPW)/DSP)/2.0*PFLOS
      RTR = 1.0 + RTRC*DRCM*SALP*(R1C + DRCM*SALP/2.0)
      RTRQ = SQRT(RTR)
      A1SCAS = (RTR**GR2 -1.0 + PLOSS)/RTRQ
  320 ACAS = ACA1*A1SOAS/A1SCA1
      IF (ICHOKE.GT.1.OR.CHOKE(IROW).EQ.0.0) RETURN
      IF (AOAS - 1.0.GE.CHOKE(IROW).OR.IINC(IROW).GT.3) RETURN
      IF (BINC.GT.(DKLE(IROW,J) + 0.033)) RETURN
C ***      READJUSTMENT OF INCIDENCE ANGLE TO RELIEVE L.E. CHANNEL CHOKE
      AI = (1.0/(1.0 + P) + DKDS*DSW/(KIC(J) -KOC(J)))/(1.0-WC*DKDS/2.0)
      DSS = DSS1 + DSW
      BI = DSS + (DSS - WC*(KP + EWC - KS)/2.0)*AI
      AI = WC*AI*(1.0 + 2.0*AI)
      DI = (BI -SQRT(BI**2 -4.0*AI*(1.0 +CHOKE(IROW)-AOAS)*WC))/AI+0.001
      DIE = BINC + DI - DKLE(IROW,J) - 0.0349
C ***      LIMIT INCIDENCE ANGLE TO +2 DEG. ON L.E. OF PRESS. SURF.
      IF (DIE.GT.0.0) DI = DI - DIE
      DINC = BINC + DI
      IGO = 2
      RETURN
      END
```

```
C ***      RESET OF SUCTION SURFACE BLADE ANGLE AT SHOCK
      SUBROUTINE SBETA
      REAL INC, KIC, KIP, KIS, KM, KOC, KOP, KOS, KP, KS, KTC, KTP, KTS,
     1 KWC, MACH
      COMMON /VECTOR/
     1 BETAS(1,21), BMATL(1), BLADES(1), CHOKE(1), CHORDA(1), CHORDB(1),
     2 CHORDC(1), CPCO(6), DEV(1,21), IDEV(1), IGEO(1), IINC(1),
     3 ILOSS(1), IMAX(1), INC(1,21), ISTN(2), ITRANS(1), NOPT(1),
     4 NXCUT(1), PHI(1,21), PO(2,21), R(2,21), RBHUB(1), RBTIP(1),
     5 SLOPE(2,21), SOLID(1), TALE(1), TAMAX(1), TATE(1), TBLE(1),
     6 TBMAX(1), TBTE(1), TCLE(1), TCMAX(1), TCTE(1), TDLE(1), TDMAX(1),
     7 TDTE(1), TILT(1), TO(2,21), TRANS(1,21), VTH(2,21), VZ(2,21),
     8 Z(2,21), ZBHUB(1), ZBTIP(1), ZMAX(1,21)
      COMMON /SCALAR/
     1 BETA, CP, CPH2, CPH3, CPH4, CPH5, CPH6, CPP3, CPP4, CPP5, CPP6,
     2 [illegible], CV, DCP, DF, DFC, DHCI, DLOSC, G, GAMMA, GJ, GJ2, GR1, GR2,
```

```
      3 GR3, GR4, GR5, H, I, ICONV, ICOUNT, IERROR, IIN, IPR, IROTOR, IR,
      4 IROW, ITER, IW, J, JM, MACH, NAB, NBROWS, NHUB,NROTOR,NSTN,NSTRM,
      5 NTIP, NTUBES, OMEGA, PI, POA1, PR, RADIAN, RF, RG, ROT,TL,TOA1,TU
       COMMON
      1 BETA1(21), BETA2(21), COSA(21), COSL(21), DKLE(1,21), DL(21),
      2 GAMM(21), GBAR(21), RELM(21), RPR1(21), RE1(21), RE2(21),
      3 RE3(21), RE4(21), RE5(21), RVTH(21), SINA(21), SINL(21), SLOS(21)
      4,SONIC(21), THETAP(21,13), THETAS(21,13), TREL1(21), TSTAT(21),
      5 VM(21), VTSQ(21), XBAR(1,21), YBAR(1,21), ZP(21,13), ZS(21,13)
       COMMON /EQUIV/
      1 CHC(21), CHK(21), COSA2(21), FSM(21), KIC(21), KOC(21), RCA(21),
      2 REC(2,21), RPTE(2,21), SINA2(21), SKIC(21), SKOC(21), TALP(21),
      3 TCA(21), TEC(2,21), TGB(21),TTRP(21),TTRS(21),YCCLE(25),YCCTE(25)
      4,ZCCLE(25), ZCCTE(25), ZCDA(21), ZEC(2,21), ZTRP(21), ZTRS(21)
       COMMON /BLADES/
      1 AMACH, AOC, AISOAS, AISOA1, BINC, CALP, CCC, CEPE, CGBL, CHORD,
      2 CINC, CKTC, CKTS, C1, C2, DKAPPA, DRCE, DRCGI, DRCMST, DRCMT,
      3 DRCOI, DRCT, DRCTI, DR1, DSME, DSMT, DSOI, DSOT, DSSE, DST, DSTI,
      4 EMT, F1, F2, GBL, ICL, IGO, IPASS, KIS, KM, KTC, KTS, P, PFLOS,
      5 RCG, RCM, RCMS, RCT, RD1, RECGI, REE, REMT, RET, RETI, RMSJ, RTRC
      6,R1, R1C, R2, SALP, SEPE, SGAM, SGBL, SJ, SKTC, SKTS, SLJD, T,
      7 TEPE, TGBLL, THD, THLE, THMAX, THTE, TKTN, TLS, WC1, YB1, YB2, ZM
       COMMON /MARG/
      1 AL, AOAS, AOA1, CCHORD, DAL, DAOAS, DPW, DPWL, DRCLEP, DRCM,
      2 DRCTPI, DRCTSI, DRCWT, DSA, DSP, DSP1, DSP2, DSS, DSS1, DSS2, DSW
      3,EB, EWC, F, HC, ICHCKE, KIP, KOP, KOS, KP, KS, KTP, KWC, PI2, RCI
      4,RCC, RCP, RCS, RCTP, RCTS, RELEP, REOI, REP, RES, RETP, RETS,
      5 REWT, RTR, RTRD, RTRC, SECGBL, TCGI, TGBL, WC, ZMT
       BETAS(IROW,J) = KS
       IF (DSW.LE.DSS2) GO TO 336
       IF (ITRANS(IROW).EQ.2) TRANS(IROW,J) = 0.9
       CHK(J) = 0.0
       FSM(J) = 1.1
       IGC = 2
       RETURN
  336  IF (ITRANS(IROW).NE.2) RETURN
C ***        RESET THE TRANSITION POINT AT THE SHOCK IMPINGEMENT POINT
       IF (DSW) 337,339,338
  337  DK = KOC(J) - KOS
       DSW = DSW/(DSS2 - THTE*DK*(1.0 + DK*DK/3.0*(1.0 + 0.4*DK*DK)))
       DK = DSW*(KOC(J) - KTC)
       DSW = DSW*DSOT
       CALL EPSLON(KTC,DK,RCT,DSW,DR,RE)
       CALL RPOINT(RCI,DRCTI+DR,RETI+RE,TGBLL,DR)
       TRANS(IROW,J) = DR*SECGBL + THLE
       RETURN
  338  DK = KIS - KIC(J)
       DSW = DSW/(DSS1 - THLE*DK*(1.0 + DK*DK/3.0*(1.0 + 0.4*DK*DK)))
       DK = (KTC - KIC(J))*(1.0 + DSW)
       DSW = DSTI*(1.0 + DSW)
       CALL EPSLON(KIC(J),DK,RCI,DSW,DR,RE)
       CALL RPOINT(RCI,DR,RE,TGBLL,DR)
       TRANS(IROW,J) = DR*SECGBL + THLE
  339  RETURN
       END
```

```
      SUBROUTINE POINTS
      REAL INC, KIC, KIP, KIS, KM, KOC, KOP, KOS, KP, KS, KTC, KTP, KTS,
     X KWC, MACH
      COMMON /VECTOR/
     1 BETAS(1,21), BMATL(1), BLADES(1), CHOKE(1), CHORDA(1), CHORDB(1),
     2 CHORDC(1), CPCO(6), DEV(1,21), IDEV(1), IGEO(1), IINC(1),
     3 ILOSS(1), IMAX(1), INC(1,21), ISTN(2), ITRANS(1), NOPT(1),
     4 NXCUT(1), PHI(1,21), PO(2,21), R(2,21), RBHUB(1), RBTIP(1),
     5 SLOPE(2,21), SOLID(1), TALE(1), TAMAX(1), TATE(1), TBLE(1),
     6 TBMAX(1), TBTE(1), TCLE(1), TCMAX(1), TCTE(1), TDLE(1), TDMAX(1),
     7 TDTE(1), TILT(1), TO(2,21), TRANS(1,21), VTH(2,21), VZ(2,21),
     8 Z(2,21), ZBHUB(1), ZBTIP(1), ZMAX(1,21)
      COMMON
     1 BETA1(21), BETA2(21), COSA(21), COSL(21), DKLE(1,21), DL(21),
     2 GAMM(21), OBAR(21), RELM(21), RPR1(21), RE1(21), RE2(21),
     3 RE3(21), RE4(21), RE5(21), RVTH(21), SINA(21), SINL(21), SLOS(21)
     4,SONIC(21), THETAP(21,13), THETAS(21,13), TREL1(21), TSTAT(21),
     5 VM(21), VTSQ(21), XBAR(1,21), YBAR(1,21), ZP(21,13), ZS(21,13)
      COMMON /EQUIV/
     1 CHC(21), CHK(21), COSA2(21), FSM(21), KIC(21), KOC(21), RCA(21),
     2 REC(2,21), RPTE(2,21), SINA2(21), SKIC(21), SKOC(21), TALP(21),
     3 TCA(21), TEC(2,21), TGB(21),TTRP(21),TTRS(21),YCCLE(25),YCCTE(25)
     4,ZCCLE(25), ZCCTE(25), ZCDA(21), ZEC(2,21), ZTRP(21), ZTRS(21)
      COMMON /PTS/ FSB(13)
      COMMON /SCALAR/
     1 BETA, CP, CPH2, CPH3, CPH4, CPH5, CPH6, CPP3, CPP4, CPP5, CPP6,
     2 CP1, CV, DCP, DF, DFC, DHCI, DLOSC, G, GAMMA. GJ, GJ2, GR1, GR2,
     3 GR3, GR4, GR5, H, I, ICONV, ICOUNT, IERROR, IIN, IPR, IROTOR, IR,
     4 IROW, ITER, IW, J, JM, MACH, NAB, NBROWS, NHUB,NROTOR,NSTN,NSTRM,
     5 NTIP, NTUBES, OMEGA, PI, POA1, PR, RADIAN, RF, RG, ROT,TL,TOA1,TU
      COMMON /BLADES/
     1 AMACH, ACC, AISOAS, AISOA1, BINC, CALP, CCC, CEPE, CGBL, CHORD,
     2 CINC, CKTC, CKTS, C1, C2, DKAPPA, DRCE, DRCGI, DRCMST, DRCMT,
     3 DRCOI, DRCT, DRCTI, DR1, DSME, DSMT, DSOI, DSOT, DSSE, DST, DSTI,
     4 EMT, F1, F2, GBL, ICL, IGC, IPASS, KIS, KM, KTC, KTS, P, PFLOS,
     5 RCG, RCM, RCMS, RCT. RCI, RECGI, REE, REMT, RET, RETI, RMSJ, RTRC
     6,R1, R1C, R2, SALP, SEPE, SGAM, SGBL, SJ, SKTC, SKTS, SLJD, T,
     7 TEPE, TGBLL, THD, THLE, THMAX, THTE, TKTN, TLS, WC1, YB1, YB2, ZM
      COMMON /MARG/
     1 AL, AOAS, AOA1, CCHORD, DAL, DAOAS, DPW, DPWL, DRCLEP, DRCM,
     2 DRCTPI, DRCTSI, DRCWT, DSA, DSP, DSP1, DSP2, DSS, DSS1, DSS2, DSW
     3,EB, EWC, F, HC, ICHOKE, KIP, KOP, KOS, KP, KS, KTP, KWC, PI2, RCI
     4,RCL, RCP, RCS, RCTP, RCTS, RELEP, REOI, REP, RES, RETP, RETS,
     5 REWT, RTR, RTRD, RTRS, SECGBL, TCGI, TGBL, WC, ZMT
C ***       BLADE ELEMENT SUCTION SURFACE Z AND THETA ARRAYS REFERENCED
C *** TO THE BLADE HUB STACKING POINT
  500 ZTRS(J) = ZCDA(J) + (DRCTSI - DRCGI)*CCHORD
      RTC = R1C + (DRCTSI + THLE)*SALP
      TTRS(J) = RETS/RTC - TCA(J) - TCGI
      ZEC(I-1,J) = ZCDA(J) - DRCGI*CCHORD
      ZEC(I,J) = ZCDA(J) + (DRCOI - DRCGI)*CCHORD
      TEC(I-1,J) = -TCA(J) - TCGI
      TEC(I,J) = REOI/(R1C + (THLE + DRCOI)*SALP) + TEC(I-1,J)
      REC(I-1,J) = R(I-1,J) + THLE*CCHORD
      REC(I,J) = R(I,J) - THTE*CCHORD
      FST = DSS1/DSS
      DO 550 K=1,13
      FS = FSB(K) - FST
      IF (FS.GT.0.0) GO TO 520
      DSS = DSS1*FS/FST
      DK = (KTS - KIS)*DSS/DSS1
```

```
      GC TO 530
  52C DSS = DSS2*FS/(1.0 - FST)
      DK = (KCS - KTS)*DSS/DSS2
  530 CALL EPSLCN(KTS,DK,RCTS,DSS,DRCTS,RES)
      ZS(J,K) = ZTRS(J) + DRCTS*CCHORD
  550 THETAS(J,K) = TTRS(J) + RES/(RTC + DRCTS*SALP)
C ***       BLADE ELEMENT PRESSURE SURFACE Z AND THETA ARRAYS REFERENCED
C *** TC THE BLADE HUB STACKING POINT
      ZTRP(J) = ZCDA(J) + (DRCTPI - DRCGI)*CCHORD
      RTC = R1C + (DRCTPI + THLE)*SALP
      TTRP(J) = RETP/RTC - TCA(J) - TCGI
      FST = DSP1/DSP
      DC 600 K=1,13
      FS = FSB(K) - FST
      IF (FS.GT.C.O) GO TO 570
      DSS = DSP1*FS/FST
      DK = (KTP - KIP)*DSS/DSP1
      GC TO 580
  570 DSS = DSP2*FS/(1.0 - FST)
      DK = (KOP - KTP)*DSS/DSP2
  58C CALL EPSLCN(KTP,DK,RCTP,DSS,DRCTS,RES)
      ZP(J,K) = ZTRP(J) + DRCTS*CCHORD
  600 THETAP(J,K) = TTRP(J) + RES/(RTC + DRCTS*SALP)
      TGB(J) = TGBL
      RETLRN
      END
```

```
      SLBRCUTINE STACK
C ***      THIS RCUTINE FINCS THE CENTERS OF AREA OF BLADE SECTIONS
C *** WHICH PASS THROUGH THE INTERSECTIONS OF THE BLADE ELEMENTS WITH
C *** THE STACKING LINE.  BLADE ELEMENTS ARE TRANSLATED ON THE CONE TO
C *** GET THE BLADE SECTION CENTERS NEARER THE STACKING AXIS.
      REAL INC, KIC, KIS, KM, KOC, KTC, KTS, MACH, MCA, MCT, MDA, MDT
      CCMMCN /VECTOR/
     1 BETAS(1,21), BMATL(1), BLADES(1), CHOKE(1), CHORDA(1), CHORDB(1),
     2 CHCRDC(1), CPCC(6), DEV(1,21), IDEV(1), IGEO(1), IINC(1),
     3 ILCSS(1), IMAX(1), INC(1,21), ISTN(2), ITRANS(1), NOPT(1),
     4 NXCUT(1), PHI(1,21), PO(2,21), R(2,21), RBHUB(1), RBTIP(1),
     5 SLCPE(2,21), SOLID(1), TALE(1), TAMAX(1), TATE(1), TBLE(1),
     6 TBMAX(1), TBTE(1), TCLE(1), TCMAX(1), TCTE(1), TDLE(1), TDMAX(1),
     7 TDTE(1), TILT(1), TC(2,21), TRANS(1,21), VTH(2,21), VZ(2,21),
     8 Z(2,21), ZBHUB(1), ZBTIP(1), ZMAX(1,21)
      CCMMON /SCALAR/
     1 BETA, CP, CPH2, CPH3, CPH4, CPH5, CPH6, CPP3, CPP4, CPP5, CPP6,
     2 CP1, CV, DCP, DF, DHC, DHCI, DLOSC, G, GAMMA, GJ, GJ2, GR1, GR2,
     3 GR3, GR4, GR5, H, I, ICCNV, ICOUNT, IERROR, IIN, IPR, IROTOR, IR,
     4 IRCW, ITER, IW, J, JM, MACH, NAB, NBROWS, NHUB,NROTOR,NSTN,NSTRM,
     5 NTIP, NTUBES, OMEGA, PI, POA1, PR, RADIAN, RF, RG, ROT,TL,TOA1,TU
      CCMMCN
     1 BETA1(21), BETA2(21), CCSA(21), COSL(21), DKLE(1,21), DL(21),
     2 GAMM(21), CBAR(21), RELM(21), RPR1(21), RE1(21), RE2(21),
     3 RE3(21), RE4(21), RE5(21), RVTH(21), SINA(21), SINL(21), SLOS(21)
     4,SCNIC(21), THETAP(21,13), THETAS(21,13), TREL1(21), TSTAT(21),
     5 VM(21), VTSC(21), XBAR(1,21), YBAR(1,21), ZP(21,13), ZS(21,13)
      CCMMCN /EQUIV/
     1 CHD(21), CHK(21), CCSA2(21), FSM(21), KIC(21), KOC(21), RCA(21),
     2 REC(2,21), RETE(2,21), SINA2(21), SKIC(21), SKOC(21), TALP(21),
```

```
     3 TCA(21), TEC(2,21), TCB(21),TTRP(21),TTRS(21),YCCLE(25),YCCTE(25)
     4,ZCCLE(25), ZCCTE(25), ZCDA(21), ZEC(2,21), ZTRP(21), ZTRS(21)
      COMMON /BLADES/
     1 AMACH, ACC, AISCAS, AISCAI, BINC, CALP, CCC, CEPE, CGBL, CHORD,
     2 CINC, CKTC, CKTS, C1, C2, DKAPPA, DRCE, DRCGI, DRCMST, DRCMT,
     3 DRCOI, DRCI, DRCTI, DR1, DSME, DSMT, DSOI, DSOT, DSSE, DST, DSTI,
     4 EMT, F1, F2, GBL, ICL, IGC, IPASS, KIS, KM, KTC, KTS, P, PFLOS,
     5 RCG, RCM, RCMS, RCT, RD1, RECGI, REE, REMT, RET, RETI, RMSJ, RTRC
     6,R1, RIC, R2, SALP, SEPE, SGAM, SGBL, SJ, SKTC, SKTS, SLJD, T,
     7 TEPE, TGBLL, THC, THLE, THMAX, THTE, TKTN, TLS, WC1, YB1, YB2, ZM
      COMMON /RCUT/  AC, CCSKL, COSKU, EMTM, IOUT, IT, NP, SINKL, SINKU,
     1 CX(13), EM(14), YBP(14), YBS(14), ZBP(14), ZBS(14)
      EQUIVALENCE (JL,ICL)
      IF (ICCNV.LT.2) WRITE (IW,2000)
      ICUT = 0
      DO 290 J=1,NSTRM
      JL = J
      STC = TCA(J)*SRS(TCA(J))
      XCUT = RCA(J)*SQRT(1.0 - STC**2)
      IF (TALP(J).GT.0.0) JL = JL - 1
      IF (JL.LT.2) JL = 2
      IF (JL.GT.NSTRM-2) JL = NSTRM - 2
      JL1 = JL
      DO 20 K=1,13
   20 CALL INTERP(XCUT,2,K,YBS(K),ZBS(K))
      TANB = (YBS(13) - YBS(1))/(ZBS(13) - ZBS(1))
      CALL INTERP(XCUT,2,0,YBS(14),ZBS(14))
C ***       TRANSLATE BLADE SECTION COORDINATES TO THE STACKING POINT
C *** ORIGIN AND ROTATE TO LIE ALONG THE BLADE SECTION CHORD.
      COSB = 1.0/SQRT(1.0 + TANB**2)
      SINB = TANB*COSB
      DZ = ZCDA(J)*COSB - RCA(J)*STC*SINB
      DY = RCA(J)*STC*COSB + ZCDA(J)*SINB
      DO 24 K=1,14
      YBT = YBS(K)
      YBS(K) = YBS(K)*COSB - ZBS(K)*SINB + DY
   24 ZBS(K) = ZBS(K)*COSB + YBT*SINB - DZ
      ZBP(1) = ZBS(1)
      YBP(1) = YBS(1)
      ZBP(13) = ZBS(13)
      YBP(13) = YBS(13)
      IF (J.NE.1.OR.ICCNV.GE.2) GO TO 28
      IF (ISTN(I).LT.0.OR.BMATL(IRCTOR).LE.0.0) GO TO 28
      DO 26 K=2,12
      YBP(K) = YBS(K)
   26 ZBP(K) = ZBS(K)
   28 CALL SPLITG(ZBS,YBS,14,AP,AXP,AYP,SP1,SP2)
      JL = JL1
      DO 210 K=1,13
  210 CALL INTERP(XCUT,1,K,YBS(K),ZBS(K))
      CALL INTERP(XCUT,1,0,YBS(14),ZBS(14))
      K = 14
      DO 215 K=1,14
      YBT = YBS(K)
      YBS(K) = YBS(K)*COSB - ZBS(K)*SINB + DY
  215 ZBS(K) = ZBS(K)*COSB + YBT*SINB - DZ
      ZS2 = ZBS(13)
      YS2 = YBS(13)
      CALL SPLITG(ZBS,YBS,14,AS,AXS,AYS,SS1,SS2)
      CALL EDGES(ZS2,YS2,SS2,ZBP(13),YBP(13),SP2,AT,AXT,AYT,RTE,ZCTE,
     X YCTE)
```

```
      CALL EDGES(ZBS(1),YBS(1),SS1,ZBP(1),YBP(1),SP1,A,AX,AY,RLE,ZCLE,
     X YCLE)
      A = A + AS - AP - AT
      AX = AX + AXS - AXP - AXT
      AY = AY + AYS - AYP - AYT
      XB = AX/A
      YB = AY/A
C ***       READJUSTMENT OF XBAR, YBAR AND BLADE EDGE LOCATION.
      DZ = (XB*COSB - YB*SINB)/(1.0 - TLS*TALP(J))
      Z(I-1,J) = Z(I-1,J) - DZ
      Z(I,J) = Z(I,J) - DZ
      R(I-1,J) = R(I-1,J) - DZ*TALP(J)
      R(I,J) = R(I,J) - DZ*TALP(J)
      DM = DZ*SQRT(1.0 + TALP(J)**2)/CHD(J)
      DY = (XB*SINB + YB*COSB)/CHD(J)
      CGBL = 1.0/SQRT(1.0 + TGB(J)**2)
      SGBL = CGBL*TGB(J)
      XBAR(IROW,J) = XBAR(IROW,J) + DM*CGBL + DY*SGBL
      YBAR(IROW,J) = YBAR(IROW,J) - DM*SGBL + DY*CGBL
      IF (ICONV.LT.2) WRITE (IW,2010) ITER, J, BETA1(J), BETA2(J),
     X SKIC(J), SKOC(J), KIC(J), KOC(J), DM, DY, SINB, DZ, A
      IF (ISTN(I).LT.0.OR.BMATL(IROTOR).LE.0.0) GO TO 290
      IF (J.GT.1) GO TO 280
      AL = A
      XU = XCUT
      MCA = 0.0
      MCT = 0.0
      MDA = 0.0
      MDT = 0.0
      IF (ABS(TALP(1)).LT.0.01) GO TO 290
C ***       TAPERED ROTOR TIP MATL. CENTRIFUGAL BENDING MOMENT CORRECTION
      ZPLE = ZCLE*COSB - YCLE*SINB
      ZPTE = ZCTE*COSB - YCTE*SINB
      ZPL = ZPLE
      DO 240 K=2,13
      DZ = ZBP(K) - ZBP(K-1)
      DY = YBP(K) - YBP(K-1)
      D = DZ*COSB - DY*SINB
      AP = (DZ*SINB + DY*COSB)/D
      BP = (ZBP(K)*YBP(K-1) - ZBP(K-1)*YBP(K))/D
      IF (K.NE.13) GO TO 220
      ZPP = ZPTE
      GO TO 230
  220 ZPP = ZBP(K)*COSB - YBP(K)*SINB
  230 ZPS1 = ZPP + ZPL
      ZPS2 = ZPS1*ZPP + ZPL**2
      ZPS3 = ZPS2*ZPP + ZPL**3
      CM = (XCUT + ZPS1*TALP(1)/4.0)*(ZPP - ZPL)
      APT = AP*ZPS2/3.0 + BP*ZPS1/2.0
      MDA = MDA - CM*(AP*ZPS3/4.0 + BP*ZPS2/3.0)
      MCA = MCA - CM*APT
      MDT = MDT + CM*(AP**2*ZPS3/8.0 + BP*(AP*ZPS2/3.0 + BP*ZPS1/4.0))
      MCT = MCT - CM*APT
  240 ZPL = ZPP
      ZPL = ZPLE
      KL = 14
      IF (ZBS(14).LE.ZBS(13)) KL = 13
      DO 270 K=2,KL
      DZ = ZBS(K) - ZBS(K-1)
      DY = YBS(K) - YBS(K-1)
      D = DZ*COSB - DY*SINB
```

```
      AS = (DZ*SINB + DY*COSB)/D
      BS = (ZBS(K)*YBS(K-1) - ZBS(K-1)*YBS(K))/D
      IF (K.NE.KL) GO TO 250
      ZPP = ZPTE
      GO TO 260
  250 ZPP = ZBS(K)*COSB - YBS(K)*SINB
  260 ZPS1 = ZPP + ZPL
      ZPS2 = ZPS1*ZPP + ZPL**2
      ZPS3 = ZPS2*ZPP + ZPL**3
      CM = (XCUT + ZPS1*TALP(1)/4.0)*(ZPP - ZPL)
      APT = AS*ZPS2/3.0 + BS*ZPS1/2.0
      MDA = MDA + CM*(AS*ZPS3/4.0 + BS*ZPS2/3.0)
      MCA = MCA + CM*APT
      MDT = MDT - CM*(AS**2*ZPS3/8.0 + BS*(AS*ZPS2/3.0 + BS*ZPS1/4.0))
      MCT = MCT + CM*APT
  270 ZPL = ZPP
      CM = PI*(XCUT + ZPLE*TALP(1)/2.0)*ZPLE*RLE**2/2.0
      MDT = MDT - CM*(ZCLE*SINB + YCLE*COSB)
      MCT = MCT + CM
      MDA = MDA + CM*(ZPLE - 4.0*RLE/(3.0*PI))
      MCA = MCA  + CM
      CM = PI*(XCUT + ZPTE*TALP(1)/2.0)*ZPTE*RTE**2/2.0
      MDT = MDT - CM*(ZCTE*SINB + YCTE*COSB)
      MCT = MCT + CM
      MDA = MDA + CM*(ZPTE + 4.0*RTE/(3.0*PI))
      MCA = MCA + CM
      MDA = MDA*TALP(1)
      MCA = MCA*TALP(1)*(XCUT - RCA(NSTRM))
      MDT = MDT*TALP(1)
      MCA = MCA*TALP(1)*(XCUT - RCA(NSTRM))
      GO TO 290
C ***       SUMMATION FOR ROTOR MATERIAL CENTRIFUGAL BENDING MOMENT
  280 RM = (XU + XCUT)/2.0
      DMC = (A + AU)*RM*(RM - RCA(NSTRM))*(XU - XCUT)/2.0
      MCA = MCA + DMC
      MCT = MCT + DMC
      AU = A
      XU = XCUT
  290 CONTINUE
      IF (ICONV.GE.2) RETURN
      IF (ISTN(I).LT.0.OR.BMATL(IROTOR).LE.0.0) RETURN
      CALL GASMNT(GBA,GBT)
      TANE = BMATL(IROTOR)*OMEGA**2/(144.0*G)
      TANL = -(MDA + GBA/TANE)/MCA
      TANS = (GBT/TANE - MDT)/MCT
      TILT(IROW) = ATAN(TANE)
      DZ = ((RBTIP(IROW) - RBHUB(IROW))*TANL + ZBHUB(IROW) - ZBTIP(IROW)
     X )/(1.0 - TANL*TALP(1))
      ZBTIP(IROW) = ZBTIP(IROW) + DZ
      RBTIP(IROW) = RBTIP(IROW) + DZ*TALP(1)
C ***       READJUSTMENT OF BLADE EDGE LOCATION FOR CHANGE IN STACK LINE.
      DO 310 J=1,NTUBES
      DZ =(RCA(J) - RCA(NSTRM))*(TANL - TLS)/(1.0 - TALP(J)*TANL)
      Z(I-1,J) = Z(I-1,J) + DZ
      Z(I,J) = Z(I,J) + DZ
      R(I-1,J) = R(I-1,J) + DZ*TALP(J)
  310 R(I,J) = R(I,J) + DZ*TALP(J)
      RETURN
 2000 FORMAT (/// 1X,4HITER,3X,1HJ,4X,8HBETA1(J),3X,8HBETA2(J),4X,
     1 7HSKIC(J),4X,7HSKOC(J),4X,6HKIC(J),5X,6HKOC(J),7X,2HDM,9X,2HDY,
     2 8X,4HSINB,8X,2HDZ,10X,1HA //)
```

```
 201C FORMAT (1X,I3,2X,I3,F12.6,5F11.6,2F11.7,F11.6,F11.7,F11.6)
      END
```

```
      SUBROUTINE INTERP(XC,ISURF,K,YC,ZC)
C ***       FOR A GIVEN X (BLADE SECTION) THIS ROUTINE FINDS BLADE SURF.
C *** CARTESIAN COORDINATES, Y AND Z, AT A GIVEN K (FRACTION OF BLADE
C *** ELEMENT SURFACE DISTANCE).  THIS IS DONE BY INTERPOLATION FROM
C *** PIECEWISE CUBIC FITS OF APPROPRIATE BLADE ELEMENT SURFACE COORD.
C *** INTERPOLATIONS ARE BETWEEN THE 2 INNERMOST CUBIC POINTS WHENEVER
C *** POSSIBLE.
      REAL KIC, KIS, KM, KCC, KTC, KTS, MACH
      COMMON /SCALAR/
     1 BETA, CP, CPH2, CPH3, CPH4, CPH5, CPH6, CPP3, CPP4, CPP5, CPP6,
     2 CP1, CV, DCP, DF, DHC, DHCI, DLOSC, G, GAMMA, GJ, GJ2, GR1, GR2,
     3 GR3, GR4, GR5, H, I, ICONV, ICOUNT, IERROR, IIN, IPR, IROTOR, IR,
     4 IROW, ITER, IW, J, JM, MACH, NAB, NBROWS, NHUB,NROTOR,NSTN,NSTRM,
     5 NTIP, NTUBES, OMEGA, PI, POA1, PR, RADIAN, RF, RG, ROT,TL,TOA1,TU
      COMMON
     1 BETA1(21), BETA2(21), COSA(21), COSL(21), DKLE(1,21), DL(21),
     2 GAMM(21), OBAR(21), RELM(21), RPR1(21), RE1(21), RE2(21),
     3 RE3(21), RE4(21), RE5(21), RVTH(21), SINA(21), SINL(21), SLOS(21)
     4,SONIC(21), THETAP(21,13), THETAS(21,13), TREL1(21), TSTAT(21),
     5 VM(21), VTSQ(21), XBAR(1,21), YBAR(1,21), ZP(21,13), ZS(21,13)
      COMMON /EQUIV/
     1 CHC(21), CHK(21), COSA2(21), FSM(21), KIC(21), KOC(21), RCA(21),
     2 REC(2,21), RPTE(2,21), SINA2(21), SKIC(21), SKOC(21), TALP(21),
     3 TCA(21), TEC(2,21), TGB(21),TTRP(21),TTRS(21),YCCLE(25),YCCTE(25)
     4,ZCCLE(25), ZCCTE(25), ZCDA(21), ZEC(2,21), ZTRP(21), ZTRS(21)
      COMMON /BLADES/
     1 AMACH, ACC, AISCAS, AISCAI, BINC, CALP, CCC, CEPE, CGBL, CHORD,
     2 CINC, CKTC, CKTS, C1, C2, DKAPPA, DRCE, DRCGI, DRCMST, DRCMT,
     3 DRCOI, DRCT, DRCTI, DR1, DSME, DSMT, DSOI, DSOT, DSSE, DST, DSTI,
     4 EMT, F1, F2, GBL, ICL, IGO, IPASS, KIS, KM, KTC, KTS, P, PFLOS,
     5 RCG, RCM, RCMS, RCT, RCI, RECGI, REE, REMT, RET, RETI, RMSJ, RTRC
     6,R1, RIC, R2, SALP, SEPE, SGAM, SGBL, SJ, SKTC, SKTS, SLJD, T,
     7 TEPE, TGBLL, THD, THLE, THMAX, THTE, TKTN, TLS, WC1, YB1, YB2, ZM
      COMMON /LOCATE/ XX, X1, X2, X3, X4
      EQUIVALENCE (JL,ICL)
      IF (ISURF.EQ.2) GO TO 40
      IF (K.EQ.0) GO TO 70
C ***       CARTESIAN COORDINATES OF THE SUCTION SURFACE BLADE ELEMENT
C *** POINTS USED FOR INTERPOLATION.
   10 R2 = RCA(JL) + (ZS(JL,K) - ZCDA(JL))*TALP(JL)
      ST2 = THETAS(JL,K)*SRS(THETAS(JL,K))
      X2 = R2*SQRT(1.0 - ST2**2)
      IF (X2.GE.XC) GO TO 20
      IF (JL.EQ.2) GO TO 20
      JL = JL - 1
      GO TO 10
   20 R3 = RCA(JL+1) + (ZS(JL+1,K) - ZCDA(JL+1))*TALP(JL+1)
      ST3 = THETAS(JL+1,K)*SRS(THETAS(JL+1,K))
      X3 = R3*SQRT(1.0 - ST3**2)
      IF ( X3.LT.XC) GO TO 30
      IF (JL.EQ.NSTRM - 2) GO TO 30
      JL = JL + 1
      R2 = R3
      ST2 = ST3
```

```
      X2 = X3
      GC TC 20
   3C R1 = RCA(JL-1) + (ZS(JL-1,K) - ZCDA(JL-1))*TALP(JL-1)
      ST1 = THETAS(JL-1,K)*SRS(THETAS(JL-1,K))
      Z1 = ZS(JL-1,K)
      Z2 = ZS(JL,K)
      Z3 = ZS(JL+1,K)
      R4 = RCA(JL+2) + (ZS(JL+2,K) - ZCDA(JL+2))*TALP(JL+2)
      ST4 = THETAS(JL+2,K)*SRS(THETAS(JL+2,K))
      Z4 = ZS(JL+2,K)
      GC TC 130
   40 IF (K.EQ.0) GC TC 10C
C ***      CARTESIAN CCORDINATES OF THE PRESSURE SURFACE BLADE ELEMENT
C *** PCINTS USED FOR INTERPCLATION.
      R2 = RCA(JL) + (ZP(JL,K) - ZCDA(JL))*TALP(JL)
      ST2 = THETAP(JL,K)*SRS(THETAP(JL,K))
      X2 = R2*SQRT(1.0 - ST2**2)
      IF (X2.GE.XC) GO TC 5C
      IF (JL.EQ.2) GC TC 50
      JL = JL - 1
      GC TC 4C
   50 R3 = RCA(JL+1) + (ZP(JL+1,K) - ZCDA(JL+1))*TALP(JL+1)
      ST3 = THETAP(JL+1,K)*SRS(THETAP(JL+1,K))
      X3 = R3*SQRT(1.0 - ST3**2)
      IF ( X3.LT.XC) GO TO 60
      IF (JL.EQ.NSTRM - 2) GC TO 60
      JL = JL + 1
      R2 = R3
      ST2 = ST3
      X2 = X3
      GC TC 50
   60 R1 = RCA(JL-1) + (ZP(JL-1,K) - ZCDA(JL-1))*TALP(JL-1)
      ST1 = THETAP(JL-1,K)*SRS(THETAP(JL-1,K))
      Z1 = ZP(JL-1,K)
      Z2 = ZP(JL,K)
      Z3 = ZP(JL+1,K)
      R4 = RCA(JL+2) + (ZP(JL+2,K) - ZCDA(JL+2))*TALP(JL+2)
      ST4 = THETAP(JL+2,K)*SRS(THETAP(JL+2,K))
      Z4 = ZP(JL+2,K)
      GC TC 130
C ***      CARTESIAN CCORDINATES OF THE SUCTION SURFACE BLADE ELEMENT
C *** TRANSITICN PCINTS USEC FCR INTERPOLATION
   70 R2 = RCA(JL) + (ZTRS(JL) - ZCDA(JL))*TALP(JL)
      ST2 = TTRS(JL)*SRS(TTRS(JL))
      X2 = R2*SQRT(1.0 - ST2**2)
      IF (X2.GE.XC) GC TC 8C
      IF (JL.EQ.2) GO TO 8C
      JL = JL - 1
      GC TC 70
   80 R3 = RCA(JL+1) + (ZTRS(JL+1) - ZCDA(JL+1))*TALP(JL+1)
      ST3 = TTRS(JL+1)*SRS(TTRS(JL+1))
      X3 = R3*SQRT(1.0 - ST3**2)
      IF (X3.LT.XC) GO TO 9C
      IF (JL.EQ.NSTRM-2) GC TO 90
      JL = JL + 1
      R2 = R3
      ST2 = ST3
      X2 = X3
      GC TC 8C
   90 R1 = RCA(JL-1) + (ZTRS(JL-1) - ZCDA(JL-1))*TALP(JL-1)
      ST1 = TTRS(JL-1)*SRS(TTRS(JL-1))
```

```
      Z1 = ZTRS(JL-1)
      Z2 = ZTRS(JL)
      Z3 = ZTRS(JL+1)
      R4 = RCA(JL+2) + (ZTRS(JL+2) - ZCDA(JL+2))*TALP(JL+2)
      ST4 = TTRS(JL+2)*SRS(TTRS(JL+2))
      Z4 = ZTRS(JL+2)
      GO TO 130
C ***     CARTESIAN COORDINATES OF THE PRESSURE SURFACE BLADE ELEMENT
C *** TRANSITION POINTS USED FOR INTERPOLATION
  100 R2 = RCA(JL) + (ZTRP(JL) - ZCDA(JL))*TALP(JL)
      ST2 = TTRP(JL)*SRS(TTRP(JL))
      X2 = R2*SQRT(1.0 - ST2**2)
      IF (X2.GE.XC) GO TO 110
      IF (JL.EQ.2) GO TO 110
      JL = JL - 1
      GO TO 100
  110 R3 = RCA(JL+1) + (ZTRP(JL+1) - ZCDA(JL+1))*TALP(JL+1)
      ST3 = TTRP(JL+1)*SRS(TTRP(JL+1))
      X3 = R3*SQRT(1.0 - ST3**2)
      IF (X3.LT.XC) GO TO 120
      IF (JL.EQ.NSTRM-2) GO TO 120
      JL = JL + 1
      R2 = R3
      ST2 = ST3
      X2 = X3
      GO TO 110
  120 R1 = RCA(JL-1) + (ZTRP(JL-1) - ZCDA(JL-1))*TALP(JL-1)
      ST1 = TTRP(JL-1)*SRS(TTRP(JL-1))
      Z1 = ZTRP(JL-1)
      Z2 = ZTRP(JL)
      Z3 = ZTRP(JL+1)
      R4 = RCA(JL+2) + (ZTRP(JL+2) - ZCDA(JL+2))*TALP(JL+2)
      ST4 = TTRP(JL+2)*SRS(TTRP(JL+2))
      Z4 = ZTRP(JL+2)
  130 X1 = R1*SQRT(1.0 - ST1**2) - X2
      Y1 = R1*ST1
      Y2 = R2*ST2
      Y3 = R3*ST3
      X4 = R4*SQRT(1.0 - ST4**2) - X2
      Y4 = R4*ST4
      X3 = X3 - X2
      XX = XC - X2
      T1 = (Y3 - Y2)/X3
      T2 = ((Y1 - Y2)/X1 - T1)/(X1 - X3)
      C4 = (T2 - (T1 - (Y4 - Y2)/X4)/(X3 - X4))/(X1 - X4)
      C3 = T2 - C4*(X1 + X3)
      C2 = T1 - (C3 + C4*X3)*X3
      YC = Y2 + XX*(C2 + XX*(C3 + XX*C4))
      T1 = (Z3 - Z2)/X3
      T2 = ((Z1 - Z2)/X1 - T1)/(X1 - X3)
      C4 = (T2 - (T1 - (Z4 - Z2)/X4)/(X3 - X4))/(X1 - X4)
      C3 = T2 - C4*(X1 + X3)
      C2 = T1 - (C3 + C4*X3)*X3
      ZC = Z2 + XX*(C2 + XX*(C3 + XX*C4))
      RETURN
      END
```

```
      SUBROUTINE SPLITG(X,Y,N,A,AX,AY,S1,S2)
C ***       THIS ROUTINE INTEGRATES UNDER A CUBIC SPLINE FIT OF BLADE
C *** SECTION SURFACE COORDINATES.  THE END POINT CURVATURES ARE SET
C *** EQUAL TO THE NEXT POINT CURVATURE AS DETERMINED FROM A CIRCULAR
C *** ARC FIT OF THE 3 END POINTS.  SLOPE BUT NOT CURVATURE IS
C *** CONTINUOUS AT THE TRANSITION POINT.  THE CURVE FIT IS USED TO GET
C *** AREA, XBAR, AND YBAR.
      COMMON /RCUT/  AC, COSKL, COSKU, EMTM, IOUT, IT, NP, SINKL, SINKU,
     1 DX(13), EM(14), YBP(14), YBS(14), ZBP(14), ZBS(14)
      DIMENSION H(14), X(N), Y(N)
      CALL ARCS(X(1),X(2), X(3), Y(1), Y(2), Y(3), F1,DI)
      CALL ARCS(X(N-1),X(N-2), X(N-3),Y(N-1),Y(N-2),Y(N-3),F2,DI)
C ***       LOCATE TRANSITION POINT IN THE ARRAY OF SURFACE POINTS.
      NP = N
      NF = N - 3
      DI = 1.0 + FLOAT(NF)*(X(N) - X(1))/(X(N-1) - X(1))
      IT = DI
   10 IF (X(N).GE.X(IT)) GO TO 20
      IT = IT - 1
      GO TO 10
   20 IF (X(N).LE.X(IT+1)) GO TO 30
      IT = IT + 1
      GO TO 20
   30 FXI = (X(N) - X(IT))/(X(IT+1) - X(IT))
      IF (FXI.LT.0.1) GO TO 60
      IF (FXI.GT.0.9) GO TO 50
C ***       PLACE TRANSITION POINT IN THE ARRAY.
      XT = X(N)
      YT = Y(N)
      NI = N - IT - 1
      NN = N + 1
      DO 40 I=1,NI
      II = NN - I
      X(II) = X(II-1)
   40 Y(II) = Y(II-1)
      II = N - NI
      X(II) = XT
      Y(II) = YT
      IT = IT + 1
      GO TO 70
   50 IT = IT + 1
   60 NP = N - 1
C ***     SOLVE FOR SECOND DERIVATIVE VALUES AT THE SURFACE ARRAY POINTS.
   70 DX(1) = X(2) - X(1)
      DS = (Y(2) - Y(1))/DX(1)
      EM(1) = -F1
      H(1) = 0.0
      IF (IT.EQ.2) GO TO 90
      ITM = IT - 1
      DO 80 I=2,ITM
      DSL = DS
      DX(I) = X(I+1) - X(I)
      DS = (Y(I+1) - Y(I))/DX(I)
      D = 2.0*(1.0 + DX(I)/DX(I-1)) - EM(I-1)
      EM(I) = DX(I)/(D*DX(I-1))
   80 H(I) = (6.0*(DS - DSL)/DX(I-1) - H(I-1))/D
      CM = (DS - DSL)/(DX(ITM) + DX(ITM-1))
   90 NC = NP - 1
      DX(NC) = X(NP) - X(NC)
      DS2 = (Y(NP) - Y(NC))/DX(NC)
      EM(NP) = -F2
```

```
      H(NP) = 0.0
      IF (IT.EQ.NC) GO TO 110
      ITP = NC - IT
      DO 100 IB=1,ITP
      I = NO - IB
      DSL2 = DS2
      DX(I) = X(I+1) - X(I)
      DS2 = (Y(I+1) - Y(I))/DX(I)
      D = 2.0*(1.0 + DX(I)/DX(I+1)) - EM(I+2)
      EM(I+1) = DX(I)/(D*DX(I+1))
  100 H(I+1) = (6.0*(DSL2 - DS2)/DX(I+1) - H(I+2))/D
      CP = (DSL2 - DS2)/(DX(IT+1) + DX(IT))
      IF (IT.LE.2) GO TO 110
      IF (CM.EQ.0.0) GO TO 130
      C = CP/CM*((1.0 + ((DSL2*DX(IT) + DS2*DX(IT+1))/(DX(IT) +
     X DX(IT+1)))**2)/(1.0 + ((DS*DX(ITM-1) + DSL*DX(ITM))/(DX(ITM) +
     X DX(ITM-1)))**2))**1.5
      C = C/(ABS(C))**0.3
      GO TO 120
  110 C = 1.0
  120 EMTM = (6.0*(DS2 - DS)/DX(IT-1) - H(IT-1) - H(IT+1)*DX(IT)/
     X DX(IT-1))/(2.0 - EM(IT-1) + (2.0 - EM(IT+1))*DX(IT)/DX(IT-1)*C)
      EMTP = EMTM*C
      GO TO 150
  130 EMTM = 0.0
      EMTP = (6.0*(DS2 - DS)/DX(IT-1) - H(IT-1) - H(IT+1)*DX(IT)/
     X DX(IT-1))/((2.0 - EM(IT+1))*DX(IT)/DX(IT-1))
  150 EM(IT) = EMTM
      IF (IT.EQ.2) GO TO 170
      ITM = IT - 2
      DO 160 IB = 1,ITM
      I = IT - IB
  160 EM(I) = H(I) - EM(I)*EM(I+1)
  170 EM(1) = EM(2)*F1
      EM(IT) = EMTP
      IF (IT.EQ.NO) GO TO 190
      IB = IT + 1
      DO 180 I=IB,NC
  180 EM(I) = H(I) - EM(I)*EM(I-1)
  190 EM(NP) = EM(NC)*F2
      S1 = (Y(2) - Y(1))/DX(1) - DX(1)*(2.0*EM(1) + EM(2))/6.0
      S2 = (Y(NP) - Y(NO))/DX(NO) + DX(NO)*(2.0*EM(NP) + EM(NO))/6.0
      A = 0.0
      AX = 0.0
      AY = 0.0
      DO 240 I=1,NC
      EML = EM(I)
      IF (IT.EQ.I+1) GO TO 220
      EMU = EM(I+1)
      GO TO 230
  220 EMU = EMTM
  230 A = A + (Y(I) + Y(I+1) - (EMU + EML)*DX(I)**2/12.0)*DX(I)/2.0
      DXS = DX(I)**2/60.0
      AX = AX + (Y(I+1)*(2.0*X(I+1) + X(I)) + Y(I)*(X(I+1) + 2.0*X(I)) -
     X DXS*(EMU*(8.0*X(I+1) + 7.0*X(I)) + EML*(7.0*X(I+1) + 8.0*X(I))))*
     X DX(I)/6.0
      AY = AY + (Y(I+1)**2 + Y(I)*(Y(I+1) + Y(I)) - DXS*((8.0*(Y(I+1)*
     X EML + Y(I)*EML) + 7.0*(Y(I+1)*EML + Y(I)*EMU)) - (16.0*(EMU**2 +
     X EML**2) + 31.0*EMU*EML)*DXS/7.0))*DX(I)/6.0
  240 CONTINUE
      RETURN
      END
```

```
C ***       THIS ROUTINE MAKES A CIRCULAR ARC FIT OF 3 POINTS TO FIND
C *** SLOPES AT THE POINTS.  THESE ARE USED TO DETERMINE SPLINE END
C *** POINT FACTORS FOR THE SECOND DERIVATIVE TERMS WHICH KEEP THE
C *** CURVATURE CONSTANT FOR THE END POINTS.
      SUBROUTINE ARCS(X1,X2,X3,Y1,Y2,Y3,F,YD1)
      DX1 = X2 - X1
      DX2 = X3 - X2
      DY1 = Y2 - Y1
      DY2 = Y3 - Y2
      DXY1 = DX1*DY2
      DXY2 = DX2*DY1
      DXXX = DX1*DX2*(X3 - X1)
      DYYY = DY1*DY2*(Y3 - Y1)
      YD1 = (DYYY - DXY1*DX1 + DXY2*(DX1 + X3 - X1))/(DXXX + DXY1*(DY1 +
     X Y3 - Y1) - DXY2*DY1)
      YD2 = (DYYY + DXY1*DX1 + DXY2*DX2)/(DXXX + DXY1*DY2 + DXY2*DY1)
      F = ((1.0 + YD1**2)/(1.0 + YD2**2))**1.5
      RETURN
      END
```

```
C ***       THIS ROUTINE FINDS THE BLADE SECTION AREA AND MOMENT
C *** ADDITIONS OF A BLADE EDGE CIRCLE.
      SUBROUTINE EDGES(XU,YU,SU,XL,YL,SL,A,AX,AY,R,XC,YC)
      COMMON /PCUT/  AC, COSKL, COSKU, EMTM, IOUT, IT, NP, SINKL, SINKU,
     1 DX(13), EM(14), YBP(14), YBS(14), ZBP(14), ZBS(14)
      COSU = 1.0/SQRT(1.0 + SU**2)
      SINU = SU*COSU
      COSL = 1.0/SQRT(1.0 + SL**2)
      SINL = SL*COSL
      SS = SINU + SINL
      SC = COSU + COSL
      XD = XU - XL
      DY = YU - YL
      TANDK = (XD*SC + DY*SS)/(XD*SS - DY*SC)
      COSDK = 1.0/SQRT(1.0 + TANDK**2)
      SINDK = TANDK*COSDK
      R = DY/(SC*COSDK - SS*SINDK)
      SINKU = SINU*COSDK + SINDK*COSU
      SINKL = SINL*COSDK + SINDK*COSL
      COSKU = COSU*COSDK - SINDK*SINU
      COSKL = COSL*COSDK - SINDK*SINL
      DXC = R*SINKU
      XC = XU + DXC
      YC = R*COSKL + YL
      IF (IOUT.EQ.1) RETURN
      ASUM = ARSIN(SINKL*COSKU - SINKU*COSKL)
      IF (XU.LT.0.0) GO TO 10
      ASUM = ASUM - 3.1415927
      GO TO 20
   10 ASUM = ASUM + 3.1415927
   20 AC = R**2*ASUM/2.0
      A = AC + (YD*(YC + YL) - DXC*DY)/2.0
      AX = AC*XC - R**3*(COSKU + COSKL)/3.0 - (DXC*((2.0*XC + XU)*YC +
     1 (2.0*XU + XC)*YU)) - (XD + DXC)*((XC + 2.0*XL)*YL + (XL + 2.0*XC)*
     2 YC))/6.0
      AY = AC*YC - R**3*(SINKU + SINKL)/3.0 - (DXC*(YC**2 + YU*(YU + YC)
     1 ) - (XD + DXC)*(YC**2 + YL*(YL + YC)))/6.0
      RETURN
      END
```

```
      SUBROUTINE GASMNT(GBA,GBT)
C ***      CALCULATION OF ROTOR GAS BENDING MOMENTS ABOUT HUB STACK PT.
      REAL INC, MACH
      COMMON /VECTOR/
     1 BETAS(1,21), BMATL(1), BLADES(1), CHOKE(1), CHORDA(1), CHORDB(1),
     2 CHORDC(1), CPCO(6), DEV(1,21), IDEV(1), IGEO(1), IINC(1),
     3 ILOSS(1), IMAX(1), INC(1,21), ISTN(2), ITRANS(1), NOPT(1),
     4 NXCUT(1), PHI(1,21), PO(2,21), R(2,21), RBHUB(1), RBTIP(1),
     5 SLOPE(2,21), SOLID(1), TALE(1), TAMAX(1), TATE(1), TBLE(1),
     6 TBMAX(1), TBTE(1), TCLE(1), TCMAX(1), TCTE(1), TDLE(1), TDMAX(1),
     7 TDTE(1), TILT(1), TO(2,21), TRANS(1,21), VTH(2,21), VZ(2,21),
     8 Z(2,21), ZBHUB(1), ZBTIP(1), ZMAX(1,21)
      COMMON /SCALAR/
     1 BETA, CP, CPH2, CPH3, CPH4, CPH5, CPH6, CPP3, CPP4, CPP5, CPP6,
     2 CP1, CV, DCP, DF, DHC, DHCI, DLOSC, G, GAMMA, GJ, GJ2, GR1, GR2,
     3 GR3, GR4, GR5, H, I, ICONV, ICOUNT, IERROR, IIN, IPR, IROTOR, IR,
     4 IROW, ITER, IW, J, JM, MACH, NAB, NBROWS, NHUB,NROTOR,NSTN,NSTRM,
     5 NTIP, NTUBES, OMEGA, PI, POA1, PR, RADIAN, RF, RG, ROT,TL,TOA1,TU
      RHS = 2.0*RBHUB(IROW)
      GB1 = 0.0
      GB2 = 0.0
      GBVX = 0.0
      GBVT = 0.0
      HR = (VZ(I-1,1)**2*(1.0 + SLOPE(I-1,1)**2) + VTH(I-1,1)**2)/GJ2
      TU = TO(I-1,1)
      TL = TEMP(HR)
      PS1U = PO(I-1,1)/PRATIO(TO(I-1,1))
      RVZRU = PS1U*VZ(I-1,1)*R(I-1,1)/(RF*TL)
      HR = (VZ(I,1)**2*(1.0 + SLOPE(I,1)**2) + VTH(I,1)**2)/GJ2
      TU = TO(I,1)
      TL = TEMP(HR)
      PS2U = PO(I,1)/PRATIO(TO(I,1))
      PT1 = PS1U
      PT2 = PS2U
      DO 10 J=1,NTUBES
      HR = (VZ(I-1,J+1)**2*(1.0 + SLOPE(I-1,J+1)**2) + VTH(I-1,J+1)**2)/
     X GJ2
      TU = TO(I-1,J+1)
      TL = TEMP(HR)
      PS1L = PO(I-1,J+1)/PRATIO(TO(I-1,J+1))
      RVZRL = PS1L*VZ(I-1,J+1)*R(I-1,J+1)/(RF*TL)
      DPF1 = (PS1U + PS1L)*(R(I-1,J)**2 - R(I-1,J+1)**2)
      GB1 = GB1 + DPF1*(R(I-1,J) + R(I-1,J+1) - RHS)
      PS1U = PS1L
      HR = (VZ(I,J+1)**2*(1.0 + SLOPE(I,J+1)**2) + VTH(I,J+1)**2)/GJ2
      TU = TO(I,J+1)
      TL = TEMP(HR)
      PS2L = PO(I,J+1)/PRATIO(TO(I,J+1))
      DPF2 = (PS2U + PS2L)*(R(I,J)**2 - R(I,J+1)**2)
      GB2 = GB2 + DPF2*(R(I,J) + R(I,J+1) - RHS)
      PS2U = PS2L
      RMA = ((R(I-1,J) + R(I-1,J+1) + R(I,J) + R(I,J+1))/2.0 - RHS)*
     X (RVZRU + RVZRL)*(R(I-1,J) - R(I-1,J+1))
      GBVX = GBVX + (VZ(I,J) + VZ(I,J+1) - VZ(I-1,J) - VZ(I-1,J+1))*RMA
      GBVT = GBVT + (VTH(I,J) + VTH(I,J+1) - VTH(I-1,J) - VTH(I-1,J+1))*
     X RMA
   10 RVZRU = RVZRL
      GBA = PI*(GBVX/G + GB1 - GB2 + (PT1 + PT2)*(R(I-1,1)**2 - R(I,1)
     X **2)*(R(I-1,1) + R(I,1) - RHS)/(6912.0*BLADES(IROW)))
      GBT = -GBVT*PI/(6912.0*G*BLADES(IROW))
      RETURN
      END
```

```
      SUBROUTINE MARGIN
C ***  CALC. OF LOCATION AND VALUE OF BLADE ELEMENT MINIMUM CHOKE MARGIN
      REAL KIC, KIP, KIS, KM, KOC, KOP, KOS, KP, KS, KTC, KTP, KTS, KWC,
     X MACH
      COMMON
     1 BETA1(21), BETA2(21), COSA(21), COSL(21), DKLE(1,21), DL(21),
     2 GAMM(21), OBAR(21), RELM(21), RPR1(21), RE1(21), RE2(21),
     3 RE3(21), RE4(21), RE5(21), RVTH(21), SINA(21), SINL(21), SLOS(21)
     4,SONIC(21), THETAP(21,13), THETAS(21,13), TREL1(21), TSTAT(21),
     5 VM(21), VTSQ(21), XBAR(1,21), YBAR(1,21), ZP(21,13), ZS(21,13)
      COMMON /EQUIV/
     1 CHC(21), CHK(21), COSA2(21), FSM(21), KIC(21), KOC(21), RCA(21),
     2 REC(2,21), RPTE(2,21), SINA2(21), SKIC(21), SKOC(21), TALP(21),
     3 TCA(21), TEC(2,21), TGB(21),TTRP(21),TTRS(21),YCCLE(25),YCCTE(25)
     4,ZCCLE(25), ZCCTE(25), ZCDA(21), ZEC(2,21), ZTRP(21), ZTRS(21)
      COMMON /SCALAR/
     1 BETA, CP, CPH2, CPH3, CPH4, CPH5, CPH6, CPP3, CPP4, CPP5, CPP6,
     2 CP1, CV, DCP, DF, DHC, DHCI, DLOSC, G, GAMMA, GJ, GJ2, GR1, GR2,
     3 GR3, GR4, GR5, H, I, ICONV, ICOUNT, IERROR, IIN, IPR, IROTOR, IR,
     4 IROW, ITER, IW, J, JM, MACH, NAB, NBROWS, NHUB,NROTOR,NSTN,NSTRM,
     5 NTIP, NTUBES, OMEGA, PI, POA1, PR, RADIAN, RF, RG, ROT,TL,TOA1,TU
      COMMON /BLADES/
     1 AMACH, ACC, A1SOAS, A1SCA1, BINC, CALP, CCC, CEPE, CGBL, CHORD,
     2 CINC, CKTC, CKTS, C1, C2, DKAPPA, DRCE, DRCGI, DRCMST, DRCMT,
     3 DRCOI, DRCT, DRCTI, DR1, DSME, DSMT, DSOI, DSOT, DSSE, DST, DSTI,
     4 EMT, F1, F2, GBL, ICL, IGC, IPASS, KIS, KM, KTC, KTS, P, PFLOS,
     5 RCG, RCM, RCMS, RCT, RD1, RECGI, REE, REMT, RET, RETI, RMSJ, RTRC
     6,R1, R1C, R2, SALP, SEPE, SGAM, SGBL, SJ, SKTC, SKTS, SLJD, T,
     7 TEPE, TGBLL, THD, THLE, THMAX, THTE, TKTN, TLS, WC1, YB1, YB2, ZM
      COMMON /MARG/
     1 AL, AOAS, AOA1, CCHORD, DAL, DAOAS, DPW, DPWL, DRCLEP, DRCM,
     2 DRCTPI, DRCTSI, DRCWT, DSA, DSP, DSP1, DSP2, DSS, DSS1, DSS2, DSW
     3,EB, EWC, F, HC, ICHOKE, KIP, KOP, KOS, KP, KS, KTP, KWC, PI2, RCI
     4,RCO, RCP, RCS, RCTP, RCTS, RELEP, REOI, REP, RES, RETP, RETS,
     5 REWT, RTR, RTRD, RTRQ, SECGBL, TCGI, TGBL, WC, ZMT
  320 IGC = 0
C ***      ESTIMATE DERIVATIVE OF AOAS WITH RESPECT TO F
      CKM = COS((KP + KS)/2.0)
      DACA1 = DSA*(HC*(KP + EWC - KS) - WC*CCHORD*SLJD*CKM/RD1)/WC1
      DRTR = RTRD*(R1C + DRCM*SALP)*CKM
      DA1SAS = (GR2*RTR**GR1 - A1SCAS/2.0)*DRTR/RTR - PFLOS/RTRQ
      DAOAS = (A1SOAS*DACA1 + AOA1*DA1SAS)/A1SOA1
      IF (ICHOKE-2) 330,430,440
  330 F1 = F
      DPW1 = DPW
      GO TO 445
C ***      SETUP OF CALCULATION FOR TRAILING EDGE CHANNEL WIDTH
  340 IF (KOS + KOP) 345,420,350
  345 KP = KOP
      CALL EPSLON(KOP+PI2,0.0,RCO,-THTE,DRCLEP,RELEP)
      RCP = RCO + DRCLEP
      REP = RCP*EB + RELEP + REOI*RCP/RCO
      DRCLEP = DRCLEP + DRCOI
      DRCWT = DRCLEP - DRCTSI
      REWT = REP - RETS*RCP/RCTS
      DPW = DSP2
      CALL CHAN
      GO TO 320
C ***      CAL. OF T.E. CHANNEL WIDTH WHEN BLADE EXIT ANGLE IS POSITIVE
  350 KS = KOS
      KP = KTP
```

```
      CALL EPSLCN(KOS+PI2,C.C,RCO,THTE,DRCLEP,RELEP)
      RCS = RCO + DRCLEP
      RES = RELEP + REOI*RCS/RCO
      DRCWT = CRCCI + CRCLEP - DRCTPI
      REWT = RES - RETP*RCS/RCTP - RCS*EB
      DRCWC = CRCWT
      REWC = REWT
      DSW = DSS2
      DPW = 0.0
      ICL = 1
      RCP = RCTP
  360 CALL TANKAP(RCP,CRCWC,REWC,TK)
      WC = SQRT(1.0 + TK**2)
      IF (ABS(TK).GT.100.0) GO TO 370
      WC = WC*ABS(DRCWC)
      GO TO 380
  370 WC = WC*ABS(REWC/TK)
  380 KWC = ATAN(-1.0/TK)
      IF (REWC.GT.0.0) KWC = PI + KWC
      DK = 2.0*KWC - KS - KP
      IF (ABS(DK).LT.0.0001) GC TO 410
      IF (ICL.GT.1) GO TC 400
      ICL = 2
      IF (DK.GT.C.0) GO TO 390
      DKDS = (KTP - KIP)/DSP1
      GC TO 400
  39C DKDS = (KCP - KTP)/DSP2
  4CC DPW = DK*WC/(2.0 + DKCS*WC) + DPW
      DK = DKCS*CPW
      CALL EPSLCN(KTP,DK,RCTP,CPW,CRCP,REP)
      KP = KTP + DK
      DRCWC = CRCWT - CRCP
      RCP = RCTP + DRCP
      REWC = REWT - REP*RCS/RCP
      GC TO 360
  410 DRCM = CRCCI + THLE - CRCWC/2.0 +DRCLEP
      EWC = - REWC/RCS
      GC TO 500
  42C DSW = DSS2
      DPW = DSP2
      SKCP = KOP*SRS(KOP)
      DRCM = CRCCI + THLE + THLE*SKOP
      EWC = RCO + THTE*SKOP
      WC = EWC*EB - 2.0*THTE*SCRT(1.0 - SKOP**2)
      EWC = WC/EWC
      GC TC 500
C ***       SEARCH FOR MINIMUM CHANNEL AREA TO CHOKE AREA
  43C F2 = F
      DPW2 = DPW
      IF (AOAS.GE.AL) GC TC 432
      ALCW = AOAS
      DPLCW = DPW
      IF (DAOAS.LE.0.0) GO TC 433
      GC TC 434
  432 ALCW = AL
      DPWLOW = CPWL
      IF (CAL.LT.C.C) GO TC 434
  433 IF (CAL- DACAS.GE.-0.0001) GC TO 478
  434 CI = DPWL - CPW
      DI = (DAL + DAOAS - 2.C*(AL - AOAS)/CI)/CI**2
      CI = (DAOAS - DAL)/(2.0*CI) + 1.5*DI*(DPWL + DPW)
```

```
      BI = DACAS + (2.0*CI - 3.0*DI*DPW)*DPW
      IF (DI.EQ.0.0) GC TO 435
      BQ = CI**2 - 3.0*DI*BI
      IF (BQ.LT.0.0) GO TO 478
      BC = SQRT(BQ)/(3.0*DI)
      CQ = CI/(3.0*DI)
      DPWN = CQ + BC
      IF (3.0*DI*DPWN - CI.GT.0.0) GO TO 438
      DPWN = CQ - BC
      GC TC 438
  435 DPWN = BI/(2.0*CI)
  438 IF (ICHCKE.EQ.3) GC TC 444
      IF (DPWN.LE.DPWL.OR.DPWN.GE.DPW) GO TO 478
      A = AL + (DPWN - DPWL)*(BI - CI*(DPWN + DPWL) + DI*(DPWN*(DPWN +
     X DPWL) + DPWL**2))
      IF (A.GT.ACAS.OR.A.GT.AL) GO TO 4..
      IF (AOAS.LT.AL) GC TC 450
      GC TC 445
  440 IF (ICHOKE.GT.3) GO TC 442
      IF (ABS(DACAS).GT.0.001) GO TO 434
      ICHCKE = 4
  442 IF (AOAS.LT.ALCW + 0.00001) GO TO 480
      DPWN = (DPW + DPWLCW)/2.0
      GC TC 445
  444 IF (DPWN.LE.DPW1) DPWN = (DPW + DPW1)/2.0
      IF (DPWN.GE.DPW2) DPWN = (DPW + DPW2)/2.0
      IF (AOAS.GT.ALOW) GO TC 445
      ALCW = AOAS
      DPWLCW = DPW
  445 AL = AOAS
      DAL = DACAS
      DPWL = DPW
  450 IF (ICHOKE.LT.3) ICHCKE = ICHOKE + 1
      IF (ICHOKE.EQ.2) GO TC 340
      DPW = DPWN
      IF (DPW) 455,470,460
  455 DKCS = (KTP - KIP)/DSP1
      GC TC 465
  460 DKCS = (KCP - KTP)/DSP2
  465 DK = DPW*DKDS
      KP = KTP + DK
      CALL EPSLCN (KTP,DK,RCTP,DPW,DRCP,REP)
      RCP = RCTP + DRCP
      REP = RCP*EB + RETP*RCP/RCTP + REP
      DRCLEP = DRCTPI + DRCP
      DRCWT = DRCLEP - DRCTSI
      GC TC 490
  470 KP = KTP
      RCP = RCTP
      REP = RCP*EB + RETP
      DRCWT = DRCTPI - DRCTSI
      GC TC 490
  478 IF (AOAS.LT.AL) GC TC 480
      ACAS = AL
      F = F1
  480 CHK(J) = ACAS - 1.0
      FSM(J) = (F - F1)/(F2 - F1)
      RETURN
  490 REWT = REP - RETS*RCP/RCTS
      CALL CHAN
      GC TC 320
```

```
500 IGC = 2
    CALL CHAN
    GO TO 320
    END
```

```
      SUBROUTINE COORD
C ***       GENERATION OF THE OUTPUT BLADE SECTION PROPERTIES AND COORD.
      REAL INC, KIC, KIS, KM, KOC, KTC, KTS, MACH
      COMMON /VECTOR/
     1 BETAS(1,21), BMATL(1), BLADES(1), CHOKE(1), CHORDA(1), CHORDB(1),
     2 CHORDC(1), CPCO(6), DEV(1,21), IDEV(1), IGEO(1), IINC(1),
     3 ILOSS(1), IMAX(1), INC(1,21), ISTN(2), ITRANS(1), NOPT(1),
     4 NXCUT(1), PHI(1,21), PO(2,21), R(2,21), RBHUB(1), RBTIP(1),
     5 SLOPE(2,21), SOLID(1), TALE(1), TAMAX(1), TATE(1), TBLE(1),
     6 TBMAX(1), TBTE(1), TCLE(1), TCMAX(1), TCTE(1), TDLE(1), TDMAX(1),
     7 TDTE(1), TILT(1), TO(2,21), TRANS(1,21), VTH(2,21), VZ(2,21),
     8 Z(2,21), ZBHUB(1), ZBTIP(1), ZMAX(1,21)
      COMMON /SCALAR/
     1 BETA, CP, CPH2, CPH3, CPH4, CPH5, CPH6, CPP3, CPP4, CPP5, CPP6,
     2 CPI, CV, DCP, DF, DHC, DHCI, DLOSC, G, GAMMA, GJ, GJ2, GR1, GR2,
     3 GR3, GR4, GR5, H, I, ICONV, ICOUNT, IERROR, IIN, IPR, IROTOR, IR,
     4 IROW, ITER, IW, J, JM, MACH, NAB, NBROWS, NHUB,NROTOR,NSTN,NSTRM,
     5 NTIP, NTUBES, OMEGA, PI, POA1, PR, RADIAN, RF, RG, ROT,TL,TOA1,TU
      COMMON
     1 BETA1(21), BETA2(21), COSA(21), COSL(21), DKLE(1,21), DL(21),
     2 GAMM(21), LPAR(21), RELM(21), RPR1(21), RE1(21), RE2(21),
     3 RE3(21), RE4(21), RE5(21), RVTH(21), SINA(21), SINL(21), SLOS(21)
     4,SONIC(21), THETAP(21,13), THETAS(21,13), TREL1(21), TSTAT(21),
     5 VM(21), VTSQ(21), XBAR(1,21), YBAR(1,21), ZP(21,13), ZS(21,13)
      COMMON /EQUIV/
     1 CHL(21), CHK(21), COSA2(21), FSM(21), KIC(21), KOC(21), RCA(21),
     2 REC(2,21), RPTE(2,21), SINA2(21), SKIC(21), SKOC(21), TALP(21),
     3 TCA(21), TEC(2,21), TCB(21),TTRP(21),TTRS(21),YCCLE(25),YCCTE(25)
     4,ZCCLE(25), ZCCTE(25), ZCOA(21), ZFC(2,21), ZTRP(21), ZTRS(21)
      COMMON /BLADES/
     1 AMACH, ACC, AISCAS, AISCA1, BINC, CALP, CCC, CEPE, CGBL, CHORD,
     2 CINC, CKTC, CKTS, C1, C2, CKAPPA, DRCE, DRCGI, DRCMST, DRCMT,
     3 DRCOI, DRCI, DRCTI, DRI, DSME, DSMT, DSOI, DSOT, DSSE, DST, DSTI,
     4 EMI, F1, F2, GBL, ICL, IGC, IPASS, KIS, KM, KTC, KTS, P, PFLOS,
     5 RCG, RCM, RCMS, RCT, RDI, RECCI, REE, REMT, RET, RETI, RMSJ, RTRC
     6,RI, RIC, R2, SALP, SEPE, SGAM, SGBL, SJ, SKTC, SKTS, SLJD, T,
     7 TEPE, TGBLL, THE, THLE, THMAX, THTE, TKTN, TLS, WC1, YB1, YB2, ZM
      COMMON /ROUT/  AC, COSKL, COSKU, EMTM, IOUT, IT, NP, SINKL, SINKU,
     1 EX(13), EM(14), YBP(14), YBS(14), ZBP(14), ZBS(14)
      COMMON /LABEL/ TITLE(18)
      DIMENSION EMS(14), FMD(13), FMS(10), NSP(4), SHP(43), SHS(43),
     1 SL(43), WORD(1), XCUT(25), YCP(43,4), YCS(43,4), ZC(43,4)
      EQUIVALENCE (JL,ICL)
      DATA FMD /        4H(5X,, 4H3F9., 4H4   , 4H,4X,, 4H3F9., 4H4    ,
     1 4H,4X,, 4H3F9., 4H4    , 4H,4X,, 4H3F9., 4H4    , 4H)        /
      DATA FMS /        4H1(4X, 4H2(4X, 4H3(4X, 4H4(4X, 4H3(9X, 4H)    ,
     1 4H7A4,, 4H15X , 4H3F5., 4H4        /
      DATA WORD / 4H        /
      ICONV = 3
      IS = 1
```

```
      DO 40 J=1,NSTRM
      CALL BLADE
   46 CALL POINTS
C *** ESTABLISH THE RADIAL LOCATION OF THE BLADE SECTION PLANES
      NC = NXCUT(IROW)
      IF (NC.GE.0) GO TO 50
      NC = -NC
      READ (IR,1000) (XCUT(J),J=1,NC)
      GO TO 260
   50 CALL XCUTS(NC,XCUT)
  260 JL = 2
      TLS = (ZBTIP(IROW) - ZBHUB(IROW))/(RBTIP(IROW) - RBHUB(IROW))
      IF (ABS(TILT(IROW)).GE.100.0) GO TO 264
      TANT = TILT(IROW)*SRS(TILT(IROW))
      TANT = TANT/SQRT(1.0 - TANT**2)
      IF (ISTN(I).LT.0) TANT = -TANT
      GO TO 266
  264 HUBT = TILT(IROW)/100.0
      IH = HUBT
      TIPT = TAN((TILT(IROW) - 100.0*FLOAT(IH))/RADIAN)
      IH = IH - (IH/100)*100
      HUBT = TAN(FLOAT(IH)/RADIAN)
  266 J = 1
  268 IP = 1
      NMIN = 43
      NMAX = 23
      WRITE (IW,2000) (TITLE(IJ),IJ=1,18)
      WRITE (IW,2020) BLADES(IROW), ZBHUB(IROW)
C *** INTERPOLATION FOR REF. COORDINATES ON THE DESIRED BLADE SECTIONS.
  290 DO 300 K=1,13
      CALL INTERP(XCUT(J),1,K,YBS(K),ZBS(K))
  300 CALL INTERP(XCUT(J),2,K,YBP(K),ZBP(K))
      CALL INTERP(XCUT(J),1,0,YBS(14),ZBS(14))
      CALL INTERP(XCUT(J),2,0,YBP(14),ZBP(14))
C *** CALCULATION OF THE BLADE SECTION CHORD ANGLE
      CALL ARCS(ZBS(1),ZBS(2),ZBS(3),YBS(1),YBS(2),YBS(3),SP1,SS1)
      CALL ARCS(ZBP(1),ZBP(2),ZBP(3),YBP(1),YBP(2),YBP(3),TANB,SP1)
      ICUT = 1
      CALL EDGES(ZBS(1),YBS(1),SS1,ZBP(1),YBP(1),SP1,A,AX,AY,RLE,
     X ZCCLE(J),YCCLE(J))
      CALL ARCS(ZBS(13),ZBS(12),ZBS(11),YBS(13),YBS(12),YBS(11),SP1,SS1)
      CALL ARCS(ZBP(13),ZBP(12),ZBP(11),YBP(13),YBP(12),YBP(11),TANB,
     X SP1)
      CALL EDGES(ZBS(13),YBS(13),SS1,ZBP(13),YBP(13),SP1,A,AX,AY,RTE,
     X ZCCTE(J),YCCTE(J))
      DY = YCCTE(J) - YCCLE(J)
      DZ = ZCCTE(J) - ZCCLE(J)
      DR = RLE - RTE
      CHORD = SQRT(DY**2 + DZ**2 - DR**2)
      TANB = (DY*CHORD + DR*DZ)/(DZ*CHORD - DR*DY)
C ***        TRANSLATE THE BLADE SECTION COORDINATES TO THE STACKING POINT
C *** ORIGIN AND ROTATE TO LIE ALONG THE BLADE SECTION CHORD
      COSB = 1.0/SQRT(1.0 + TANB**2)
      SINB = TANB*COSB
      DZ = XCUT(J) - RBHUB(IROW)
      IF (ABS(TILT(IROW)).GE.100.0) GO TO 304
      DTH = DZ*TANT
      GO TO 308
  304 RCCC = XCUT(J)
      DTHL = 0.0
  305 GT = (RCCC - RBHUB(IROW))/(RBTIP(IROW) - RBHUB(IROW))*(TIPT -HUBT)
```

```
      DTH = GT + (HUBT - RBHUB(IROW))/(RBTIP(IROW) - RBHUB(IROW))*(TIPT -
     1 HUBT))*ALOG(RCCG/RBHUB(IROW))
      IF (ABS(DTH - DTHL).LT.1.0E-7) GO TO 306
      RCCG = RCCG + (XCUT(J)/COS(DTH) - RCCG)/(1.0 - DTH*(GT + HUBT))
      DTHL = DTH
      GO TO 305
  306 DTH = XCUT(J)*TAN(DTH)
      IF (ISTN(I).LT.0) DTH = -DTH
  308 DZ = TLS*DZ
      DY = DTH*COSB + DZ*SINB
      DZ = DZ*COSB - DTH*SINB
      DO 310 K=1,14
      YBT = YBS(K)
      YBS(K) = YBS(K)*COSB - ZBS(K)*SINB + DY
  310 ZBS(K) = ZBS(K)*COSB + YBT*SINB - DZ
      ZS2 = ZBS(13)
      YS2 = YBS(13)
      CALL SPLITG(ZBS,YBS,14,AS,AXS,AYS,SS1,SS2)
      NPS = NP
      ITS = IT
      EMTS = EMTM
      DO 320 K=1,NP
  320 EMS(K) = EM(K)
      CALL IMOM(ZBS,YBS,NP,AXXS,AXYS,AYYS,AXXXXS, AXXYYS,AYYYYS)
      DO 360 K=1,14
      YBT = YBP(K)
      YBP(K) = YBP(K)*COSB - ZBP(K)*SINB + DY
  360 ZBP(K) = ZBP(K)*COSB + YBT*SINB - DZ
      ZP2 = ZBP(13)
      YP2 = YBP(13)
      CALL SPLITG(ZBP,YBP,14,AP,AXP,AYP,SP1,SP2)
      CALL IMOM(ZBP,YBP,NP,AXX,AXY,AYY,AXXXX,AXXYY,AYYYY)
  370 AXXS = AXXS - AXX
      AXYS = AXYS - AXY
      AYYS = AYYS - AYY
      AXXXXS = AXXXXS - AXXXX
      AXXYYS = AXXYYS - AXXYY
      AYYYYS = AYYYYS - AYYYY
      ICUT = 0
      CALL EDGES(ZS2,YS2,SS2,ZP2,YP2,SP2,AT,AXT,AYT,RTE,ZCTE,YCTE)
      CALL ENDS(ZS2,YS2,ZP2,YP2,ZCTE,YCTE,RTE,AC,AXXT,AXYT,AYYT,AXXXXT,
     X AXXYYT,AYYYYT)
      CALL EDGES(ZBS(1),YBS(1),SS1,ZBP(1),YBP(1),SP1,A,AX,AY,RLE,ZCLE,
     X YCLE)
      CALL ENDS(ZBS(1),YBS(1),ZBP(1),YBP(1),ZCLE,YCLE,RLE,AC,AXX,AXY,
     X AYY, AXXXX, AXXYY, AYYYY)
      A = A + AS - AP - AT
      AX = AX + AXS - AXP - AXT
      AY = AY + AYS - AYP - AYT
      AXX = AXX + AXXS - AXXT
      AXY = AXY + AXYS - AXYT
      AYY = AYY + AYYS - AYYT
      AXXXX = AXXXX + AXXXXS - AXXXXT
      AXXYY = AXXYY + AXXYYS - AXXYYT
      AYYYY = AYYYY + AYYYYS - AYYYYT
      XB = AX/A
      YB = AY/A
      AIP = AXX + AYY
      BETA = RADIAN*ARSIN(SINB)
      TANTBI = 2.0*AXY/(AXX - AYY)
      TANBI = TANTBI/(1.0 + SQRT(1.0 + TANTBI**2))
```

```
      BETAI = RADIAN*ATAN(TANBI) + BETA
      COSBI = 1.0/SQRT(1.0 + TANBI**2)
      SINBI = TANBI*COSBI
      AIMIN = AYY*COSBI**2 + SINBI*(AXX*SINBI - 2.0*AXY*COSBI)
      AIMAX = AIP - AIMIN
      CALL TORSN(ITS,NPS,EMS,EMTS,RLE,SS1,SP1,SS2,SP2,U,TORS)
      TORS = TORS/(3.0 + 4.0*TORS/(A*U**2))
      TWIST = AXXXX + AXXYY + AYYYY - AIP**2/A
      YCG = RLE - YCLE
      ZCG = RLE - ZCLE
      YST = YCG + DY
      ZST = ZCG - DZ
      WRITE (IW,2030) J, XCUT(J), ZST, YST, BETA, ZCG, YCG, A, AIMIN,
     X AIMAX, BETAI, TORS, TWIST
C ***       SET THE BLADE COORD. DEFINITION INCREMENT TO GIVE BETWEEN 20
C *** AND 40 POINTS AT A ROUND DECIMAL VALUE
      CHORD = RTE + ZCTE - ZCLE + RLE
      DI = CHORD/20.0
      DIL = ALOG10(DI)
      IDIL = DIL
      IF (DI.LT.1.0) IDIL = IDIL - 1
      RL = DIL - FLOAT(IDIL)
      IF (RL.GE.0.30103) GO TO 430
      DI = 1.0
      GO TO 455
  430 IF (RL.GE.0.39794) GO TO 440
      DI = 2.0
      GO TO 455
  440 IF (RL.GE.0.69897) GO TO 450
      DI = 2.5
      GO TO 455
  450 DI = 5.0
  455 DI = DI*10.0**IDIL
      PN = CHORD/DI - 0.00001
      NPT = PN
      NPT = NPT + 4
C *** INTERPOLATION FOR BLADE SECTION SURF. COORD. AT THE DESIRED LOCS.
      ZC(1,IP) = 0.0
      YCS(1,IP) = RLE
      YCP(1,IP) = RLE
      ZCTE = ZCTE + ZCG
      ZLE = RLE - ZCLE + ZBS(1)
      ZTE = ZCG + ZS2
      DO 460 K=1,14
      ZBS(K) = ZBS(K) + ZCG
  460 ZBP(K) = ZBP(K) + ZCG
      K = 2
      KS = 2
      IE = 0
  465 IF (RLE.GE.ZC(K-1,IP) + DI) GO TO 470
      ZC(K,IP) = RLE
      IE = 1
      KLE = K
      GO TO 480
  470 ZC(K,IP) = ZC(K-1,IP) + DI
  480 IF (ZC(K,IP).GT.ZLE) GO TO 490
      YCS(K,IP) = RLE + SQRT((2.0*RLE - ZC(K,IP))*ZC(K,IP))
      GO TO 530
  490 IF (ZC(K,IP).LT.ZTE) GO TO 500
      YCS(K,IP) = YCTE + YCG + SQRT(RTE**2 - (ZC(K,IP) - ZCTE)**2)
      GO TO 530
```

```
500 IF (ZC(K,IP).LE.ZBS(KS)) GO TO 505
    KS = KS + 1
    GO TO 500
505 EMU = EM(KS)
    IF (KS.EQ.ITS) EMU = EMTS
    DZ = ZBS(KS) - ZBS(KS-1)
    DZM = ZC(K,IP) - ZBS(KS-1)
    ZR = DZM/DZ
    IF (ZR.GT.0.0001) GO TO 510
    YCS(K,IP) = YCG + YBS(KS-1) + ZR*(YBS(KS) - YBS(KS-1)) -DZM*DZ*
   X (2.0*EMS(KS-1) + EMU)/6.0
    GO TO 530
510 DZP = ZBS(KS) - ZC(K,IP)
    ZR = DZP/DZ
    IF (ZR.GT.0.0001) GO TO 520
    YCS(K,IP) = YCG + YBS(KS) - ZR*(YBS(KS) - YBS(KS-1)) + DZM*DZ*(
   X 2.0*EMU + EMS(KS-1))/6.0
    GO TO 530
520 YCS(K,IP) = YCG + DZM*(YBS(KS)/DZ + EMU*(DZM**2/DZ - DZ)/6.0)
   X + DZP*(YBS(KS-1)/DZ + EMS(KS-1)*(DZP**2/DZ - DZ)/6.0)
530 K = K + 1
    IF (IE-1) 465,540,550
540 IE = 2
545 ZC(K,IP) = ZC(K-2,IP) + DI
    GO TO 480
550 IF (ZCTE.GE.ZC(K-1,IP) + DI) GO TO 470
    IF (K.EQ.NPT) GO TO 570
    IF (IE.GE.3) GO TO 560
    ZC(K,IP) = ZCTE
    IE = 3
    KTE = K
    GO TO 490
560 IF (IE.NE.3) GO TO 470
    IE = 4
    GO TO 545
570 K = 2
    KS = 2
    ZTE = ZCG + ZP2
580 IF (ZC(K,IP).GT.ZBP(1)) GO TO 590
    YCP(K,IP) = RLE - SQRT((2.0*RLE - ZC(K,IP))*ZC(K,IP))
    GO TO 630
590 IF (ZC(K,IP).LT.ZTE) GO TO 600
    YCP(K,IP) = YCTE + YCG - SQRT(RTE**2 - (ZC(K,IP) - ZCTE)**2)
    GO TO 630
600 IF (ZC(K,IP).LE.ZBP(KS)) GO TO 605
    KS = KS + 1
    GO TO 600
605 EMU = EM(KS)
    IF (KS.EQ.IT) EMU = EMTM
    DZ = ZBP(KS) - ZBP(KS-1)
    DZM = ZC(K,IP) - ZBP(KS-1)
    ZR = DZM/DZ
    IF (ZR.GT.0.0001) GO TO 610
    YCP(K,IP) = YCG + YBP(KS-1) + ZR*(YBP(KS) - YBP(KS-1)) - DZM*DZ*
   X (2.0*EM(KS-1) + EMU)/6.0
    GO TO 630
610 DZP = ZBP(KS) - ZC(K,IP)
    ZR = DZP/DZ
    IF (ZR.GT.0.0001) GO TO 620
    YCP(K,IP) = YCG + YBP(KS) - ZR*(YBP(KS) - YBP(KS-1)) + DZM*DZ*
   X (2.0*EMU + EM(KS-1))/6.0
```

```
      GO TO 630
  620 YCP(K,IP) = YCG + DZM*(YBP(KS)/DZ + EMU*(DZM**2/DZ - DZ)/6.0) +
     * DZP*(YBP(KS-1)/DZ + EM(KS-1)*(DZP**2/DZ - DZ)/6.0)
  630 IF (K.EQ.NPT-1) GO TO 640
      K = K + 1
      GO TO 580
  640 ZC(NPT,IP) = CHORD
      YCS(NPT,IP) = YCTE + YCG
      YCP(NPT,IP) = YCS(NPT,IP)
      IF (NOPT(IROW).LT.10) GO TO 648
      NPS = NPT - 2
      DO 642 K=1,NPS
      KS = K+1
      IF (K.LT.KLE) KS = K
      IF (K.GE.KTE-1) KS = K+2
      SL(K) = ZC(KS,IP)
      SHP(K) = YCP(KS,IP)
  642 SHS(K) = YCS(KS,IP)
      IF (NOPT(IROW).LT.20) GO TO 646
      PUNCH 1900, XCUT(J), (TITLE(IJ),IJ=1,4)
      PUNCH 1910, NPS, BETA, ZST, YST, RLE, RLE, RTE, ZCTE
      PUNCH 1920, (SL(K),SHP(K),SHS(K),K=1,NPS)
      IF (NOPT(IROW).LT.30) GO TO 648
  646 CONTINUE
  648 IF (NPT.GT.NMAX) NMAX = NPT
      IF (NPT.LT.NMIN) NMIN = NPT
      NSP(IP) = NPT
      IF (IP.NE.4) GO TO 790
      JS = J + 1 - IP
      JF = J
      WRITE (IW,2070) (J,J=JS,JF)
  650 DO 660 K=1,NMIN
  660 WRITE (IW,FMD) (ZC(K,IJ), YCP(K,IJ), YCS(K,IJ),IJ=1,IP)
      IPI = 1
      IF (NMAX.NE.NMIN) GO TO 665
      IF (IP.NE.4) GO TO 775
      GO TO 780
  665 NMIN = NMIN + 1
      DO 770 K=NMIN,NMAX
      GO TO (760,720,680,670),IP
  670 IF (NSP(4).GE.K) GO TO 680
      IP = 3
      FMD(11) = FMS(5)
      FMD(12) = FMS(6)
  680 IF (NSP(3).GE.K) GO TO 720
      IF (IP.EQ.3) GO TO 700
      IF (IPI.LT.3) GO TO 710
      IPI = 4
  690 FMD(8) = FMS(5)
      FMD(9) = FMS(6)
      GO TO 720
  700 IP = 2
      GO TO 690
  710 FMD(8) = FMS(7)
      FMD(9) = FMS(8)
      ZC(K,3) = WORD(1)
      YCP(K,3) = WORD(1)
      YCS(K,3) = WORD(1)
  720 IF (NSP(2).GE.K.OR.IPI.GT.2) GO TO 760
      IF (IP.EQ.2) GO TO 740
      IF (IPI.EQ.1) GO TO 750
      IPI = 3
```

```
730 FMD(5) = FMS(5)
    FMD(6) = FMS(6)
    GC TO 760
740 IP = 1
    GC TC 730
750 FMD(5) = FMS(7)
    FMD(6) = FMS(8)
    ZC(K,2) = WORD(1)
    YCP(K,2) = WORD(1)
    YCS(K,2) = WCRC(1)
760 IF (NSP(1).GE.K.OR.IPI.GT.1) GO TO 770
    IPI = 2
    FMD(2) = FMS(5)
    FMD(3) = FMS(6)
770 WRITE (IW,FMD) (ZC(K,IJ),YCP(K,IJ),YCS(K,IJ),IJ=IPI,IP)
    FMD(2) = FMS(9)
    FMD(3) = FMS(10)
775 FMD(5) = FMS(9)
    FMD(6) = FMS(10)
    FMD(8) = FMS(9)
    FMC(9) = FMS(10)
    FMD(11) = FMS(9)
    FMD(12) = FMS(10)
780 IF (J.EC.NC) GO TC 840
    J = J + 1
    GC TO 268
790 IF (J.EQ.NC) GO TO 80C
    J = J + 1
    IP = IP + 1
    GC TC 290
8CC FMD(11) = FMS(5)
    FMD(12) = FMS(6)
    JS = J + 1 - IP
    JF = J
    IF (IP.LT.3) GC TC 810
    WRITE (IW,2060) (J,J=JS,JF)
    GC TC 650
810 FMC(8) = FMS(5)
    FMC(9) = FMS(6)
    IF (IP.LT.2) GO TO 82C
    WRITE (IW,2050) JS,JF
    GC TC 650
82C FMD(5) = FMS(5)
    FMC(6) = FMS(6)
    WRITE (IW,2040) J
    GC TC 650
84C CALL BCOORC(IS,NC,XCUT,YCCLE,ZCCLE,YCCTE,ZCCTE)
85C RETURN
10CC FCRMAT (8F10.4)
19CC FCRMAT (3X,3HX =,F10.4,2X,4A6)
191C FCRMAT (I5,5X,7F10.5)
192C FCRMAT (9F8.4)
20CC FCRMAT (1H1 / 27X,32H** BLADE SECTION PROPERTIES OF    , 18A4 )
2C2C FCRMAT ( / 20X,18HNUMBER OF BLADES =,F6.1,10X,47HAXIAL LOCATION OF
    1 STACKING LINE IN COMPRESSCR =,F7.3,4H IN.// 4X,13HBLADE SECTION,
    2 5X,14HSTACKING POINT,5X,7HSECTION,5X,13HBLADE SECTION,4X,
    3 7HSECTICN,3X,18HMOMENTS OF INERTIA,4X,4HIMAX,4X,7HSECTION,3X,
    4 7HSECTICN  / 13X,4HRAC.,7X,11HCOORDINATES,6X,7HSETTING,3X,
    5 16HC.G. CCCRDINATES,4X,4HAREA,8X,12HTHROUGH C.G.,6X,7HSETTING,2X,
    6 7HTCRSICN,4X,5HTWIST / 5X,3HNO.,5X,4HLOC.,6X,1HL,9X,1HH,8X,
    7 5HANGLE,6X,1HL,9X,1HH,17X,4HIMIN,6X,4HIMAX,7X,5HANGLE,3X,
```

```
    8 8HCONSTANT,1X,9HSTIFFNESS /  3X,5H(IN.),4X,5H(IN.),5X,5H(IN.),5X,
    9 6H(DEG.),4X,5H(IN.),5X,5H(IN.),3X,5H(IN.)**2,1X,2(2X,8H(IN.)**4),
    . 3X,6H(DEG.),3X,8H(IN.)**4,2X,    ***)
 2030 FORMAT (5X,I2,F10.3,2F10.4,F1 ,3 ,  4,F10.5,F11.6,F9.5,F10.3.
    1 F11.6,F10.5 )
 2040 FORMAT (/      7X,11HSECTION NO.,I3,1  COORDINATES  /      10X,
    1 1HL,8X,2HHP,7X,2HHS,7X  /   4X,3(4X,  IN.) ))
 2050 FORMAT (/ 2X,2(5X,11HSECTION NO.,I3,12H COORDINATES) / 6X,2(4X,
    1 1HL,8X,2HHP,7X,2HHS,7X) / 2(4X,3(4X,5H IN.))))
 2060 FORMAT (/ 2X,3(5X,11HSECTION NO.,I3,12H COORDINATES) / 6X,3(4X,
    1 1HL,8X,2HHP,7X,2HHS,7X) / 3(4X,3(4X,5H(IN.))))
 2070 FORMAT (/ 2X,4(5X,11HSECTION NO.,I3,12H COORDINATES) / 6X,4(4X,
    1 1HL,8X,2HHP,7X,2HHS,7X) / 4(4X,3(4X,5H(IN.))))
      END
```

```
      SUBROUTINE XCUTS(NC,XCUT)
C ***       THIS ROUTINE SETS THE RADIAL LOCATION OF THE BLADE SECTION
C *** PLAINS TO COVER THE BLADE SPAN IN ROUND DECIMAL INCREMENTS
      REAL INC, KIC, KOC, MACH
      COMMON /VECTOR/
     1 BETAS(1,21), BMATL(1), BLADES(1), CHOKE(1), CHORDA(1), CHORDB(1),
     2 CHORDC(1), CPCO(6), DEV(1,21), IDEV(1), IGEO(1), IINC(1),
     3 ILOSS(1), IMAX(1), INC(1,21), ISTN(2), ITRANS(1), NOPT(1),
     4 NXCUT(1), PHI(1,21), PO(2,21), R(2,21), RBHUB(1), RBTIP(1),
     5 SLOPE(2,21), SOLID(1), TALE(1), TAMAX(1), TATE(1), TBLE(1),
     6 TBMAX(1), TBTE(1), TCLE(1), TCMAX(1), TCTE(1), TDLE(1), TDMAX(1),
     7 TDTE(1), TILT(1), TO(2,21), TRANS(1,21), VTH(2,21), VZ(2,21),
     8 Z(2,21), ZBHUB(1), ZBTIP(1), ZMAX(1,21)
      COMMON /SCALAR/
     1 BETA, CP, CPH2, CPH3, CPH4, CPH5, CPH6, CPP3, CPP4, CPP5, CPP6,
     2 CP1, CV, DCP, DF, DHC, DHCI, DLOSC, G, GAMMA, GJ, GJ2, GR1, GR2,
     3 GR3, GR4, GR5, H, I, ICONV, ICOUNT, IERROR, IIN, IPR, IROTOR, IR,
     4 IROW, ITER, IW, J, JM, MACH, NAB, NBROWS, NHUB,NROTOR,NSTN,NSTRM,
     5 NTIP, NTUBES, OMEGA, PI, POA1, PR, RADIAN, RF, RG, ROT,TL,TOA1,TU
      COMMON
     1 BETA1(21), BETA2(21), COSA(21), COSL(21), DKLE(1,21), DL(21),
     2 GAMM(21), OBAR(21), RELM(21), RPR1(21), RE1(21), RE2(21),
     3 RE3(21), RE4(21), RE5(21), RVTH(21), SINA(21), SINL(21), SLOS(21)
     4,SONIC(21), THETAP(21,13), THETAS(21,13), TREL1(21), TSTAT(21),
     5 VM(21), VTSQ(21), XBAR(1,21), YBAR(1,21), ZP(21,13), ZS(21,13)
      COMMON /EQUIV/
     1 CHD(21), CHK(21), COSA2(21), FSM(21), KIC(21), KOC(21), RCA(21),
     2 REC(2,21), RPTE(2,21), SINA2(21), SKIC(21), SKOC(21), TALP(21),
     3 TCA(21), TEC(2,21), TGB(21),TTRP(21),TTRS(21),YCCLE(25),YCCTE(25)
     4,ZCCLE(25), ZCCTE(25), ZCDA(21), ZEC(2,21), ZTRP(21), ZTRS(21)
      DIMENSION XCUT(25)
      IF (NC.GT.0) GO TO 60
      XN = 20.0*(1.0 - EXP(-0.5*(RBTIP(IROW) - RBHUB(IROW))/CHD(JM))) +
     X 5.0
      NC = XN
   60 IF (NC.LT.5) NC = 5
      IF (NC.GT.24) NC = 24
      NI = NC - 1
      IF (R(I,1).GE.R(I-1,1)) GO TO 70
      XHIGH = R(I-1,1)
      DXHIGH = R(I-1,1) - R(I,1)
      GO TO 80
```

```
 70 XHIGH = R(I,1)
    DXHIGH = R(I,1) - R(I-1,1)
 80 XLOW = R(I-1,NSTRM)*COS(THETAP(NSTRM,1))
    DXLOW = R(I,NSTRM)*COS(THETAS(NSTRM,1)) - XLOW
    IF (DXLOW.GE.0.0) GO TO 90
    XLOW = XLOW + DXLOW
    DXLOW = -DXLOW
 90 DX = XHIGH - XLOW
    DIL = ALOG10(DX)
    IDIL = DIL
    IF (DX.LT.1.0) IDIL = IDIL - 1
    RL = DIL - FLOAT(IDIL)
    IF (RL.GE.0.30103) GO TO 100
    DI = 1.0
    GO TO 130
100 IF (RL.GE.0.39794) GO TO 110
    DI = 2.0
    GO TO 130
110 IF (RL.GE.0.69897) GO TO 120
    DI = 2.5
    GO TO 130
120 DI = 5.0
130 DI = DI*10.0**(IDIL - 2)
    XCUT(1) = XHIGH/DI
    ICUT = XCUT(1)
    XCUT(1) = DI*(FLOAT(ICUT) + 1.0)
    XN = (XCUT(1) - XLOW)/DI + 1.0
    NX = XN
    XCUT(NC) = XCUT(1) - DI*FLOAT(NX)
    IF (NC.LT.7) GO TO 215
    XNI = NI
    FN = 1.0
    DXCUT = XCUT(1) - XCUT(NC)
140 F = DXCUT*(FN + 0.2)/XNI
    IF (DXHIGH.LT.F) GO TO 150
    FN = FN + 1.0
    GO TO 140
150 XT = DXHIGH/DI + 1.0
    NT = XT
    IF (NT.LE.NX/NI/5) GO TO 170
    NF = FN
    XCUT(NF+1) = XCUT(1) - DI*FLOAT(NT)
    IT = 1
    IF (NF.EQ.1) GO TO 180
    NTI = (NT + 1)/NF
160 IT = IT + 1
    XCUT(IT) = XCUT(IT-1) - DI*FLOAT(NTI)
    IF (IT.EQ.NF) GO TO 180
    GO TO 160
170 NT = 0
    IT = 0
180 FN = 1.0
190 F = DXCUT*(FN + 0.2)/XNI
    IF (DXLOW.LT.F) GO TO 200
    FN = FN + 1.0
    GO TO 190
200 XT = DXLOW/DI + 1.0
    NH = XT
    IF (NH.LE.NX/NI/5) GO TO 220
    NF = FN
    NFH = NC - NF
```

```
      XCUT(NFH) = XCUT(NC) + DI*FLOAT(NH)
      IH = 1
      IF (NF.EQ.1) GO TO 230
      NTI = (NH + 1)/NF
  210 IH = IH + 1
      INH = NC + 1 - IH
      XCUT(INH) = XCUT(INH+1) + DI*FLOAT(NTI)
      IF (IH.EQ.NF) GO TO 230
      GO TO 210
  215 NT = 0
      IT = 0
  220 NH = 0
      IH = 0
  230 NX = NX - NT - NH
      NI = NI - IT - IH
  240 II = NX/NI
      NL = NX - II*NI
      JL = IT + 2
      N = NI + IT
      IC = 0
      DO 250 J=JL,N
      IC = IC + II
      IF (J.LT.JL+NL) IC = IC + 1
  250 XCUT(J) = XCUT(IT+1) - FLOAT(IC)*DI
      NC = NC + 1
      XCUT(NC) = RBTIP(IROW)
      IF (ISTN(I).GT.0) XCUT(NC) = RBHUB(IROW)
      RETURN
      END
```

```
      SUBROUTINE IMOM(Z,Y,N,AXX,AXY,AYY,AXXXX,AXXYY,AYYYY)
C *** MOMENTS OF INERTIA USING THE SPLINE CURVE AS THE SURFACE BOUNDARY
      COMMON /RCUT/  AC, COSKL, COSKU, EMTM, IOUT, IT, NP, SINKL, SINKU,
     1 DX(13), EM(14), YBP(14), YBS(14), ZBP(14), ZBS(14)
      DIMENSION Y(N), Z(N)
      AXX = 0.0
      AXY = 0.0
      AYY = 0.0
      AXXXX = 0.0
      AXXYY = 0.0
      AYYYY = 0.0
      NI = NP - 1
      DO 30 K=1,NI
      EL = EM(K)
      IF (IT.EQ.K+1) GO TO 10
      EU = EM(K+1)
      GO TO 20
   10 EU = EMTM
   20 DXS = DX(K)**2
      DXSE = DXS*(EL + EU)/2.0
      YM = Y(K)
      YP = Y(K+1)
      YS = YM*YM
      YC = YS*YM
      YQ = YS*YS
      ES = EL*EL
```

```
      EC = ES*EL
      ZM = Z(K)
      ZP = Z(K+1)
      ZS = ZM*ZM
      ZC = ZS*ZM
      ZQ = ZS*ZS
      AXX = AXY + DX(K)*(ES*(YP*(ZP + 2.0*ZM) + 3.0*ZS) + YP*(ZS + ZP*
     1 (2.0*ZM + 3.0*ZP)))/2.0 - DXS*(EL*(ZP*(ZP/15.0 + ZM/10.0) + ZS/
     2 12.0) + EU*(ZP*(ZP/12.0 + ZM/10.0) + ZS/15.0)))/6.0
      AXY = AXY + DX(K)/24.0*(YS*(3.0*ZM + ZP) + YP*(2.0*(ZM + ZP)*YM +
     1 YP*(ZM + 3.0*ZP)) - DXS/15.0*(YM*(ZM*(5.0*EL + 4.0*EU) + 3.0*ZP*
     2 (EL + EU)) + YP*(3.0*ZM*(EL + EU) + ZP*(4.0*EL + 5.0*EU))) - DXS/
     3 168.0*(ES*(35.0*ZM + 29.0*ZP) + EU*(62.0*EL*(ZM + ZP) + EU*(29.0*
     4 ZM + 35.0*ZP)))))
      AYY = AYY + DX(K)/12.0*(YC + (YS + (YM + YP)*YP)*YP - DXS/30.0*((
     1 5.0*YS + (6.0*YM + 4.0*YP)*YP)*EL + (4.0*YS + (6.0*YM + 5.0*YP)*
     2 YP)*EU - DXS/84.0*((35.0*ES + (62.0*EL + 29.0*EU)*EU)*YM + (29.0*
     3 ES + (62.0*EL + 35.0*EU)*EU)*YP - DXS/6.0*(7.0*EC + (20.0*ES +
     4 (20.0*EL + 7.0*EU)*EU)*EU))))
      AXXXX = AXXXX + DX(K)*(YP*((((5.0*ZP + 4.0*ZM)*ZP + 3.0*ZS)*ZP +
     1 2.0*ZC)*ZP + ZQ) + YM*((((ZP + 2.0*ZM)*ZP + 3.0*ZS)*ZP + 4.0*ZC)*
     2 ZP + 5.0*ZQ) - DXS*(EL*(35.0*ZQ + ZP*(52.0*ZC + ZP*(54.0*ZS + ZP*
     3 (44.0*ZM + 25.0*ZP)))) + EU*((((35.0*ZP + 52.0*ZM)*ZP + 54.0*ZS)*
     4 ZP + 44.0*ZC)*ZP + 25.0*ZQ))/168.0)/30.0
      AXXYY = AXXYY + DX(K)*(YC*(ZP*(ZP + 4.0*ZM) + 10.0*ZS) + YP*(YS*(
     1 3.0*ZP*(ZP + 2.0*ZM) + 6.0*ZS) + YP*(YM*(6.0*ZP*(ZP + ZM) + 3.0*
     2 ZS) + YP*(ZP*(10.0*ZP + 4.0*ZM) + ZS))) - DXS*(YS*(EL*(ZP*(9.0*ZP
     3 + 26.0*ZM) + 35.0*ZS) + EU*(ZP*(9.0*ZP + 22.0*ZM) + 25.0*ZS)) +YP
     4 *(YM*(EL*(ZP*(22.0*ZP + 36.0*ZM) + 26.0*ZS) + EU*(ZP*(26.0*ZP +
     5 36.0*ZM) + 22.0*ZS)) + YP*(EL*(ZP*(25.0*ZP + 22.0*ZM) + 9.0*ZS) +
     6 EU*(ZP*(35.0*ZP + 26.0*ZM) + 9.0*ZS))) - DXS*(ES*(YM*(ZP*(19.0*ZP
     7 + 44.0*ZM) + 42.0*ZS) + YP*(ZP*(27.0*ZP + 38.0*ZM) + 22.0*ZS)) +
     8 EU*(EL*(YM*(40.0*ZP*(ZP + 2.0*ZM) + 66.0*ZS) + YP*(ZP*(66.0*ZP +
     9 80.0*ZM) + 40.0*ZS)) + EU*(YM*(ZP*(22.0*ZP + 38.0*ZM) + 27.0*ZS)+
     . YP*(ZP*(42.0*ZP + 44.0*ZM) + 19.0*ZS))) - DXS*(EC*(ZP*(52.0*ZP +
     1 102.0*ZM) + 77.0*ZS) + EU*(ES*(ZP*(171.0*ZP + 294.0*ZM) + 195.0*
     2 ZS) + EU*(EL*(ZP*(195.0*ZP + 294.0*ZM) + 171.0*ZS) + EU*(ZP*(77.0
     3 *ZP + 102.0*ZM) + 52.0*ZS)))))/66.0)/18.0)/28.0)/90.0
   30 AYYYY = AYYYY + DX(K)*(((((YP + YM)*YP + YS)*YP + YC)*YP + YQ)*YP
     1 + YM*YQ) - DXSE*(((((5.0*YP + 6.0*YM)*YP + 9.0*YS)*YP + 8.0*YC)*
     2 YP + 5.0*YQ) - DXSE*((((5.0*YP + 9.0*YM)*YP + 9.0*YS)*YP + 5.0*YC
     3 ) - DXSE*(((5.0*YP + 8.0*YM)*YP + 5.0*YS) - DXSE*((YP + YM) -
     4 DXSE/22.0)/2.0)/6.0)/4.0)/14.0)/30.0
      RETURN
      END
```

```
C ***       THIS ROUTINE CALCULATES THE MOMENT OF INERTIA CORRECTIONS
C *** ASSOCIATED WITH THE PROPER TREATMENT OF THE BLADE END CIRCLES.
      SUBROUTINE ENDS(ZS,YS,ZP,YP,ZC,YC,R,A,AXX,AXY,AYY,AXXXX,AXXYY,
     X AYYYY)
      COMMON /ROOT/  AC, COSKL, COSKU, EMTM, IOUT, IT, NP, SINKL, SINKU,
     1 DX(13), EM(14), YBP(14), YBS(14), ZBP(14), ZBS(14)
      DZU = ZC - ZS
      DZL = ZC - ZP
      DYU = YC - YS
      DYL = YC - YP
```

```
      RS = R*R
      RC = R*RS
      YCS = YC**2
      ZCS = ZC**2
      YCC = YC*YCS
      YCQ = YCS*YCS
      ZCC = ZC*ZCS
      ZCQ = ZCS*ZCS
      SINS = SINKL + SINKU
      COSS = COSKL + COSKU
      SIN2KL = 2.0*SINKL*COSKL
      SIN2KU = 2.0*SINKU*COSKU
      SIND = SIN2KL - SIN2KU
      RT = R*(SIN2KL - SIN2KU)/16.0
      RD = RS*(SIN2KL*(1.0 - 2.0*SINKL**2) - SIN2KU*(1.0 - 2.0*SINKU**2
     X ))/48.0
      AXX = (ZCS + RS/4.0)*A - RC*(2.0*ZC*COSS/3.0 + RT) -
     1 (DZU*YC/3.0 - ZC*DYU/12.0)*(ZCS + ZS*(ZC + ZS)) + (DZL*YC/3.0 -
     2 ZC*DYL/12.0)*(ZCS + ZP*(ZC + ZP)) - (DYU*ZS**3 - DYL*ZP**3)/4.0
      AXY = ZC*YC*A - RC*((ZC*SINS + YC*COSS)/3.0 +
     1 R*(SINKL - SINKU)*SINS/8.0) - (DZU*(ZS*(YS*(3.0*YS +
     2 2.0*YC) + YCS) + ZC*(YS*(YS + 2.0*YC) + 3.0*YCS)) - DZL*(ZP*(YP*
     3 (3.0*YP + 2.0*YC) + YCS) + ZC*(YP*(YP + 2.0*YC) + 3.0*YCS)))/24.0
      AYY = (YCS + RS/4.0)*A - RC*(2.0*YC*SINS/3.0 - RT) -
     1 (DZU*(YCS + YS**2)*(YC + YS) - DZL*(YCS + YP**2)*(YC + YP))/12.0
      AXXXX = (ZCQ + RS*(1.5*ZCS + RS/8.0))*A - RC*(ZC*((10.0*ZCS + 4.0*
     1 RS)*COSS + RS*(SIN2KL*SINKL + SIN2KU*SINKU))/7.5 + R*((3.0*ZCS +
     2 RS/3.0)*SIND - RD)/8.0) - ((6.0*YC*DZU - ZC*DYU)*(ZCQ + ZS*(ZCC +
     3 ZS*(ZCS + ZS*(ZC + ZS)))) - (6.0*YC*DZL - ZC*DYL)*(ZCQ + ZP*(ZCC
     4 + ZP*(ZCS + ZP*(ZC + ZP)))))/30.0 + (DYL*ZP**5 - DYU*ZS**5)/6.0
      AXXYY = (ZCS*YCS + RS*(ZCS + YCS + RS/6.0)/4.0)*A - RC*(ZC*YC*((ZC
     1 *SINS + YC*COSS)/1.5 + R*SINS*(SINKL - SINKU)/2.0) + RS*(ZC*(
     2 COSKL**3 + COSKU**3) + YC*(SINKL**3 + SINKU**3))/7.5 - R*((ZCS -
     3 YCS)*SIND - 2.0*RD)/16.0) + (DZL*(ZP*(ZP*(YCC + YP*(3.0*YCS + YP*
     4 (6.0*YC + 10.0*YP))) + ZC*(4.0*YCC + YP*(6.0*YCS + YP*(6.0*YC +
     5 4.0*YP)))) + ZCS*(10.0*YCC + YP*(6.0*YCS + YP*(3.0*YC + YP)))) -
     6 DZU*(ZS*(ZS*(YCC + YS*(3.0*YCS + YS*(6.0*YC + 10.0*YS))) + ZC*(
     7 4.0*YCC + YS*(6.0*YCS + YS*(6.0*YC + 4.0*YS)))) + ZCS*(10.0*YCC +
     8 YS*(6.0*YCS + YS*(3.0*YC + YS)))))/180.0
      AYYYY = (YCQ + RS*(1.5*YCS + RS/8.0))*A - RC*(YC*((10.0*YCS + 4.0*
     1 RS)*SINS + RS*(SIN2KL*COSKL + SIN2KU*COSKU))/7.5 - R*((3.0*YCS +
     2 RS/3.0)*SIND + RD)/8.0) + (DZL*(YCQ*YC + YP*(YCQ + YP*(YCC + YP*(
     3 YCS + YP*(YC + YP))))) - DZU*(YCQ*YC + YS*(YCQ + YS*(YCC+ YS*(
     4 YCS + YS*(YC + YS))))))/30.0
      RETURN
      END
```

```
      SUBROUTINE TORSN(ITS,NPS,EMS,EMTS,RLE,SS1,SP1,SS2,SP2,U,TORS)
C ***       CALCULATION OF THE BLADE SECTION TORSION CONSTANT
      COMMON /RCUT/  AC, COSKL, COSKU, EMTM, IOUT, IT, NP, SINKL, SINKU,
     1 DX(13), EM(14), YBP(14), YBS(14), ZBP(14), ZBS(14)
      DIMENSION EMS(NPS)
      U = 0.0
      TORS = 0.0
      TALPAL = (ZBP(1) - ZBS(1))/(YBS(1) - YBP(1))
      XAL = (ZBP(1) + ZBS(1))/2.0
      YAL = (YBP(1) + YBS(1))/2.0
```

```
      TL = SQRT((ZBP(1) - ZBS(1))**2 + (YBS(1) - YBP(1))**2)
      SOL = (SS1 - SP1)/(1.0 + SS1*SP1)
C ***       INTEGRATION OF T**3*DU FOR THE SPLINE SEGMENTS
      KS = 1
      DO 100 K=2,NP
      IF (K.NE.IT) GO TO 25
      EMU = EMTM
      IF (NPS-NP) 10,30,20
   10 IF (KS.LT.2) KS = 2
      GO TO 40
   20 KS = KS + 2
      GO TO 40
   25 EMU = EM(K)
   30 KS = KS + 1
   40 XL = ZBS(KS)
      YL = YBS(KS)
      IF (K.EQ.NP) GO TO 80
      TALPL = (YBP(K) - YBP(K-1))/(ZBP(K) - ZBP(K-1)) + (2.0*EMU +
     X EM(K-1))*(ZBP(K) - ZBP(K-1))/6.0
      EMU = EMS(KS)
      IF (KS.EQ.ITS) EMU = EMTS
      TALPU = (YBS(KS) - YBS(KS-1))/(ZBS(KS) - ZBS(KS-1)) + (2.0*EMU
     X + EMS(KS-1))*(ZBS(KS) - ZBS(KS-1))/6.0
   50 TLAM = (ZBP(K) - XL)/(YL - YBP(K))
      TALPA = (TALPU + TALPL)/(1.0 - TALPU*TALPL + SQRT((1.0 + TALPU**2)
     X *(1.0 + TALPL**2)))
      IF (ABS(TALPA - TLAM).LE.0.0001) GO TO 90
      XL = XL + ((YBP(K) - YL)*TALPA + ZBP(K) - XL)/(1.0 + TALPU*TALPA)
      IF (XL.LE.ZBS(KS)) GO TO 60
      KU = KS + 1
      KL = KS
      EMU = EMS(KU)
      IF (KU.EQ.ITS) EMU = EMTS
      GO TO 70
   60 KU = KS
      KL = KS - 1
      EMU = EMS(KS)
      IF (KS.EQ.ITS) EMU = EMTS
   70 DZ = ZBS(KU) - ZBS(KL)
      DXU = ZBS(KU) - XL
      DXL = XL - ZBS(KL)
      YL = DXL*(YBS(KU)/DZ + EMU*(DXL**2/DZ - DZ)/6.0) + DXU*
     X (YBS(KL)/DZ + EMS(KL)*(DXU**2/DZ - DZ)/6.0)
      TALPU = (YBS(KU) - YBS(KL) + (EMU*DXL**2 - EMS(KL)*DXU**2)/
     X 2.0)/DZ + (EMS(KL) - EMU)*DZ/6.0
      GO TO 50
   80 SD = (SS2 - SP2)/(1.0 + SS2*SP2)
      TALPA = (SS2 + SP2)/(1.0 - SS2*SP2 + SQRT((1.0 + SS2**2)*(1.0 +
     X SP2**2)))
      GO TO 100
   90 SD = (TALPU - TALPL)/(1.0 + TALPU*TALPL)
  100 XA = (ZBP(K) + XL)/2.0
      YA = (YBP(K) + YL)/2.0
      T = SQRT((ZBP(K) - XL)**2 + (YL - YBP(K))**2)
      ANG = ((ATAN((TALPAL - TALPA)/(1.0 + TALPAL*TALPA)))/2.0)**2
      UK = (SQRT((XA - XAL)**2 + (YA - YAL)**2))/(1.0 - ANG/6.0*(1.0 -
     X ANG/20.0))
      U = U + UK
      TORS = TORS + UK/140.0*((43.0*TL + 27.0*T)*TL**2 + (27.0*TL +
     1 43.0*T)*T**2 + UK/6.0*(((97.0*TL + 70.0*T)*TL + 43.0*T**2)*SOL -
     2 ((43.0*TL + 70.0*T)*TL + 97.0*T**2)*SD + UK*(((16.0*TL + 8.0*T)*
```

```
     3 SDL - 13.0*(TL + T)*SD)*SDL + (8.0*TL + 16.0*T)*SD**2 + UK*
     4 (((SDL - SD)*SDL + SD**2)*(SDL - SD)))))
      XAL = XA
      YAL = YA
      TALPAL = TALPA
      TL = T
  110 SDL = SD
C ***        END CIRCLE INTEGRATIONS FOR T**3*DU
      SIN2A = SINKU*COSKL - SINKL*COSKU
      COS2A = COSKU*COSKL + SINKL*SINKU
      UK = RLE*(1.0 - SIN2A/SQRT(2.0*(1.0 + COS2A)))
      U = U + UK
      TORS = TORS + RLE**4*((3.1415927 - ARSIN(SIN2A))*3.0 - SIN2A*(4.0
     X + COS2A))/8.0
      ICUT = 1
      CALL EDGES(ZBS(NPS),YBS(NPS),SS2,ZBP(NP),YBP(NP),SP2,UK,UK,UK,RTE,
     X UK,UK)
      SIN2A = SINKL*COSKU - SINKU*COSKL
      COS2A = COSKU*COSKL + SINKL*SINKU
      UK = RTE*(1.0 - SIN2A/SQRT(2.0*(1.0 + COS2A)))
      U = U + UK
      TORS = TORS + RTE**4*((3.1415927 - ARSIN(SIN2A))*3.0 - SIN2A*(4.0
     X + COS2A))/8.0
      RETURN
      END
```

```
      SUBROUTINE BCCORD(IS,NC,XCUT,YLE,ZLE,YTE,ZTE)
C *** PRINTOUT OF UNROTATED COORDINATES WITH HUB STACKING POINT REF.
      REAL INC, KIS, KM, KTS, MACH
      COMMON /VECTOR/
     1 BETAS(1,21), BMATL(1), BLADES(1), CHOKE(1), CHORDA(1), CHORDB(1),
     2 CHORDC(1), CPCO(6), DEV(1,21), IDEV(1), IGEO(1), IINC(1),
     3 ILOSS(1), IMAX(1), INC(1,21), ISTN(2), ITRANS(1), NOPT(1),
     4 NXCUT(1), PHI(1,21), PO(2,21), R(2,21), RBHUB(1), RBTIP(1),
     5 SLOPE(2,21), SOLID(1), TALE(1), TAMAX(1), TATE(1), TBLE(1),
     6 TBMAX(1), TBTE(1), TCLE(1), TCMAX(1), TCTE(1), TDLE(1), TDMAX(1),
     7 TDTE(1), TILT(1), TC(2,21), TRANS(1,21), VTH(2,21), VZ(2,21),
     8 Z(2,21), ZBHUB(1), ZBTIP(1), ZMAX(1,21)
      COMMON /SCALAR/
     1 BETA, CP, CPH2, CPH3, CPH4, CPH5, CPH6, CPP3, CPP4, CPP5, CPP6,
     2 CP1, CV, DCP, DF, DHC, DHCI, DLOSC, G, GAMMA, GJ, GJ2, GR1, GR2,
     3 GR3, GR4, GR5, H, I, ICONV, ICOUNT, IERROR, IIN, IPR, IROTOR, IR,
     4 IROW, ITER, IW, J, JM, MACH, NAB, NBROWS, NHUB,NROTOR,NSTN,NSTRM,
     5 NTIP, NTUPES, OMEGA, PI, POA1, PR, RADIAN, RF, RG, ROT,TL,TOA1,TU
      COMMON /BLADES/ DUM(35), ICL, DUMM(44)
      COMMON /PTS/ FSB(13)
      COMMON /LABEL/ TITLE(18)
      DIMENSION XCUT(25), YCP(14,3), YCS(14,3), YLE(25), YTE(25),
     1 ZC(28,3), ZLE(25), ZTE(25)
      EQUIVALENCE (JL,ICL)
      J = 1
      JL = 2
      IP = 1
      IC = 1
   10 IF (IP.NE.1) GO TO 30
      WRITE (IW,2000) (TITLE(IJ),IJ=1,18)
```

```
 30 DO 40 K=1,13
    CALL INTERP(XCUT(J),1,K,YCS(K,IC),ZC(K,IC))
 40 CALL INTERP(XCUT(J),2,K,YCP(K,IC),ZC(K+14,IC))
    IF (IC.NE.3) GO TO 80
    JS = J - 2
    JF = J
    WRITE (IW,2020) (J,XCUT(J),J=JS,JF)
 60 DO 70 K=1,13
 70 WRITE (IW,2030) FSP(K), (ZC(K,IJ), YCS(K,IJ), ZC(K+14,IJ),
   1 YCP(K,IJ),IJ=1,IC)
    WRITE (IW,2040) (ZLE(J),YLE(J),J=JS,JF)
    WRITE (IW,2050) (ZTE(J),YTE(J),J=JS,JF)
    IC = 0
    IP = IP + 1
    IF (IP.GT.2) IP = 1
 80 IF (J.EQ.NC) GO TO 100
    IC = IC + 1
    J = J + 1
    IF (IC.EQ.1) GO TO 10
    GO TO 30
100 IF (IC.EQ.0) RETURN
    JF = NC
    IF (IC.NE.2) GO TO 110
    JS = J - 1
    WRITE (IW,2015) JS, XCUT(JS), NC, XCUT(NC)
    GO TO 60
110 WRITE (IW,2010) NC, XCUT(NC)
    JS = JF
    GO TO 60
2000 FORMAT (1H1 /// 1X,58H** BLADE SECTION COORDINATES IN TURBOMACHINE
   1 ORIENTATION -   ,18A4 )
2010 FORMAT (// 4X,6HFRACT.,  4X,7HSECTION,I3,12H FOR XCUT OF,F8.4,
   1 4H IN.,2X  / 5X,2HOF,      6X,15HSUCTION SURFACE,4X,16HPRESSURE SU
   2RFACE  / 4X,5HSURF.,   7X,1HZ,8X,1HY,9X,1HZ,8X,1HY,4X  /      14X,
   3 5H(IN.),4X,5H(IN.),5X,5H(IN.),4X,5H(IN.)    // )
2015 FORMAT (// 4X,6HFRACT.,2(4X,7HSECTION,I3,12H FOR XCUT OF,F8.4,
   1 4H IN.,2X) / 5X,2HOF,1X,2(5X,15HSUCTION SURFACE,4X,16HPRESSURE SU
   2RFACE) / 4X,5HSURF.,2(7X,1HZ,8X,1HY,9X,1HZ,8X,1HY,4X) / 7X,2(7X,
   3 5H(IN.),4X,5H(IN.),5X,5H(IN.),4X,5H(IN.) ) // )
2020 FORMAT (// 4X,6HFRACT.,3(4X,7HSECTION,I3,12H FOR XCUT OF,F8.4,
   1 4H IN.,2X) / 5X,2HOF,1X,3(5X,15HSUCTION SURFACE,4X,16HPRESSURE SU
   2RFACE) / 4X,5HSURF.,3(7X,1HZ,8X,1HY,9X,1HZ,8X,1HY,4X) / 7X,3(7X,
   3 5H(IN.),4X,5H(IN.),5X,5H(IN.),4X,5H(IN.) ) // )
2030 FORMAT (4X,F4.2,2X,3(2F9.4,1X,2F9.4,3X))
2040 FORMAT (/4X,18HL.E. CIRCLE CENTER,7X,2F9.4,2(22X,2F9.4))
2050 FORMAT (4X,18HT.E. CIRCLE CENTER,7X,2F9.4,2(22X,2F9.4))
    END
```

*** INPUT DATA FOR COMPRESSOR DESIGN PROGRAM ***

A ROTOR TEST CASE

THE SPECIFIC HEAT POLYNOMIAL IS IN THE FOLLOWING FORM

[illegible] = [illegible].23747E+00 + [illegible].21362E-04*T + -0.87791E-07*T**2 + 0.13991E-09*T**3 + -0.78056E-13*T**4 + 0.15043E-16*T**5

NUMBER OF SPECIES	MOLECULAR WEIGHT	ROTATIONAL SPEED (RPM)	TIP AXIAL STACK LOC. (INCHES)	TIP RADIAL STACK LOC. (INCHES)	HUB AXIAL STACK LOC. (INCHES)	HUB RADIAL STACK LOC. (INCHES)	NUMBER OF BLADES	TIP SOLIDITY	STACK LINE TANG. TILT (DEGREES)
11	28.970	1[illegible]042.8	6.8400	10.0000	6.8400	5.5300	38.0	1.3000	0.

* POLYNOMIAL CONSTANTS FOR THE FOLLOWING FUNCTIONS OF RADIUS WITH TIP = 0 AND HUB = 1 *

	L.E. RADIUS/CHORD	T.E. RADIUS/CHORD	MAX. THICKNESS/CHORD	CHORD/TIP CHORD
CONSTANT	0.0060	0.0060	0.0340	
LINEAR	0.0090	0.0090	0.0490	-0.
QUADRATIC	-0.	-0.	-0.	-0.
CUBIC	-0.	-0.	-0.	-0.

* INPUT BLADE ELEMENT DEFINITION OPTIONS *

INCIDENCE ANGLE	DEVIATION ANGLE	TURNING RATE RATIO	TRANSITION POINT	MAX. THICKNESS POINT	CHOKE MARGIN	BLADE MATERIAL DENSITY LB/(IN)**3
[illegible]	MODIFIED CARTERS	OPTIMUM	S.S. SHOCK	TABLE (L.E.REF.)	NONE	0.

* TABLE OF BLADE SECTION DESIGN VARIABLES INPUT *

(VARIABLES CONTROLLED BY OTHER OPTIONS WILL APPEAR AS MINUS ZEROS IN THE TABLE.)

STREAMLINE NUMBER	INCIDENCE ANGLE (DEGREES)	DEVIATION ANGLE (DEGREES)	INLET/OUTLET TURNING RATE RATIO	TRANSITION/CHORD LOCATION	MAX. THICKNESS LOCATION/CHORD
1	-0.	-0.	-0.	-0.	0.5000
2	-0.	-0.	-0.	-0.	0.5000
3	-0.	-0.	-0.	-0.	0.5000
4	-0.	-0.	-0.	-0.	0.5000
5	-0.	-0.	-0.	-0.	0.5000
6	-0.	-0.	-0.	-0.	0.5000
7	-0.	-0.	-0.	-0.	0.5000
8	-0.	-0.	-0.	-0.	0.5000
9	-0.	-0.	-0.	-0.	0.5000
10	-0.	-0.	-0.	-0.	0.5000
11	-0.	-0.	-0.	-0.	0.5000

** INLET STATION INPUT DATA **

STREAMLINE NUMBER	STREAMLINE RADIUS (INCHES)	AXIAL LOCATION (INCHES)	AXIAL VELOCITY (FT/SEC)	TANGENTIAL VELOCITY (FT/SEC)	STREAMLINE SLOPE (DEGREES)	STAGNATION TEMPERATURE (DEG.R.)	STAGNATION PRESSURE (PSIA)
1	9.4040	6.3460	629.890	0.	-5.16000	610.44	23.476
2	9.0900	6.3220	641.430	0.	-3.81000	607.13	23.532
3	8.7690	6.2980	648.830	0.	-2.45000	605.15	23.550
4	8.4380	6.2730	652.850	0.	-1.07000	603.38	23.559
5	8.0950	6.2470	653.440	0.	0.37000	602.65	23.539
6	7.7350	6.2180	650.720	0.	1.87000	601.99	23.511
7	7.3550	6.1860	644.380	0.	3.51000	601.41	23.469
8	6.9480	6.1500	632.970	0.	5.35000	600.90	23.408
9	6.5040	6.1080	612.590	0.	7.41000	601.28	23.301
10	6.0040	6.0570	576.300	0.	9.71000	601.67	23.090
11	5.4030	6.0120	484.820	0.	11.18000	599.88	22.735

** OUTLET STATION INPUT DATA **

STREAMLINE NUMBER	STREAMLINE RADIUS (INCHES)	AXIAL LOCATION (INCHES)	AXIAL VELOCITY (FT/SEC)	TANGENTIAL VELOCITY (FT/SEC)	STREAMLINE SLOPE (DEGREES)	STAGNATION TEMPERATURE (DEG.R.)	STAGNATION PRESSURE (PSIA)
1	9.3010	7.3760	521.320	419.420	-5.42000	700.96	35.759
2	9.0100	7.3980	529.570	413.660	-3.82000	693.64	35.759
3	8.7140	7.4200	533.240	417.210	-2.43000	689.56	35.759
4	8.4110	7.4440	535.250	423.340	-1.11000	686.07	35.759
5	8.0990	7.4720	536.050	437.560	0.20000	684.93	35.759
6	7.7730	7.5040	536.870	454.330	1.52000	683.99	35.759
7	7.4330	7.5400	539.100	474.480	2.93000	683.32	35.759
8	7.0780	7.5810	541.670	499.060	4.47000	682.93	35.759
9	6.7020	7.6300	542.290	536.620	6.13000	684.79	35.759
10	6.2970	7.6870	543.600	588.760	7.86000	687.75	35.759
11	5.9650	7.7400	587.100	646.820	7.70000	687.97	35.759

*** PRINTOUT FOR EACH ITERATION ***

ITER	J	BETA1(J)	BETA2(J)	SKIC(J)	SKOC(J)	KIC(J)	KOC(J)	DM	DY	SINB	CZ	A
1	1	1.122965	1.035364	1.078972	0.962065	1.078591	0.961833	-0.0014941	-0.0016014	0.863464	-0.0029887	0.105966
1	2	1.103039	1.011423	1.054179	0.937387	1.053945	0.937133	-0.0016557	-0.0007175	0.849930	-.0033179	0.118244
1	3	1.084724	0.984042	1.030393	0.908321	1.030267	0.908175	-0.0016315	-0.0000015	0.834847	-0.0032733	0.130715
1	4	1.065851	0.953506	1.006895	0.877318	1.006854	0.877279	-0.0013791	0.0004974	0.818561	-0.0027689	0.143538
1	5	1.047765	0.914705	0.983499	0.836550	0.983507	0.836550	-0.0009571	0.0008301	0.798969	-.0019226	0.156804
1	6	1.029476	0.867904	0.959639	0.786910	0.959684	0.786868	-0.0003322	0.0009906	0.775330	-.0006669	0.1706[illegible]
1	7	1.010781	0.809204	0.935064	0.723906	0.935169	0.723733	0.0005841	0.0009570	0.745740	.0011717	0.185375
1	8	0.991916	0.735724	0.909902	0.643730	0.910026	0.643220	0.0020492	0.0006[illegible]93	0.707695	0.0041053	0.20[illegible]
1	9	0.974695	0.634764	0.865814	0.530192	0.885811	0.529333	0.0044997	0.0000328	0.653655	.0089365	0.218899
1	10	0.963043	0.490169	0.866431	0.364188	0.865705	0.362042	0.0082337	-0.0014[illegible]5	0.572271	.0165171	0.239800
1	11	0.992077	0.286107	0.886176	0.119859	0.878639	0.116873	0.0158352	-0.0039423	0.450722	.0314021	0.269275

C-3

ITER	J	BETA1(J)	BETA2(J)	SKIC(J)	SKOC(J)	KIC(J)	KOC(J)	DM	DY	SINB	DZ	A
2	1	1.122969	1.035357	1.078290	0.957334	1.078109	0.957006	-0.0003980	0.0003409	0.862768	-0.0007960	0.105945
2	2	1.103031	1.011410	1.053378	0.935906	1.053294	0.935503	-0.0001288	0.0002378	0.849729	-0.0002582	0.118215
2	3	1.084196	0.984091	1.029475	0.909443	1.029470	0.909155	0.0000621	0.0001039	0.835154	0.0001246	0.130699
2	4	1.065841	0.953552	1.005910	0.879078	1.005958	0.878939	0.0001057	0.0000444	0.819023	0.0002122	0.143524
2	5	1.047733	0.914757	0.982428	0.838258	0.982509	0.838250	0.0001130	0.0000249	0.799415	0.0002269	0.156772
2	6	1.029463	0.867933	0.958555	0.788492	0.958671	0.788598	0.0001092	-0.0000034	0.775750	0.0002192	0.170628
2	7	1.010775	0.809249	0.934022	0.725340	0.934223	0.725502	0.0000965	-0.0000587	0.746328	0.0001936	0.185237
2	8	0.991902	0.735773	0.909061	0.644947	0.909266	0.645600	0.0001027	-0.0001265	0.708766	0.0002056	0.200911
2	9	0.974571	0.634834	0.885608	0.530739	0.885604	0.533106	0.0001187	-0.0002451	0.656150	0.0002372	0.218261
2	10	0.962807	0.490325	0.868124	0.363638	0.867178	0.371345	-0.0001271	-0.0004973	0.583578	-0.0002534	0.238352
2	11	0.991121	0.286311	0.892363	0.115524	0.885434	0.157319	-0.0023871	-0.0023909	0.487182	-0.0047338	0.264145

ITER	J	BETA1(J)	BETA2(J)	SKIC(J)	SKOC(J)	KIC(J)	KOC(J)	DM	DY	SINB	DZ	A
3	1	1.122953	1.035432	1.078273	0.957392	1.078056	0.957064	0.0000178	-0.0000082	0.862721	0.0000356	0.105461
3	2	1.103029	1.011443	1.053381	0.935909	1.053281	0.935499	0.0000049	-0.0000155	0.849688	0.0000098	0.118240
3	3	1.084211	0.984269	1.029497	0.909403	1.029475	0.909104	-0.0000055	-0.0000166	0.835122	-0.0000110	0.130724
3	4	1.065860	0.953519	1.005940	0.879030	1.005976	0.878863	-0.0000110	-0.0000120	0.819010	-0.0000222	0.143563
3	5	1.047750	0.914723	0.982461	0.838211	0.982530	0.838203	-0.0000130	-0.0000128	0.799400	-0.0000260	0.156825
3	6	1.029479	0.867897	0.958592	0.788446	0.958736	0.788552	-0.0000146	-0.0000158	0.775750	-0.0000334	0.170697
3	7	1.010795	0.809208	0.934070	0.725291	0.934273	0.725538	-0.0000237	-0.0000179	0.746334	-0.0000476	0.185320
3	8	0.991934	0.735710	0.909258	0.644739	0.909472	0.645400	-0.0000470	-0.0000019	0.708796	-0.0000741	0.201005
3	9	0.974649	0.634712	0.886195	0.530484	0.886191	0.532466	-0.0000986	0.0000487	0.656246	-0.0001971	0.218373
3	10	0.963053	0.490129	0.869780	0.363160	0.868804	0.368932	-0.0001152	0.0002922	0.583192	-0.0002296	0.238621
3	11	0.992341	0.285963	0.897587	0.115240	0.893158	0.143341	0.0002952	0.0017152	0.482626	0.0005955	0.265632

ITER	J	BETA1(J)	BETA2(J)	SKIC(J)	SKOC(J)	KIC(J)	KOC(J)	DM	DY	SINB	DZ	A
4	1	1.122951	1.035431	1.078272	0.957391	1.078063	0.957068	-0.0000012	-0.0000002	0.862727	[illegible]	[illegible]
4	2	1.103028	1.011442	1.053375	0.935911	1.053276	0.935501	0.0000002	-0.0000000	0.849686	0.0000004	[illegible]
4	3	1.084210	0.984070	1.029485	0.909409	1.029464	0.909110	0.0000018	0.0000007	0.835121	0.0000036	0.130724
4	4	1.065860	0.953521	1.005922	0.879038	1.005958	0.878892	0.0000031	0.0000012	0.819008	0.0000062	0.143556
4	5	1.047750	0.914724	0.982436	0.838222	0.982537	0.838214	0.0000039	0.0000008	0.799405	0.0000079	0.156815
4	6	1.029480	0.867895	0.958561	0.788459	0.958676	0.788565	0.0000039	-0.0000002	0.775785	0.0000079	0.170684
4	7	1.010797	0.805211	0.934035	0.725307	0.934239	0.725551	0.0000057	0.000001	0.746325	0.0000114	[illegible]
4	8	0.991940	0.735716	0.909223	0.644759	0.909438	0.645411	0.0000073	0.0000039	0.708776	0.0000146	[illegible]
4	9	0.974662	0.634730	0.886167	0.530514	0.886163	0.532481	0.0000108	0.0000111	0.656207	0.0000215	0.218363
4	10	0.963052	0.490163	0.869741	0.363200	0.864741	0.369323	0.0000295	-0.0000162	0.579891	0.0000589	[illegible]
4	11	0.992119	0.28607[illegible]	0.897269	0.115374	0.889284	0.143022	0.0001511	-0.0001806	0.480024	[illegible]	[illegible]

ITER	J	BETA1(J)	BETA2(J)	SKIC(J)	SKOC(J)	KIC(J)	KOC(J)	DM	DY	SINB	DZ	A
5	1	1.122952	1.035431	1.078272	0.957391	1.078063	0.957068	0.0000000	0.0000000	.862727	.0000001	[illegible]
5	2	1.103028	1.011440	1.053376	0.935911	1.053277	0.935500	0.0000000	0.0000002	.849686	.0000001	0.118236
5	3	1.084210	0.984070	1.029487	0.909408	1.029466	0.909109	-0.0000000	0.0000005	0.835121	-.0000000	0.130723
5	4	1.065860	0.953520	1.005925	0.879037	1.005961	0.878890	-0.0000001	0.0000006	0.819008	-.0000002	0.143554
5	5	1.047750	0.914724	0.982441	0.838220	0.982511	0.838212	-0.0000002	0.0000007	0.799405	[illegible]	0.156813
5	6	1.029480	0.867899	0.958567	0.788457	0.959681	0.788563	-0.0000002	0.0000008	.775785	-.0000005	0.170681
5	7	1.010796	0.809210	0.934040	0.725304	0.934244	0.725549	-0.0000000	0.0000011	.746326	-.0000001	[illegible]
5	8	0.991939	0.735716	0.909229	0.644756	0.909444	0.645411	0.0000004	0.0000013	.708777	.0000009	0.200987
5	9	0.974660	0.634728	0.886173	0.530510	0.886169	0.532493	0.0000004	-0.0000004	.656204	[illegible]	0.218354
5	10	0.963049	0.490158	0.869739	0.363186	0.868746	0.369186	-0.0000118	-0.0000086	0.583047	-.0000235	0.238576
5	11	0.992076	0.286064	0.897224	0.115248	0.889369	0.144756	-0.0001110	-0.0001090	0.481438	-.0002201	0.265375

ITER	J	BETA1(J)	BETA2(J)	SKIC(J)	SKOC(J)	KIC(J)	KOC(J)	DM	DY	SINB	DZ	A
6	1	1.122952	1.035431	1.078272	0.957391	1.078063	0.957068	-0.0000000	0.0000000	0.862727	-0.0000001	0.105960
6	2	1.103028	1.01144[illegible]	1.053376	0.935911	1.053277	0.935500	-0.0000001	-0.0000001	0.849686	-0.0000002	0.118237
6	3	1.084210	0.984070	1.029487	0.909407	1.029466	0.909109	-0.0000002	-0.0000003	0.835121	-0.0000004	0.130724
6	4	1.065860	0.95352[illegible]	1.005926	0.879036	1.005962	0.878890	-0.0000003	-0.0000004	0.819008	-0.0000006	0.143556
6	5	1.047750	0.914724	0.982442	0.838220	0.982512	0.838211	-0.0000004	-0.0000005	0.799406	-0.0000009	0.156815
6	6	1.029480	0.867899	0.958568	0.788456	0.958683	0.788562	-0.0000005	-0.0000005	0.775786	-0.0000010	0.170684
6	7	1.010796	0.809213	0.934042	0.725304	0.934246	0.725549	-0.0000006	-0.0000006	0.746327	-0.0000012	0.185306
6	8	0.991939	0.735716	0.909231	0.644755	0.909446	0.645410	-0.0000008	-0.0000007	0.708778	-0.0000016	0.200991
6	9	0.974660	0.634728	0.886175	0.530509	0.886171	0.532489	-0.0000010	-0.0000010	0.656209	-0.0000020	0.218359
6	10	0.963054	0.490156	0.869745	0.363188	0.868754	0.369127	0.0000008	0.0000050	0.580024	0.0000016	0.238597
6	11	0.992125	0.286054	0.897269	0.115277	0.889464	0.144251	0.0000168	0.0000574	0.481287	0.0000133	0.2654[illegible]

ITER	J	BETA1(J)	BETA2(J)	SKIC(J)	SKOC(J)	KIC(J)	KOC(J)	DM	DY	SINB	DZ	A
7	1	1.122952	1.035431	1.078272	0.957391	1.078063	0.957068	0.0000000	0.0000001	0.862727	0.0000001	0.105960
7	2	1.103028	1.01144[illegible]	1.053376	0.935911	1.053277	0.935500	0.0000000	0.0000000	0.849686	0.0000001	0.118236
7	3	1.084210	0.984073	1.029487	0.909408	1.029466	0.909109	0.0000001	0.0000000	0.835121	0.0000001	0.130724
7	4	1.065960	0.953520	1.005925	0.879037	1.005961	0.878890	0.0000001	0.0000000	0.819008	0.000000[illegible]	0.1435[illegible]
7	5	1.047750	0.914724	0.982441	0.838220	0.982511	0.838212	0.0000002	0.0000001	0.799405	.0000004	0.156815
7	6	1.029480	0.867899	0.958567	0.788457	0.958682	0.788563	0.0000002	0.0000000	0.775785	0.0000004	0.170684
7	7	1.010796	0.809213	0.934040	0.725304	0.934244	0.725549	0.0000002	0.0000001	0.746326	0.0000005	0.1853[illegible]
7	8	0.991939	0.735716	0.909229	0.644756	0.909444	0.645411	0.0000002	-0.0000000	0.708777	0.0000005	0.20[illegible]
7	9	0.974660	0.634728	0.886173	0.530510	0.886169	0.532490	0.0000003	0.0000003	0.656209	0.0000007	0.218358
7	10	0.963053	0.490157	0.869743	0.363189	0.868750	0.369130	0.0000012	-0.0000006	0.580015	.0000025	0.238586
7	11	0.992115	0.286057	0.897257	0.115281	0.889431	0.144237	0.0000061	-0.0000066	0.481188	0.0000120	0.2554[illegible]

ITER	J	BETA1(J)	BETA2(J)	SKIC(J)	SKOC(J)	KIC(J)	KOC(J)	DM	DY	SINB	DZ	A
8	1	1.122952	1.035431	1.078272	0.957391	1.078063	0.957068	-0.0000001	-0.0000001	0.862727	-0.0000001	0.105960
8	2	1.103028	1.011440	1.053376	0.935911	1.053277	0.935500	-0.0000000	0.0000000	0.849686	-0.0000000	0.118236
8	3	1.084210	0.984073	1.029487	0.909407	1.029466	0.909109	0.0000000	0.0000000	0.835121	0.0000000	0.130723
8	4	1.065860	0.953520	1.005925	0.879036	1.005961	0.878890	-0.0000000	0.0000000	0.819008	-0.0000001	0.143555
8	5	1.047750	0.914724	0.982441	0.838220	0.982511	0.838212	-0.0000000	0.0000000	0.799406	-0.0000001	0.156815
8	6	1.029480	0.867899	0.958567	0.788457	0.958682	0.788563	-0.0000000	0.0000000	0.775786	-0.0000000	0.170694
8	7	1.010796	0.809213	0.934041	0.725304	0.934245	0.725549	-0.0000000	0.0000001	0.746326	-0.0000000	0.185305
8	8	0.991939	0.735716	0.909229	0.644755	0.909444	0.645411	-0.0000000	-0.0000000	0.708777	-0.0000000	0.200990
8	9	0.974660	0.634728	0.886173	0.530510	0.886169	0.532490	-0.0000000	-0.0000001	0.656209	-0.0000001	0.218358
8	10	0.963053	0.490157	0.869743	0.363188	0.868751	0.369135	-0.0000005	-0.0000[illegible]	0.580027	-0.0000004	0.238565
8	11	0.992113	0.286057	0.897256	0.115[illegible]	0.889433	0.144295	-0.0000037	-0.0000038	0.481236	-0.0000074	0.265426

*** TERMINAL CALCULATIONS WITH THE STACKED BLADE ***

** INPUT DATA CORRECTED TO THE BLADE EDGES **

INLET				OUTLET			
STREAMLINE RADIUS (INCHES)	AXIAL LOCATION (INCHES)	AXIAL VELOCITY (FT/SEC)	TANGENTIAL VELOCITY (FT/SEC)	STREAMLINE RADIUS (INCHES)	AXIAL LOCATION (INCHES)	AXIAL VELOCITY (FT/SEC)	TANGENTIAL VELOCITY (FT/SEC)
9.4040	6.3456	629.914	0.	9.3008	7.3778	521.221	419.428
9.0990	6.3217	641.449	0.	9.0100	7.3984	529.547	413.661
8.7690	6.2977	648.853	0.	8.7140	7.4208	533.202	417.212
9.4390	6.2732	652.936	0.	8.4110	7.4444	535.232	423.343
9.0950	6.2467	653.462	0.	8.0990	7.4724	536.029	437.560
7.7350	6.2181	650.715	0.	7.7730	7.5039	536.875	454.330
7.3550	6.1863	644.360	0.	7.4330	7.5401	539.094	474.480
6.9490	6.1503	632.941	0.	7.0780	7.5809	541.677	499.061
6.5339	6.1075	612.630	0.	6.7019	7.6296	542.316	536.624
6.0040	6.0571	576.290	0.	6.2970	7.6869	543.605	588.762
5.4031	6.0125	484.793	0.	5.8649	7.7395	587.106	646.827

L.E.RAD. /CHORD	MAX.TH. /CHORD	T.E.RAD. /CHORD	MAX.TH PT.LOC. /CHORD	TRAN.PT. LOCATION /CHORD	SEGMENT IN/OUT TURN.RATE	1ST SEG. S.S.CAM. (DEG)	BLD.SET ANGLE (DEG)	ELEMENT SOLIDITY	AERO. CHORD (IN.)	LOC.OF MAX CAMB.PT. /CHORD	LOCAL BLADE FORCES RADIUS (IN.)	FOR.AXIAL (LBS/IN)	TANG. (LBS/IN)
0.0060	0.0340	0.0060	0.5000	0.6653	0.2933	5.98	59.33	1.3000	2.0133	0.6562	9.352	13.7117	-8.2505
0.0067	0.0378	0.0068	0.5000	0.6350	0.3116	6.01	57.92	1.3429	2.0096	0.6452	9.050	13.1524	-8.0700
0.0074	0.0418	0.0075	0.5000	0.6042	0.3483	6.20	56.41	1.3898	2.0087	0.6243	8.741	12.5357	-7.9760
0.0082	0.0459	0.0083	0.5000	0.5728	0.4017	6.50	54.80	1.4417	2.0083	0.6018	8.424	11.5185	-7.8669
0.0089	0.0500	0.0091	0.5000	0.5400	0.4824	7.04	52.89	1.4999	2.0081	0.5771	8.097	11.2370	-7.8312
0.0098	0.0544	0.0100	0.5000	0.5056	0.5798	7.74	50.69	1.5665	2.0084	0.5534	7.754	10.5255	-7.7726
0.0106	0.0591	0.0109	0.5000	0.4695	0.6868	8.64	48.39	1.6435	2.0094	0.5333	7.394	9.7686	-7.7180
0.0115	0.0641	0.0118	0.5000	0.4313	0.7928	9.73	44.97	1.7347	2.0116	0.5173	7.013	8.5541	-7.6366
0.0125	0.0695	0.0128	0.5000	0.3903	0.8901	11.22	40.95	1.8467	2.0162	0.5056	6.603	7.9838	-7.5678
0.0136	0.0756	0.0139	0.5000	0.3462	0.9641	13.16	35.68	1.9921	2.0259	0.4980	6.150	6.7686	-7.3981
0.0150	0.0830	0.0150	0.5000	0.3042	1.0000	15.82	29.90	2.2035	2.0527	0.4931	5.634	5.3788	-7.5650

INC. ANGLE (DEG)	S.S.INC. ANGLE (DEG)	IN.FLOW ANGLE (DEG)	IN.BLADE ANGLE (DEG)	IN.ANGLE ON CONE (DEG)	DEV. ANGLE (DEG)	OUT.FLOW ANGLE (DEG)	OUT.BLADE ANGLE (DEG)	OUT.ANG. ON CONE (DEG)	TRAN.PT. BL.ANGLE (DEG)	SP.LOC. AS FRACT OF S.S.	COV.CHAN. AS FRACT OF S.S.	MIN.CHK. AREA MARGIN	MIN.CHK. PT.LOC.IN COV.CHAN.
2.56	-0.00	64.34	61.78	61.77	4.47	59.33	54.85	54.84	59.27	0.6666	0.3334	0.0399	0.3884
2.84	-0.00	63.20	60.35	60.35	4.33	57.95	53.62	53.60	57.96	0.6362	0.3638	0.0315	0.3800
3.14	-0.00	62.12	58.99	58.98	4.28	56.38	52.11	52.09	56.58	0.6052	0.3946	0.0239	0.3642
3.43	-0.00	61.07	57.64	57.64	4.27	54.63	50.37	50.36	55.09	0.5734	0.426[illegible]	0.0190	0.3398
3.74	-0.00	60.03	56.29	56.29	4.38	52.41	48.03	48.03	53.30	0.5401	0.4[illegible]	0.0161	0.2933
4.06	-0.00	58.98	54.92	54.93	4.55	49.73	45.18	45.19	51.30	0.5[illegible]53	0.4547	0.0165	0.2443
4.40	-0.00	57.91	53.52	53.53	4.81	46.36	41.56	41.57	49.01	0.4685	0.5[illegible]1	0.0180	0.1988
4.74	-0.	56.83	52.10	52.11	5.21	42.15	36.94	36.98	46.45	0.4296	0.570[illegible]	0.0225	0.1502
5.07	0.00	55.84	50.77	50.77	5.97	36.37	30.41	30.51	43.46	0.3874	0.6121	0.0334	0.[illegible]744
5.35	-0.00	55.18	49.83	49.78	7.27	28.08	20.81	21.15	40.19	0.3433	0.6567	0.0498	0.0067
5.43	0.00	56.84	51.41	50.96	9.78	16.39	6.6[illegible]	8.27	19.07	0.3714	0.65[illegible]	.1200	0.

** BLADE SECTION PROPERTIES OF A ROTOR TEST CASE

NUMBER OF BLADES = 38.0 AXIAL LOCATION OF STACKING LINE IN COMPRESSOR = 6.840 IN.

BLADE NO.	SECTION RAD. LOC. (IN.)	STACKING POINT COORDINATES L (IN.)	STACKING POINT COORDINATES H (IN.)	SECTION SETTING ANGLE (DEG.)	BLADE SECTION C.G. COORDINATES L (IN.)	BLADE SECTION C.G. COORDINATES H (IN.)	SECTION AREA (IN.)**2	MOMENTS OF INERTIA THROUGH C.G. IMIN (IN.)**4	MOMENTS OF INERTIA THROUGH C.G. IMAX (IN.)**4	IMAX SETTING ANGLE (DEG.)	SECTION TORSION CONSTANT (IN.)**4	SECTION TWIST STIFFNESS (IN.)**6
1	[illegible]	0.9965	.0223	60.948	0.9965	0.0243	0.10312	0.000031	0.02657	60.146	0.000108	0.007107
2	[illegible]	0.9976	.0247	59.369	0.9975	0.0247	0.10819	0.000035	0.02789	59.561	0.000125	0.007457
3	[illegible]	0.9993	.0312	58.170	0.9993	0.0312	0.11830	0.000045	0.03052	58.350	0.000161	0.008155
4	[illegible]	1.0009	.0335	56.92[illegible]	1.0009	0.0335	0.12840	0.000058	0.03314	57.094	0.000208	0.008851

SECTION NO. 1 COORDINATES L (IN.)	HP (IN.)	HS (IN.)	SECTION NO. 2 COORDINATES L (IN.)	HP (IN.)	HS (IN.)	SECTION NO. 3 COORDINATES L (IN.)	HP (IN.)	HS (IN.)	SECTION NO. 4 COORDINATES L (IN.)	HP (IN.)	HS (IN.)
0.	0.0114	0.0114	0.	0.0124	0.0124	0.	0.0135	0.0135	.	0.0146	0.0146
0.0114	-0.	0.0231	0.0124	-0.	0.0247	0.0135	-0.0000	0.0270	0.0146	-0.0000	0.0293
0.1000	-0.0002	0.0301	0.1000	-0.0004	0.0321	0.1000	-0.0006	0.0367	0.1000	-0.0007	0.0375
0.2000	-0.0003	0.0381	0.2000	-0.0007	0.0381	0.2000	-0.0012	0.0426	0.2000	-0.0014	0.0460
0.3000	-0.0005	0.0444	0.3000	-0.0010	[illegible]	0.3000	-0.0018	.0497	0.3000	.0020	0.0536
0.4000	-0.0005	0.0504	0.4000	-0.0013	0.0492	0.4000	-0.0022	0.0559	0.4000	0.0025	0.0603
0.5000	-0.0005	[illegible]	.5000	-0.0014	0.0554	0.5000	-0.0025	0.0609	.5000	-0.0029	0.0658
0.6000	-0.0004	[illegible]	0.6000	-0.0014	0.0611	0.6000	-0.0027	0.0656	.6000	-0.0030	0.0707
0.7000	-0.0003	0.0622	0.7000	-0.0013	0.0641	.7000	-0.0027	0.0688	.7000	-0.0031	0.0743
0.8000	0.0001	0.0644	0.8000	-0.0011	0.0663	0.8000	[illegible]	0.0716	.8000	0.0029	0.0774
0.9000	0.0005	0.0663	0.9000	-0.0007	[illegible]	0.9000	[illegible]	0.0732	.9000	-0.0025	0.0791
1.0000	0.0011	0.0674	1.0000	-0.0001	[illegible]	1.0000	[illegible]	.0744	1.0000	-0.0019	0.0805
1.1000	0.0017	0.0677	1.1000	0.0007	[illegible]	1.1000	-0.0007	0.0744	1.1000	-0.0010	0.0805
1.2000	0.0024	0.0676	1.2000	0.0017	[illegible]	1.2000	[illegible]	0.0741	1.2000	0.0001	0.0801
1.3000	0.0041	0.0659	1.3000	0.0031	0.0678	1.3000	0.0017	0.0727	1.3000	.0012	0.0783
1.4000	0.0057	0.0638	1.4000	0.0041	0.0657	1.4000	0.0027	0.0702	1.4000	.0021	0.0755
1.5000	0.0060	0.0608	1.5000	0.0048	0.0621	1.5000	0.0034	0.0660	1.5000	0.0026	0.0708
1.6000	0.0060	0.0557	1.6000	0.0055	0.0572	1.6000	0.0035	0.0606	1.6000	.0027	0.0652
1.7000	0.0055	0.0494	1.7000	0.0046	0.0512	1.7000	0.0032	0.0544	1.7000	0.0025	0.0578
1.8000	0.0043	0.0417	1.8000	0.0036	0.0431	1.8000	0.0026	0.0459	1.8000	.0020	0.0491
1.9000	0.0024	0.0326	1.9000	0.0021	0.0338	1.9000	0.0014	0.0365	1.9000	0.0011	0.0394
1.9956	0.0000	0.0224	1.9949	0.0000	0.0247	1.9934	0.0000	0.0264	1.9920	.0000	0.0291
2.0000	0.0009	0.0214	2.0000	0.0012	[illegible]	2.0000	0.0018	0.0246	2.0000	0.0024	[illegible]
2.0067	0.0112	0.01[illegible]	2.0067	0.0116	0.0118	2.0066	0.0132	0.0132	2.0065	.0145	[illegible]

** BLADE SECTION PROPERTIES OF A ROTOR TEST CASE

NUMBER OF BLADES = 38.0 AXIAL LOCATION OF STACKING LINE IN COMPRESSOR = 6.840 IN.

BLADE NO.	SECTION RAD. LOC. (IN.)	STACKING POINT COORDINATES L (IN.)	STACKING POINT COORDINATES H (IN.)	SECTION SETTING ANGLE (DEG.)	BLADE SECTION C.G. COORDINATES L (IN.)	BLADE SECTION C.G. COORDINATES H (IN.)	SECTION AREA (IN.)**2	MOMENTS OF INERTIA THROUGH C.G. IMIN (IN.)**4	MOMENTS OF INERTIA THROUGH C.G. IMAX (IN.)**4	IMAX SETTING ANGLE (DEG.)	SECTION TORSION CONSTANT (IN.)**4	SECTION TWIST STIFFNESS (IN.)**6
5	8.550	1.0022	.0363	55.645	1.0022	[illegible]	0.13850	[illegible]	0.03576	[illegible]	[illegible]	[illegible]
6	8.300	1.0035	.0397	54.286	1.0035	0.0397	0.14861	[illegible]	[illegible]	[illegible]	[illegible]	[illegible]
7	8.050	1.0047	.0445	52.783	1.0047	0.0445	0.15871	0.000115	[illegible]	[illegible]	[illegible]	[illegible]
8	7.800	1.0058	.0500	51.188	1.0058	.0500	0.16880	0.000147	0.04359	51.313	0.00047[illegible]	[illegible]

SECTION NO. 5 COORDINATES L (IN.)	HP (IN.)	HS (IN.)	SECTION NO. 6 COORDINATES L (IN.)	HP (IN.)	HS (IN.)	SECTION NO. 7 COORDINATES L (IN.)	HP (IN.)	HS (IN.)	SECTION NO. [illegible] COORDINATES L (IN.)	HP (IN.)	HS (IN.)
0.	0.0158	0.0158	0.	0.0169	0.0169	0.	0.0180	0.0180	0.	0.0192	0.0192
0.0158	-0.0000	0.0316	0.0169	-0.0000	0.0339	0.0180	0.0000	0.0362	0.0192	-0.	0.0386
0.1000	-0.0007	0.0403	0.1000	-0.0004	0.0434	0.1000	0.0000	0.0466	0.1000	0.0006	0.0501
0.2000	-0.0014	0.0496	0.2000	-0.0009	0.0536	0.2000	0.0000	0.0581	0.2000	0.0014	0.0629
0.3000	-0.0020	0.0579	0.3000	-0.0013	0.0627	0.3000	0.0001	0.0683	0.3000	0.0021	0.0744
0.4000	-0.0024	0.0652	0.4000	-0.0016	0.0708	0.4000	0.0002	0.0773	0.4000	0.0028	0.0846
0.5000	-0.0027	0.0711	0.5000	-0.0017	0.0774	0.5000	0.0004	0.0847	0.5000	0.0034	0.0929
0.6000	-0.0029	0.0765	0.6000	-0.0018	0.0833	0.6000	0.0007	0.0913	0.6000	0.0041	0.1003
0.7000	-0.0029	0.0804	0.7000	-0.0016	0.0876	0.7000	0.0010	0.0962	0.7000	0.0048	0.1058
0.8000	-0.0027	0.0838	0.8000	-0.0014	0.0913	0.8000	0.0015	0.1003	0.8000	0.0054	0.1104
0.9000	-0.0022	0.0857	0.9000	-0.0009	0.0934	0.9000	0.0021	0.1027	0.9000	0.0062	0.1131
1.0000	-0.0016	0.0872	1.0000	-0.0003	0.0950	1.0000	0.0028	0.1044	1.0000	0.0069	0.1150
1.1000	-0.0007	0.0875	1.1000	0.0007	0.0952	1.1000	0.0036	0.1046	1.1000	0.0076	0.1148
1.2000	0.0004	0.0868	1.2000	0.0016	0.0943	1.2000	0.0043	0.1034	1.2000	0.0080	0.1134
1.3000	0.0014	0.0845	1.3000	0.0022	0.0915	1.3000	0.0046	0.1001	1.3000	0.0079	0.1096
1.4000	0.0020	0.0813	1.4000	0.0026	0.0878	1.4000	0.0046	0.0958	1.4000	0.0075	0.1047
1.5000	0.0023	0.0761	1.5000	0.0027	0.0820	1.5000	0.0044	0.0893	1.5000	0.0069	0.0975
1.6000	0.0024	0.0700	1.6000	0.0025	0.0754	1.6000	0.0039	0.0819	1.6000	0.0059	0.0891
1.7000	0.0022	0.0621	1.7000	0.0022	0.0667	1.7000	0.0031	0.0724	1.7000	0.0047	0.0786
1.8000	0.0017	0.0533	1.8000	0.0016	0.0569	1.8000	0.0022	0.0616	1.8000	0.0032	0.0667
1.9000	0.0005	0.0425	1.9000	0.0009	0.0458	1.9000	0.0011	0.0493	1.9000	0.0016	0.0531
1.9906	-0.0000	0.0318	1.9891	0.	0.0345	1.9876	0.0000	0.0373	1.9861	0.0000	0.0400
2.0000	0.0031	0.0286	2.0000	0.0039	0.0305	2.0000	0.0047	0.0324	2.0000	0.0057	0.0341
2.0064	0.0158	0.0158	2.0063	0.0172	0.0172	2.0062	0.0185	0.0185	2.0060	0.0199	0.0199

** BLADE SECTION PROPERTIES OF A ROTOR TEST CASE

NUMBER OF BLADES = 38.0 AXIAL LOCATION OF STACKING LINE IN COMPRESSOR = 6.840 IN.

BLADE SECTION NO.	SECTION RAD. LOC. (IN.)	STACKING POINT COORDINATES L (IN.)	STACKING POINT COORDINATES H (IN.)	SECTION SETTING ANGLE (DEG.)	BLADE SECTION C.G. COORDINATES L (IN.)	BLADE SECTION C.G. COORDINATES H (IN.)	SECTION AREA (IN.)**2	MOMENTS OF INERTIA THROUGH C.G. IMIN (IN.)**4	MOMENTS OF INERTIA THROUGH C.G. IMAX (IN.)**4	IMAX SETTING ANGLE (DEG.)	SECTION TORSION CONSTANT (IN.)**4	SECTION TWIST STIFFNESS (IN.)**6
9	7.550	1.0068	0.0567	49.449	1.0068	0.0567	0.17892	0.000173	0.04621	49.562	0.000560	0.012296
10	7.300	1.0078	0.0646	47.555	1.0078	0.0646	0.18909	0.000214	0.04883	47.662	0.0006[illegible]	0.012981
11	7.050	1.0089	0.0743	45.484	1.0089	0.0743	0.19936	0.000267	0.05146	45.595	0.000773	0.013665
12	6.800	1.0100	0.0869	43.135	1.0100	0.0869	0.20979	0.000341	0.05414	43.269	0.000899	0.014356

SECTION NO. 9 COORDINATES L (IN.)	HP (IN.)	HS (IN.)	SECTION NO. 10 COORDINATES L (IN.)	HP (IN.)	HS (IN.)	SECTION NO. 11 COORDINATES L (IN.)	HP (IN.)	HS (IN.)	SECTION NO. 12 COORDINATES L (IN.)	HP (IN.)	HS (IN.)
0.	0.0203	0.0203	0.	0.0214	0.0214	0.	0.0225	0.0225	0.	0.0237	0.0237
0.0203	-0.	0.0409	0.0214	-0.	0.0432	0.0225	0.0000	0.0456	0.0237	-0.	0.0481
0.1000	0.0015	0.0537	0.1000	0.0025	0.0576	0.1000	0.0039	0.0618	0.1000	0.0057	0.0666
0.2000	0.0032	0.0683	0.2000	0.0056	0.0742	0.2000	0.0086	0.0808	0.2000	0.0127	0.0885
0.3000	0.0048	0.0813	0.3000	0.0083	0.0890	0.3000	0.0128	0.0978	0.3000	0.0191	0.1082
0.4000	0.0063	0.0928	0.4000	0.0108	0.1021	0.4000	0.0167	0.1127	0.4000	0.0247	0.1256
0.5000	0.0076	0.1023	0.5000	0.0130	0.1129	0.5000	0.0200	0.1251	0.5000	0.0297	0.1400
0.6000	0.0088	0.1107	0.6000	0.0149	0.1224	0.6000	0.0229	0.1360	0.6000	0.0340	0.1527
0.7000	0.0099	0.1169	0.7000	0.0166	0.1295	0.7000	0.0254	0.1441	0.7000	0.0374	0.1621
0.8000	0.0109	0.1221	0.8000	0.0180	0.1354	0.8000	0.0274	0.1509	.8000	0.0403	0.1700
0.9000	0.0119	0.1255	0.9000	0.0192	0.1391	0.9000	0.0289	0.1551	0.9000	0.0423	0.1746

1.0000	0.0127	0.1272	1.0000	0.0200	0.1410	1.0000	0.0297	0.1571	1.0000	0.0431	0.1771
1.1000	0.0134	0.1267	1.1000	0.0203	0.1403	1.1000	0.0297	0.1562	1.1000	0.0430	0.1761
1.2000	0.0131	0.1250	1.2000	0.0199	0.1382	1.2000	0.0290	0.1538	1.2000	0.0420	0.1733
1.3000	0.0127	0.1206	1.3000	0.0190	0.1332	1.3000	0.0274	0.1481	1.3000	0.0399	0.1669
1.4000	0.0118	0.1150	1.4000	0.0176	0.1268	1.4000	0.0254	0.1409	1.4000	0.0368	0.1586
1.5000	0.0106	0.1068	1.5000	0.0156	0.1176	1.5000	0.0226	0.1305	1.5000	0.0327	0.1467
1.6000	0.0090	0.0975	1.6000	0.0132	0.1071	1.6000	0.0191	0.1184	1.6000	0.0276	0.1328
1.7000	0.0070	0.0857	1.7000	0.0103	0.0938	1.7000	0.0149	0.1033	1.7000	0.0216	0.1153
1.8000	0.0048	0.0724	1.8000	0.0070	0.0787	1.8000	0.0101	0.0861	1.8000	0.0146	0.0952
1.9000	0.0023	0.0572	1.9000	0.0033	0.0616	1.9000	0.0047	0.0665	1.9000	0.0066	0.0722
1.9844	0.0000	0.0429	1.9824	0.0000	0.0458	1.9799	0.0000	0.0489	1.9768	0.0000	0.0522
2.0000	0.0068	0.0358	2.0000	0.0083	0.0370	2.0000	0.0107	0.0376	2.0000	0.0148	0.0365
2.3057	0.0213	0.0213	2.0051	0.0227	0.0227	2.0041	0.0241	0.0241	2.0024	0.0257	0.0257

** BLADE SECTION PROPERTIES OF A ROTOR TEST CASE

NUMBER OF BLADES = 38.0 AXIAL LOCATION OF STACKING LINE IN COMPRESSOR = 6.840 IN.

BLADE SECTION NO.	RAD. LOC. (IN.)	STACKING POINT COORDINATES L (IN.)	H (IN.)	SECTION SETTING ANGLE (DEG.)	BLADE SECTION C.G. COORDINATES L (IN.)	H (IN.)	SECTION AREA (IN.)**2	MOMENTS OF INERTIA THROUGH C.G. IMIN (IN.)**4	IMAX (IN.)**4	IMAX SETTING ANGLE (DEG.)	SECTION TORSION CONSTANT (IN.)**4	SECTION TWIST STIFFNESS (IN.)**6
13	6.550	1.0111	0.1031	40.451	1.0111	0.1031	0.22047	0.000447	0.05688	40.641	0.001040	0.015053
14	6.300	1.0119	0.1226	37.426	1.0119	0.1226	0.23143	0.000597	0.05965	37.701	0.001199	0.015746
15	6.075	1.0126	0.1430	34.537	1.0126	0.1430	0.24191	0.000787	0.06226	34.957	0.001363	0.016380
16	5.850	1.0132	0.1666	31.608	1.0132	0.1666	0.25318	0.001051	0.06502	32.252	0.001554	0.017023

SECTION NO. 13 COORDINATES L (IN.)	HP (IN.)	HS (IN.)	SECTION NO. 14 COORDINATES L (IN.)	HP (IN.)	HS (IN.)	SECTION NO. 15 COORDINATES L (IN.)	HP (IN.)	HS (IN.)	SECTION NO. 16 COORDINATES L (IN.)	HP (IN.)	HS (IN.)
0.	0.0248	0.0248	0.	0.0259	0.0259	0.	0.0269	0.0269	0.	0.0279	0.0279
0.0248	-0.	0.0506	0.0259	-0.	0.0533	0.0269	-0.	0.0558	0.0279	-0.	0.0587
0.0500	0.0026	0.0579	0.0500	0.0034	0.0615	0.0500	0.0040	0.0649	0.0500	0.0046	0.0686
0.1000	0.0080	0.0719	0.1000	0.0108	0.0780	0.1000	0.0136	0.0839	0.1000	0.0165	0.0904
0.1500	0.0131	0.0851	0.1500	0.0179	0.0935	0.1500	0.0227	0.1018	0.1500	0.0280	0.1110
0.2000	0.0180	0.0976	0.2000	0.0247	0.1083	0.2000	0.0314	0.1188	0.2000	0.0389	0.1304
0.2500	0.0227	0.1097	0.2500	0.0312	0.1224	0.2500	0.0397	0.1350	0.2500	0.0493	0.1490
0.3000	0.0272	0.1207	0.3000	0.0373	0.1354	0.3000	0.0476	0.1499	0.3000	0.0591	0.1661
0.3500	0.0314	0.1311	0.3500	0.0431	0.1476	0.3500	0.0550	0.1640	0.3500	0.0684	0.1824
0.4000	0.0353	0.1410	0.4000	0.0486	0.1593	0.4000	0.0620	0.1775	0.4000	0.0772	0.1978
0.4500	0.0390	0.1498	0.4500	0.0536	0.1696	0.4500	0.0685	0.1895	0.4500	0.0856	0.2119
0.5000	0.0424	0.1579	0.5000	0.0583	0.1792	0.5000	0.0746	0.2006	0.5000	0.0934	0.2249
0.5500	0.0456	0.1656	0.5500	0.0626	0.1882	0.5500	0.0802	0.2111	0.5500	0.1004	0.2369
0.6000	0.0485	0.1729	0.6000	0.0666	0.1968	0.6000	0.0853	0.2208	0.6000	0.1066	0.2478
0.6500	0.0512	0.1791	0.6500	0.0704	0.2042	0.6500	0.0898	0.2293	0.6500	0.1119	0.2573
0.7000	0.0536	0.1846	0.7000	0.0737	0.2108	0.7000	0.0939	0.2367	0.7000	0.1170	0.2659
0.7500	0.0557	0.1894	0.7500	0.0764	0.2162	0.7500	0.0975	0.2432	0.7500	0.1219	0.2738
0.8000	0.0574	0.1933	0.8000	0.0786	0.2209	0.8000	0.1006	0.2489	0.8000	0.1262	0.2808
0.8500	0.0588	0.1963	0.8500	0.0805	0.2244	0.8500	0.1032	0.2532	0.8500	0.1296	0.2861
0.9000	0.0600	0.1987	0.9000	0.0820	0.2273	0.9000	0.1052	0.2567	0.9000	0.1323	0.2903
0.9500	0.0608	0.2005	0.9500	0.0831	0.2295	0.9500	0.1067	0.2594	0.9500	0.1343	0.2936
1.0000	0.0613	0.2018	1.0000	0.0838	0.2311	1.0000	0.1077	0.2613	1.0000	0.1356	0.2960
1.0500	0.0614	0.2017	1.0500	0.0840	0.2311	1.0500	0.1080	0.2616	1.0500	0.1363	0.2966
1.1000	0.0612	0.2009	1.1000	0.0838	0.2304	1.1000	0.1079	0.2610	1.1000	0.1363	0.2963
1.1500	0.0606	0.1996	1.1500	0.0830	0.2290	1.1500	0.1071	0.2596	1.1500	0.1356	0.2950
1.2000	0.0597	0.1978	1.2000	0.0819	0.2269	1.2000	0.1057	0.2574	1.2000	0.1341	0.2928

1.2500	0.0584	0.1944	1.2500	0.0802	0.2232	1.2500	0.1038	0.2534	1.2500	0.1319	0.2886
1.3000	0.0568	0.1905	1.3000	0.0781	0.2188	1.3000	0.1012	0.2485	1.3000	0.1289	0.2834
1.3500	0.0548	0.1863	1.3500	0.0755	0.2136	1.3500	0.0980	0.2428	1.3500	0.1250	0.2770
1.4000	0.0525	0.1813	1.4000	0.0724	0.2078	1.4000	0.0941	0.2362	1.4000	0.1203	0.2696
1.4500	0.0498	0.1744	1.4500	0.0688	0.2002	1.4500	0.0896	0.2276	1.4500	0.1147	0.2601
1.5000	0.0468	0.1671	1.5000	0.0647	0.1918	1.5000	0.0844	0.2180	1.5000	0.1082	0.2492
1.5500	0.0434	0.1593	1.5500	0.0601	0.1826	1.5500	0.0785	0.2075	1.5500	0.1007	0.2371
1.6000	0.0396	0.1509	1.6000	0.0549	0.1726	1.6000	0.0718	0.1959	1.6000	0.0922	0.2237
1.6500	0.0355	0.1409	1.6500	0.0492	0.1608	1.6500	0.0644	0.1823	1.6500	0.0827	0.2077
1.7000	0.0310	0.1303	1.7000	0.0429	0.1482	1.7000	0.0561	0.1674	1.7000	0.0719	0.1902
1.7500	0.0261	0.1191	1.7500	0.0361	0.1348	1.7500	0.0471	0.1515	1.7500	0.0600	0.1713
1.8000	0.0209	0.1064	1.8000	0.0287	0.1194	1.8000	0.0371	0.1332	1.8000	0.0468	0.1492
1.8500	0.0152	0.0929	1.8500	0.0207	0.1031	1.8500	0.0263	0.1136	1.8500	0.0322	0.1253
1.9000	0.0092	0.0787	1.9000	0.0120	0.0857	1.9000	0.0145	0.0923	1.9000	0.0160	0.0989
1.9500	0.0028	0.0631	1.9500	0.0027	0.0665	1.9500	0.0016	0.0688	1.9500	0.0000	0.0692
1.9725	0.0000	0.0559	1.9669	0.0000	0.0598	1.9600	0.0000	0.0639	1.9506	0.0000	0.0689
1.9998	0.0272	0.0272	1.9957	0.0288	0.0288	1.9903	0.0302	0.0302	1.9823	0.0317	0.0317

** BLADE SECTION PROPERTIES OF A ROTOR TEST CASE

NUMBER OF BLADES = 38.0 AXIAL LOCATION OF STACKING LINE IN COMPRESSOR = 6.84C IN.

BLADE SECTION NO.	RAD. LOC. (IN.)	STACKING POINT COORDINATES L (IN.)	STACKING POINT COORDINATES H (IN.)	SECTION SETTING ANGLE (DEG.)	BLADE SECTION C.G. COORDINATES L (IN.)	BLADE SECTION C.G. COORDINATES H (IN.)	SECTION AREA (IN.)**2	MOMENTS OF INERTIA THROUGH C.G. IMIN (IN.)**4	MOMENTS OF INERTIA THROUGH C.G. IMAX (IN.)**4	IMAX SETTING ANGLE (DEG.)	SECTION TORSION CONSTANT (IN.)**4	SECTION TWIST STIFFNESS (IN.)**6
17	5.600	1.0132	0.1976	28.417	1.0132	0.1976	0.26681	0.001476	0.06828	29.425	0.001803	0.017719
18	5.350	1.0115	0.2346	25.397	1.0115	0.2346	0.28179	0.002109	0.07168	26.910	0.002100	0.018329
19	5.530	1.0130	0.2073	27.550	1.0130	0.2073	0.27087	0.001628	0.06922	28.685	0.001881	0.017902

SECTION NO. 17 COORDINATES L (IN.)	HP (IN.)	HS (IN.)	SECTION NO. 18 COORDINATES L (IN.)	HP (IN.)	HS (IN.)	SECTION NO. 19 COORDINATES L (IN.)	HP (IN.)	HS (IN.)
0.	0.0292	0.0292	0.	0.0305	0.0305	0.	0.0295	0.0295
0.0292	-0.	0.0622	0.0305	-0.	0.0663	0.0295	-0.	0.0633
0.0500	0.0051	0.0731	0.0500	0.0053	0.0781	0.0500	0.0052	0.0744
0.1000	0.0201	0.0985	0.1000	0.0239	0.1077	0.1000	0.0211	0.1009
0.1500	0.0345	0.1223	0.1500	0.0418	0.1353	0.1500	0.0364	0.1258
0.2000	0.0482	0.1450	0.2000	0.0589	0.1617	0.2000	0.0511	0.1494
0.2500	0.0613	0.1666	0.2500	0.0752	0.1867	0.2500	0.0650	0.1719
0.3000	0.0738	0.1866	0.3000	0.0907	0.2100	0.3000	0.0783	0.1928
0.3500	0.0856	0.2055	0.3500	0.1053	0.2321	0.3500	0.0908	0.2126
0.4000	0.0967	0.2235	0.4000	0.1192	0.2529	0.4000	0.1026	0.2313
0.4500	0.1071	0.2403	0.4500	0.1321	0.2722	0.4500	0.1137	0.2485
0.5000	0.1167	0.2553	0.5000	0.1442	0.2902	0.5000	0.1240	0.[illegible]645
0.5500	0.1256	0.2694	0.5500	0.1554	0.3067	0.5500	0.1335	0.[illegible]793
0.6000	0.1338	0.2821	0.6000	0.1657	0.3216	0.6000	0.1423	0.2926
0.6500	0.1413	0.2934	0.6500	0.1751	0.3351	0.6500	0.1502	0.[illegible]045
0.7000	0.1480	0.3036	0.7000	0.1837	0.3475	0.7000	0.15[illegible]4	0.3154
0.7500	0.1540	0.3132	0.7500	0.1914	0.3589	0.7500	0.1638	0.3253
0.8000	0.1592	0.3214	0.8000	0.1983	0.3687	0.8000	0.16[illegible]5	0.3339
0.8500	0.1637	0.3279	0.8500	0.2042	0.3767	0.8500	0.1743	0.3408
0.9000	0.1674	0.3332	0.9000	0.2092	0.3834	0.9000	0.1783	0.3465
0.9500	0.1703	0.3375	0.9500	0.2132	0.3890	0.9500	0.1815	0.3511

1.0000	0.1723	0.3407	1.0000	0.2162	0.3930	1.0000	0.1838	0.3545
1.0500	0.1736	0.3420	1.0500	0.2182	0.3952	1.0500	0.1852	0.3560
1.1000	0.1739	0.3421	1.1000	0.2190	0.3960	1.1000	0.1857	0.3563
1.1500	0.1733	0.3411	1.1500	0.2187	0.3955	1.1500	0.1852	0.3554
1.2000	0.1718	0.3389	1.2000	0.2172	0.3933	1.2000	0.1837	0.3532
1.2500	0.1693	0.3346	1.2500	0.2145	0.3890	1.2500	0.1811	0.3489
1.3000	0.1658	0.3290	1.3000	0.2104	0.3831	1.3000	0.1774	0.3432
1.3500	0.1612	0.3221	1.3500	0.2048	0.3755	1.3500	0.1726	0.3361
1.4000	0.1554	0.3137	1.4000	0.1978	0.3662	1.4000	0.1665	0.3275
1.4500	0.1494	0.3029	1.4500	0.1891	0.3539	1.4500	0.1591	0.3163
1.5000	0.1402	0.2904	1.5000	0.1785	0.3395	1.5000	0.1503	0.3034
1.5500	0.1306	0.2764	1.5500	0.1660	0.3231	1.5500	0.1400	0.2887
1.6000	0.1195	0.2605	1.6000	0.1514	0.3041	1.6000	0.1280	0.2721
1.6500	0.1068	0.2415	1.6500	0.1343	0.2839	1.6500	0.1143	0.2520
1.7000	0.0925	0.2203	1.7000	0.1146	0.2549	1.7000	0.0986	0.2296
1.7500	0.0762	0.1969	1.7500	0.0918	0.2252	1.7500	0.0808	0.2046
1.8000	0.0578	0.1692	1.8000	0.0654	0.1894	1.8000	0.0606	0.1750
1.8500	0.0371	0.1388	1.8500	0.0348	0.1493	1.8500	0.0376	0.1423
1.9000	0.0138	0.1039	1.9000	0.0016	0.1003	1.9000	0.0116	0.1042
1.9349	-0.0000	0.0766	1.9105	-0.0000	0.0890	1.9292	-0.0000	0.0795
1.9500	0.0036	0.0643	1.9463	0.0357	0.0357	1.9500	0.0071	0.0609
1.9684	0.0335	0.0335				1.9632	0.0340	0.0340

** BLADE SECTION COORDINATES IN TURBOMACHINE ORIENTATION - A ROTOR TEST CASE

FRACT. OF SURF.	SECTION 1 FOR XCUT OF 9.4250 IN. SUCTION SURFACE Z (IN.)	Y (IN.)	PRESSURE SURFACE Z (IN.)	Y (IN.)	SECTION 2 FOR XCUT OF 9.3000 IN. SUCTION SURFACE Z (IN.)	Y (IN.)	PRESSURE SURFACE Z (IN.)	Y (IN.)	SECTION 3 FOR XCUT OF 9.0500 IN. SUCTION SURFACE Z (IN.)	Y (IN.)	PRESSURE SURFACE Z (IN.)	Y (IN.)
0.	-0.4887	-0.8562	-0.4677	-0.8670	-0.4982	-0.8513	-0.4763	-0.8628	-0.5169	-0.8405	-0.4934	-0.8541
0.05	-0.4460	-0.7662	-0.4179	-0.7812	-0.4547	-0.7617	-0.4255	-0.7777	-0.4721	-0.7522	-0.4406	-0.7703
0.12	-0.3848	-0.6407	-0.3481	-0.6609	-0.3926	-0.6369	-0.3543	-0.6584	-0.4080	-0.6286	-0.3668	-0.6529
0.20	-0.31[illegible]	-0.4982	-0.2684	-0.5234	-0.3197	-0.4951	-0.2730	-0.5220	-0.3328	-0.4884	-0.2825	-0.5186
0.30	-0.2239	-0.3215	-0.1690	-0.3514	-0.2259	-0.3194	-0.1718	-0.3513	-0.2360	-0.3146	-0.1777	-0.3505
0.40	-0.1259	-0.1463	-0.0699	-0.1792	-0.1292	-0.1452	-0.0710	-0.1803	-0.1362	-0.1425	-0.0733	-0.1820
0.50	-0.0282	0.0273	0.0286	-0.0068	-0.0300	0.0274	0.0293	-0.0090	-0.0336	0.0275	0.0304	-0.0131
0.60	0.0718	0.1994	0.1265	0.1658	0.0718	0.1983	0.1288	0.1626	0.0716	0.1965	0.1333	0.1562
0.70	0.1743	0.3699	0.2238	0.3386	0.1760	0.3676	0.2277	0.3343	0.1797	0.3632	0.2357	0.3257
0.80	0.2807	0.5375	0.3223	0.5105	0.2843	0.5339	0.3279	0.5052	0.2921	0.5266	0.3394	0.4941
0.88	0.3691	0.6692	0.4026	0.6470	0.3742	0.6646	0.4093	0.6408	0.3851	0.6550	0.4233	0.6282
0.95	0.4489	0.7826	0.4739	0.7655	0.4552	0.7771	0.4814	0.7588	0.4686	0.7655	0.4973	0.7448
1.00	0.5072	0.8625	0.5254	0.8496	0.5147	0.8563	0.5335	0.8426	0.5294	0.8434	0.5506	0.8278
L.E. CIRCLE CENTER			-0.4780	-0.8611			-0.4870	-0.8566			-0.5048	-0.8469
T.E. CIRCLE CENTER			0.5160	0.8557			0.5235	0.8491			0.53[illegible]7	0.8351

FRACT. CF SURF.	SECTION 4 FOR XCUT OF 8.8000 IN. SUCTION SURFACE Z (IN.)	Y (IN.)	PRESSURE SURFACE Z (IN.)	Y (IN.)	SECTION 5 FOR XCUT OF 8.5500 IN. SUCTION SURFACE Z (IN.)	Y (IN.)	PRESSURE SURFACE Z (IN.)	Y (IN.)	SECTION 6 FOR XCUT OF 8.3000 IN. SUCTION SURFACE Z (IN.)	Y (IN.)	PRESSURE SURFACE Z (IN.)	Y (IN.)
0.	-0.5355	-0.8300	-0.5102	-0.8447	-0.5537	-0.8185	-0.5268	-0.8350	-0.5722	-0.8062	-0.5437	-0.8244
0.05	-0.4894	-0.7420	-0.4556	-0.7624	-0.5064	-0.7314	-0.4705	-0.7540	-0.5238	-0.7198	-0.4858	-0.7447
0.12	-0.4234	-0.6197	-0.3793	-0.6469	-0.4387	-0.6102	-0.3918	-0.6404	-0.4544	-0.5998	-0.4049	-0.6331
0.20	-0.3460	-0.4809	-0.2923	-0.5148	-0.3591	-0.4729	-0.3020	-0.5104	-0.3727	-0.4639	-0.3124	-0.5054
0.30	-0.2462	-0.3091	-0.1838	-0.3492	-0.2564	-0.3030	-0.1902	-0.3476	-0.2671	-0.2961	-0.1972	-0.3454
0.40	-0.1432	-0.1391	-0.0760	-0.1833	-0.1503	-0.1353	-0.0789	-0.1843	-0.1577	-0.1307	-0.0824	-0.1849
0.50	-0.0373	0.0290	0.0312	-0.0169	-0.0410	0.0304	0.0318	-0.0206	-0.0448	0.0324	0.0319	-0.0240
0.60	0.0715	0.1951	0.1375	0.1500	0.0714	0.1949	0.1417	0.1437	0.0716	0.1930	0.1457	0.1373
0.70	0.1837	0.3588	0.2438	0.3168	0.1878	0.3545	0.2518	0.3077	0.1925	0.3501	0.2601	0.2981
0.80	0.3003	0.5192	0.3512	0.4827	0.3087	0.5116	0.3630	0.4710	0.3179	0.5035	0.3753	0.4583
0.88	0.3966	0.6450	0.4378	0.6148	0.4084	0.6347	0.4524	0.6010	0.4213	0.6235	0.4679	0.5860
0.95	0.4830	0.7532	0.5141	0.7300	0.4978	0.7405	0.5311	0.7144	0.5139	0.7265	0.5492	0.6974
1.00	0.5458	0.8295	0.5688	0.8119	0.5628	0.8150	0.5875	0.7952	0.5812	0.7989	0.6074	0.7768
L.E. CIRCLE CENTER			-0.5225	-0.8367			-0.5398	-0.8260			-0.5574	-0.8144
T.E. CIRCLE CENTER			0.5569	0.8201			0.5746	0.8044			0.5936	0.7871

** BLADE SECTION COORDINATES IN TURBOMACHINE ORIENTATION - A ROTOR TEST CASE

FRACT. CF SURF.	SECTION 7 FOR XCUT OF 8.0500 IN. SUCTION SURFACE Z (IN.)	Y (IN.)	PRESSURE SURFACE Z (IN.)	Y (IN.)	SECTION 8 FOR XCUT OF 7.8000 IN. SUCTION SURFACE Z (IN.)	Y (IN.)	PRESSURE SURFACE Z (IN.)	Y (IN.)	SECTION 9 FOR XCUT OF 7.5500 IN. SUCTION SURFACE Z (IN.)	Y (IN.)	PRESSURE SURFACE Z (IN.)	Y (IN.)
0.	-0.5914	-0.7927	-0.5614	-0.8127	-0.6109	-0.7783	-0.5794	-0.8001	-0.6310	-0.7628	-0.5981	-0.7863
0.05	-0.5419	-0.7071	-0.5020	-0.7345	-0.5604	-0.6934	-0.5186	-0.7232	-0.5796	-0.6784	-0.5354	-0.7108
0.12	-0.4709	-0.5882	-0.4188	-0.6248	-0.4877	-0.5756	-0.4333	-0.6156	-0.5052	-0.5617	-0.4486	-0.6057
0.20	-0.3870	-0.4539	-0.3238	-0.4994	-0.4017	-0.4428	-0.3357	-0.4926	-0.4171	-0.4303	-0.3485	-0.4846
0.30	-0.2783	-0.2882	-0.2051	-0.3424	-0.2899	-0.2793	-0.2136	-0.3386	-0.3020	-0.2692	-0.2224	-0.3340
0.40	-0.1655	-0.1252	-0.0866	-0.1850	-0.1735	-0.1190	-0.0914	-0.1846	-0.1819	-0.1117	-0.0969	-0.1636
0.50	-0.0488	0.0350	0.0316	-0.0273	-0.0528	0.0382	0.0308	-0.0304	-0.0568	0.0421	0.0295	-0.0332
0.60	0.0721	0.1922	0.1496	0.1305	0.0728	0.1916	0.1534	0.1236	0.0738	0.1911	0.1569	0.1164
0.70	0.1978	0.3454	0.2686	0.2877	0.2036	0.3406	0.2771	0.2768	0.2102	0.3354	0.2857	0.2650
0.80	0.3283	0.4946	0.3884	0.4443	0.3394	0.4849	0.4017	0.4292	0.3515	0.4743	0.4156	0.4126
0.88	0.4359	0.6109	0.4847	0.5691	0.4513	0.5971	0.5020	0.5507	0.4683	0.5816	0.5203	0.5301
0.95	0.5322	0.7105	0.5692	0.6780	0.5516	0.6928	0.5900	0.6566	0.5725	0.6728	0.6123	0.6325
1.00	0.6022	0.7803	0.6297	0.7556	0.6245	0.7598	0.6531	0.7322	0.6490	0.7362	0.6782	0.7055
L.E. CIRCLE CENTER			-0.5757	-0.8017			-0.5944	-0.7881			-0.6137	-0.7732
T.E. CIRCLE CENTER			0.6151	0.7671			0.6378	0.7450			0.6624	0.7198

FRACT. OF SURF.	SECTION 10 FOR XCUT OF 7.3000 IN. SUCTION SURFACE Z (IN.)	SUCTION SURFACE Y (IN.)	PRESSURE SURFACE Z (IN.)	PRESSURE SURFACE Y (IN.)
0.	-0.6519	-0.7456	-0.6177	-0.7711
0.05	-0.5995	-0.6620	-0.5542	-0.6971
0.12	-0.5236	-0.5464	-0.4649	-0.5935
0.20	-0.4331	-0.4166	-0.3623	-0.4755
0.30	-0.3148	-0.2579	-0.2333	-0.3285
0.40	-0.1937	-0.1034	-0.1033	-0.1819
0.50	-0.0609	0.0465	0.0275	-0.0360
0.60	0.0750	0.1910	0.1600	0.1088
0.70	0.2169	0.3297	0.2942	0.2521
0.80	0.3645	0.4624	0.4298	0.3942
0.88	0.4864	0.5641	0.5392	0.5070
0.95	0.5958	0.6499	0.6356	0.6051
1.00	0.6753	0.7092	0.7048	0.6749
L.E. CIRCLE CENTER			-0.6338	-0.7570
T.E. CIRCLE CENTER			0.6887	0.6909

FRACT. OF SURF.	SECTION 11 FOR XCUT OF 7.0500 IN. SUCTION SURFACE Z (IN.)	SUCTION SURFACE Y (IN.)	PRESSURE SURFACE Z (IN.)	PRESSURE SURFACE Y (IN.)
0.	-0.6735	-0.7274	-0.6379	-0.7548
0.05	-0.6232	-0.6443	-0.5733	-0.6821
0.12	-0.5426	-0.5297	-0.4822	-0.5836
0.20	-0.4590	-0.4014	-0.3772	-0.4653
0.30	-0.3282	-0.2452	-0.2447	-0.3214
0.40	-0.1999	-0.0940	-0.1108	-0.1796
0.50	-0.0652	0.0517	0.0248	-0.0385
0.60	0.0763	0.1910	0.1625	0.1007
0.70	0.2243	0.3235	0.3023	0.2380
0.80	0.3784	0.4489	0.4440	0.3735
0.88	0.5059	0.5440	0.5588	0.4806
0.95	0.6203	0.6233	0.6600	0.5735
1.00	0.7037	0.6776	0.7328	0.6393
L.E. CIRCLE CENTER			-0.6546	-0.7396
T.E. CIRCLE CENTER			0.7166	0.6572

FRACT. OF SURF.	SECTION 12 FOR XCUT OF 6.8000 IN. SUCTION SURFACE Z (IN.)	SUCTION SURFACE Y (IN.)	PRESSURE SURFACE Z (IN.)	PRESSURE SURFACE Y (IN.)
0.	-0.6962	-0.7074	-0.6594	-0.7368
0.05	-0.6420	-0.6248	-0.5937	-0.6653
0.12	-0.5630	-0.5111	-0.5010	-0.5659
0.20	-0.4681	-0.3842	-0.3937	-0.4532
0.30	-0.3427	-0.2306	-0.2579	-0.3137
0.40	-0.2100	-0.0829	-0.1198	-0.1760
0.50	-0.0699	0.0581	0.0207	-0.0406
0.60	0.0777	0.1914	0.1640	0.0923
0.70	0.2324	0.3156	0.3100	0.2224
0.80	0.3938	0.4333	0.4586	0.3497
0.88	0.5275	0.5201	0.5793	0.4496
0.95	0.6477	0.5912	0.6962	0.5356
1.00	0.7353	0.6390	0.7632	.5962
L.E. CIRCLE CENTER			-0.6766	-0.7235
T.E. CIRCLE CENTER			0.7472	0.6163

** BLADE SECTION COORDINATES IN TURBOMACHINE ORIENTATION - 4 ROTOR TEST CASE

FRACT. OF SURF.	SECTION 13 FOR XCUT OF 6.5500 IN. SUCTION SURFACE Z (IN.)	SUCTION SURFACE Y (IN.)	PRESSURE SURFACE Z (IN.)	PRESSURE SURFACE Y (IN.)
0.	-0.7202	-0.6855	-0.6821	-0.7169
0.05	-0.6652	-0.5032	-0.6156	-0.6466
0.12	-0.5846	-0.4903	-0.5213	-0.5491
0.20	-0.4874	-0.3648	-0.4119	-0.4390
0.30	-0.3582	-0.2137	-0.2722	-0.3036
0.40	-0.2207	-0.0697	-0.1303	-0.1710
0.50	-0.0748	0.0659	0.0154	-0.0419
0.60	0.0795	0.1924	0.1646	0.0835
0.70	0.2415	0.3093	0.3173	0.2050
0.80	0.4110	0.4149	0.4734	0.3222
0.88	0.5515	0.4914	0.6007	0.4129
0.95	0.6780	0.5519	0.7139	0.4898
1.00	0.7793	0.5912	0.7958	0.5433
L.E. CIRCLE CENTER			-0.6999	-0.6995
T.E. CIRCLE CENTER			0.7808	0.5660

FRACT. OF SURF.	SECTION 14 FOR XCUT OF 6.3000 IN. SUCTION SURFACE Z (IN.)	SUCTION SURFACE Y (IN.)	PRESSURE SURFACE Z (IN.)	PRESSURE SURFACE Y (IN.)
0.	-0.7455	-0.6612	-0.7062	-0.6946
0.05	-0.6897	-0.5790	-0.6389	-0.6253
0.12	-0.6076	-0.4666	-0.5432	-0.5295
0.20	-0.5078	-0.3423	-0.4317	-0.4220
0.30	-0.3745	-0.1938	-0.2889	-0.2910
0.40	-0.2317	-0.0541	-0.1427	-0.1642
0.50	-0.0795	0.0757	0.0090	-0.0421
0.60	0.0819	0.1943	0.1643	0.0749
0.70	0.2517	0.3008	0.3239	0.1861
0.80	0.4297	0.3938	0.4878	0.2912
0.88	0.5774	0.4577	0.6221	0.3705
0.95	0.7103	0.5050	0.7419	0.4359
1.00	0.8073	0.5335	0.8287	0.4803
L.E. CIRCLE CENTER			-0.7243	-0.6761
T.E. CIRCLE CENTER			0.9154	0.5058

FRACT. OF SURF.	SECTION 15 FOR XCUT OF 6.0750 IN. SUCTION SURFACE Z (IN.)	SUCTION SURFACE Y (IN.)	PRESSURE SURFACE Z (IN.)	PRESSURE SURFACE Y (IN.)
0.	-0.7681	-0.6388	[illegible]	-0.6734
0.05	-0.7117	-0.5566	-0.6598	-0.6054
0.12	-0.6281	-0.4445	[illegible]	-0.5111
0.20	-0.5262	-0.3211	-0.4497	-0.4057
0.30	-0.3891	-0.1746	-0.3033	-0.2787
0.40	-0.2416	-0.0386	-0.1532	-0.1572
0.50	-0.0837	0.0855	[illegible]	-0.0414
0.60	0.0840	0.1972	0.1624	0.0675
0.70	0.2610	0.2935	[illegible]	0.1684
0.80	0.4464	0.3740	[illegible]	.2517
0.88	0.6034	0.4246	[illegible]	.3293
0.95	0.7387	0.4575	[illegible]	0.3842
1.00	[illegible]	0.4700	[illegible]	.4162
L.E. CIRCLE CENTER			-0.7462	-0.6545
T.E. CIRCLE CENTER			[illegible]	.4441

FRACT. OF SURF.	SECTION 16 FOR XCUT OF 5.8500 IN. SUCTION SURFACE Z (IN.)	Y (IN.)	PRESSURE SURFACE Z (IN.)	Y (IN.)
0.	-0.7891	-0.6182	-0.7473	-0.6549
0.05	-0.7322	-0.5357	-0.6792	-0.5868
0.12	-0.6476	-0.4235	-0.5816	-0.4936
0.20	-0.5437	-0.3005	-0.4670	-0.3901
0.30	-0.4033	-0.1557	-0.3186	-0.2663
0.40	-0.2514	-0.0224	-0.1646	-0.1493
0.50	-0.0881	0.0973	-0.0049	-0.0398
0.60	0.0858	0.2016	0.1693	0.0612
0.70	0.2696	0.2881	0.3311	0.1523
0.80	0.4621	0.3541	0.5076	0.2318
0.88	0.6216	0.3996	0.6528	0.2855
0.95	0.7645	0.4059	0.7828	0.3239
1.00	0.8679	0.4380	0.8772	0.3458
L.E. CIRCLE CENTER			-0.7664	-0.6345
T.E. CIRCLE CENTER			0.8691	0.3764

FRACT. OF SURF.	SECTION 17 FOR XCUT OF 5.6000 IN. SUCTION SURFACE Z (IN.)	Y (IN.)	PRESSURE SURFACE Z (IN.)	Y (IN.)
0.	-0.8090	-0.5994	-0.7653	-0.6377
0.05	-0.7520	-0.5162	-0.6974	-0.5697
0.12	-0.6667	-0.4032	-0.5996	-0.4768
0.20	-0.5613	-0.2797	-0.4841	-0.3745
0.30	-0.4179	-0.1353	-0.3337	-0.2533
0.40	-0.2617	-0.0040	-0.1769	-0.1404
0.50	-0.0931	0.1115	-0.0137	-0.0369
0.60	0.0871	0.2086	0.1556	0.0558
0.70	0.2776	0.2839	0.3311	0.1354
0.80	0.4771	0.3332	0.5126	0.1990
0.88	0.6416	0.3499	0.6619	0.2359
0.95	0.7879	0.3446	0.7955	0.2555
1.00	0.8910	0.3275	0.8924	0.2610
L.E. CIRCLE CENTER			-0.7853	-0.6165
T.E. CIRCLE CENTER			0.8888	0.2943

FRACT. OF SURF.	SECTION 18 FOR XCUT OF 5.3500 IN. SUCTION SURFACE Z (IN.)	Y (IN.)	PRESSURE SURFACE Z (IN.)	Y (IN.)
0.	-0.8236	-0.5076	-0.7776	-0.6272
0.05	-0.7671	-0.5029	-0.7104	-0.5584
0.12	-0.6820	-0.3881	-0.6133	-0.4648
0.20	-0.5760	-0.2628	-0.4979	-0.3623
0.30	-0.4307	-0.1170	-0.3467	-0.2421
0.40	-0.2713	0.0141	-0.1883	-0.1318
0.50	-0.0983	0.1271	-0.0231	-0.0327
0.60	0.0871	0.2183	0.1488	0.0526
0.70	0.2833	0.2825	0.3271	0.1211
0.80	0.4881	0.3144	0.5114	0.1682
0.88	0.6559	0.3104	0.6628	0.1864
0.95	0.8036	0.2800	0.7976	0.1843
1.00	0.9082	0.2400	0.8950	0.1703
L.E. CIRCLE CENTER			-0.7987	-0.6051
T.E. CIRCLE CENTER			0.8974	0.2060

** BLADE SECTION COORDINATES IN TURBOMACHINE ORIENTATION - A ROTOR TEST CASE

FRACT. OF SURF.	SECTION 19 FOR XCUT OF 5.5300 IN. SUCTION SURFACE Z (IN.)	Y (IN.)	PRESSURE SURFACE Z (IN.)	Y (IN.)
0.	-0.8137	-0.5953	-0.7694	-0.6340
0.05	-0.7568	-0.5118	-0.7016	-0.5659
0.12	-0.6715	-0.3983	-0.6040	-0.4729
0.20	-0.5658	-0.2745	-0.4883	-0.3707
0.30	-0.4217	-0.1299	-0.3376	-0.2499
0.40	-0.2645	0.0011	-0.1802	-0.1380
0.50	-0.0945	0.1157	-0.0163	-0.0358
0.60	0.0873	0.2110	0.1539	0.0546
0.70	0.2795	0.2833	0.3304	0.1311
0.80	0.4806	0.3277	0.5129	0.1962
0.88	0.6463	0.3387	0.5631	0.2220
0.95	0.7932	0.3268	0.7971	0.2355
1.00	0.8984	0.3036	0.8945	0.2361
L.E. CIRCLE CENTER			-0.7897	-0.6125
T.E. CIRCLE CENTER			0.8925	0.2701

APPENDIX J

MICROFILM SUBROUTINES FROM LEWIS LIBRARY

The following NASA Lewis Library subroutines - LRMRGN, LRSIZE, LRGRID, LRANGE, LRCURV, LREON, LRCPLT, LRCHSZ, LRLEGN, LRION, LRIOFF, LRCNVT - are called in program subroutine BLUEPT to produce tables of blade-section coordinates that can be attached to blueprint drawings. These systems routines are a part of a microfilm plotting package called CINEMATIC, which is described in reference 8. The following descriptions of the subroutines are condensed from those given in the reference.

Subroutine LRMRGN

Purpose. - LRMRGN is used to change the width of plot margins.

Usage. - CALL LRMRGN (XLEFT, XRIGHT, YBOTM, YTOP). XLEFT (floating point) is the left margin width in absolute positioning units. XRIGHT (floating point) is the right margin width in absolute positioning units. YBOTM (floating point) is the lower margin width in absolute positioning units. YTOP (floating point) is the upper margin width in absolute positioning units.

Method. - A frame of film contains 10 absolute positioning units in the horizontal direction and 10 in the vertical direction. CINEMATIC sets margins around the plotting area as follows: LEFT and BOTTOM, 1.0 absolute positioning unit; RIGHT and TOP, 0.4 of an absolute positioning unit. A call to LRMRGN before LRCURV will change the width of the margins.

Subroutine LRSIZE

Purpose. - LRSIZE is used to change the size of a plot.

Usage. - CALL LRSIZE (XLEFT, XRIGHT, YBOTM, YTOP). XLEFT is the left end point of a plot in absolute positioning units. XRIGHT is the right end point of a plot in absolute positioning units. YBOTM is the lower end point of a plot in absolute positioning units. YTOP is the upper end point of a plot in absolute positioning units.

Method. - CINEMATIC uses one frame of film as the size of a plot (including margins). A call to LRSIZE before a curve-plotting routine will change the size of the plot. Plot size may be expanded in the X (horizontal) direction to be several frames wide.

Restrictions. - LRSIZE must be called before the plotting routine it applies to. The settings of LRSIZE remain in effect until changed by another call to LRSIZE. CALL LRSIZE(0.0, 10.0, 0.0, 10.0) will set the size back to one frame of film.

Subroutine LRGRID

Purpose. - LRGRID is used to specify grid-line changes.

Usage. - CALL LRGRID (IXCODE, IYCODE, DX, DY). IXCODE (fixed point) is a switch which applies to vertical grid lines and is used as follows:

IXCODE=0 means return to using CINEMATIC's built-in grid format (11 grid lines).

IXCODE=±1 means DX specifies how many grid lines; IXCODE=-1 suppresses grid labels.

IXCODE=±2 means DX specifies grid intervals; IXCODE=-2 suppresses grid labels.

IXCODE=±3 means DX specifies how many "tick marks" instead of grid lines; IXCODE=-3 suppresses grid labels.

IXCODE=±4 means DX specifies the interval between "tick marks"; IXCODE=-4 suppresses grid labels.

DX (floating point) specifies grid-line or "tick mark" frequency or intervals, depending on how IXCODE is set. IYCODE (fixed point) is the same as IXCODE, but it applies to horizontal grid lines. DY (floating point) is the same as DX but for horizontal grid lines.

Method. - CINEMATIC puts 11 horizontal and 11 vertical grid lines on every plot, unless LRGRID is called. When a grid-line frequency is specified, CINEMATIC sets the interval between the specified number of grid lines to be equal to $Z \times 10^n$, where Z = 1.0, 2.0, 2.5, or 5.0 and n depends on the magnitude of the user's data. To get these intervals, CINEMATIC will adjust the end points of the plot, if necessary.

Subroutine LRANGE

Purpose. - LRANGE is used to set the range of (X, Y) curve points.

Usage. - CALL LRANGE (XLEFT, XRIGHT, YBOTM, YTOP). XLEFT is the left end point of a plot in the user's units. XRIGHT is the right end point of a plot in the user's units. YBOTM is the lower end point of a plot in the user's units. YTOP is the upper end point of a plot in the user's units.

Method. - The curve-plotting subroutine LRCURV searches the (X, Y) coordinates for maximums and minimums and scales the rest of the user's points to fit between them. A call to LRANGE before LRCURV suppresses the search. The settings of LRANGE remain in effect for all successive plots until changed by another call to LRANGE.

Subroutine LRCURV

Purpose. - LRCURV is used to plot one curve of a multiple-curve plot.

Usage. - CALL LRCURV (X, Y, N, ITYPE, SYMBOL, EOP). X (floating point) is an array of X-coordinates for the curve. Y (floating point) is an array of Y-coordinates for the curve. N (fixed point) is the number of (X, Y) points to be plotted. ITYPE is a switch that indicates the type of plot desired:

ITYPE=1 specifies a dot plot; each (X, Y) point is represented by a dot.

ITYPE=2 specifies a vector plot; successive (X, Y) points are joined by straight lines.

ITYPE=3 specifies a symbol plot; each (X, Y) point is represented by a symbol. The FORTRAN character in SYMBOL specifies the symbol used.

ITYPE=4 specifies a special symbol plot; each (X, Y) point is represented by a special symbol taken from a SPECIAL CHARACTER TABLE.

SYMBOL specifies the plotting symbol when ITYPE=3 or 4. EOP is a switch that indicates when the last subroutine call for a given plot is being made:

EOP=0.0 means the current plot is not yet complete. More subroutine calls for this plot will follow.

EOP=1.0 means the current plot is complete. No more printing or plotting subroutines will be called for this plot.

Method. - LRCURV provides greater flexibility in drawing curves. LRCURV is useful for the plotting situation in which not all (X, Y) points for a plot are in the computer memory at the same time. Several calls to LRCURV may be made for the same plot.

The X and Y arrays are in whatever units the user is working with. LRCURV scales his data range to fit the size of the plot on film. The user should call LRANGE before LRCURV to supply the range of his data points to CINEMATIC. If the user does not call LRANGE, LRCURV will take the user's data range from the first call to LRCURV for any given plot.

LRCURV does not destroy the contents of X, Y, N, ITYPE, SYMBOL, or EOP during plotting.

Subroutine LREON

LREON is used to expand a frame in all directions so that the edges of adjacent frames touch.

Subroutine LRCPLT

Purpose. - LRCPLT is used to specify a multiple-curve plot.

Usage. - CALL LRCPLT (X, Y, KKK). X (floating point) is an array of X-coordinates for all the curves. Y (floating point) is an array of Y-coordinates for all the curves. KKK (fixed point) is an array at least six words long. It is used as follows: KKK(1) is a switch that indicates whether CINEMATIC should duplicate any of the coordinates in the X or Y arrays:

KKK(1)=1 means duplicate X-coordinates.

KKK(1)=2 means duplicate Y-coordinates.

KKK(1)=3 means no duplication.

KKK(2) indicates the type of plot desired:

KKK(2)=0 means that all successive points on a curve are connected by straight lines (a vector plot).

KKK(2)=N specifies a vector plot with a plotting symbol placed at every Nth point. KKK(5) indicates the symbol.

KKK(2)=-N means that every Nth point is represented by a plotting symbol. KKK(5) indicates the symbol.

KKK(2)=999 means that several curves with different KKK(2) numbers are being plotted. Let KN be the number of such curves. Then the KKK(2) number for each curve is supplied in KKK(KN+6) through KKK(2KN+5)

KKK(3) is the number of curves to be plotted.

KKK(4) is a switch that indicates whether a call to LRLABL will follow this call to LRCPLT. LRLABL labels a curve point.

KKK(4)=0 means no call to LRLABL will follow (moves to next frame).

KKK(4)=1 means a call to LRLABL will follow (holds a frame).

Whenever symbols are plotted, KKK(5) equals the number of the symbol used to plot the first curve. Symbols for successive curves are chosen in order.

KKK(6) gives the number of points in each curve when KKK(1) equals 1 or 2. KKK(6) gives the number of points in the first curve when KKK(1) equals 3. The number of points for successive curves appear in KKK(7) through KKK(KN+5), where KN is the number of curves being plotted.

Duplication of coordinates: When the set of X-coordinates for all the curves is the same, it may appear only once in the X array. KKK(1)=1 indicates this arrangement of the user's data. LRCPLT will use the one set of X's for all the curves to be plotted. The Y-coordinates for all the curves must appear in the Y array. LRCPLT does not destroy the contents of X and Y during plotting.

Grid: Ten grid intervals are specified in each direction. Grid intervals are equal to $Z \times 10^n$ where Z = 1, 2, 2.5, or 5 and n depends on the range of the user's data.

LRCPLT will adjust the range of the user's data to get 10 equal intervals of $Z \times 10^n$. Use LRGRID to change the grid.

Margins: A margin of 0.10 frame is allowed at the left and bottom, 0.04 frame at the right and top. These margins allow enough space for a title and legends, which are printed by LRTLEG, LRXLEG, AND LRYLEG. Use LRMRGN to change margins.

Plot size: The size of the entire plot is one frame of film. If needed, the size may be expanded to several continuous frames of film by a call to LRSIZE. With the previously described margins, the user's data range is scaled to a coordinate system of 981 × 981 distinct points.

Subroutine LRCHSZ

Purpose. - LRCHSZ is used to change the size of printed characters.

Usage. - CALL LRCHSZ (ISIZE), where ISIZE (fixed point) gives the size:

ISIZE=0 means let CINEMATIC resume selecting the size.

ISIZE=1 means miniature characters.

ISIZE=2 means small characters.

ISIZE=3 means medium characters.

ISIZE=4 means large characters.

Method. - LRCHSZ changes the character size for all character printing that follows. The specified size remains in effect until changed by another call to LRCHSZ.

Large: 43 characters per line, 22 lines per frame.

Medium: 64 characters per line, 32 lines per frame.

Small: 86 characters per line, 43 lines per frame.

Miniature: 128 characters per line, 64 lines per frame.

Subroutine LRLEGN

Purpose. - LRLEGN is used to print a legend anywhere on a plot.

Usage. - CALL LRLEGN (CHARS, N, IORIEN, XY, EOP). CHARS is an array of characters to be printed. N (fixed point) is the number of characters to be printed. IORIEN (fixed point) is a switch:

IORIEN=0 causes horizontal printing.

IORIEN=1 causes vertical printing.

X (floating point) is the X-coordinate of the starting point in absolute positioning units.
Y (floating point) is the Y-coordinate of the starting point in absolute positioning units.
EOP (floating point) is a switch:

EOP=0 indicates the current plot is not yet complete.

EOP=1 indicates the current plot is complete. No more calls to plotting or printing subroutines for this plot will occur.

Method. - The user expresses the (X, Y) starting point of a line of printing in absolute positioning units. LRLEGN prints medium-size characters. The user may also get other character sizes, italics, lower case, and special symbols.

Subroutines LRION and LRIOFF

Purpose. - These subroutines italicize printed characters.

Usage. - CALL LRION causes all printed characters that follow to be italicized. CALL LRIOFF turns off the italicized mode of printing.

Subroutine LRCNVT

Purpose. - LRCNVT converts a fixed- or floating-point number into printable characters.

Usage. - CALL LRCNVT (X, ITYPE, CHARS, IFORM, N, M). X is the number to be converted. ITYPE specifies X:

ITYPE=1 means X is fixed point.

ITYPE=2 means X is INTEGER*2

ITYPE=3 means X is floating point.

CHARS is the array to receive printable characters. CHARS must be dimensioned large enough to hold the N characters requested. IFORM is a switch that describes the format of the characters:

IFORM=1 means convert to FORTRAN "I" format.

IFORM=2 means convert to FORTRAN "Z" format.

IFORM=3 means convert to FORTRAN "F" format.

IFORM=4 means convert to FORTRAN "E" format.

N is the total number of characters desired. M is the number of characters to the right of the decimal point. M=0 for "I" or "Z" format.

REFERENCES

1. Crouse, James E.; Janetzke, David C.; and Schwirian, R. E.: A Computer Program for Composing Compressor Blading from Simulated Circular-Arc Elements on Conical Surfaces. NASA TN D-5437, 1969.
2. Johnsen, Irving A.; and Bullock, Robert O.; eds.: Aerodynamic Design of Axial-Flow Compressors. NASA SP-36, 1965.
3. Ames Research Staff: Equations, Tables, and Charts for Compressible Flow. NACA Rep. 1135, 1953.
4. Schwenk, Francis C.; Lewis, George W.; and Hartmann, Melvin J.: A Preliminary Analysis of the Magnitude of Shock Losses in Transonic Compressors. NACA RM E57A30, 1957.
5. Isakson, G. J.; and Eisley, J. G.: Natural Frequencies in Coupled Bending and Torsion of Twisted and Nonrotating Blades. NASA CR-65, 1964.
6. Roark, Raymond J.: Formulas for Stress and Strain. Third ed., McGraw-Hill Book Co., Inc., Table IX, p. 176, case 15.
7. Walsh, J. L.; Ahlberg, J. H.; and Nilson, E. N.: Best Approximation Properties of the Spline Fit. J. Math. Mech., vol. 11, no. 2, 1962, pp. 225-234.
8. Kannenberg, Robert G.: CINEMATIC - FORTRAN Subprograms for Automatic Computer Microfilm Plotting. NASA TM X-1866, 1969.

TABLE I. - VALUES OF $\frac{\kappa}{2}$ WHICH MAKE $\tanh^{-1} X$

EQUAL TO $+\infty$ OR $-\infty$

$$\left[\tanh^{-1} X = \tanh^{-1}\left[\frac{\sqrt{1 - (R_0C - \sin\kappa_0)^2}\left(\tan\frac{\kappa}{2} - \tan\frac{\kappa_0}{2}\right)}{(R_0C - \sin\kappa_0)\left(1 + \tan\frac{\kappa}{2}\tan\frac{\kappa_0}{2}\right) + \tan\frac{\kappa}{2} + \tan\frac{\kappa_0}{2}}\right]\right]$$

$R_0C - \sin\kappa_0$	X = 1		X = -1	
	$\tan\frac{\kappa}{2}$	$\frac{\kappa}{2}$, deg	$\tan\frac{\kappa}{2}$	$\frac{\kappa}{2}$, deg
-1.0	1.0000	45.00	1.0000	45.00
-.9	1.5954	57.92	.6268	32.08
-.8	2.0000	63.43	.5000	26.57
-.7	2.4488	67.79	.4084	22.21
-.6	3.0000	71.57	.3333	18.43
-.5	3.7321	75.00	.2679	15.00
-.4	4.7913	78.21	.2087	11.79
-.3	6.5131	81.27	.1535	8.73
-.2	9.8990	84.23	.1010	5.77
-.1	19.950	87.13	.0501	2.87
0	$\pm\infty$	$\pm$90.00	0	0
.1	-19.950	-87.13	-.0501	-2.87
.2	-9.8990	-84.23	-.1010	-5.77
.3	-6.5131	-81.27	-.1535	-8.73
.4	-4.7913	-78.21	-.2087	-11.79
.5	-3.7321	-75.00	-.2679	-15.00
.6	-3.0000	-71.57	-.3333	-18.43
.7	-2.4488	-67.79	-.4084	-22.21
.8	-2.0000	-63.43	-.5000	-26.57
.9	-1.5954	-57.92	-.6268	-32.08
1.0	-1.0000	-45.00	-1.0000	-45.00

TABLE II. - COEFFICIENTS FOR SERIES

REPRESENTATION OF $\sqrt{\frac{R}{R_0}} - 1$

Series term	Series coefficient	Ratio of coefficients	
		Decimal form	Fractional form
1	0.5	--------	-----
2	-.125	-0.25	1/4
3	.0625	-.50	3/6
4	-.039063	-.625	5/8
5	.027344	-.70	7/10
6	-.020508	-.75	9/12
7	.016113	-.78571	11/14
8	-.013092	-.8125	13/16
9	.010910	-.83333	15/18

TABLE [illegible] – MAXIMUM VALUES OF X_2^2 OVER R_0C [illegible]

$$\left[X_2^2 = \frac{\left[1-(R_0C-\sin\kappa_0)^2\right]\sin^2\frac{\kappa-\kappa_0}{2}}{\left[(R_0C-\sin\kappa_0)\cos\frac{\kappa-\kappa_0}{2}+\sin\frac{\kappa+\kappa_0}{2}-CR_0\sqrt{\frac{R}{R_0}}\right]^2}\right]$$

$R_0C - \sin\kappa_0$	R_0C	κ_0, deg	κ, deg	R/R_c	X_2^2	Turbomachinery limit imposed
1 000 000.0	1 000 000.9	70.00	70.00	0.99998	-0.4903	$\kappa - \kappa_0 = 140°$
10 000.0	10 000.94			.99981		
1 000.0	1 000.940			.99812		
100.0	100.9397			.98138		
10.0	10.9397			.82820	-.4886	
5.0	5.9397			.68359	-.4834	
3.0	3.9397			.52296	-.4704	
2.8191	3.7583			.50000	-.46760	
2.8191	3.7588	70.00	-70.00	0.50000	-0.4676	$R/R_0 = 0.5$
2.8	3.7397		-68.46		-.4467	
2.7	3.6396		-61.66		-.3719	
2.5	3.4397		-51.27		-.2732	
2.2	3.1397		-39.06		-.1798	
1.8	2.7397		-25.48		-.0986	
1.4	2.3397		-13.31		-.0421	
1.0	1.9397		-1.73		0	
0.6	1.5397		9.78		.0318	
0.2	1.1397		21.71		.0552	
-0.2	0.7397		34.74		.0697	
-0.5	0.4397		46.04		.0720	
-0.7	0.2397		55.07		.0654	
-0.9	0.0397		66.90		.0405	
-0.9396	0.0001		66.99		.0295	
-0.9397	-0.0000	70.00	70.00	2.0000	0.0294	$R/R_0 = 2.0$
-0.95	-0.0103		68.34		.0230	
-0.97	-0.0303		65.42		.0125	
-1.0	-0.0603		61.57		0	
-1.2	-0.2603		42.80		-.0494	
-1.4	-0.4603		28.64		-.0830	
-1.8	-0.8603		4.55		-.1449	
-2.2	-1.2603		-18.70		-.2197	
-2.5	-1.5603		-38.36		-.2991	
-2.7	-1.7603		-55.15		-.3815	
-2.8	-1.8603		-67.02		-.4492	
-2.8191	-1.8794		-70.00		-.4676	
-2.8191	-1.8794	70.00	-70.00	2.0000	-0.4676	$\kappa - \kappa_0 = -140°$
-3.0	-2.0603			1.9122	-.4704	
-5.0	-4.0603			1.4629	-.4834	
-10.0	-9.0603			1.2074	-.4886	
-100.0	-99.0603			[illegible]	-.4903	
-1 000.0	-999.06			1.0019		
-10 000.0	-9999.06			1.0002		
-1 000 000.0	-999 999.1			1.0000		

TABLE V. - RANGE OF ϵ EQUATION APPLICABILITY

Equation	Conditions
B12	$\lvert \kappa - \kappa_0 \rvert \leq 0.00001$ and $\dfrac{\lvert R_0 \rvert}{s - s_0} \leq 100.0$
B36	$\dfrac{\lvert R_0 \rvert}{s - s_0} > 10\,000.0$
	$\lvert \kappa - \kappa_0 \rvert < 0.00001$ and $\dfrac{\lvert R_0 \rvert}{s - s_0} > 100.0$
	$\left(\dfrac{R_0}{s - s_0}\right)^2 \dfrac{1}{\lvert \kappa - \kappa_0 \rvert} > 1.7\times10^9$
B28	Everything else

TABLE IV. - NUMBER OF TERMS FOR SERIES $\frac{X_2^2}{3} + \frac{X_2^4}{5} + \frac{X_2^6}{7} + \frac{X_2^8}{9} + \ldots + \frac{X_2^{2n}}{2n+1}$ NEEDED TO KEEP RELATIVE ERROR TO 10^{-8} FOR VARIOUS X_2^2

Independent variable, X_2^2	Number of series terms, n	First series term, $\frac{X_2^2}{3}$	n^{th} series term, $\frac{X_2^{2n}}{2n+1}$	Relative error,[a] $\frac{3X_2^{2(n-1)}}{2n+1}$
0.5	23	0.1667	0.2536×10^{-8}	$1.522\cdot10^{-8}$
.4	18	.1333	.1857	1.393
.3	14	.1000	.[illegible]9	1.649
.2	11	.06667	.08904	1.336
.1	8	.03333	.05882	1.765
.05	7	.01667	.005208	.3125
.01	5	.003333	.0009091	.2727
.001	4	.0003333	.00001111	.03333

[a]The n^{th} series term divided by the first series term.

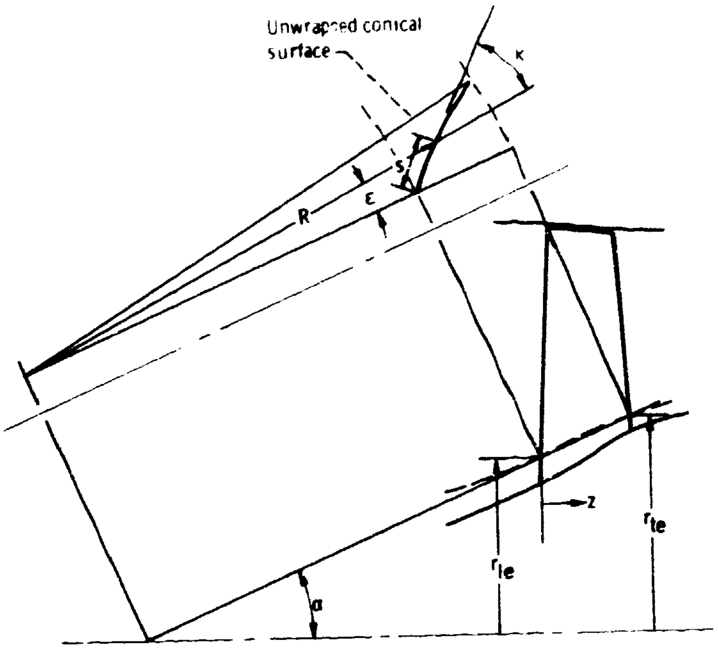

Figure 1. - Conical coordinate system for blade-element layout.

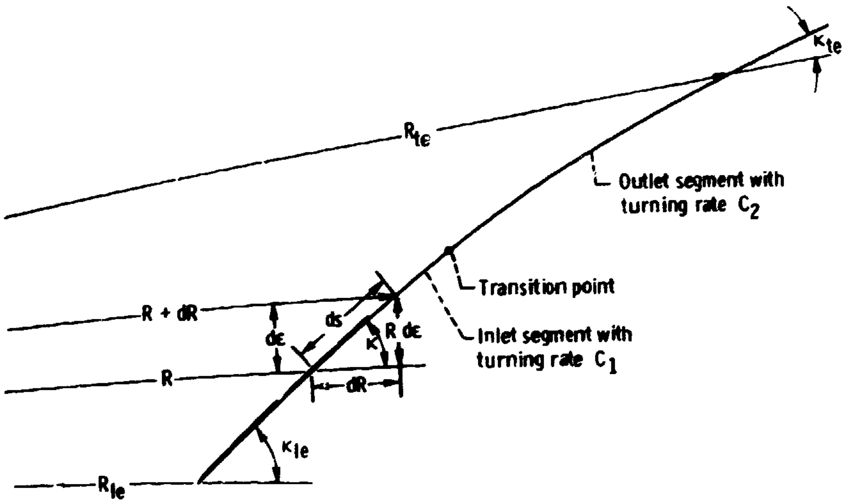

Figure 2. - Blade-element centerline nomenclature.

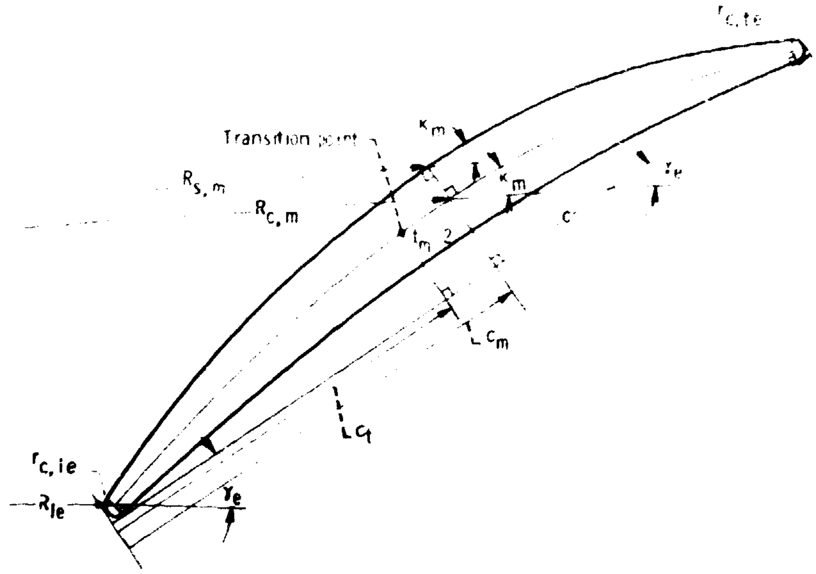

Figure 3. - Blade-element layout parameters.

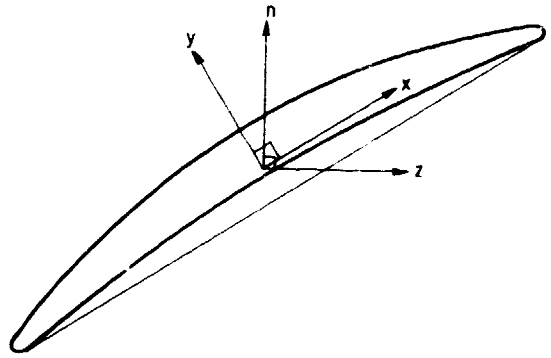

Figure 4. - Blade-section coordinate systems.

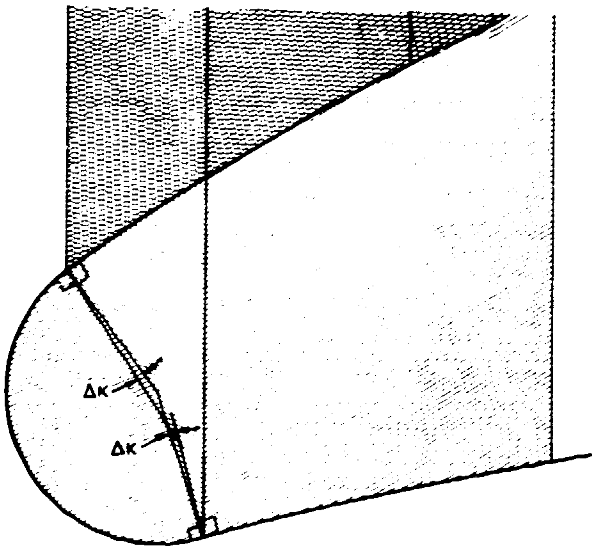

Figure 5. - Breakdown of blade-section end area for area and moment calculations.

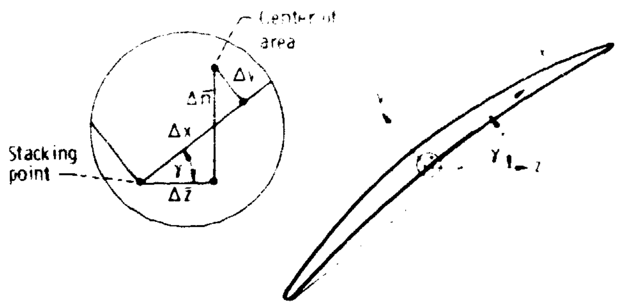

(a) Blade-section coordinates between center of area and stacking point.

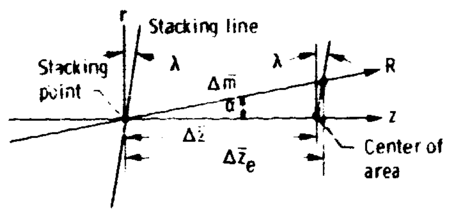

(b) Relation between blade-element and blade-section axial shifts in meridional plane.

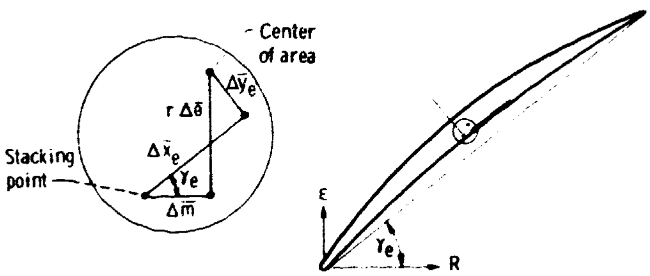

(c) Blade-element center-of-area chordwise and normal coordinate component adjustments.

Figure 6. - Stacking adjustment components between center of area and stacking point.

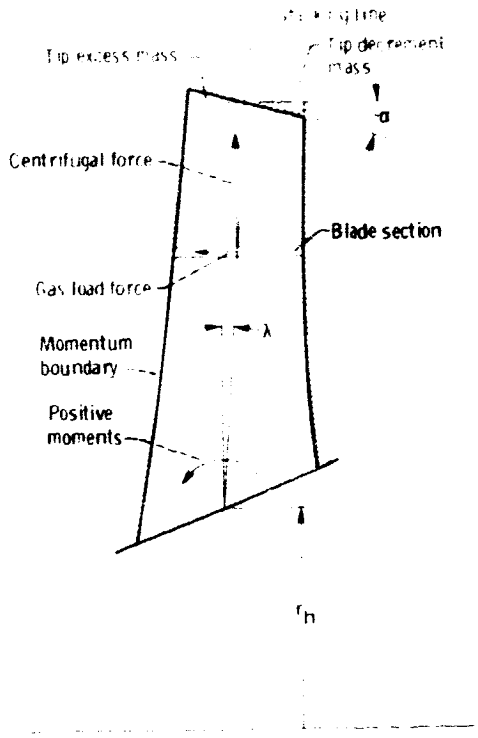

Figure 7. - Moments in meridional plane.

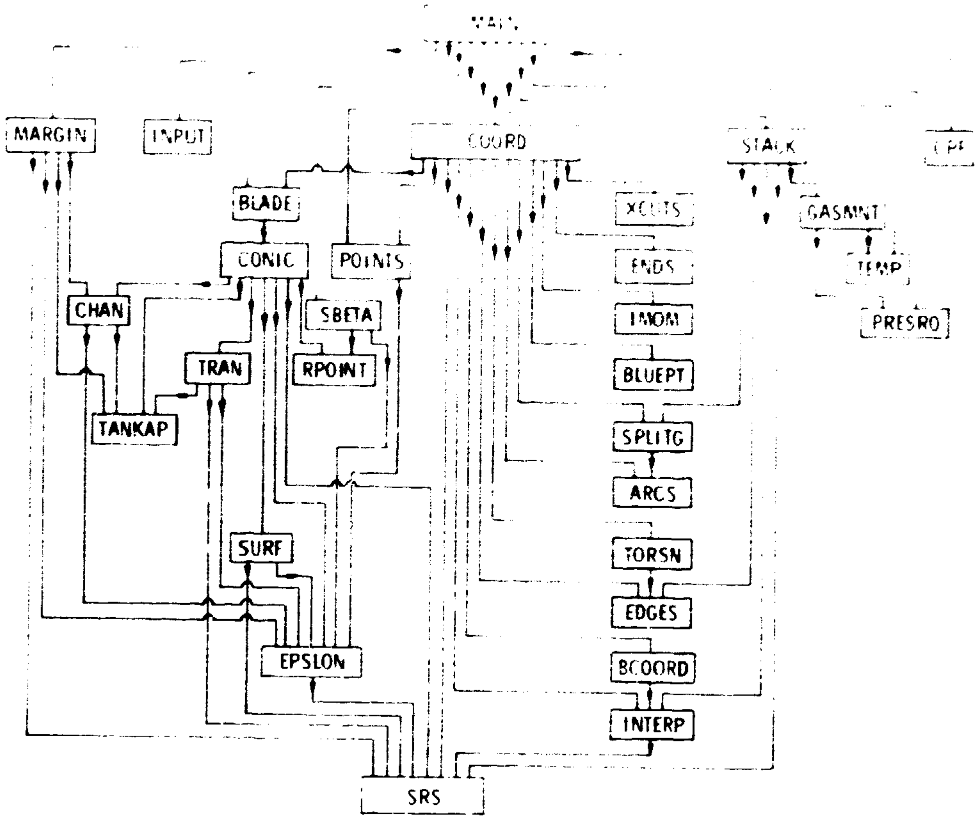

Figure 8. - Call sequence of computer program subroutines.

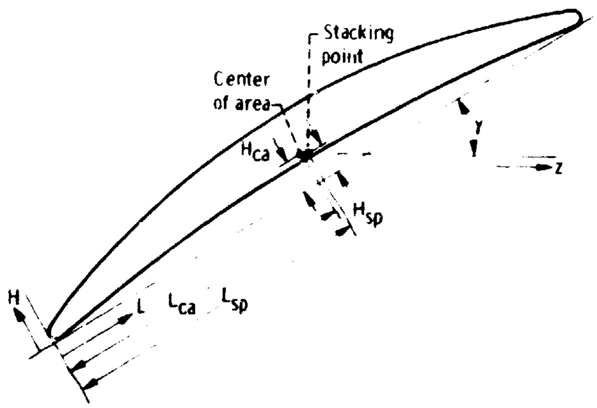

Figure 9. - Coordinate system for blade-section output data.

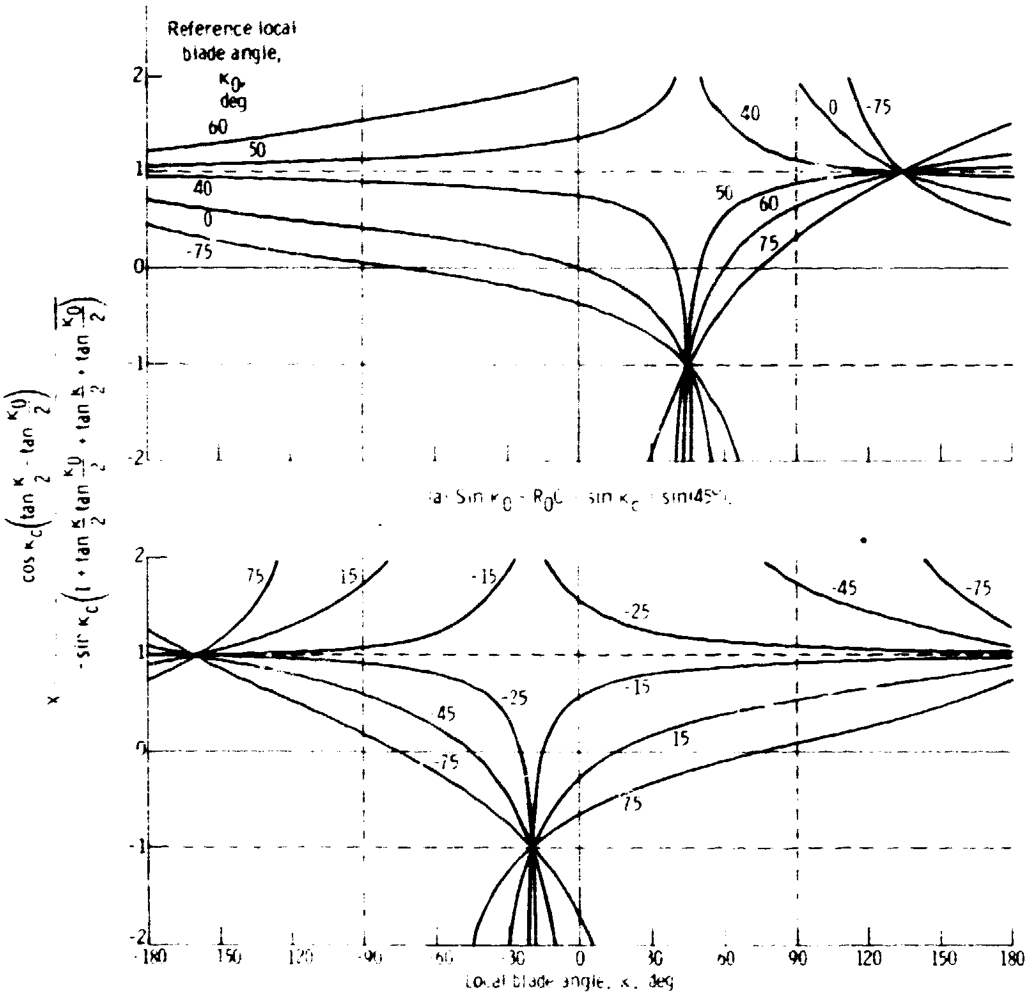

(a) $\sin\kappa_0 - R_0C = \sin\kappa_c = \sin(45^\circ)$.

(b) $\sin\kappa_0 - R_0C = \sin\kappa_c = \sin(-20^\circ)$.

Figure 10. - Variation of argument of $\tanh^{-1} X$ with κ.

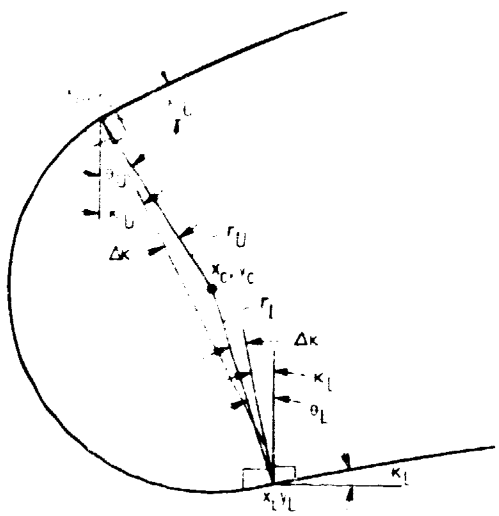

Figure 11. - Geometric placement of blade-section end circle.

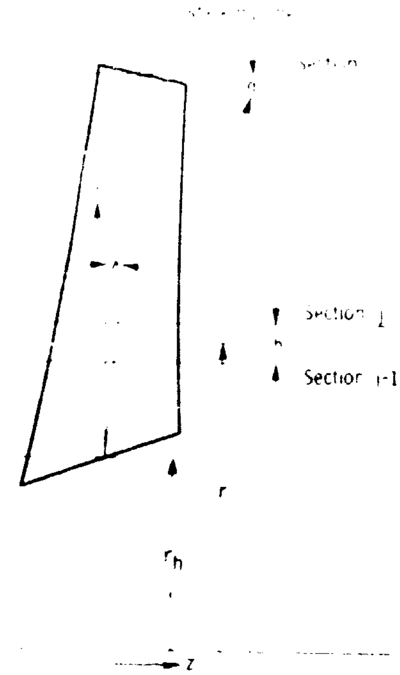

Figure 12. - Meridional plane stacking-axis lean.

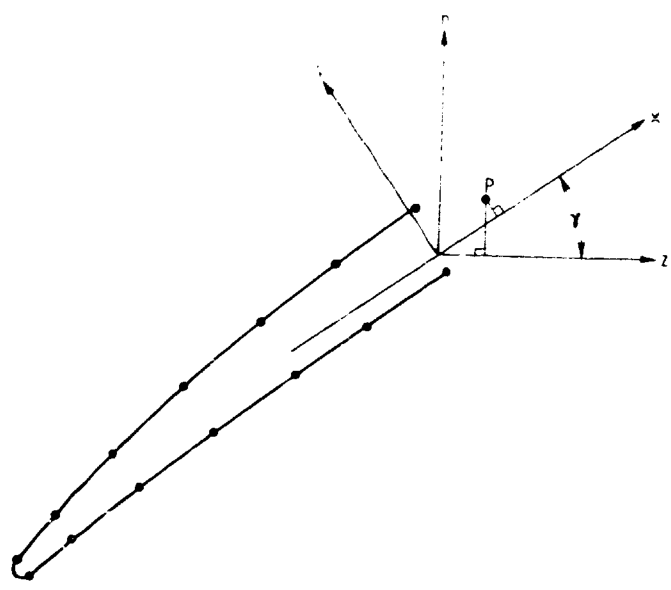

Figure 13. - Coordinate rotation about blade-section stacking point.

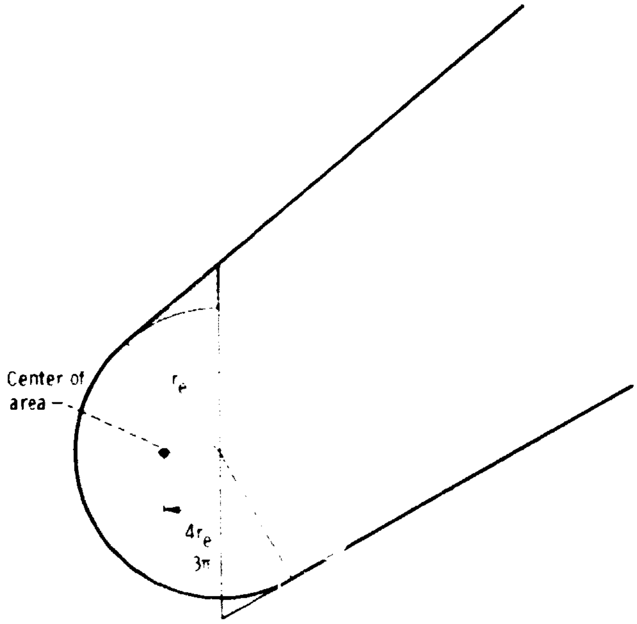

Figure 14. - Treatment of blade-section ends for excess end mass moment.

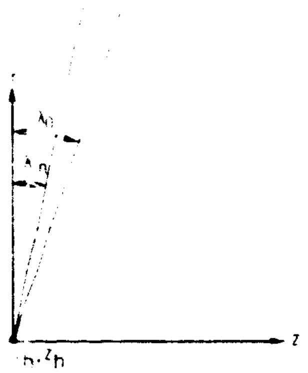

Figure 15. - Blade-element coordinate shifts due to change in meridional stacking-axis lean.

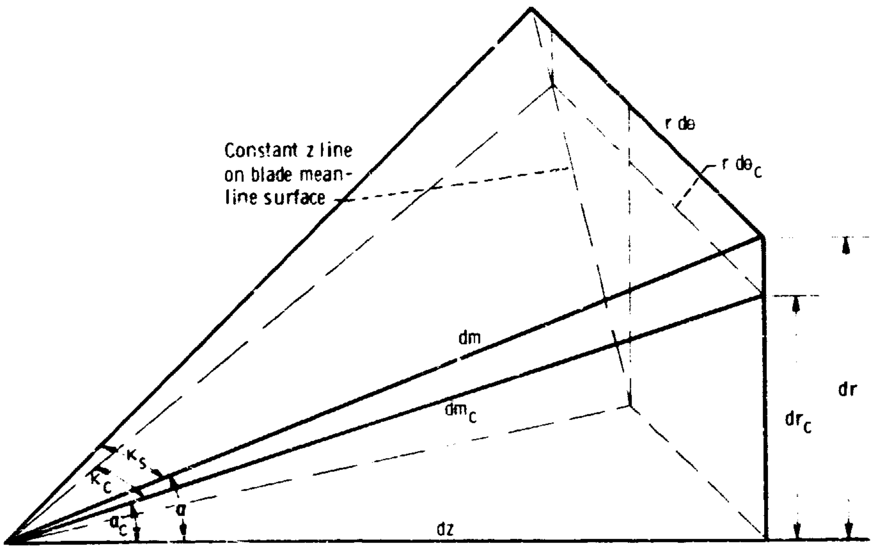

Figure 16. - Blade-angle correction from local streamline slope to cone slope.

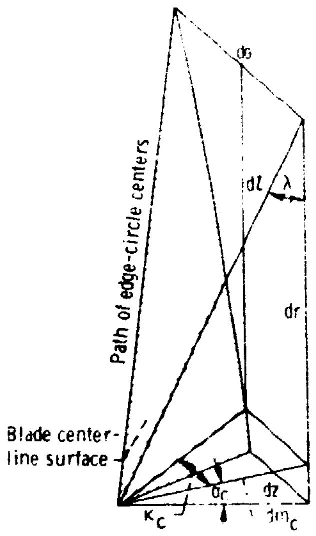

Figure 17. - Differential components at blade edge.

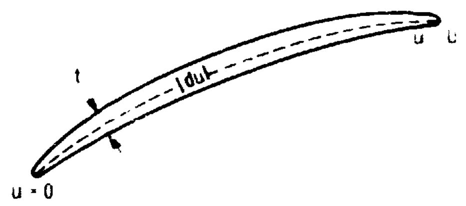

Figure 18. - Blade-section geometry parameters for torsion constant integration.

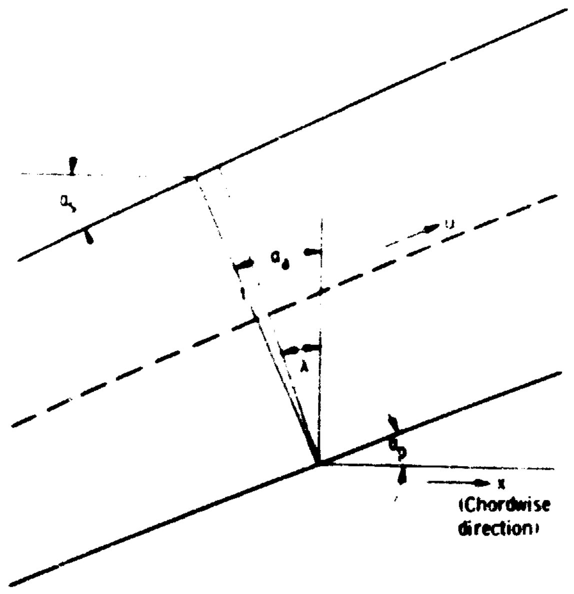

Figure 19. - Parameters for blade-section thickness definition.

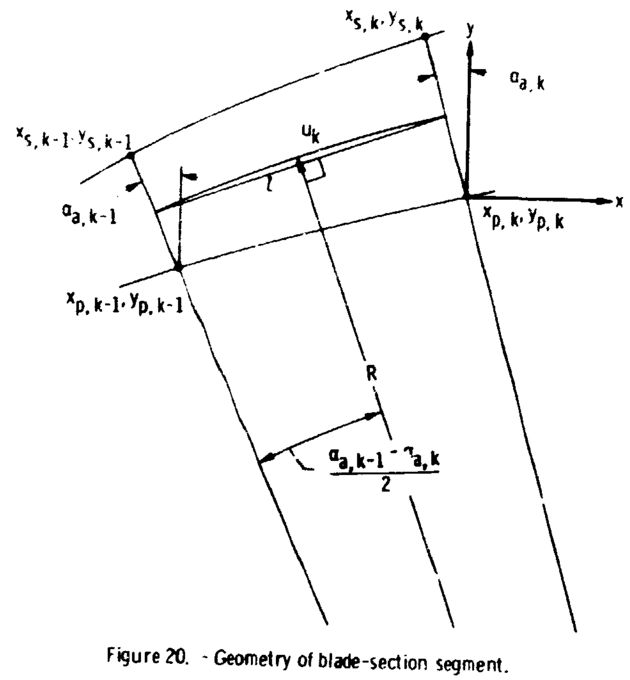

Figure 20. - Geometry of blade-section segment.

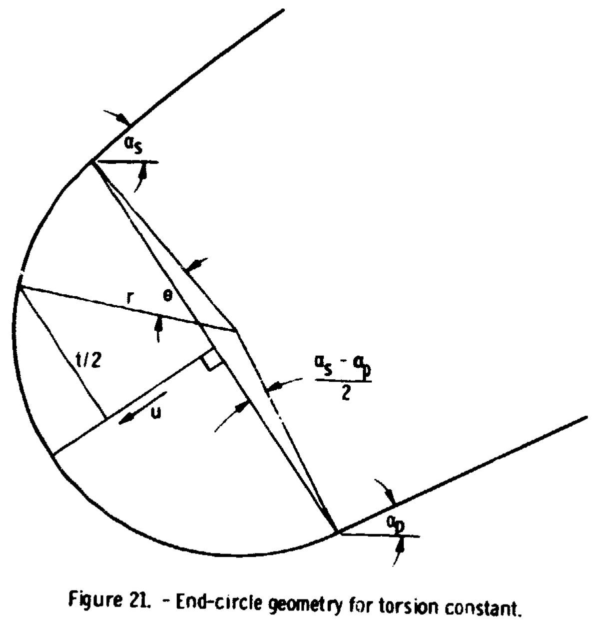

Figure 21. - End-circle geometry for torsion constant.

TITLE(1)							
OPCO(1)		OPCO([illegible])		[illegible]			
OPCO(4)		OPCO([illegible])		[illegible]			
NSTRM	[illegible]	[illegible]	ROT	[illegible](IROW)	[illegible](IROW)	[illegible](IROW)	[illegible](IROW)
BLADES(IROW)	SOLID(IROW)	TILT(IROW)	RMATL(IROW)	[illegible](IROW)			
TALE(IROW)	TBLE(IROW)	T[illegible]E(IROW)	TBLE(IROW)	[illegible](IROW)	[illegible](IROW)	[illegible](IROW)	[illegible]
TAMAX(IROW)	TBMAX(IROW)	TCMAX(IROW)	T[illegible]MAX(IROW)	[illegible](IROW)	[illegible](IROW)	[illegible](IROW)	
OP	OPE	A[illegible] AF	IF [illegible]	[illegible]	[illegible]	[illegible]	
INC(IROW,1)	INC(IROW,2)	...	INC(IROW,NSTRM)	[illegible]	[illegible]	[illegible]	
DEV(IROW,1)	DEV(IROW,2)	...	DEV(IROW,NSTRM)	[illegible]	[illegible]	[illegible]	
PHI(IROW,1)	PHI(IROW,2)	...	PHI(IROW,NSTRM)	[illegible]	[illegible]	TABLE	
TRANS(IROW,1)	TRANS(IROW,2)	...	TRANS(IROW,NSTRM)	[illegible]	[illegible]	TABLE	
ZMAX(IROW,1)	ZMAX(IROW,2)	...	ZMAX(IROW,NSTRM)	[illegible]	[illegible]	TABLE	
R(1,1)	Z(1,1)	VZ(1,1)	VTH(1,1)	SLOPE(1,1)	TO(1,1)	PO(1,1)	
R(1,2)	Z(1,2)	VZ(1,2)	VTH(1,2)	SLOPE(1,2)	TO(1,2)	PO(1,2)	
⋮	⋮	⋮	⋮	⋮	⋮	⋮	
R(1,NSTRM)	Z(1,NSTRM)	VZ(1,NSTRM)	VTH(1,NSTRM)	SLOPE(1,NSTRM)	TO(1,NSTRM)	PO(1,NSTRM)	tip
R(2,1)	Z(2,1)	VZ(2,1)	VTH(2,1)	SLOPE(2,1)	TO(2,1)	PO(2,1)	
R(2,2)	Z(2,2)	VZ(2,2)	VTH(2,2)	SLOPE(2,2)	TO(2,2)	PO(2,2)	
⋮	⋮	⋮	⋮	⋮	⋮	⋮	
R(2,NSTRM)	R(2,NSTRM)	VZ(2,NSTRM)	VTH(2,NSTRM)	SLOPE(2,NSTRM)	TO(2,NSTRM)	PO(2,NSTRM)	
XCUT(1)	XCUT(2)	XCUT(3)	XCUT(4)	XCUT([illegible])	XCUT([illegible])	XCUT([illegible])	[illegible]
XCUT([illegible])	... XCUT(NXCUT(IROW))			[illegible]			

Figure [illegible]

☆U.S. GOVERNMENT PRINTING OFFICE: 1974-739-157/84

END

DATE

FILMED

APR 19 1974